ADVANCED HYBRID PARTICULATE COLLECTOR

Final Technical Report for Phase I

Prepared for:

AAD Document Control
U.S. Department of Energy
National Energy Technology Laboratory
PO Box 10940, MS 921-143
Pittsburgh, PA 15236-0940

DOE Contract No. DE-AC22-95PC95258

Prepared by:

Stanley J. Miller
Grant L. Schelkoph
Grant E. Dunham

Energy & Environmental Research Center
University of North Dakota
PO Box 9018
Grand Forks, ND 58202-9018

Ken Walker

W.L. Gore & Associates, Inc.
101 Lewisville Road
Elkton, MD 21922-1100

Henry V. Krigmont
Alex V. Potapov

Allied Environmental Technologies Company
One Pacific Plaza
7755 Central Avenue, Suite 1118
Huntington Beach, CA 92647

2000-EERC-12-01

December 2000

DISCLAIMER

EERC DISCLAIMER

ADVANCED HYBRID PARTICULATE COLLECTOR

ABSTRACT

A new concept in particulate control, called an advanced hybrid particulate collector (AHPC), is being developed under funding from the U.S. Department of Energy. The AHPC combines the best features of electrostatic precipitators (ESPs) and baghouses in an entirely novel manner. The AHPC concept combines fabric filtration and electrostatic precipitation in the same housing, providing major synergism between the two methods, both in the particulate collection step and in transfer of dust to the hopper. The AHPC provides ultrahigh collection efficiency, overcoming the problem of excessive fine-particle emissions with conventional ESPs, and solves the problem of reentrainment and recollection of dust in conventional baghouses.

Phase I of the development effort consisted of design, construction, and testing of a 5.7-m^3/min (200-acfm) working AHPC model. Results from both 8-hour parametric tests and 100-hour proof-of-concept tests with two different coals demonstrated excellent operability and greater than 99.99% fine-particle collection efficiency.

TABLE OF CONTENTS

Continued . . .

TABLE OF CONTENTS (continued)

Continued . . .

TABLE OF CONTENTS (continued)

LIST OF FIGURES

Continued . . .

LIST OF FIGURES (continued)

Continued . . .

LIST OF FIGURES (continued)

Continued . . .

LIST OF FIGURES (continued)

Continued . . .

LIST OF FIGURES (continued)

Continued . . .

LIST OF FIGURES (continued)

Continued . . .

LIST OF FIGURES (continued)

Continued . . .

LIST OF FIGURES (continued)

Continued . . .

LIST OF FIGURES (continued)

Continued . . .

LIST OF FIGURES (continued)

LIST OF TABLES

Continued . . .

LIST OF TABLES (continued)

UNITS AND ACRONYMS USED

acf	actual cubic feet
acfm	actual cubic feet per minute
AHPC	advanced hybrid particulate collector
APS	aerodynamic particle sizer
A/C	air-to-cloth (ratio)
As	arsenic
C	Celsius
Cd	cadmium
cfm	cubic feet per minute
cm	centimeter
cm^3	cubic centimeter
CO	carbon monoxide
CO_2	carbon dioxide
CPC	condensation particle counter
Cr	chromium
DC	direct current
DI	deionized
DOE	U.S. Department of Energy
dP	differential pressure
DPD	dry powder disperser
EERC	Energy & Environmental Research Center
EPA	U.S. Environmental Protection Agency
EPRI	Electric Power Research Institute
ESP	electrostatic precipitator
F	Fahrenheit
FD	forced draft
ft	foot
ft^2	square foot
g	gram
gr	grain
HCl	hydrochloric acid
Hg	mercury
Hg^0	elemental mercury
Hg^{2+}	oxidized mercury
H_2O_2	hydrogen peroxide
hr	hour
IAC	iodine-impregnated activated carbon
ID	induced draft, inside diameter
in.	inch
$KMnO_4$	potassium permanganate
kPa	kilopascal
kV	kilovolt
LAC	lignite-based activated carbon
LOI	loss on ignition
m	meter
m^2	square meter
m^3	cubic meter
mA	milliampere
mg	milligram
µg	microgram
min	minute

NH_3	ammonia
Ni	nickel
NO_x	nitrogen oxides
NSPS	New Source Performance Standard
OD	outside diameter
pc	pulverized coal
Pb	lead
ppm	parts per million
psig	pounds per square inch gage
PRDA	Program Research and Development Announcement
PTC	particulate test combustor
PTFE	polytetrafluoroethylene
RGFF	reverse-gas fabric filter
RSD	relative standard deviation
s	second
S	sulfur
SCA	specific collection area
scf	standard cubic feet
Se	selenium
SMPS	scanning mobility particle sizer
$SnCl_2$	stannous chloride
SO_2	sulfur dioxide
SO_3	sulfur trioxide
SS	stainless steel
STDV	standard deviation
W.C.	water column

ADVANCED HYBRID PARTICULATE COLLECTOR

EXECUTIVE SUMMARY

The goal for improved fine-particle control is to achieve as high a level of control as is practically possible, while at the same time providing high reliability, smaller size, and economic benefits. The primary technologies for state-of-the-art particulate control are fabric filters (baghouses) and electrostatic precipitators (ESPs). However, each of these has limitations that prevent it from achieving ultrahigh collection of fine particulate matter. A major limitation of ESPs is that the fractional penetration of 0.1- to 1.0-μm particles is typically at least an order of magnitude greater than for 10-μm particles, so a situation exists where the particles that are of greatest health concern are collected with the lowest efficiency. Fabric filters are currently considered to be the best available control technology for fine particles, but they also have weaknesses that limit their application. Emissions are dependent on ash properties and typically increase if the air-to-cloth (A/C) ratio is increased. In addition, many fabrics cannot withstand the rigors of high-SO_3 flue gases, which are typical for bituminous fuels. Fabric filters may also have problems with bag cleanability and high pressure drop, which has resulted in conservatively designed, large, costly baghouses.

The objective of the advanced hybrid particulate collector (AHPC) is to overcome the deficiencies of ESPs and fabric filters and achieve >99.99% particulate collection efficiency for all particle sizes from 0.01 to 50 μm, to be applicable for use with all U.S. coals, and to be cost-competitive with existing technologies.

An approach to making fabric filters more economical is to employ smaller baghouses that operate at much higher A/C ratios. The challenge is to increase the A/C ratio for economic benefits and to achieve ultrahigh collection efficiency at the same time. The solution is to employ a sophisticated fabric that can ensure ultrahigh collection efficiency and endure frequent high-energy cleaning. In addition, the fabric should be reliable under the most severe chemical

environment likely to be encountered (such as high SO_3). A fabric that meets these requirements is GORE-TEX® membrane on GORE-TEX® felt.

Pulse-jet baghouses have the potential to operate at high face velocities because bags can be cleaned more often and adequate pulse energy can usually prevent excessive residual dust cake buildup. The potential for high-ratio operation is much greater if a significant portion of the dust is precollected. That is accomplished in the AHPC by employing only enough ESP plate area to precollect approximately 90% of the dust and by also utilizing this plate area to enhance bag cleaning.

The electrostatic and filtration zones are uniquely oriented to maximize fine-particle collection and minimize pressure drop. The geometric configuration of the AHPC is similar to that of a conventional pulse-jet baghouse with three of every four rows of bags removed and a grounded plate placed between adjacent remaining rows of bags. Directional high-voltage corona discharge electrodes are installed between each plate and row of bags so that the corona is forced to the plate side rather than to the bag side. Flue gas is directed by baffles into the AHPC so that the particles become charged before they can reach the filtration surface. Since the electrostatic migration velocity of the particles moving toward the plates is greater than the gas velocity component moving toward the bags, most of the dust is collected on the plates. Ultrahigh fine-particle collection is achieved by removing over 90% of the dust before it reaches the fabric and using a GORE-TEX® membrane fabric to collect with a high efficiency the particles that reach the filtration surface.

The Phase I scope of work consisted of the following:

- Design and construction of a 5.7-m^3/min (200-acfm) working model
- Cold-flow tests using reentrained dust
- 8-hr tests on coal
- 100-hr tests on coal

The primary parameters evaluated to determine the success of the concept were:

- Fine-particle collection efficiency.
- Operating pressure drop.
- Bag-cleaning interval.
- A/C ratio.
- Coal type.

Highlights of the results are:

- Greater than 99.99% fine-particle collection efficiency was achieved by a wide margin. The GORE-TEX® fabric performed very well, and no further development of the fabric is necessary to move forward with the AHPC concept.

- Results demonstrated successful 100-hr operation at an A/C ratio of 3.7 m/min (12 ft/min) and 8-hr operation at 4.9 m/min (16 ft/min).

- Pressure drop was well controlled, at a 2.0-kPa (8-in. W.C.) bag-cleaning set point with a pulse-cleaning interval of 25 min. The average pressure drop was in the range of 1.5–1.75 kPa (6–7 in.) Never in the Phase I testing was it necessary to increase the 2.0-kPa (8-in. W.C.) set point to demonstrate the AHPC operability.

- Results demonstrated significant synergism between the ESP and filtration modes. Tests with only the ESP demonstrated 95% collection, but with the bags included, emissions were over 1000 times lower. With the ESP, the bag-cleaning interval was over 10 times greater than without the ESP. The presence of the two collection mechanisms overcomes any weakness in either technology by itself and results in a combined device that is significantly smaller, but superior to either technology alone.

- Flow baffling is not highly critical to direct flow to the ESP zone. This was one of the pleasant surprises of the Phase I testing. Visual monitoring of the AHPC showed that the dust and gas flow is directed toward the grounded plates, even with minimal baffling. Because the electrical migration velocity toward the plates is much greater than the filtration velocity toward the bags, the dirty inlet gas and dust are transferred into the ESP zone before they reach the filter. This indicates that a simpler inlet configuration with an inlet just below the bags and plates would also work well.

- The use of conductive bags and a directional corona discharge electrode prevent electrical damage to the bags. Since the conductive bags are already available at about the same cost as nonconductive ones, this is not a developmental concern. For most cases, grounded bags are likely to be unnecessary, but until that is proven, the safest approach is to use them.

- The AHPC is projected to be economically competitive with conventional ESPs and baghouses, even for meeting the old NSPS (New Source Performance Standard) requirement of 0.03 lb/million Btu. For a new $PM_{2.5}$ emission standard of 99.9% control, the AHPC is projected to be the economic choice over ESPs by a wide margin. The AHPC is projected to also be the economic choice over conventional baghouses for a $PM_{2.5}$ standard.

- All of the developmental goals of Phase I were met and the approach is ready for scaleup.

ADVANCED HYBRID PARTICULATE COLLECTOR

1.0 INTRODUCTION

This project report summarizes the Phase I development for a new concept in particulate control called an advanced hybrid particulate collector (AHPC). The project was funded under the U.S. Department of Energy (DOE) Program Research and Development Announcement (PRDA) No. DE-RA22-94PC92291, Contract No. DE-AC22-95PC95258, Advanced Environmental Control Technologies for Coal-Based Power Systems Phases I and II, and addresses Topic 7: Advanced Concepts for Control of Fine Particles and Vapor-Phase Toxic Emissions. In addition to DOE, the project team includes the Energy & Environmental Research Center (EERC) as the primary contractor, Allied Environmental Technologies Company as a subcontractor, and W.L. Gore & Associates, Inc., as a technical and financial partner.

1.1 Background

Significant concern exists over the impact of increasing energy consumption on ambient air quality. Emissions of fine particles from coal combustion are of concern because these particles can be deposited in the lower respiratory system through normal breathing. The potential problem is further compounded because hazardous trace elements such as mercury, cadmium, selenium, and arsenic are known to be concentrated on such fine particles. Recent studies indicate that current levels of fine particles in the atmosphere are causing up to 60,000 premature deaths per year and that the current ambient air quality standard for PM_{10} may not adequately protect public health (1–3). In addition to adverse health effects, fine particles, including secondary sulfates, are the primary cause of visibility impairment in the atmosphere. The U.S. Environmental Protection Agency (EPA) has responded with the recent ambient air quality standard based on particles smaller than 2.5 μm (4). The new standard for $PM_{2.5}$ is a broad and wide-sweeping regulation designed to ensure that all Americans can enjoy clean air whether they live in remote, pristine regions or in major urban centers. The standard has major implications for industry, including transportation, power production, oil refining, incineration, chemical

production, and agriculture. The number of counties nationwide that are out of compliance will increase from the present 41 counties that are not in compliance with PM_{10} to 167 that are projected to not meet the new standard (5). The noncompliance areas represent major urban areas in 37 of the 50 states. States will be required to set up monitoring networks and then develop state implementation plans to bring all areas into compliance. Achieving compliance will require significant reductions in emissions from the mobile and stationary sources of $PM_{2.5}$ contamination in the atmosphere. Superior, economical technologies will have to be developed that allow efficient operation of processes while at the same time preventing unacceptable pollution of the atmosphere.

The primary technologies for state-of-the-art particulate control are fabric filters (baghouses) and electrostatic precipitators (ESPs). However, each of these has limitations that prevent it from achieving ultrahigh collection of fine particulate matter. A major limitation of ESPs is that the fractional penetration of 0.1- to 1.0-μm particles is typically at least an order of magnitude greater than for 10-μm particles, so a situation exists where the particles that are of greatest health concern are collected with the lowest efficiency. Fabric filters are currently considered to be the best available control technology for fine particles, but they also have weaknesses that limit their application. Emissions depend on ash properties and typically increase if the air-to-cloth (A/C) ratio is increased. In addition, many fabrics cannot withstand the rigors of high-SO_3 flue gases, which are typical for bituminous fuels. Fabric filters may also have problems with bag cleanability and high pressure drop, which has resulted in conservatively designed, large, costly baghouses.

The intent of the AHPC is to overcome the deficiencies of ESPs and fabric filters and yet capitalize on the best features of electrostatics and filtration and combine them into a single device. The AHPC concept consists of a combination of fabric filtration and electrostatic precipitation in the same device, providing major synergism between the two collection methods, both in the particulate collection step and in transfer of the dust from the bags or plates to the hopper.

1.2 Objective

The objective of the project is to develop a highly reliable AHPC that can provide >99.99% particulate collection efficiency for all particle sizes from 0.01 to 50 μm, is applicable for use with all U.S. coals, and is cost-competitive with existing technologies.

2.0 THEORY AND CONCEPT

2.1 Fine-Particle Collection Efficiency

The goal in developing a new approach for particulate control is to achieve as high a level of control as is practically possible, while at the same time providing high reliability, smaller size, and economic benefits. For dusts that are primarily larger than 20 μm, inertial separation methods, such as cyclones, are reasonably effective and are much more economical than conventional ESPs or baghouses. However, fine particles smaller than 2.5 μm pass through cyclones with little or no collection. If emission of even a small amount of fine dust is unacceptable, then cyclones are not a viable control method and only ESPs and baghouses are capable of achieving any reasonable level of control. Fabric filters collect fine particles much better than ESPs because fabric filters do not have the same theoretical (and actual) minimum collection efficiency for particles in the range from 0.1 to 0.3 μm. For these particles, the collection efficiency of a cyclone is close to zero, the efficiency of a modern ESP could approach about 99%, and the efficiency of a well-designed fabric filter would be about 99.9%. Higher levels of control might be possible with an ESP, but only by a significant increase in the size or specific collection area (SCA). Since the goal for the AHPC is to be much smaller and more economical than conventional approaches, achieving better fine-particle collection with electrostatic collection alone does not appear to be viable. That means that the advanced concept must employ filtration or some combination of electrostatics and filtration to achieve an ultrahigh fine-particle collection efficiency.

Fabric filters cannot routinely achieve 99.9% fine-particle collection efficiency for all coals within economic constraints, and studies have shown that collection efficiency is likely to deteriorate significantly when the face velocity is increased (6,7). An approach to make fabric filters more economical is to employ smaller baghouses that operate at much higher A/C ratios. The challenge is to increase the A/C ratio for economic benefits and to achieve ultrahigh collection efficiency at the same time. To achieve high collection efficiency, the pores in the filter media must be effectively bridged (assuming they are larger than the average particle size).

With conventional fabrics at low A/C ratios, the residual dust cake serves as part of the collection medium, but at high A/C ratios, only a very light residual dust cake is acceptable, so the cake cannot be relied on to help achieve high collection efficiency. The solution is to employ a sophisticated fabric that can ensure ultrahigh collection efficiency and endure frequent high-energy cleaning. In addition, the fabric should be reliable under the most severe chemical environment likely to be encountered (such as high SO_3). Such a fabric is already commercially available but is not widely applied to coal-fired boilers because of its higher cost compared to conventional fabrics. The fabric is GORE-TEX® membrane on GORE-TEX® felt, which can achieve very high collection efficiencies at high A/C ratios. GORE-TEX® membrane filter bags consist of a microporous, expanded polytetrafluoroethylene (PTFE) membrane laminated to a felted or fabric backing material. Consequently, even fine, nonagglomerating particles do not penetrate the filter, resulting in significant improvements in filtration efficiency, especially for submicron particles. This fabric is also rugged enough to hold up under rigorous cleaning, and the all-PTFE construction alleviates concern over chemical attack under the most severe chemical environments. Although GORE-TEX® membrane filter medium is more expensive than conventional fabrics, the much smaller surface area required for the AHPC will make the use of the GORE-TEX® membrane filter medium economical.

2.2 Collector Size and Pressure Drop

Assuming that the use GORE-TEX® fabric will achieve ultrahigh collection efficiency at high A/C ratios, the challenge is to control pressure drop. The following analysis will show that there is a good theoretical basis for operating fabric filters at much higher A/C ratios than typically employed. The size of fabric filters and bag-cleaning frequency are determined by pressure drop. If we assume viscous flow, pressure drop across a fabric filter is dependent on three components:

$$dP = K_f V + K_2 W_R V + K_2 C V^2 t /1000 \qquad \text{[Eq. 1]}$$

where:

dP = differential pressure (dP) across baghouse tube sheet (kPa [in. W.C.])

K_f = fabric resistance coefficient (kPa min/m [in. W.C.-min/ft])

V = face velocity or A/C ratio (m/min [ft/min])

K_2 = specific dust cake resistance coefficient (kPa m-min/kg [in. W.C.-ft-min/lb])

W_R = residual dust cake weight (kg/m^2 [lb/ft^2])

C = dust loading (g/m^3 [gr/acf])

t = filtration time between bag cleaning (min)

The first term in Eq. 1 accounts for the pressure drop across the fabric. For conventional fabrics, the pore size is quite large and the corresponding fabric permeability is high, so the pressure drop across the fabric alone is negligible. To achieve better collection efficiency, the pore size can be significantly reduced without making the fabric resistance a significant contributor to pressure drop. The GORE-TEX® fabric allows for this optimization by providing a microfine pore structure while maintaining a sufficient fabric permeability to permit operation at high A/C ratios. The second term in Eq. 1 accounts for the pressure drop contribution from the permanent residual dust cake that exists on the surface of the fabric. For operation at high A/C ratios, the bag cleaning must be sufficient to maintain a very light residual dust cake and ensure that the pressure drop contribution from this term is not unreasonable (e.g., up to 50% of the total).

The third term in Eq. 1 accounts for the pressure drop contribution from the dust accumulated on the bags since the last bag cleaning. The flow resistance of the dust is determined primarily by the fly ash particle-size distribution and the porosity of the dust cake and is modeled with a single term, the specific dust cake resistance coefficient, K_2. Typical K_2 values for pulverized coal (pc)-fired fly ash range from about 0.5 to 2.5 kPa-m-min/kg (3 to 15 in. W.C.-ft-min/lb), but may, in extreme cases, cover a wider range. Of interest is the maximum A/C ratio at which a baghouse can be expected to operate reliably for the range of K_2 values likely to be encountered. All three terms in Eq. 1 may require increased bag-cleaning frequency with increased A/C ratio, but the third term dictates the minimum bag-cleaning interval. From Eq. 1,

with a face velocity of 0.6 m/min (2 ft/min), a dust loading of 6.0 g/m^3 (2.6 gr/acf), and a dP increase of 1.0 kPa (4 in. W.C.), the required bag-cleaning frequency is greater than 100 min when K_2 is less than 4.6 kPa m-min/kg (28 in. W.C.-ft-min/lb). In a reverse-gas utility baghouse, cleaning takes place off-line and may require several minutes per compartment and more than an hour to clean all of the compartments. This is one reason why most reverse-gas baghouses are conservatively designed for a face velocity of 0.6 m/min (2 ft/min). To ensure that adequate cleaning time is available when K_2 is not known demands a conservative approach. On the other hand, if K_2 were known to be less than 1.2 kPa m-min/kg (7 in. W.C.-ft-min/lb), Eq. 1 implies that a face velocity of 1.2 m/min (4 ft/min) could be employed. However, to date, reverse-gas baghouses have not been designed much above face velocities of 0.6 m/min (2 ft/min) because an effective method of controlling K_2 has not existed and excessive residual dust cake weight is frequently encountered.

Pulse-jet baghouses have the potential to operate at much higher face velocities because bags can be cleaned more often and adequate pulse energy can usually prevent excessive residual dust cake buildup. Assuming that bag life is acceptable and that low particulate emissions can be maintained through the use of advanced filter materials, face velocities much greater than 1.2 m/min (4 ft/min) should be possible. Assuming 10 min is the minimum cleaning cycle time for a pulse-jet baghouse, a face velocity of 1.2 m/min (4 ft/min) is adequate to handle a dust with a K_2 greater than 12 kPa m-min/kg (72 in. W.C.-ft-min/lb) (see Figure 2.1-1). If K_2 is less than 2.9 kPa m-min/kg (18 in. W.C.-ft-min/lb), the face velocity can be increased to 2.4 m/min (8 ft/min). For many dusts, this might be possible with conventional systems. Doubling face velocity again to 4.9 m/min (16 ft/min) implies that K_2 would have to be less than 0.7 kPa m-min/kg (4 in. W.C.-ft-min/lb). This is lower than most typical K_2 values; however, through the use of flue gas conditioning, it may be possible. Increasing the face velocity beyond 4.9 m/min (16 ft/min) appears to be stretching the theoretical limit for a full dust loading of 0.6 g/m^3 (3 gr/scf). However, if the actual dust loading that reached the fabric were reduced by a factor of 10, the allowable K_2 would increase by a factor of 10, while keeping the cleaning interval at 10 min. If a process could collect 90% of the dust before it reached the bags, a K_2 of up to

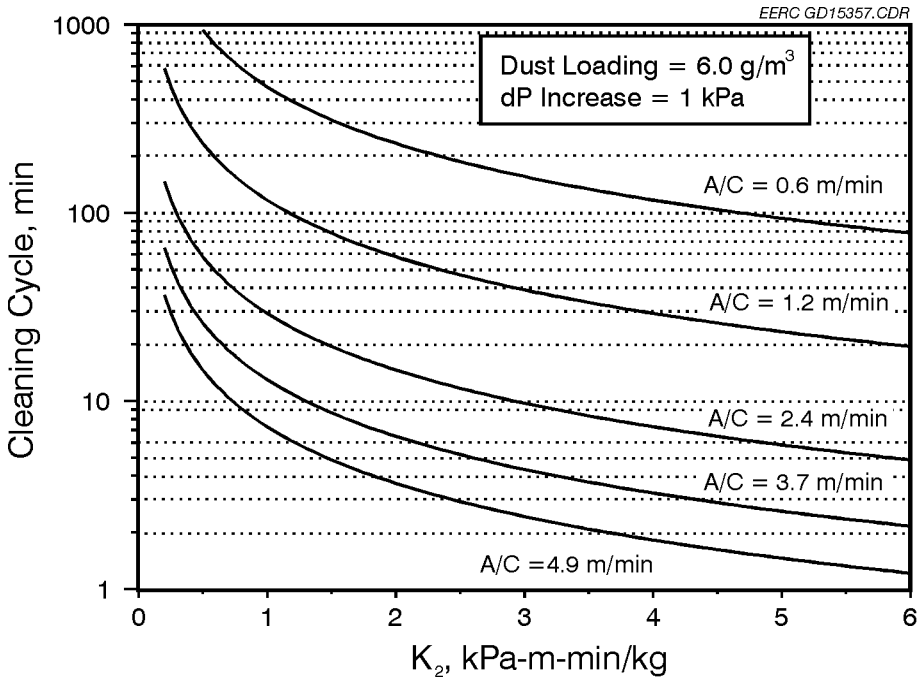

Figure 2.1-1. Cleaning cycle requirements for full dust loading.

6.9 kPa m-min/kg (42 in.W.C.-ft-min/lb) would be allowable at an A/C ratio of 4.9 m/min (16 ft/min) and a 10-min bag-cleaning interval (see Figure 2.1-2). The K_2 for almost all coal fly ash dusts is likely to be less than 6.9 kPa m-min/kg (42 in.W.C.-ft-min/lb), even allowing for some size fractionating between the precollected dust and the dust that reaches the bags. Therefore, a theoretical basis exists to operate a fabric filter at a reduced dust loading and high A/C ratio with a reasonable bag-cleaning frequency.

The preceding analysis is valid as long as the dust can be effectively removed from the bags and transferred to the hopper without significant redispersion and recollection. With pulse-jet cleaning, heavy residual dust cakes are not typically a problem because of the fairly high cleaning energy that can be employed. However, the high cleaning energy can lead to significant redispersion of the dust and subsequent recollection on the bags. The combination of a very high-energy pulse and a very light dust cake tends to make the problem of redispersion much worse. The barrier that limits operation at high A/C ratios is not so much the dislodging of dust from the bags as it is transferring the dislodged dust to the hopper. Therefore, any improvement that

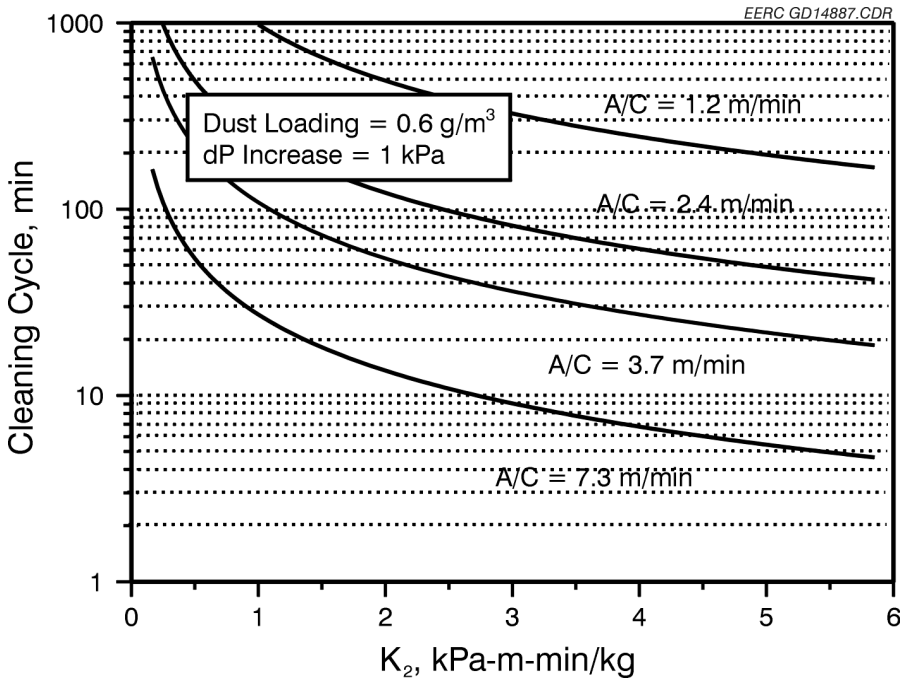

Figure 2.1-2. Cleaning cycle requirements for reduced dust loading.

facilitates transfer of the dislodged dust to the hopper without recollection on the bags will greatly enhance operation at higher A/C ratios. The AHPC achieves enhanced bag cleaning by employing electrostatic effects to precollect a significant portion of the dust and to facilitate moving the dust from the bags to the hopper. A more detailed description of how that is achieved is given the next section.

2.3 AHPC Concept Description

While very large ESPs are required to achieve >99% collection of the fine particles, a small ESP can remove 90% to 95% of the dust. Including rapping puffs, 90% to 95% collection efficiency can be achieved with full-scale precipitators with a SCA of less than 20 m^2 of collection area/m^3/s (100 ft^2 of collection area/1000 acfm) (8). In the AHPC concept, the goal is to employ only enough ESP plate area to remove approximately 90% of the dust. Similarly, the cloth area should be held to a minimum to keep the cost reasonable. If the fabric is operated at an A/C ratio of 3.7 m/min (12 ft/min) and the SCA of the ESP is 17 m^2/m^3/s (83 ft^2/1000 acfm) the

filtration collection area will be the same as the plate collection area. A SCA of 17 $m^2/m^3/s$ (83 ft^2/1000 acfm) should be sufficient to easily remove at least 90% of the dust. (Note that an alternative definition of SCA is simply the inverse of A/C ratio multiplied by 1000.) A baghouse operating at an A/C ratio of 0.6 m/min (2 ft/min) has the same collection area as an ESP with a SCA of 100 $m^2/m^3/s$ (500 ft^2/1000 acfm). Both of these are typical of the size of collectors employed for new power plants. Therefore, an AHPC operating at an A/C ratio of 3.7 m/min (12 ft/min) and a SCA of 17 $m^2/m^3/s$ (83 ft^2/1000 acfm) would offer an 83% reduction in fabric area over a conventional baghouse operating at 0.6 m/min (2 ft/min) and an 83% reduction in plate area over a conventional ESP with a SCA of 100 $m^2/m^3/s$ (500 ft^2/1000 acfm). The combined collection area in the AHPC would be 67% lower than either the conventional baghouse or the ESP. These key aspects of the AHPC are shown in Figure 2.3-1.

The electrostatic and filtration zones are oriented differently from any previous approaches and they also function in a manner superior to previous methods. The geometric configuration of the AHPC concept can be understood by comparing the configuration with a conventional pulse-jet baghouse. In a typical pulse-jet baghouse, the individual bags or filtration tubes are

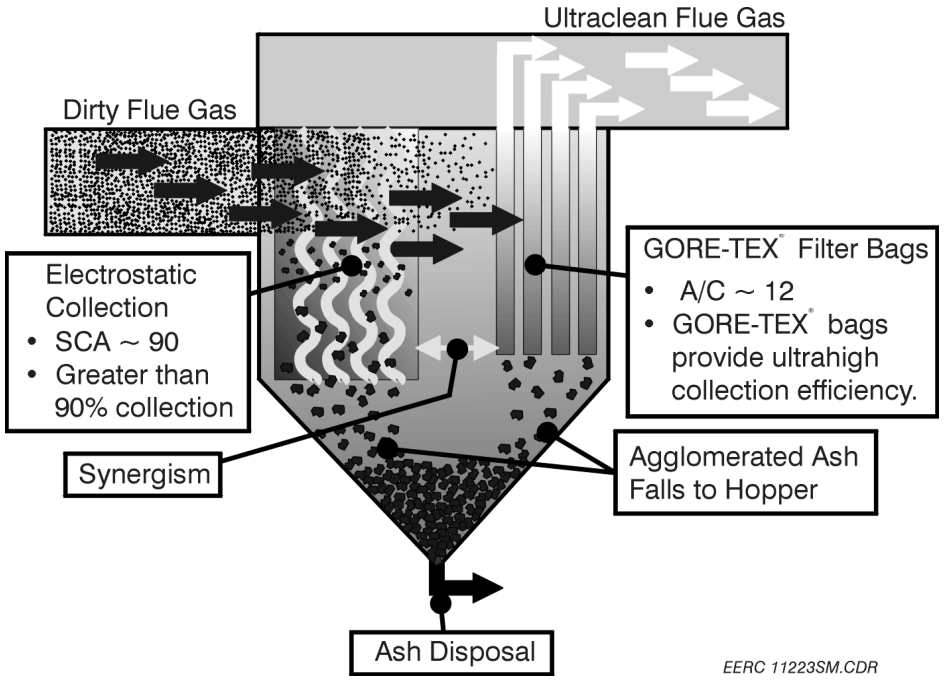

Figure 2.3-1. Key features of the AHPC.

0.10–0.15 m (4–6 in.) in diameter, 2.4–6.0 m (8–20 ft) long, and mounted in and suspended from a tube sheet. The dust is collected on the outside of the bags while the flue gas passes through the fabric to the inside, then exits through the top of the bags into the clean air plenum and subsequently out the stack. Cages are installed inside the bags to prevent them from collapsing during normal filtration. Air nozzles are installed above each bag to clean the bags with a quick burst of high-pressure air directed inside the bags. The burst of air, or cleaning pulse, causes a rapid expansion of the bag and momentarily reverses the direction of gas through the bag, which both help to clean the dust off the bags. Typically, pulse-jet bags are oriented in a rectangular array spaced only a few inches apart. The bags are usually pulse-cleaned one row at a time in sequence, with approximately 15 bags per row. Because of the narrow bag spacing and forward filtration through the two adjacent rows, much of the dust that is removed from one row of bags is simply recollected on the adjacent bags. Only very large agglomerates of dust reach the hopper after pulsing. The phenomenon of redispersion and recollection of dust after bag-cleaning is one of the major obstacles to operation of baghouses at higher filtration velocity (also called A/C ratio).

To understand the AHPC concept, consider the configuration if approximately three out of every four rows of bags are removed from a conventional pulse-jet baghouse and a grounded plate is placed between adjacent remaining rows of bags. High-voltage corona discharge electrodes (wires or rigid frame) are installed between each plate and row of bags. The spacing from the wires to the plates is greater than the spacing from the wires to the bags, which forces any sparking from the wires to the plates rather than to the bags. Conventional discharge electrodes may be employed, but the preferred configuration is to use directional corona electrodes that force the corona to the plate side rather than to the bag side. An optional variation of the configuration to help protect the bags is a row of grounded wires between the high-voltage electrode and the bags; however, this extra row of grounded wires is not necessary, except under severe sparking conditions.

Two different inlet configurations of the AHPC are possible. For the first case, the flue gas can enter the collection chamber either on one or on two opposite sides and the flow is directed

into the space between the wires and plates by baffling. Another possible configuration is introducing the flue gas to the collection chamber in the hopper plenum area so that it must pass upward into the channels defined by adjacent grounded plates in order to reach the bags. The side inlet case was tested in Phase I, but the bottom inlet configuration is simpler. The basic function and operation of the AHPC for either configuration is similar.

Operation of the AHPC can be considered a two-step process. In Step 1, the particles are collected on either the grounded plates or the filtration surface, and in Step 2 the dust is transferred to the hopper. In Step 1, dirty gas flow enters the AHPC vessel and is directed into the ESP zone by appropriate baffling. The particles in the ESP zone immediately become charged and migrate toward the grounded plate at a velocity (electrical migration velocity) dependent upon the particle charge and electric field strength. For 10-μm particles, the actual migration velocity is approximately 0.6 m/s (2 ft/s), or 10 times the filtration velocity of 3.7 m/min (12 ft/min or 0.2 ft/s). This rapid movement of dust toward the grounded plate pulls the gas flow with it and, along with electric wind effects from the movement of charged gas molecules toward the plate, produces a "suction action" of the gas flow toward the plate. The gas cannot accumulate at the plate, so there is a resulting recirculation pattern produced by the combination of the forward entrance velocity parallel to the plate and the migration velocity perpendicular to the plate. Since all of the gas flow must eventually pass through the bags, a portion of the recirculation flow is drawn toward the bags. The greater migration velocities of particles moving toward the plates ensures that most of the particles will first be exposed to the ESP zone and will collect on the plates before they have a chance to reach the filter. Under ideal laminar flow conditions, only particles with migration velocities smaller than the gas velocity toward the bags would reach the bags during normal filtration. However, because of some flow maldistribution, recirculation patterns, and the presence of turbulent flow, a small fraction of the dust (less than 10%) reaches the bags during normal collection operation. The particles that do reach the filtration surface will likely retain some charge. Charged particle are more readily collected because there is an additional coulombic force to drive the particles to a grounded or neutral surface. In addition, a dust cake formed from charged particles will be more porous, which produces a lower pressure drop. Ultrahigh fine-particle collection is achieved by removing over

90% of the dust before it reaches the fabric, precharging the particles, and using a GORE-TEX® membrane fabric to collect with a high efficiency the particles that do reach the filtration surface.

In Step 2, the dust that accumulates on the grounded plates and filtration surfaces must be periodically removed and transferred from the bags and plates to the hopper. One row of bags at a time is cleaned with a reverse pulse of pressurized air or gas with sufficient energy to dislodge most of the dust from the bags. A few larger agglomerates may fall directly to the hopper; however, much of the dust is reentrained into particles too small to fall directly to the hopper. While these are small particles, they are agglomerated into larger particles than are originally collected on the bags. In conventional baghouses, these particles would immediately be recollected on the bags. In the AHPC, the unique method of bag cleaning and transfer of dust to the hopper prevents the recollection of dust on the filter surface. The bags are pulsed with sufficient energy and volume to propel the reentrained dust past the high-voltage wires and back into the ESP zone, where they immediately become charged and are trapped on the plates. Since this reentrained cloud is composed of agglomerated particles larger than originally collected on the bags, they are trapped in the ESP zone much more easily than the original fine particles. The alternative rows of bags, wires, and plates act as an "electronic trap" to prevent the reentrained dust from being recollected on the same bags, and the plates prevent the dust from being recollected on adjacent rows of bags. This effect greatly reduces the accumulation of a residual dust cake, and makes control of pressure drop at high A/C ratios much easier. The excess cleaning air passes into the hopper area and is eventually filtered by adjacent rows of bags. Since most of the dust collects on the grounded plates, these plates are rapped periodically and the dust is released from the plates in large agglomerates that easily reach the hopper. A fraction of the dust is reentrained as particles too small to reach the hopper. But these particles are primarily recollected on the plates. Any remaining fine dust that penetrates the ESP zone will be collected at an ultrahigh collection efficiency by the bags. This completely eliminates any spike in emissions due to a rapping puff and makes redundant downstream fields completely unnecessary, compared to conventional ESPs that require multiple fields to minimize rapping reentrainment. In the AHPC, there is major synergism between the ESP and filtration modes, each improving the operation of the other. The filter will collect the excess ESP emissions during normal

operation and during rapping, and the ESP will collect the reentrained dust from the bags upon cleaning, which will greatly enhance the ability to control pressure drop and operate at high A/C ratios. The AHPC is also superior to ESPs because it completely eliminates the problem of sneakage in conventional ESPs, because in the AHPC all of the flow must pass through the bags.

The benefits of this approach are that the AHPC:

- Solves the problem of excessive fine-particle emissions with conventional ESPs and eliminates the problem of sneakage.

- Greatly reduces the problem of higher emissions from conventional baghouses when the A/C ratio is increased.

- Solves the problem of reentrainment and recollection of dust in conventional pulse-jet baghouses caused by the close bag spacing and the effect of cleaning one row of bags at a time.

- Breaks down the barriers that prevent operation of fabric filters at high A/C ratios.

- Requires significantly less total collection area than conventional ESPs or baghouses.

- Solves the bag problem of chemical attack that limits application of baghouses to low-sulfur coals.

- Reduces the applicability problem for ESPs with high-resistivity dusts.

- Improves the potential for mercury capture with sorbents in ESPs.

- Is suitable for new installations or as a retrofit replacement technology for existing particulate collectors as well as an add-on retrofit technology.

3.0 SCOPE OF WORK

The project was organized into three tasks:

Task 1 – Project Management, Reporting, and Subcontract Consulting

Task 2 – Applied Modeling, Design, and Construction of 5.7-m^3/min (200-acfm) AHPC Model

Task 3 – Experimental Testing and Subcontract Consulting

3.1 Task 1 – Project Management, Reporting, and Subcontract Consulting

The purpose of Task 1 was to separate the project management aspects of the project from the design and experimental work. Hence this task included all project management activities such as planning, coordination, communication, travel, and reporting. Project organization is illustrated in Figure 3.1-1. ALENTEC served as a consultant to the EERC for Phase I and provided the following:

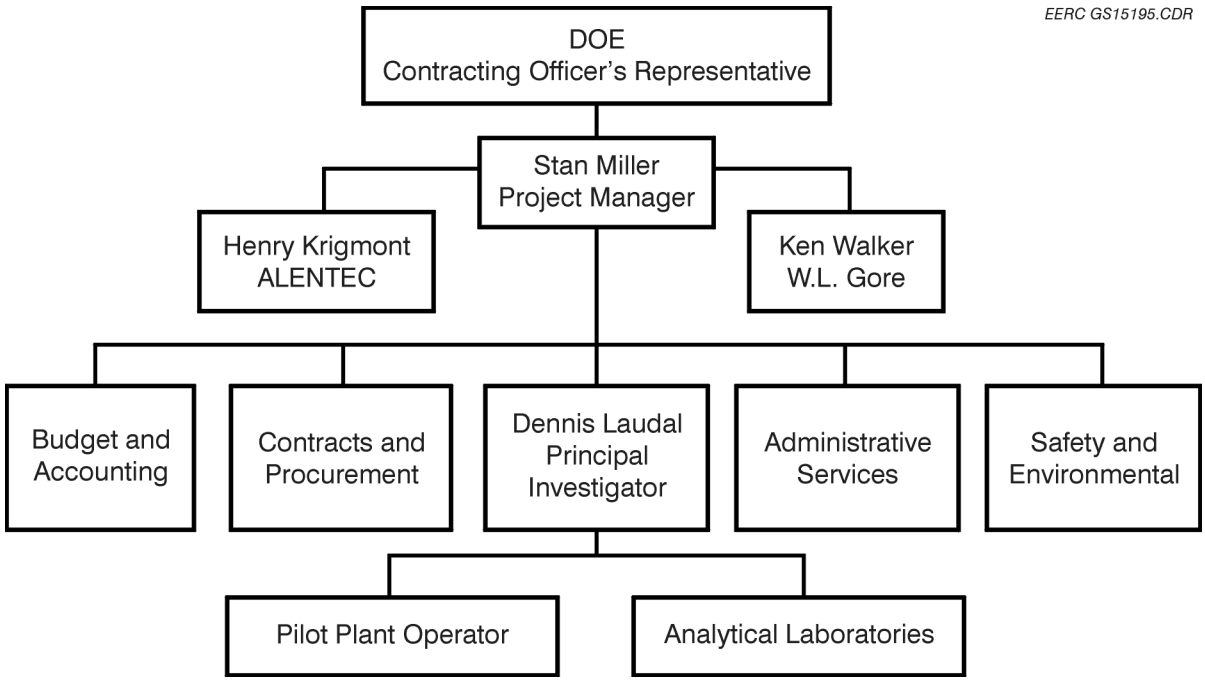

Figure 3.1.1. Project organization chart.

- Review of the AHPC design and recommendations for improvements to the 5.7-m^3/min (200-acfm) working model

- Review of the planned tests and recommendations for refinements to the experimental approach

- Review and interpretation of results

- Recommendations for scaleup of the device

- Specific theoretical ESP and fluid dynamic modeling

In addition to providing significant cost share for the work, W. L. Gore and Associates provided all of the test bags and cages. Mr. Ken Walker at W.L. Gore also reviewed the test plans and results and provided technical advice for the entire Phase I effort.

3.2 Task 2 – Applied Modeling, Design, and Construction

The primary purpose of Task 2 was to design, construct, and install a working AHPC model on the existing EERC particulate test combustor (PTC). The design effort included some flow modeling to help scale the AHPC to the appropriate dimensions. Details of the design are given in Section 4.1.

3.3 Task 3 – Experimental Testing

The experimental work for Phase I was divided into three subtasks, intended to follow a logical sequence from initial shakedown of the AHPC model through 100-hr proof-of-concept tests.

3.3.1 Subtask 3.1 – Cold-Flow Shakedown Testing

The primary purpose of the cold-flow testing with air was to properly adjust the pulse-cleaning parameters and flow baffling to achieve the best interaction between the ESP and filtration zones. Reentrained dust (fly ash) was injected into the carrier air upstream of the AHPC operating at an A/C ratio of 3.7 m/min (12 ft/min). Tests were conducted with the electric field on and off to document the benefit of the ESP section for bag cleaning. Independent variables included pulse pressure, pulse volume or duration, applied voltage, baffling, and bag type. The primary dependent variables were pressure drop before and after cleaning, time between cleaning cycles, and a visual evaluation of the cleaning dynamics. Since the reentrained dust in the carrier had a lower submicron particle concentration than real flue gas, extensive outlet particulate measurements were deferred until the tests with real flue gas. The duration for each test varied from less than 1 hr for initial adjustment of settings to 7 hr for multiple cleaning cycle tests. Cold-flow test results are given in Section 4.2

Following the cold-flow tests, the data were reviewed by DOE, ALENTEC, W.L. Gore & Associates, and the EERC. Figure 3.3-1 illustrates the decision logic.

3.3.2 Subtask 3.2 – 8-hr Verification Tests on Coal

A total of seventeen 8-hr tests were completed with two different coals. The original plan was to complete ten 8-hr tests, but additional tests were conducted to evaluate on-line and off-line cleaning, electrode type, and the baffle configuration. Other main variables included coal type, A/C ratio, and flue gas conditioning. The coals included Blacksville, an eastern bituminous Pittsburgh No. 8 seam coal, and Absaloka, a Powder River Basin western subbituminous coal. Originally A/C ratios of 3.7, 4.9, 7.3 m/min (12, 16, and 24 ft/min) were proposed, but, since results at 4.9 m/min (16 ft/min) indicated modification would be required to optimize performance at higher A/C ratios, no 7.3-m/min (24-ft/min) tests were conducted. For the flue gas conditioning tests, a combination of SO_3 and NH_3 was chosen as the conditioning agent, because SO_3 and NH_3 are known to enhance both ESP and fabric filter performance.

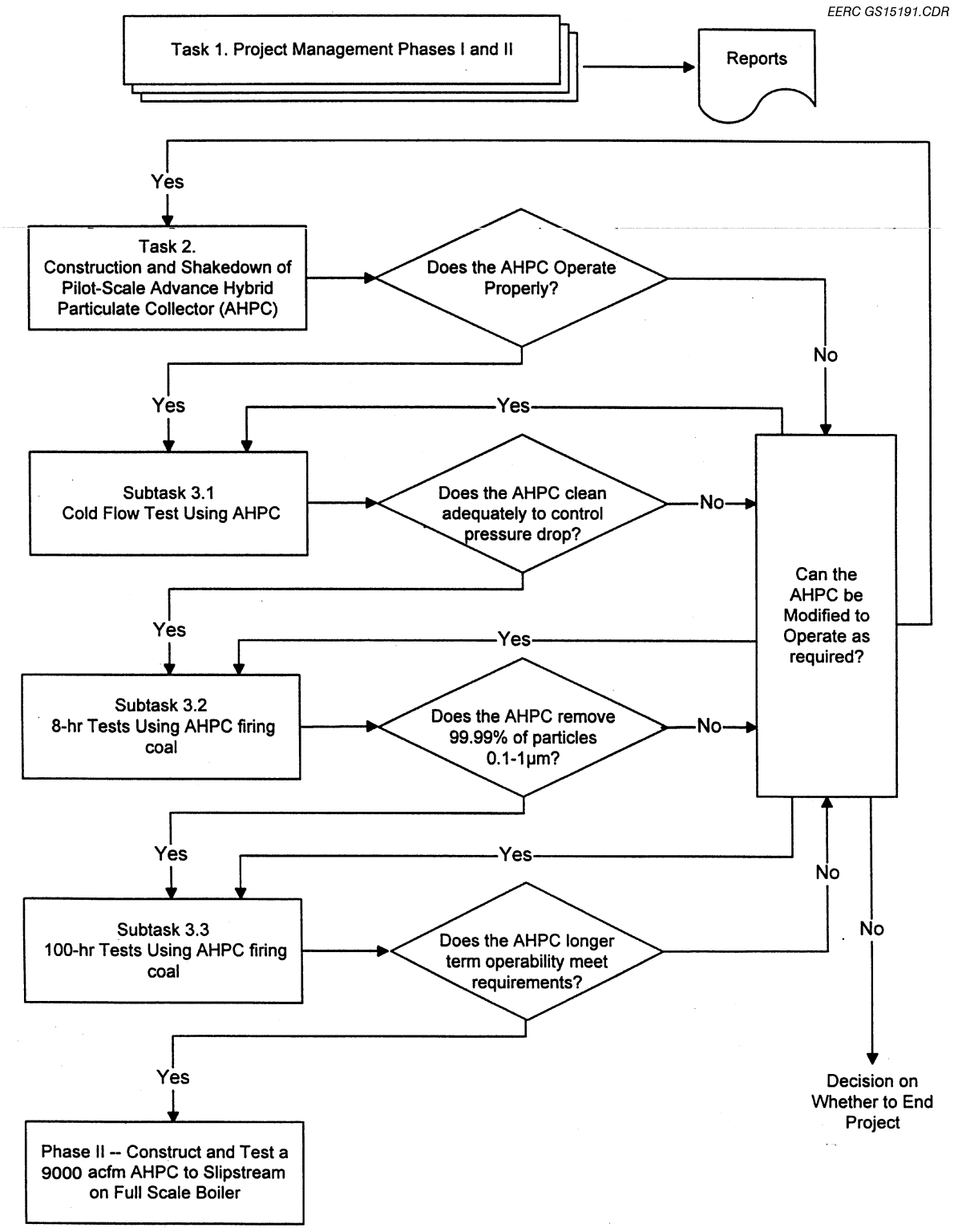

Figure 3.3-1. Project logic and decision points.

Tests were conducted at an AHPC temperature of 149°C (300°F), since that is a typical air heater outlet temperature in full-scale coal-fired boilers. Each test included inlet and outlet EPA Method 5 dust-loading measurements and continuous outlet particulate measurements with an aerodynamic particle sizer (APS) and scanning mobility particle sizer–condensation particle counter (SMPS–CPC). Results from the 8-hr tests are presented in Section 4.3. At the end of the 8-hr tests on coal, results were again evaluated by the project team. Since the main objectives for the 8-hr tests were met, the decision was made to proceed with the 100-hr tests.

3.3.3 Subtask 3.3 – 100-hr Proof-of-Concept Tests

A total of six 100-hr tests were originally planned. Since many more 8-hr tests were conducted, only three 100-hr tests were completed. The main variables evaluated included coal type, sorbent injection for mercury control, and flue gas conditioning. A/C ratio was originally planned as a variable, but, based on the 8-hr test results, the decision was made to run all of the 100-hr tests at 3.7 m/min (12 ft/min). Extensive inlet and outlet particulate measurements were completed to thoroughly document the performance of the AHPC as a function of time. Two of the tests each included four inlet and four outlet EPA Method 29 trace element measurements to evaluate the collection efficiency of arsenic, cadmium, chromium, lead, mercury, nickel, and selenium. One test served as a baseline, and the second test included the injection of a sorbent upstream of the AHPC for mercury control. Results from the 100-hr tests are given in Section 4.4.

4.0 RESULTS AND DISCUSSION

4.1 Construction of the 5.7-m^3/min (200-acfm) Working Model

4.1.1 Flow Modeling of the 5.7-m^3/min (200-acfm) AHPC

Flow modeling was completed by Alex Potapov and Henry Krigmont of ALENTEC. The initial modeling results indicated possible problems with flow turbulence behind the baffle so that some of the gas would go directly to the bags without first entering the ESP zone. However, this was based on an earlier baffle design with a greater spacing. ALENTEC completed additional flow modeling with the exact configuration shown in Figure 4.1-4. Based on this modeling, there was not a problem of flow bypassing the electrical zone or any other serious flow distribution problems. Further details on the modeling effort are given in Appendix A.

4.1.2 Construction and Description of AHPC

The 5.7-m^3/min (200-acfm) size test unit was selected because that is the amount of flue gas produced by the EERC coal-fired PTC. The filtration area of the 5.7-m^3/min (200-acfm) model consisted of a single row of four 12.7-cm (5-in.)-diameter by 96.5-cm (38-in.)-long bags. This configuration allowed the most important dimensions—the wire-to-plate spacing, wire-to-bag spacing, and bag diameter—to be similar to that of a full-scale unit and allowed operation at 3.7 m/min (12 ft/min) with all four bags or 4.9 m/min (16 ft/min) with three bags. Sketches of the front and side view of the original 5.7-m^3/min (200-acfm) AHPC are shown in Figures 4.1-1 and 4.1-2. The AHPC was integrated with a pilot furnace known as the PTC. The PTC is a 160-kW (550,000-Btu/hr) pc-fired unit designed to generate fly ash representative of that produced in a full-scale utility boiler. A schematic of the PTC with the AHPC is illustrated in Figure 4.1-3. Flue gas was extracted from three points in the combustion system: the furnace exit, baghouse inlet, and baghouse outlet. The flue gas was analyzed for O_2, CO_2, SO_2, NO_x, and CO. With the exception of CO_2 and CO, each component in the flue gas was monitored simultaneously at both the exit of the furnace and the outlet of the AHPC.

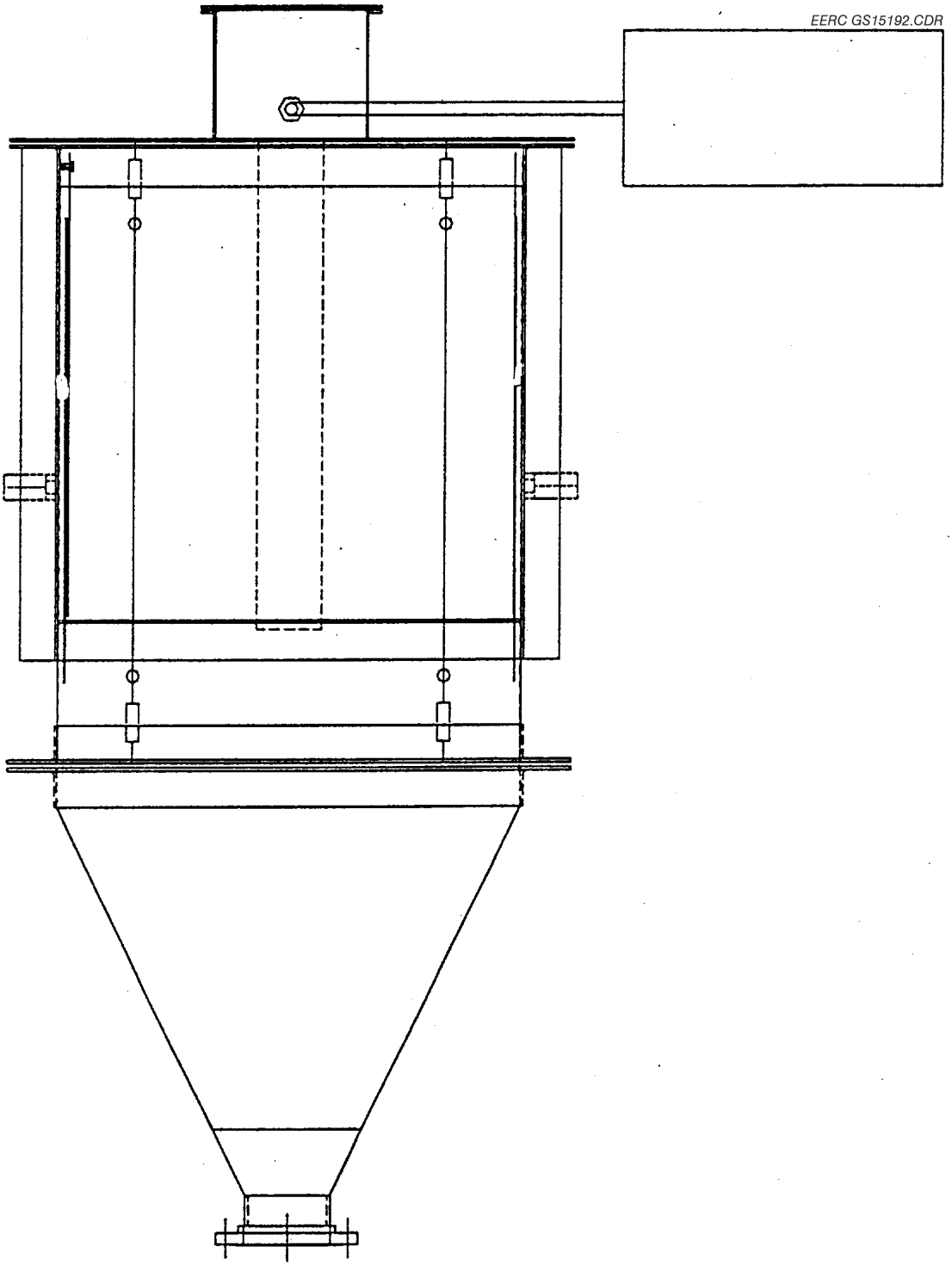

Figure 4.1-1. Original AHPC, front view.

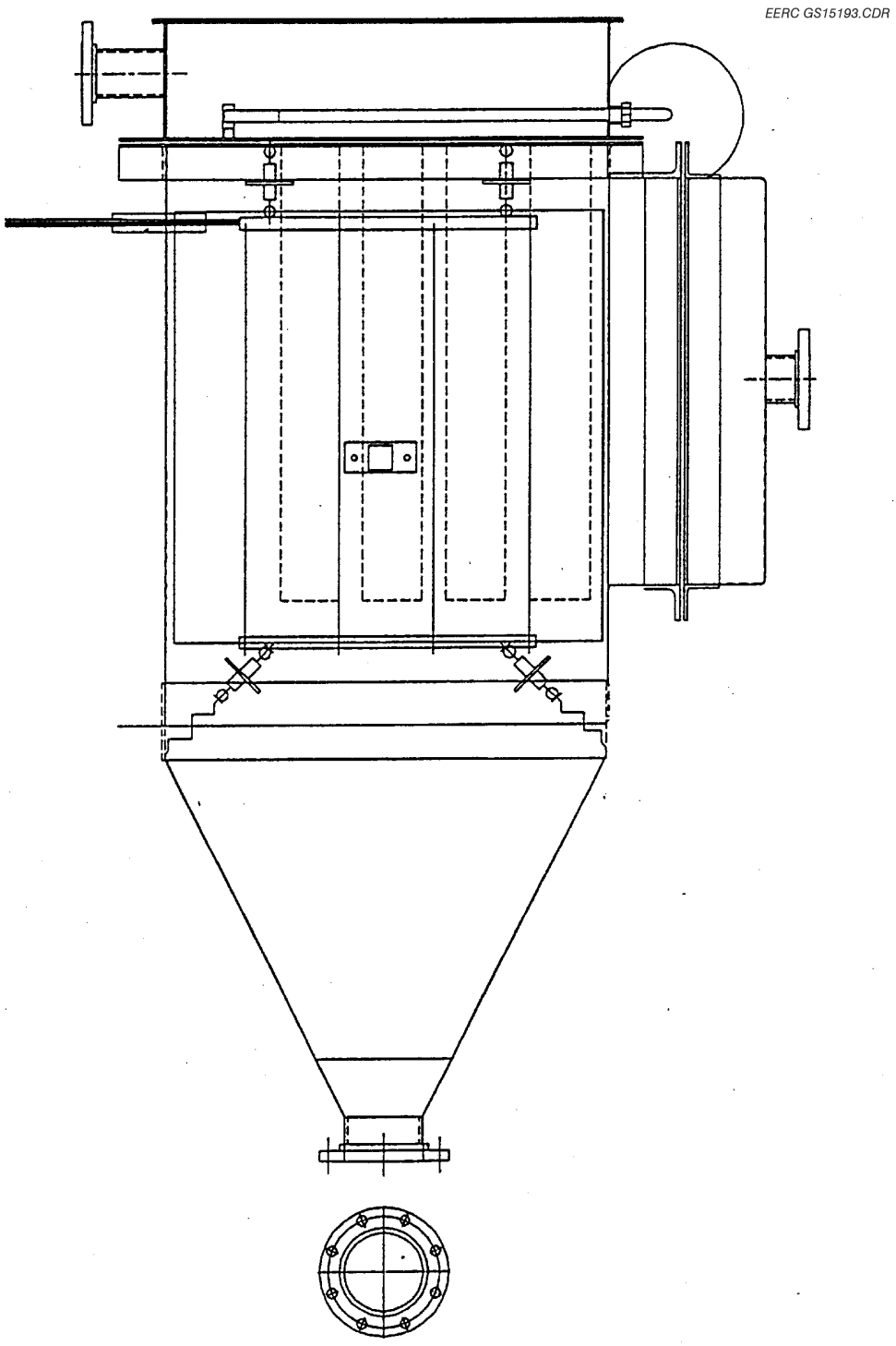

Figure 4.1-2. Original AHPC, side view.

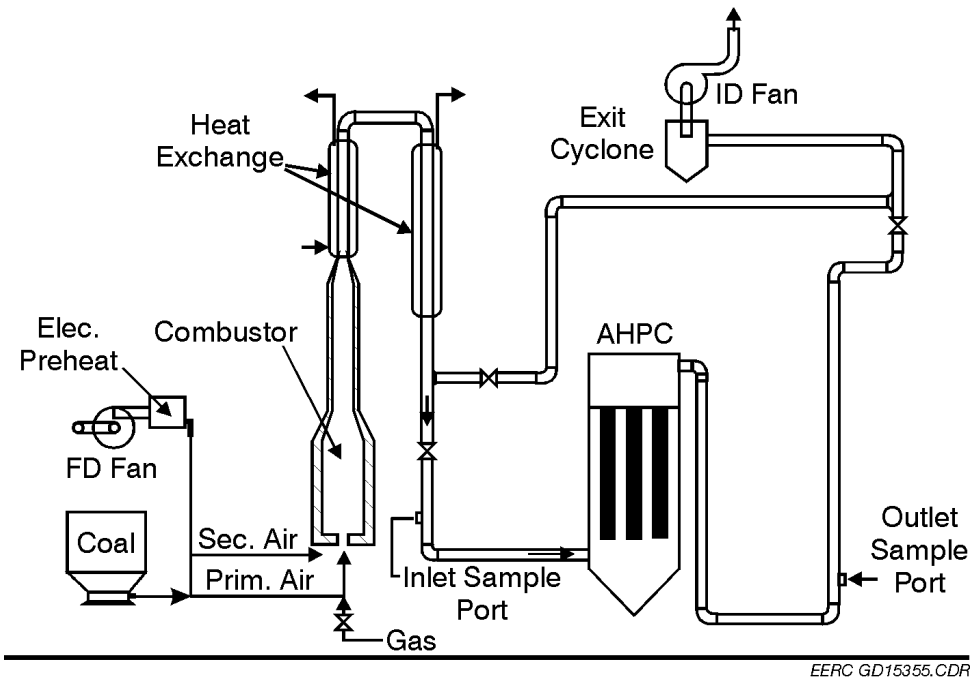

Figure 4.1-3. Sketch of the PTC with the AHPC.

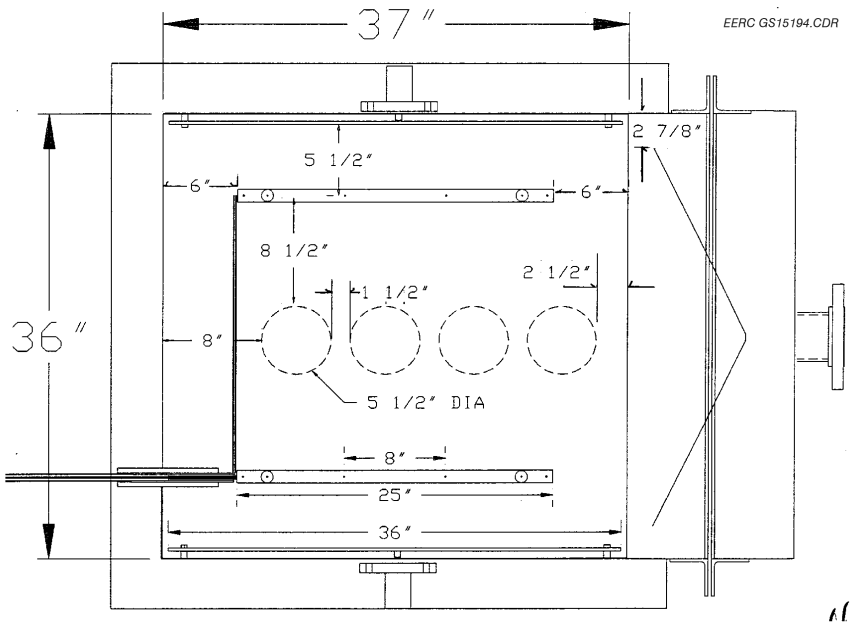

Figure 4.1-4. Top-view drawing of the AHPC showing
the arrangement and dimensions of bags, ESP grid, and V-baffle.

The AHPC was designed to simulate the wire-to-plate and wire-to-bag spacing of a full-size AHPC. Figure 4.1-4 shows these spacing dimensions in a top-view drawing of the 5.7-m^3/min (200-acfm) AHPC. Photographs of the AHPC in Figures 4.1-5 and 4.1-6 give perspective as to scale of the unit.

Changing A/C ratios was easily accomplished by plugging off flow through one bag (for an A/C of 4.9 m/min [16 ft/min]) and two bags (for an A/C ratio of 7.3 m/min [24 ft/min]). Figure 4.1-7 shows the arrangement of bags in the outlet plenum. This photograph shows how flow through one of the bags was stopped by the placement of a plug over the bag exit. The design of the outlet plenum covered only the central portion of the tube sheet, which included the mounting holes for one row of bags. This configuration allowed adequate space to install the bags, pulse blowpipe, and outlet flange and made available space on both sides of the plenum for sight ports.

Figure 4.1-5 is a front view of the AHPC showing the inlet pipe entering the center of the inlet plenum. To the upper right is the pulse pressure tank and pulse tube entering the side of the outlet plenum. Modifications to the pulsing assembly will be discussed later. In Figure 4.1-8, the inlet piping and inlet plenum cover have been removed, revealing the initial baffle configuration. The openings at each side are 5.0 cm (2 in.) wide and are intended to direct the flow between the wires and grounded plates. Figure 4.1-9 views of the inside of the vessel with the baffle and bags removed and reveals the high-voltage electrodes, grounded plates, and view ports at the top. A large sight port was installed at the lower left corner of the far wall of the vessel. Figure 4.1-10 was taken from the deck level of the AHPC and shows the bag and cage installation process. The bags have built-in snap bands that simply snap into the tube sheet openings for mounting. Also shown are three 12.7- by 12.7-cm (5- by 5-in.) sight ports on each side of the outlet plenum located on top of the vessel. These multiple sight ports greatly facilitated evaluation of the flow dynamics and interaction between the ESP and baghouse zones during filtration, bag cleaning, and plate rapping.

EERC GS15196.CDR

Figure 4.1-5. Front view of the AHPC.

Figure 4.1-6. Outlet plenum during bag installation
(notice the sight ports in the lower left of this picture).

Figure 4.1-7. The pulse-jet bag-cleaning assembly modified to increase air volume released during a bag-cleaning cycle.

The photograph shown in Figure 4.1-11, taken through one of the top sight ports, shows the main electrical connection to the high-voltage electrode and the crossover wire to the other electrode. The multiple sight ports allowed a complete view of both electrodes so that the corona characteristics could be evaluated and, if any sparking should occur, the exact location of sparking identified. Figure 4.1-12 is a closeup view of one of the electrical insulators used to suspend the high-voltage electrodes. A high-density machinable ceramic material was chosen for the insulators based on previous experience at the EERC with a pilot-scale ESP.

The insulator stock was purchased from TPI Technical Products, Inc., under the trade name of Malcor® and is a machinable glass ceramic of ultrapure aluminum oxide. Dielectric strength of the material is 3000 volts per mm at 25°C under DC voltage conditions. The insulator is a cylinder 12.7 cm (5 in.) long and 2.5 cm (1 in.) in diameter. The machinability of the Malcor® made it ideal for this application. Sections of 0.6-cm (¼-in.) threaded round stock were modified

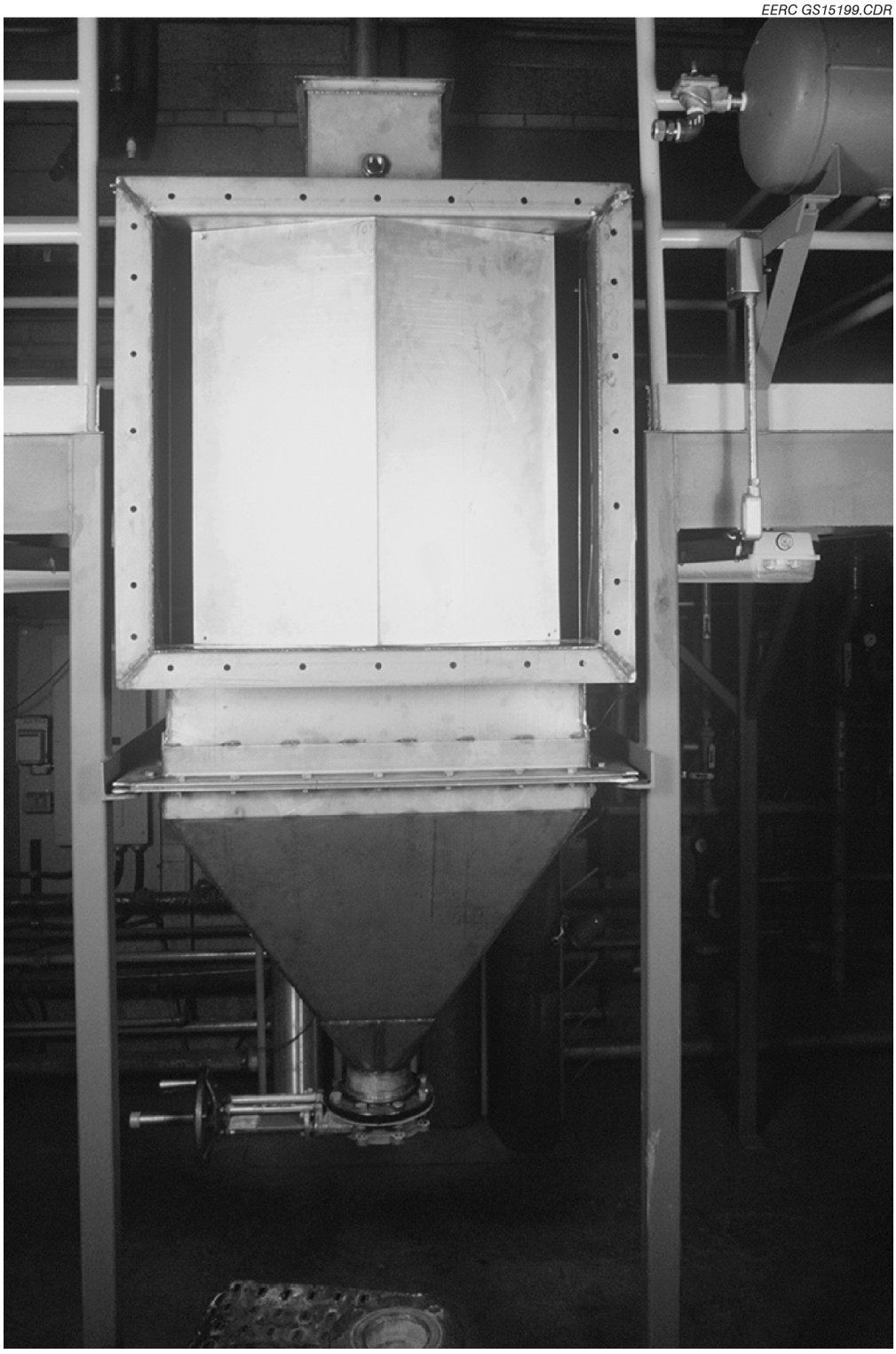

Figure 4.1-8. Front of the AHPC with the V-baffle installed.

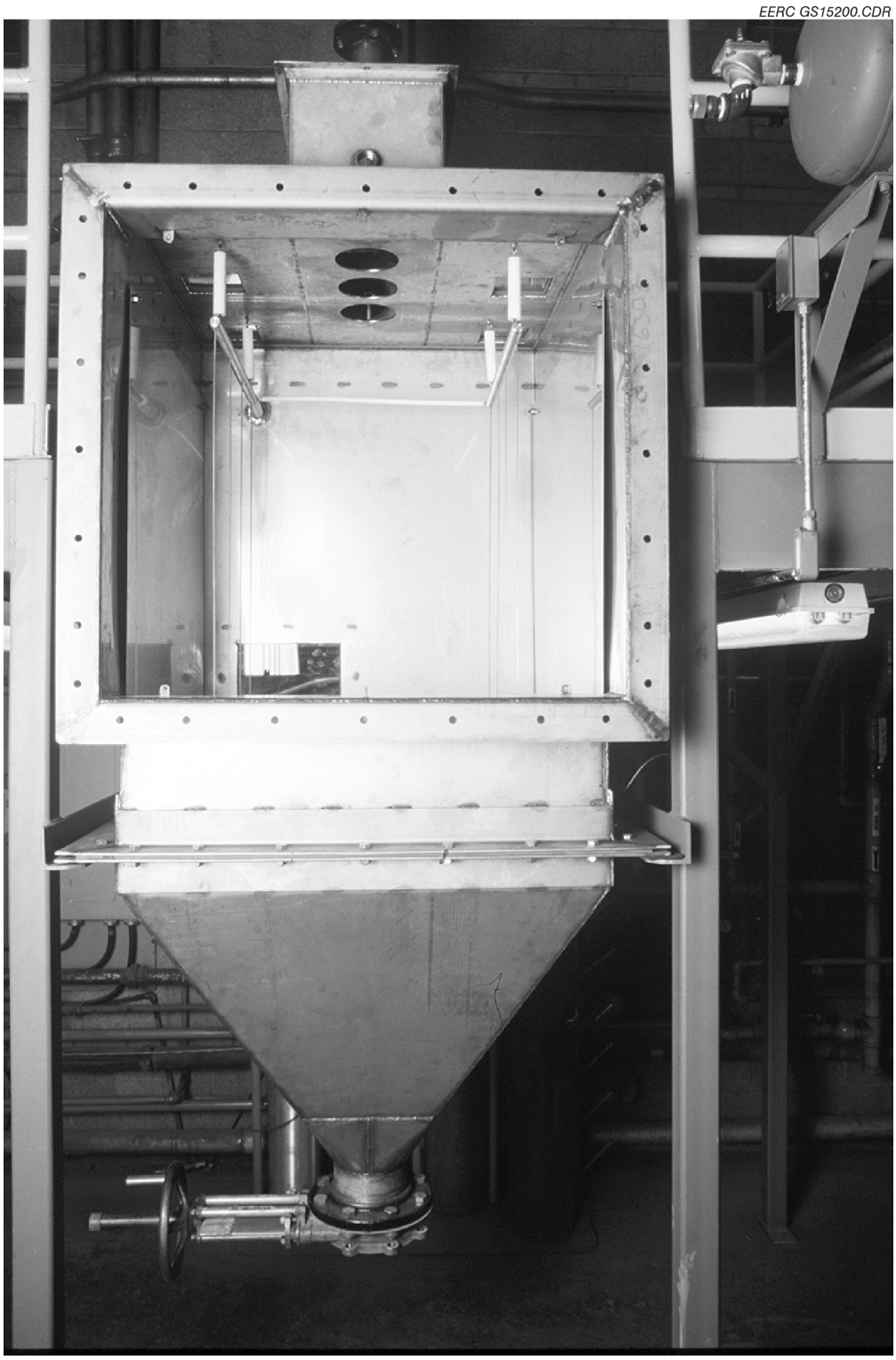

Figure 4.1-9. Front view showing interior of the AHPC without bags.

Figure 4.1-10. Outlet plenum during bag cage installation.

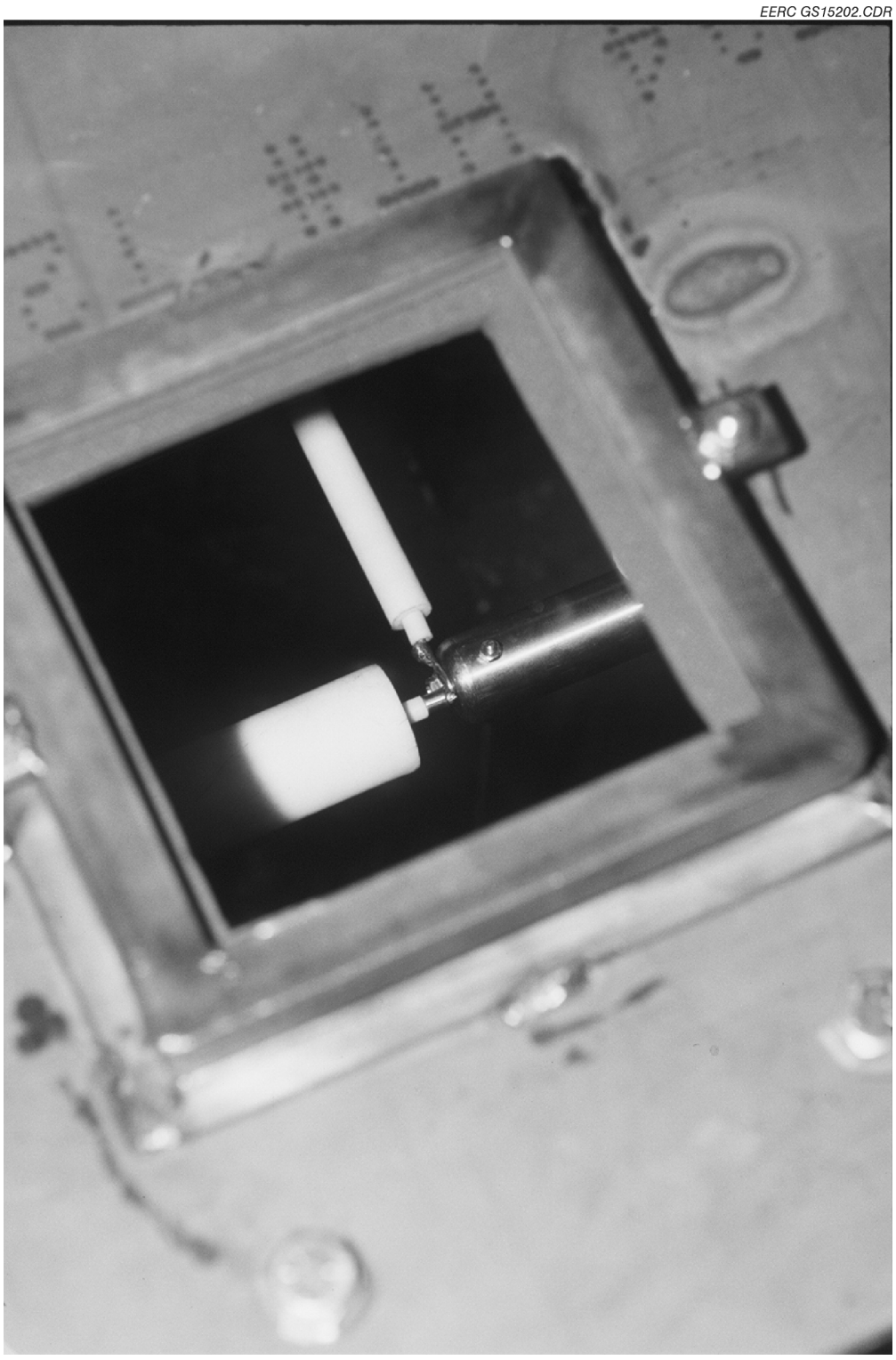

Figure 4.1-11. High-voltage power coupling bolted to the ESP grid.

Figure 4.1-12. One of the machinable ceramic insulators supporting the ESP grid.

and screwed into both ends of the insulator to provide a means of support and electrical isolation for the ESP grid.

The AHPC was preheated by electrical resistance heaters installed on the outside surfaces of the AHPC, inlet piping, and outlet piping. The heaters were covered by 2.5-cm (1-in.)-thick ceramic fiber insulation followed by 7.6 cm (3 in.) of fiberglass insulation. Stainless steel sheeting covered the insulated portions of the AHPC. The preheat system heated the AHPC to 149°C (300°F) in about 3 hr.

The AHPC panel board is pictured in Figure 4.1-13. At the top of the panel sits the high-voltage power supply provided by Spellman, Inc. A photomagnehelix located in the middle of the panel controls the dP cleaning mode for bag cleaning. For all the tests on the AHPC, the initiation dP was set at 2.0 kPa (8.0 in. W.C.). Once the photomagnehelix senses the dP across the bags greater than 2.0 kPa (8.0 in. W.C.), it initiates the cleaning sequence to timers that control the pulse duration and time between each individual bag pulse. These timers are located below the photomagnehelix. Temperature controllers, which operate the resistance heaters, are located to the side of the photomagnehelix.

4.1.3 Baffle Configurations and Modifications

A time line is presented in Figure 4.1-14 to show the development of the baffle design. The main purpose of the baffle is simply to direct the gas flow into the ESP zone to facilitate collection of most of the dust before it reaches the bags. The primary method of evaluating the effectiveness of the baffle was visual observation of the dust flow patterns. The multiple sight ports greatly enhanced flow visualization and, along with video, provided a good indication of local velocities and dust distribution. After several iterations, visual results indicated that a 5.0-cm (2-in.)-wide opening on each side of a V-shaped baffle was effective at directing the flow between the wires and plates. Figure 4.1-15 shows the position of the V-baffle in the front view of the AHPC. One further baffle modification was to block off the top 15.2 cm (6 in.) of the openings on each side to minimize flow through the space between the top of the electrodes and

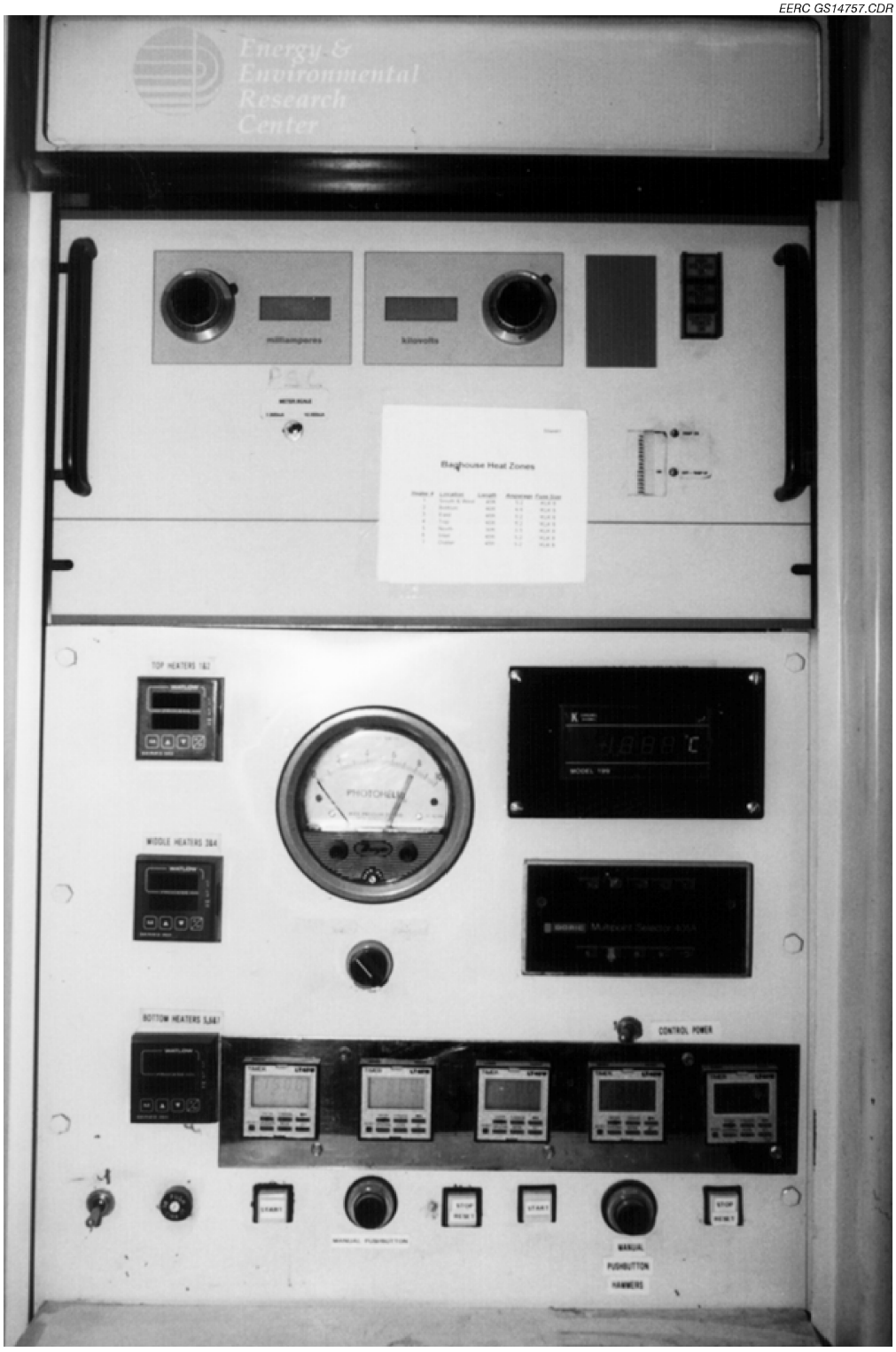

Figure 4.1-13. Panel board used to operate the AHPC.

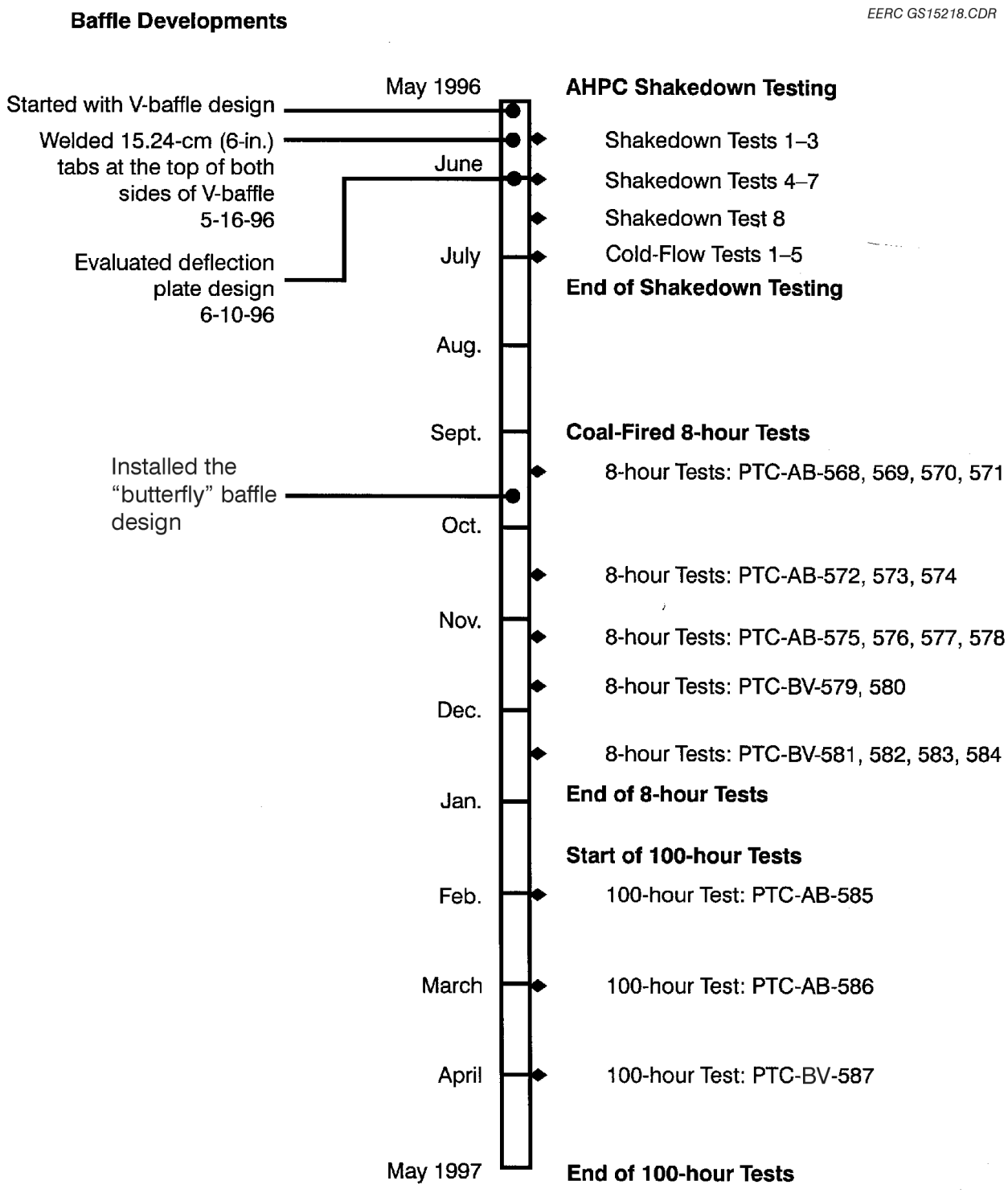

Figure 4.1-14. Time line in the development of the baffle configurations used in the AHPC.

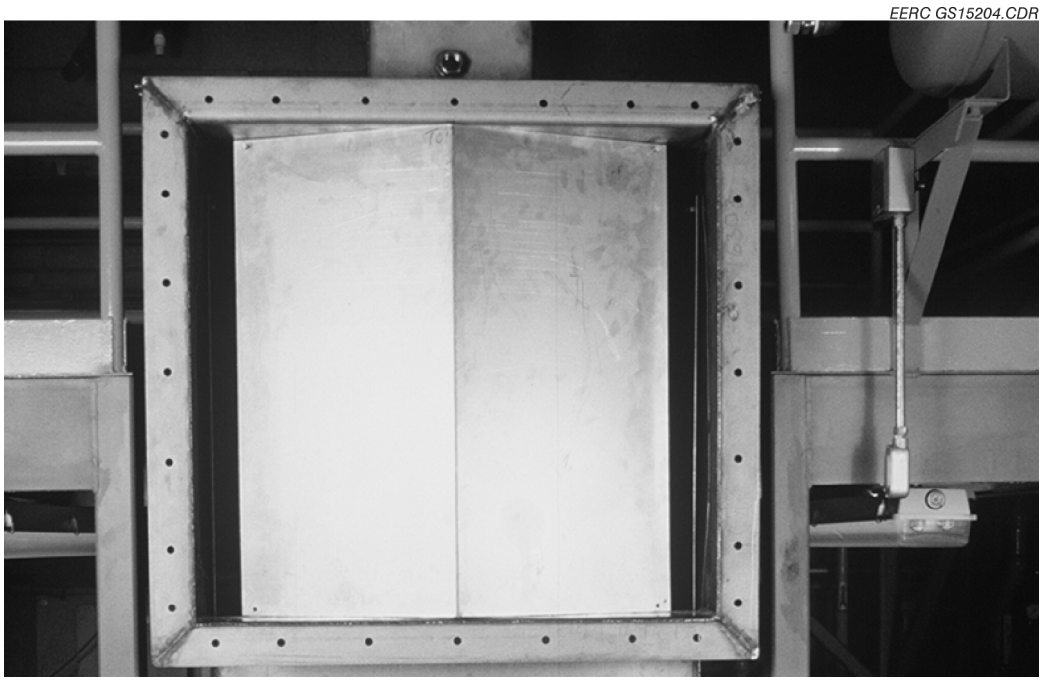

Figure 4.1-15. Front view of the V baffle installed.

top of the main AHPC compartment. This baffle configuration was used throughout the shakedown/cold-flow testing and the first four 8-hr tests firing coal.

An attempt was made to compare this V configuration with a minimum baffle configuration, consisting of a 15.2-cm (6-in.), circular deflection plate placed 12.7 cm (5 in.) in front of the 10.1-cm (4-in.)-diameter inlet. Figure 4.1-16 shows the deflection plate mounted in position on the AHPC. The purpose of the deflection plate was to protect the bags from direct impact of high-velocity, ash-laden gas, but without further flow direction. Essentially, the deflection plate was an attempt at a minimum baffle configuration. Results are presented later in this report.

As a result of that test series, PTC-AB-568 to 571, it was determined that the V-shaped baffle caused about 25% of the ash to drop out in the inlet plenum. To correct the dropout problem, the V-baffle design was replaced by a butterfly-shaped baffle before Test PTC-AB-572. The objective of the design was to reduce the volume of dead space in the inlet plenum.

Figure 4.1-16. Front view of the deflection plate installed.

Figure 4.1-17 shows the rear view of the butterfly baffle. After tests PTC-AB-572 and 573 were conducted, the dust loadings calculated from the AHPC hopper ash collected agreed within 10% of the inlet dust loadings from EPA Method 5 sampling of the inlet flue gas stream. The agreement of inlet dust loadings confirmed the improvement of the butterfly baffle design in reducing the amount of ash dropping out in the inlet plenum. Further inspection of the inlet plenum showed greatly reduced deposits of ash, so this baffle design was used for the remainder of the tests.

4.1.4 ESP Electrode Modifications

Spacing of the ESP electrode between the bags and the ESP plate remained unchanged throughout the AHPC test period. The original ESP grid design was able to operate at the specified voltages with very little arcing. To make the electric field more uniform, additional wires were added. A time line, shown in Figure 4.1-18, illustrates the development of the ESP design. The original ESP electrode design had four 0.3-cm (⅛-in.)-diameter wires, spaced

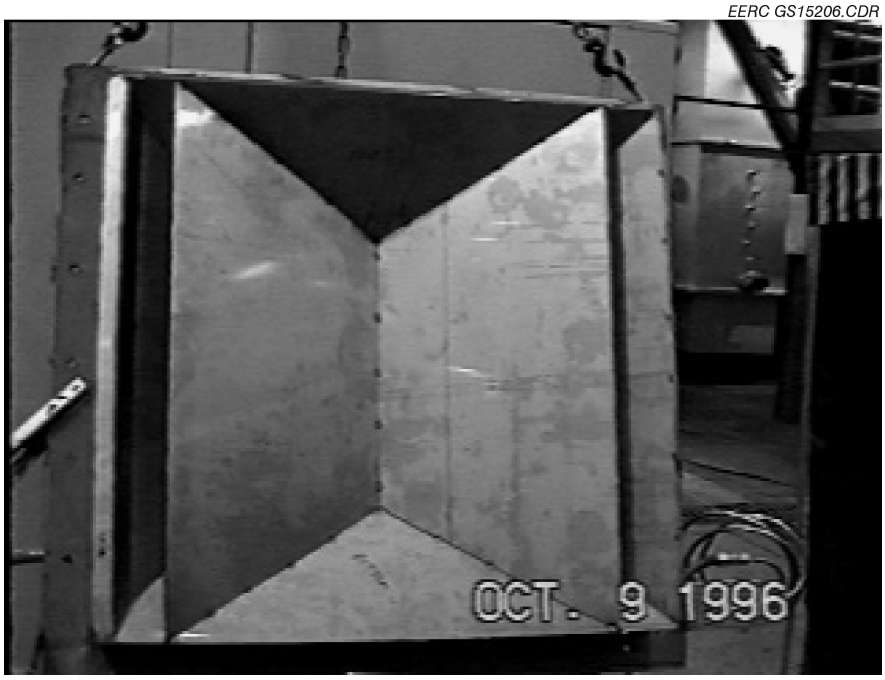

Figure 4.1-17. Rear view of the butterfly baffle under construction.

20.3 cm (8 in.) apart and bolted to 2.5-cm (1-in.)-OD SS cross members at the top and bottom for support (see Figure 4.1-19).

The first modification was made during the early cold-flow experiments in May of 1996. Three more vertical wires were added in between the other four, making a total of seven vertical wires, as shown in Figure 4.1-20. The wire spacing was reduced to 10.1 cm (4 in.).

The last grid modification was done (between Tests PTC-AB-574 and PTC-AB-575) during the last 2 weeks of October 1996. The electrode was switched from smooth wires to a directional comb-type electrode, which consisted of 2.5-cm (1-in.) spikes placed 2.5 cm (1 in.) apart on the plate side of the wires. The purpose of the change was to force the corona to the plate side of the wires and to make the field more uniform. Figure 4.1-21 shows the new grid. Each of the seven wires was sheathed with 0.6-cm (¼-in.) SS tubing. To the 0.6-cm (¼-in.) tubing, 0.2-cm (1/16-in.)-OD SS needles 2.5 cm (1 in.) long were welded at a spacing of 2.5 cm (1 in.). The comblike configuration was installed with the needles perpendicular to the mast and

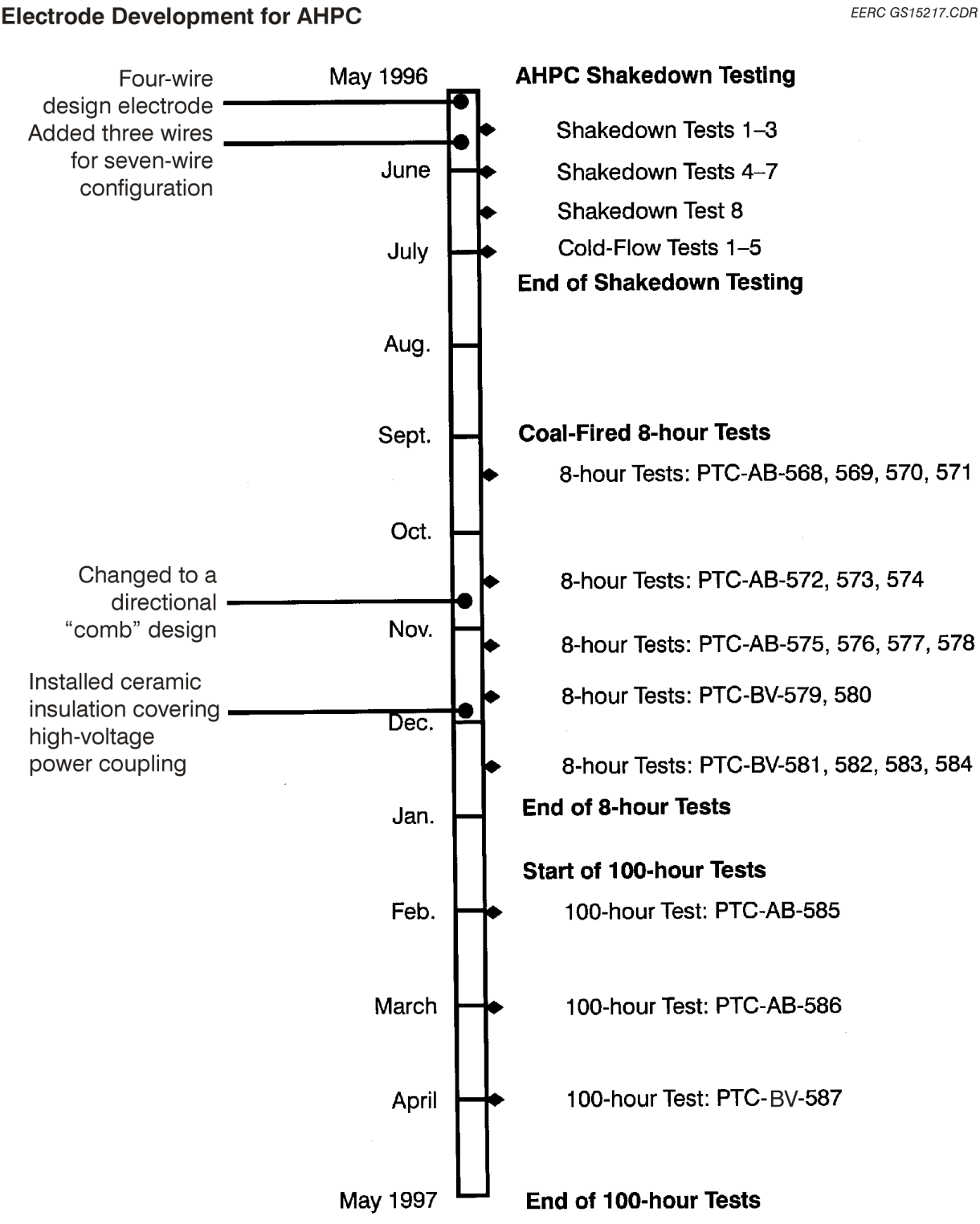

Figure 4.1-18. Time line in the development of the ESP electrode used in the AHPC.

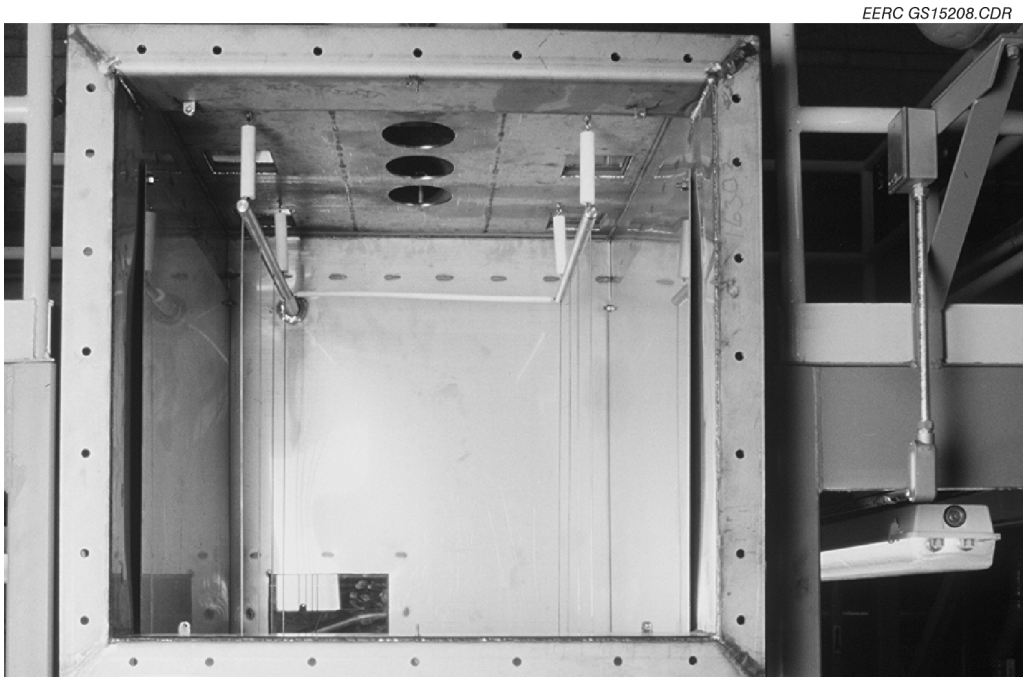

Figure 4.1-19. ESP grid showing the four-vertical-wire design.

Figure 4.1-20. ESP grid showing the seven-vertical-wire design.

Figure 4.1-21. ESP grid showing the comblike design.

pointing directly at the ESP plate. With the installation of the comb grid, the ESP current increased 10 times over the old value. The current went from 0.35 to 3.5 mA at 50 KV when the ESP was operating in flue gas conditions.

During the 8-hr Blacksville bituminous tests, arcing problems caused by the unburned carbon in the ash began to degrade PTFE material in the high-voltage power supply coupling. This coupling is connected by the high-voltage wiring from the outside to the inside of the AHPC (see Figure 4.1-11). To solve the problem, a piece of cylindrical ceramic tubing was placed around the PTFE insulator, protecting it from further harm. Figure 4.1-22 shows the coupling covered with the ceramic tube.

4.1.5 Modifications to Pulse-Jet Cleaning System

Figure 4.1-23 shows the initial pulse-jet cleaning system. One single blow tube of 2.5-cm (1-in.) SS Schedule 40 pipe was used. The centerline of the blow tube was located 6.4 cm

Figure 4.1-22. The ceramic sheath covering the PTFE high-voltage power coupling.

Figure 4.1-23. Initial pulse-jet bag-cleaning assembly design to clean the four bags simultaneously.

(2.5 in.) above the tube sheet. 0.6-cm (¼-in.)-diameter holes were drilled in the blow tube. These holes were placed such that the air pulse would be directed downward into each bag cage venturi. In this configuration, all four bags were pulsed at the same time.

In order to increase pulse air volume while not causing dramatic backpressures in the baghouse, it was decided to pulse each bag individually. A time line showing the changes of the pulse-jet cleaning assembly is found in Figure 4.1-24. A picture of the individual bag-cleaning assembly can be seen in Figure 4.1-25. SS 1.3-cm (½-in.)-OD tubing was used to direct the high-pressure air into each of the bags. In the figure, the tubing is moved to the side in order to remove the bag cages and bags. A solenoid valve was installed on each of the four pulse lines going to the bags. Timers were used to control the pulse duration and to actuate the cleaning sequence. Further modification was done at the end of October 1996 (between Tests PTC-AB-574 and 575). The purpose of this modification was to allow more flexibility over pulse pressure and volume control.

To further increase the volume of air released during each pulse, the 1.3-cm (½-in.) tubing was replaced by 2.5-cm (1-in.) SS Schedule 40 pipe. Nozzles were constructed by welding SS 0.3-cm (⅛-in.)-thick disks to the end of 12.7-cm (5-in.) pipe nipples. A 1.3-cm (½-in.)-diameter hole was drilled into each disk. The modified pipe nipples were installed pointing down into each bag cage venturi and 1.3 cm (½ in.) above the tube sheet. Figure 4.1-7 shows the 2.5-cm (1-in.) Schedule 40 SS pipe modifications to the pulse-jet cleaning system. Before the start of the 100-hr tests, the nozzles on the bag-cleaning assembly were shortened so the nozzles were 5.0 cm (2 in.) above the top of the cages.

4.1.6 Modification to ESP Plate-Rapping Assembly

Minor modifications were also made to the ESP rapping system. The original rapping of the plates occurred with the force of the rapper line perpendicular to the ESP plate surface. The new rapping configuration, shown in Figure 4.1-26, places the rapping force parallel to the ESP

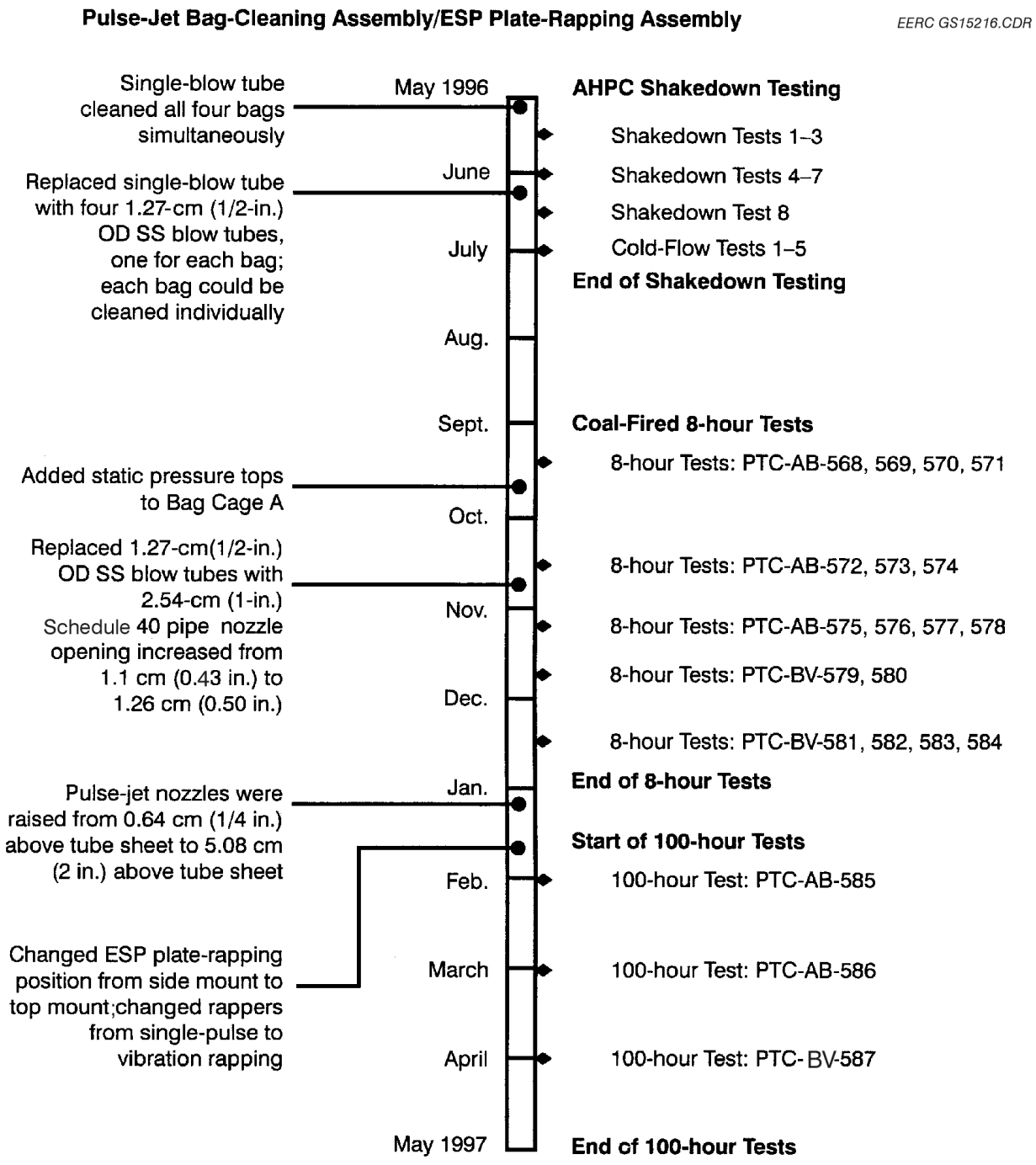

Figure 4.1-24. Time line for the development of the pulse-jet bag-cleaning assembly and ESP plate-rapping assembly.

Figure 4.1-25. Pulse-jet bag-cleaning assembly modified to pulse each bag one at a time.

Figure 4.1-26. New rapper modification places the rapping force parallel to the surface of the ESP plate.

plate surface. The single-impulse rappers were replaced with vibrating rappers. The time line for this modification is shown in Figure 4.1-24.

4.1.7 Modification to Bag Cage with Static Pressure Taps

In an attempt to determine the amount of reverse airflow back through the bags as well as the distribution of that flow, a bag cage with a venturi was fitted with six static pressure taps. Figure 4.1-24 shows the time line for the installation of this modification. These taps were made of 0.6-cm (¼-in.) SS tubing and welded to the inside of the bag cage. Figure 4.1-27 shows the tubing and orientation of the pressure tap welded to the cage. Two of the six taps were placed at the top of the cage even with the venturi bottom. Spacing between all pairs of pressure taps was 90°. Two more taps were secured in the middle of the bag cage and two at the bottom of the bag cage. The pressure taps were connected to pressure gages by flexible tubing. Figure 4.1-28 shows the pressure lines secured to the pressure taps from the top bag cage.

Figure 4.1-27. Location and orientation of the pressure taps welded to the inside member of the bag cage.

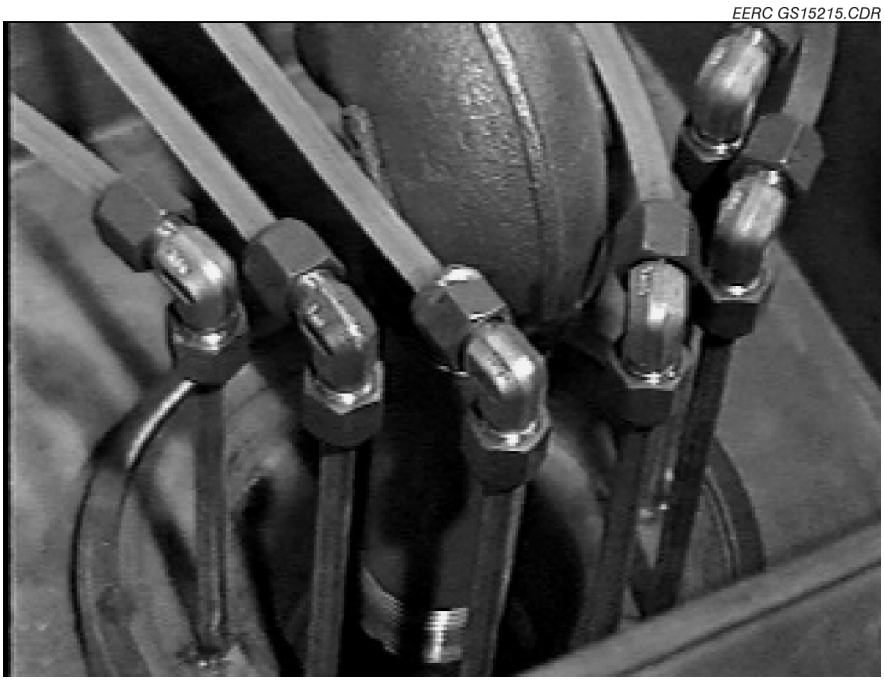

Figure 4.1-28. Top view of the modified bag cage showing the static pressure connection of each pressure tap to PTFE tubing.

4.2 Cold-Flow Testing

4.2.1 Objectives for Cold-Flow Tests

- Evaluate interactions between the ESP and filtration zones
- Evaluate multiple cleaning cycles
- Evaluate bag cleanability
- Evaluate the effect of the electric field (on or off)
- Evaluate baffling (V-baffle versus deflection plate)
- Evaluate the use of PTFE-only bags and graphite-impregnated PTFE bags

4.2.2 Initial Shakedown Tests

During the shakedown tests, the voltage was varied over a wide range to first make sure that there were no problems with the electrical insulation and that effective corona power could be generated without sparking. After one minor insulation problem was corrected, results showed

that corona could be easily generated (observed on the wires through the sight ports). At a voltage of approximately 70 kV, some back corona was noticed on the bags. It was not clear whether this was caused only by the high-resistivity fabric or by some traces of fine silica dust that was earlier tested as a flow tracer (fly ash worked just as well as a flow tracer, so the silica dust was not subsequently used). Further inspection of the bags revealed blackened spots and damage to the bags where the back corona was observed. This indicates that under severe back corona conditions, fabric damage might occur. However, 70 kV is a much higher voltage than would typically be used. At the much lower operating voltage of 50 kV chosen for subsequent tests, no back corona was observed. Should back corona be a problem, one of the ways to prevent it is to employ conductive GORE-TEX® graphite-impregnated bags. A set of these was tested to 75 kV with no corona observed on the bags. Full-scale ESPs operate with automatic voltage controls to maximize corona power (and subsequently collection efficiency) and minimize sparking. The actual operating voltage will be highly dependent on the electrode spacing, electrode alignment, dust resistivity, rapping efficiency, etc. Similarly, the operating voltage of the AHPC will be dependent on the same parameters. However, the cold-flow tests did not indicate a voltage limit problem that would impair performance.

Pulse pressure and duration are the primary operational variables that can be adjusted to provide the best bag cleaning. The goal is not only to remove most of the dust from the bags, but also to prevent recollection on the bags of the fine-particle dust cloud formed from reentrained dust. For proper operation, this dust cloud should be propelled into the ESP zone where most of it will be trapped. Fortunately, the whole AHPC compartment can be observed through the sight ports because the ESP zone traps most of the incoming dust, resulting in the whole chamber being visually clean. This allows immediate evaluation of the effects of changing pulse pressure or duration on bag-cleaning efficiency. Following multiple iterations, it was found that a lower-pressure, longer-duration pulse was more effective while cleaning one bag at a time on-line. When the pulse is initiated, larger agglomerates quickly fall to the hopper, but a cloud of reentrained dust always remains. Pushing this remaining cloud into the ESP zone appears to require a longer-duration pulse. With a longer-duration pulse, the dust is effectively transferred into the ESP zone, even though the cleaning is nonideal. Because adjacent bags are still in the

forward filtration mode, a concern is that the dust would simply transfer to the next bag. However, the cleaning velocity appeared to be sufficient to overcome the suction of the other bags so that the cloud moved back into the ESP zone, providing excellent bag cleaning.

4.2.3 AHPC Performance with Ash Injection

Reentrained dust (fly ash) was injected into the carrier air upstream of the AHPC operating at an A/C ratio of 3.7 m/min (12 ft/min), until the bags showed an increase in pressure drop of 2.0 kPa (8 in.) of water. Absaloka fly ash was injected at a rate of 1.8 kg/hr (4 lb/hr), which corresponds to a dust loading of 5.3 g/m^3 (2.3 gr/scf). The dust feed was then stopped until the compartments cleared of suspended dust to enhance visual observation of the cleaning phenomenon. Each bag was cleaned individually and on-line in rapid succession. Tests were conducted with the electric field on and off to document the benefit of the ESP section for bag cleaning. The ESP voltage was 50 kV. Test duration ranged from 2 to 7 hr, the shorter times for the tests without the electric field. The primary dependent variables were pressure drop before and after cleaning and a visual evaluation of the cleaning dynamics. Since the reentrained dust has a lower submicron particle concentration than real flue gas, extensive outlet particulate measurements were deferred until the tests with real flue gas. Cold-flow test parameters are shown in Table 4.2-1.

4.2.4 AHPC Performance with ESP On or Off

The effect of the electric field is dramatic, as shown in Figures 4.2-1 and 4.2-2. With 50 kV applied to the high-voltage electrode, the bags effectively cleaned from 2.0 to 1.0 kPa (8 to 4 in. W.C.) and only required cleaning about every 50 min. Without the electric field, the cleaning cycle interval was 7 min at the start of the test, but was less than 4 min at the end of the test. Furthermore, the bags were cleaned only down to 1.5 kPa (6 in.). From these results, the electric field not only increased pulse interval times between cleaning cycles, but also assisted in the removal of ash that would otherwise be redeposited on the bags. This test showed the enormous benefits of the synergism between of the ESP and filtration within the AHPC.

TABLE 4.2-1

Cold-Flow Multiple Cleaning Cycle Test Parameters

Test	Ash Type	A/C Ratio, m/min (ft/min)	Flow Rate, m^3/min (acfm)	Fly Ash Feed Rate, kg/hr (lb/hr)	Rapping Pressure, kPa (psig)	Rapping Duration, s	Rapping Cycle, min	Baffling	Voltage, kV	Type of Bag	No. of Bags per Pulse	Pulse Pressure, kPa (psig)	Pulse Duration, s
1	AB[1]	3.7 (12)	5.7 (200)	8.8 (4)	138 (20)	0.1	As needed	Baffle	50	PTFE	1	207 (30)	1.00
2	AB	3.7 (12)	5.7 (200)	8.8 (4)	138 (20)	0.1	As needed	Baffle	Off	PTFE	1	207 (30)	1.00
3	AB	3.7 (12)	5.7 (200)	8.8 (4)	138 (20)	0.1	As needed	Deflection plate	50	PTFE	1	207 (30)	1.00
4	AB	3.7 (12)	5.7 (200)	8.8 (4)	138 (20)	0.1	As needed	Deflection plate	Off	PTFE	1	207 (30)	1.00
5	AB	3.7 (12)	5.7 (200)	8.8 (4)	138 (20)	0.1	As needed	Baffle	50	PTFE (graphite impreg-nated)	1	207 (30)	1.00

[1] Absaloka.

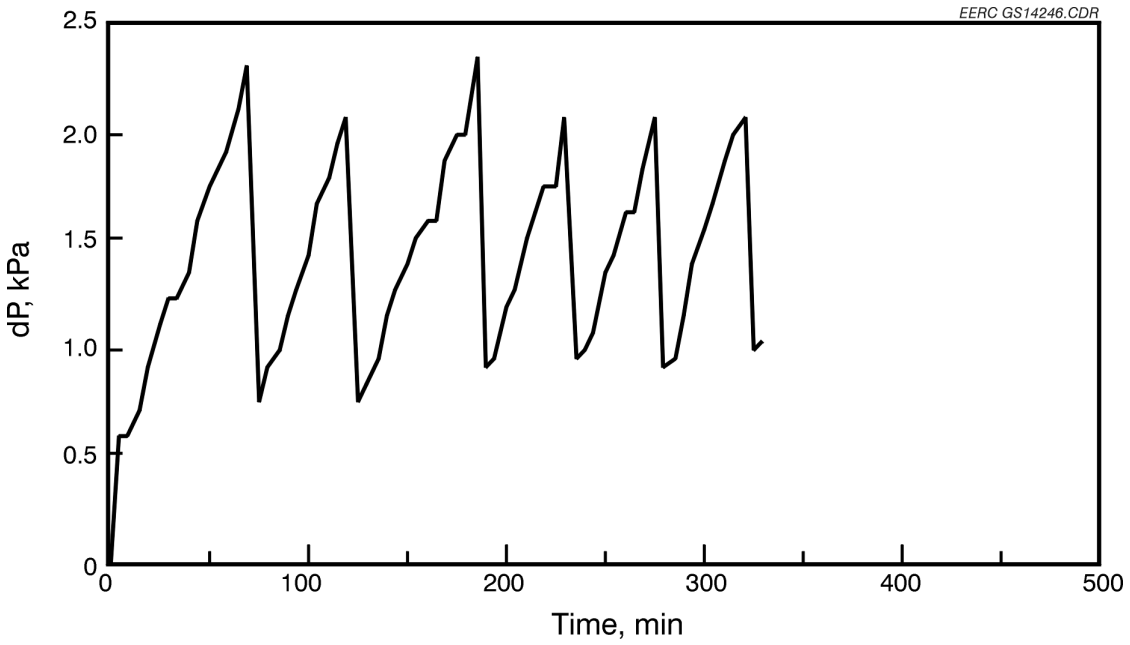

Figure 4.2-1. Pressure drop as a function of time for the AHPC V-baffle configuration with 50-kV applied voltage. Upper peak values represent pressure drop before cleaning, and lower peak values represent pressure drop immediately after cleaning.

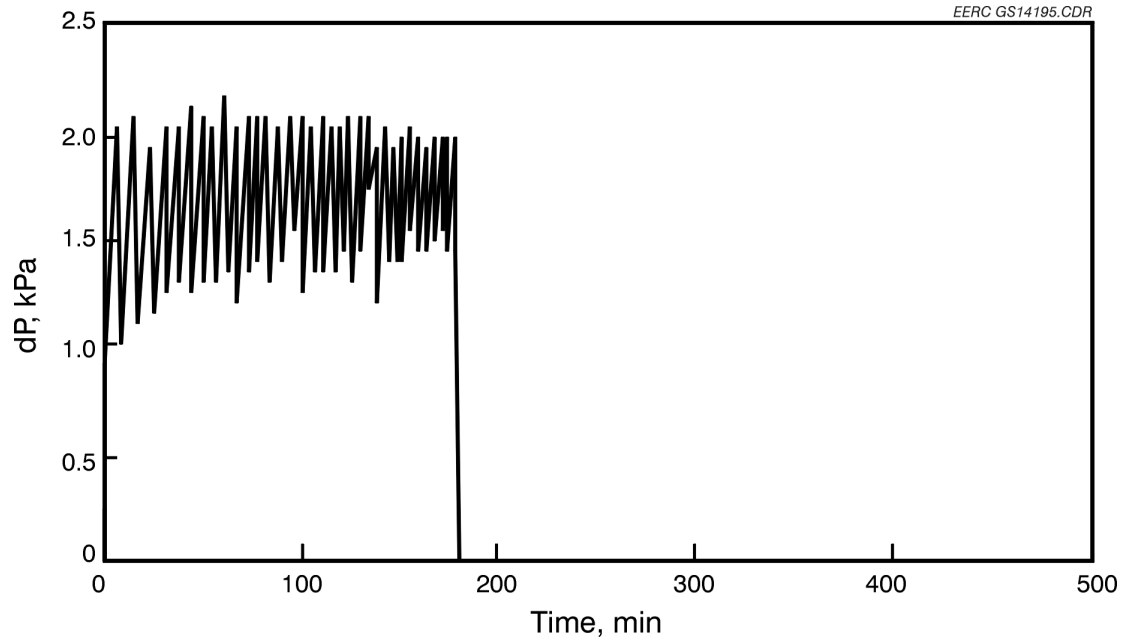

Figure 4.2-2. Pressure drop as a function of time for the AHPC V-baffle configuration with the ESP voltage off. Upper peak values represent pressure drop before cleaning, and lower peak values represent pressure drop immediately after cleaning.

4.2.5 AHPC Performance with V-Type Baffle and Deflection Plate

In order to understand the degree to which the baffle configuration effects AHPC performance, two baffle types, the V-baffle and a deflection plate, were tested during the cold-flow tests. The deflection plate was designed to try to simulate a no-baffle condition within the AHPC. The plate was placed in front of the inlet to prevent ash impinging and damaging the bags. Figures 4.2-1 and 4.2-2 illustrate the AHPC performance using the V-baffle to distribute the flue gas flow. Figures 4.2-3 and 4.2-4 are similar tests, except with the deflection plate installed. Comparing Figure 4.2-1 with Figure 4.2-3, and Figure 4.2-2 with Figure 4.2-4 demonstrates that baffling design is not as significant a priority as previously assumed. There was a moderate benefit to the V-baffle configuration, but it is totally dwarfed by the much larger ESP field effects. In actuality, the circular disk deflector was somewhat effective at diverting the flow to the sides of the vessel and into the ESP zone and therefore could not completely satisfy definition of a no-baffling configuration. These results are encouraging because they indicate that the AHPC performance is not highly sensitive to an exact baffling configuration.

4.2.6 AHPC Performance Using PTFE-Only Bags and Graphite-Impregnated PTFE Bags

A test was performed using graphite-impregnated PTFE bags. The ESP was on and the V-baffle was installed. Figure 4.2-5 shows that the conductive graphite–PTFE bags provided similar results to the PTFE-only bags shown in Figure 4.2-1. There may be advantages to the conductive bag in some applications; however, in the cold-flow tests, both bag types performed about the same. No sparking or back corona problems were observed for either of these tests.

4.2.7 Summary of Cold-Flow Results

In summary, the cold-flow tests showed the following:

- The ESP had a dramatic effect on AHPC performance.

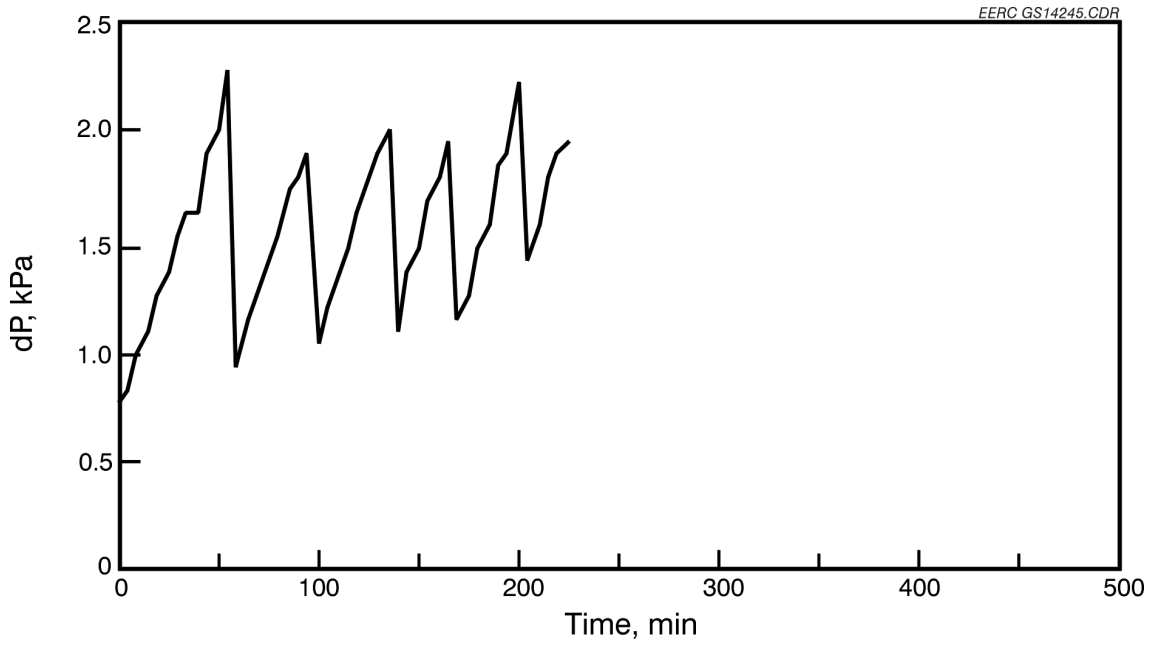

Figure 4.2-3. Pressure drop as a function of time for the AHPC with deflection plate baffle configuration and ESP voltage on. Upper peak values represent pressure drop before cleaning, and lower peak values represent pressure drop immediately after cleaning.

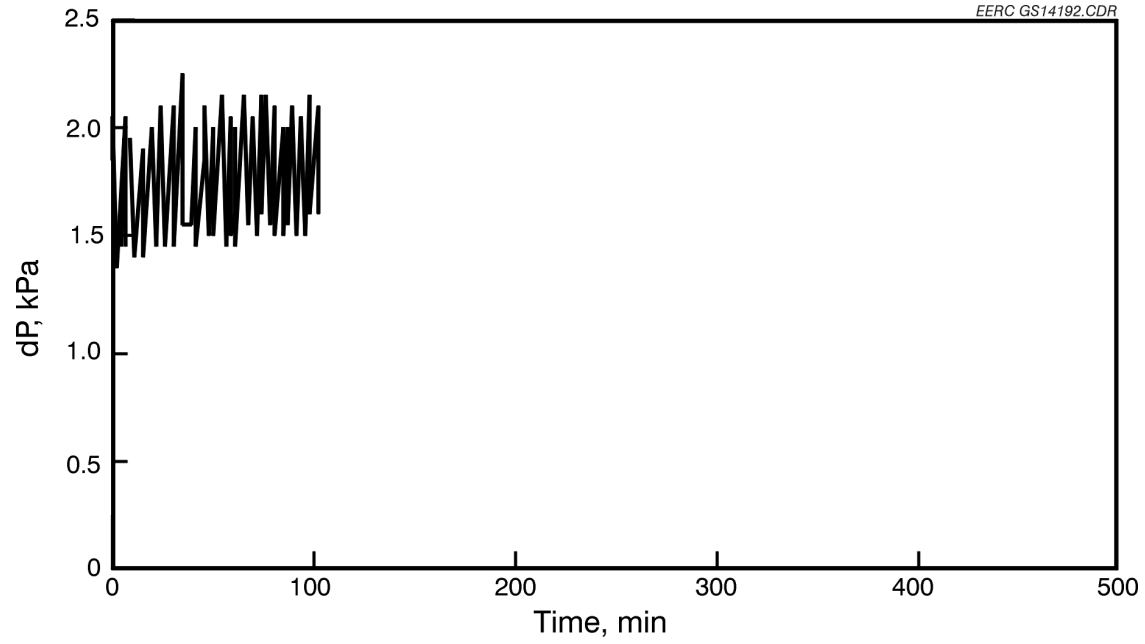

Figure 4.2-4. Pressure drop as a function of time for the AHPC with deflection plate configuration and ESP voltage off. Upper peak values represent pressure drop before cleaning, and lower peak values represent pressure drop immediately after cleaning.

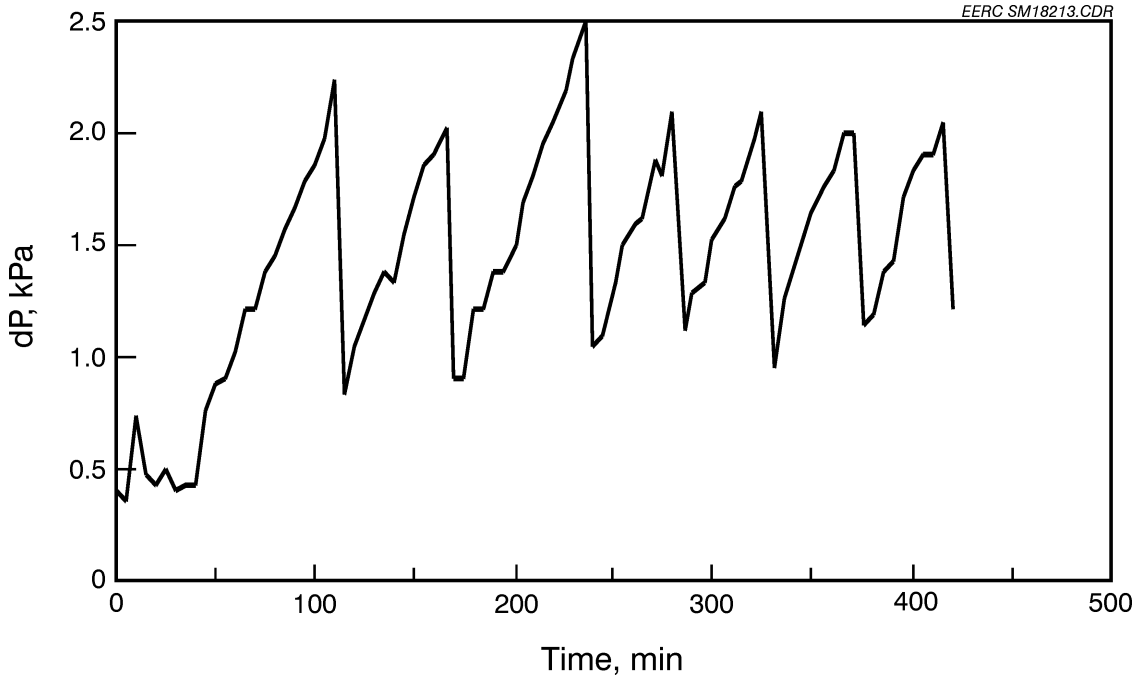

Figure 4.2-5. Pressure drop as a function of time for the AHPC with V-battle configuration and ESP voltage on using conductive graphite-impregnated PTFE bags. Upper peak values represent pressure drop before cleaning, and lower peak values represent pressure drop immediately after cleaning.

- The differences in AHPC performance between the V-baffle and the deflection plate were not significant.

- No differences in bag performance were noted between the PTFE-only bags and the conductive graphite–PTFE bags.

4.3 8-hr Tests Firing Coal

The objectives of the 8-hr tests on coal were:

- Evaluate the AHPC under real flue gas conditions firing coal.
- Test A/C ratios.
- Test on-line versus off-line cleaning.

- Test bag type.
- Test flue gas conditioning.

The variables evaluated during the 8-hr test series were:

- Coal type.
- A/C, 3.7 and 4.9 m/min (12 and 16 ft/min).
- On-line versus off-line cleaning.
- AHPC operability with the ESP alone and all bags removed.
- AHPC operability with ESP off and all bags removed.
- Bag type: graphite-impregnated, conductive PTFE bags versus the nonconductive PTFE bags.
- AHPC inlet plenum baffling: V type and butterfly.
- Reservoir tank pulse pressure: 414 and 621 kPa (60 and 90 psig).
- ESP electrode shape: smooth wire and directional comb.
- System start-up procedure.

4.3.1 8-hr Test Results Firing Absaloka Coal

Eleven 8-hr tests firing Absaloka subbituminous coal were completed. Operational variables for the 8-hr Absaloka-fired tests are found in Table 4.3-1. Particulate information is

TABLE 4.3-1

Test Parameters for Absaloka Coal

Date:	9-17-96	9-18-96	9-19-96	9-20-96	10-15-96	10-16-96	10-17-96	11-05-96	11-06-96	11-07-96	11-07-96
PTC Test No.	PTC-AB-568	PTC-AB-569	PTC-AB-570	PTC-AB-571	PTC-AB-572	PTC-AB-573	PTC-AB-574	PTC-AB-575	PTC-AB-576	PTC-AB-577	PTC-AB-578
A/C Ratio, m/min (ft/min)	3.7 (12)	3.7 (12)	3.7 (12)	3.7 (12)	3.7 (12)	3.7 (12)	No bags	3.7 (12)	3.7 (12)	4.9 (16)	4.9 (16)
Inlet Temp., °C (°F)	149 (300)	149 (300)	149 (300)	149 (300)	149 (300)	149 (300)	149 (300)	149 (300)	149 (300)	149 (300)	149 (300)
On-Line and Off-Line Cleaning	On	Off	On	Off	On	Off	NA[1]	Off	On	Off	On
Baffling	V-Type	V-Type	V-Type	V-Type	Butterfly	Butterfly	Butterfly	Butterfly	Butterfly	Butterfly	Butterfly
Voltage, kV	50, off at end	50, off at end	50, off at end	50	50, off at end	50, off at end	50, off at end	50	50	50	50
Type of Bag	PTFE Set 2	PTFE Set 2	Graphite–PTFE Set 3	Graphite–PTFE Set 3	PTFE Set 4	PTFE Set 4	No bags	PTFE Set 6	PTFE Set 6	PTFE Set 6	PTFE Set 6
No. of Bags in Use	4	4	4	4	4	4	0	4	4	3	3
Pulse Pressure, kPa (psig)	414 (60)	414 (60)	414 (60)	414 (60)	414 to 612 (60 to 90)	621 (90)	NA	621 (90)	621 (90)	621 (90)	621 (90)
Pulse Duration, s	1.00	1.00	NA	1.00	1.00	1.00	NA	1.00	1.00	1.00	1.00
Pulsing Initiation Pressure, kPa (in. W.C.)	2.0 (8.0)	2.0 (8.0)	NA	2.0 (8.0)	2.0 (8.0)	2.0 (8.0)	NA	2.0 (8.0)	2.0 (8.0)	2.0 (8.0)	2.0 (8.0)

[1] Not applicable.

presented in Table 4.3-2, and average concentrations for flue gas constituents are found in Table 4.3-3.

4.3.1.1 Effect of On-Line or Off-Line Bag Cleaning

The purpose of Run PTC-AB-568 was to evaluate the PTFE bags in the on-line cleaning mode. Natural gas was fired to heat the PTC, the AHPC, and adjacent piping. The PTC was then switched to Absaloka subbituminous fuel and flue gas was directed into the AHPC containing four newly installed PTFE bags. Flue gas composition remained fairly consistent throughout the 4-day test period. ESP voltage was set at 50 kV. With the seven-wire electrode configuration, the average current output was about 0.25 mA. Approximately 2 hr of operation was required before the bags achieved steady-state pressure drop. Figure 4.3-1 shows the dP versus time of the run. The cleaning cycle dropped the dP from 2.0 kPa (8.0 W.C.) to around 1.5 kPa (6.0 in. W.C.) on the average. For on-line cleaning, the pulse interval started at about 40 min with clean bags and decreased in time to about 18 min at steady-state conditions. This trend of pulse interval versus run time is shown in Figure 4.3-2.

The purpose of Run PTC-AB-569 was to evaluate the PTFE bags using off-line cleaning. After the successful completion of Run PTC-AB-568, the now-dirty PTFE bags were pulsed several times with the AHPC off-line. The dust-laden flue gas was again directed into the AHPC. ESP voltage was 50 kV, with an average current output during the test of 0.33 mA. Figure 4.3-3 presents the dP versus run time for Run PTC-AB-569. Once the dP reached 2.0 kPa (8 in. W.C.), the operator would bypass the flue gas flow from the AHPC and initiate a bag-cleaning cycle. During the cleaning cycle, the dP read zero, since no flow was going through the AHPC. The ESP was left on during the off-line cleaning cycle. Because the bags were already conditioned, the pulse intervals quickly reached steady-state conditions. The pulse interval for Run PTC-AB-569 was about 35–40 min at the end of the run. The pulse interval plotted against run time is shown on the graph in Figure 4.3-4. For these early tests, off-line cleaning provided better control.

TABLE 4.3-2

Dust-Loading Data for Absaloka Coal

Date	PTC Test No.	Hopper Ash, g/m^3	Inlet, g/m^3	Outlet, g/m^3	Percent Collection Efficiency	Outlet Filter Weighing Precision RSD,[1] %
9-17-96	PTC-AB-568	4.60	NA[2]	NA	NA	
9-18-96	PTC-AB-569	4.60	6.640	0.0002	99.996	2.89
9-19-96	PTC-AB-570	5.15	5.5429	0.0016	99.971	6.26
9-20-96	PTC-AB-571	4.32	6.6352	0.0006	99.991	1.86
10-15-96	PTC-AB-572	7.95	8.3791	0.0007	99.992	
10-16-96	PTC-AB-573	6.80	7.5792	0.0009	99.989	
10-17-96	PTC-AB-574	No bags	ESP on	0.2840	96.441	
		No bags	ESP on	0.3728	95.327	
		No bags	ESP on	0.3648	95.428	
		No bags	ESP off	4.4847	43.79	
		No bags	ESP off	4.0998	48.620	
		No bags	ESP off	4.1934	47.776	
11-05-96	PTC-AB-575	8.11	11.1502	0.0037	99.968[3]	
11-06-96	PTC-AB-576	9.18	9.9274	0.0046	99.955[3]	
11-07-96	PTC-AB-577	9.71	10.5306	0.0018	99.983[3]	
11-07-96	PTC-AB-578	7.83	8.6205	0.0037	99.957[3]	

[1] Relative standard deviation.

[2] Not applicable.

[3] Contamination of AHPC outlet piping.

TABLE 4.3-3

Average Flue Gas Concentrations for Tests PTC-AB-568 to PTC-AB-578[1]

O_2, % by volume	CO_2, % by volume	H_2O, % by volume	SO_2, ppm	NO_x, ppm
4.0–4.5	14–16	9.5–10.0	720	700

[1] Dry basis except for H_2O.

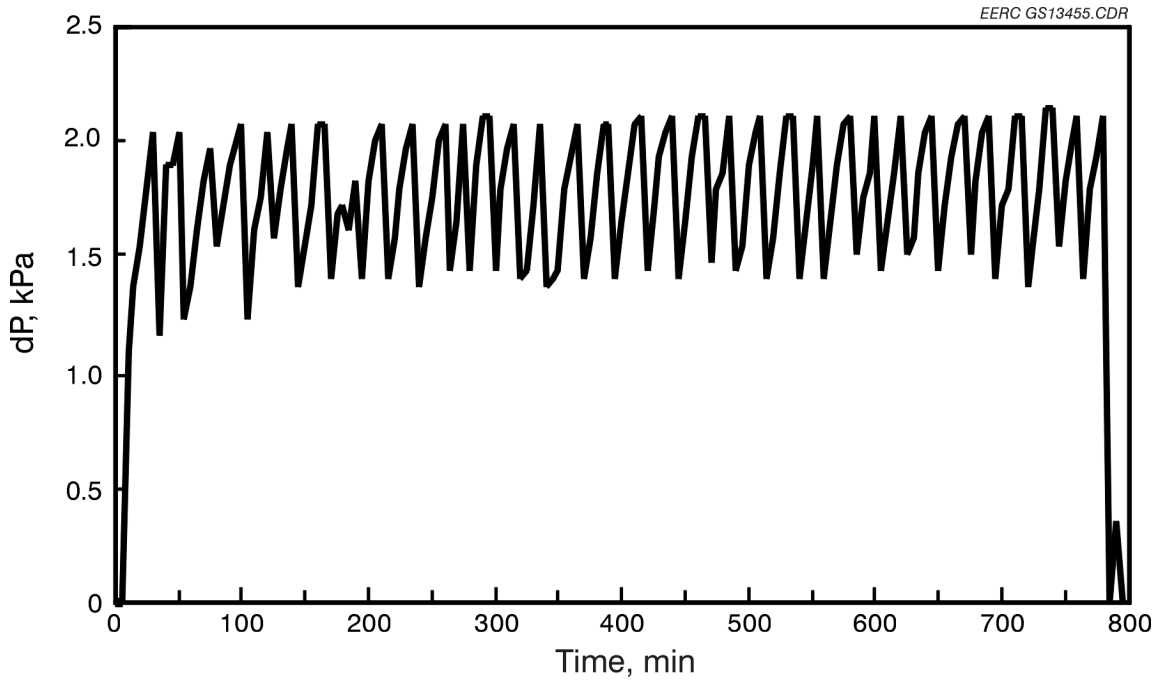

Figure 4.3-1. Pressure drop as a function of time for Test PTC-AB-568 with on-line cleaning using PTFE bags.

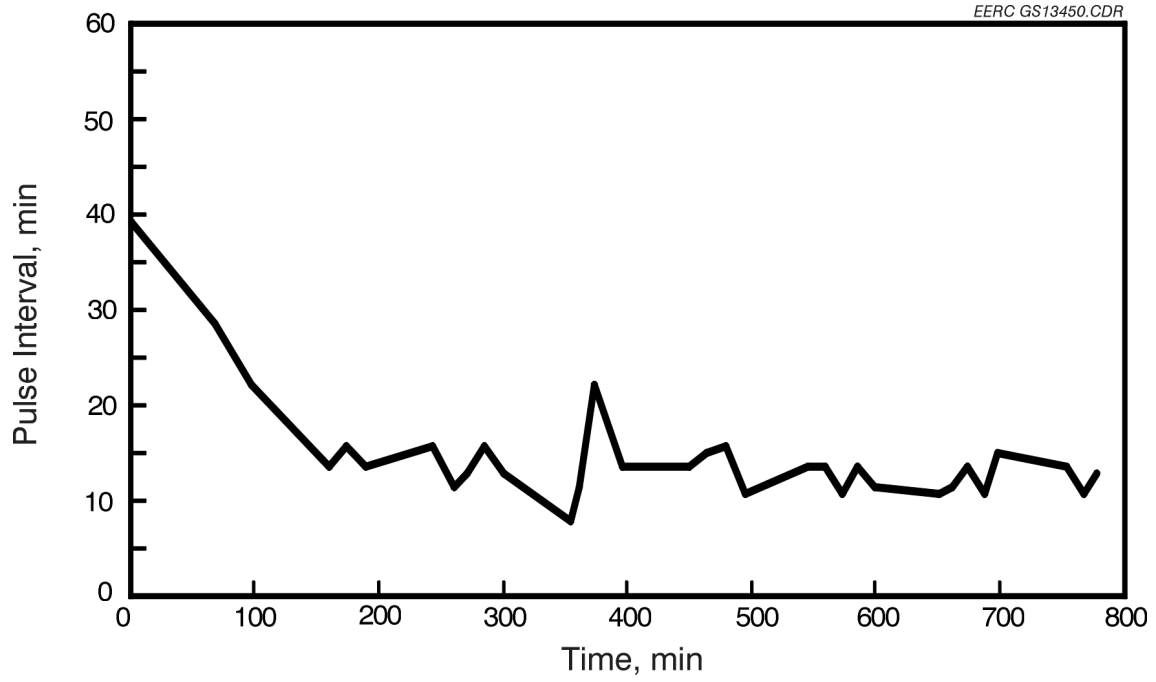

Figure 4.3-2. Pulse interval as a function of time for Test PTC-AB-568 with on-line cleaning using PTFE bags.

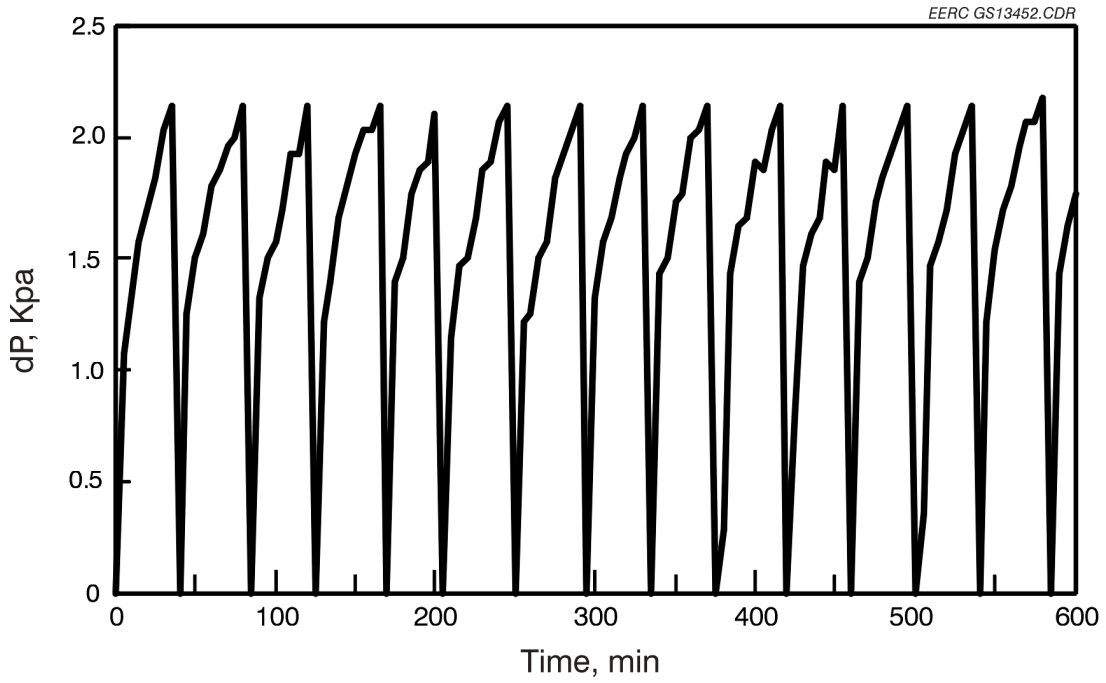

Figure 4.3-3. Pressure drop as a function of time for Test PTC-AB-569 with off-line cleaning using PTFE bags.

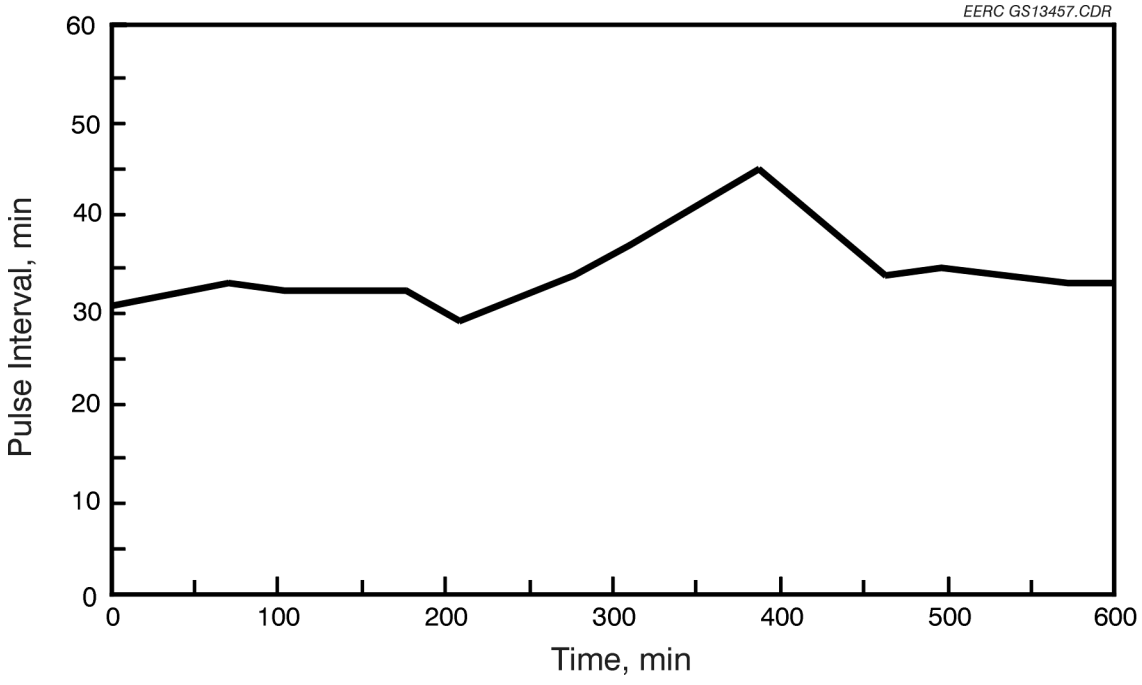

Figure 4.3-4. Pulse interval as a function of time for Test PTC-AB-569 with off-line cleaning using PTFE bags.

Particulate sampling data for these two runs are presented in Table 4.3-2. Dust loadings from Run-AB-569 of the inlet and outlet of the AHPC are 6.6400 g/m^3 and 0.0002 g/m^3 (2.9020 and 0.00010 gr/scf), respectively. This gives a dust collection efficiency of 99.996%. The weights of the outlet dust-loading samples were small, so in order to establish measurement precision of the method, these outlet filters were reweighed several times. APS data for PTC-AB-569 are shown on the graph in Figure 4.3-5. No integrated averages of respirable mass were taken during this test; however, except for the spikes due to bag cleaning, the respirable mass data remained below 0.05 mg/m^3. These APS data correspond to an AHPC dust collection efficiency of >99.99%.

4.3.1.2 Comparison of Bag Type with On-Line and Off-Line Bag Cleaning

The purpose of Run PTC-AB-570 was to evaluate the graphite-impregnated PTFE bags in the on-line cleaning mode. Four new graphite-impregnated PTFE bags were installed in the AHPC. ESP voltage was set at 50 kV, with an average current output of about 0.40 mA.

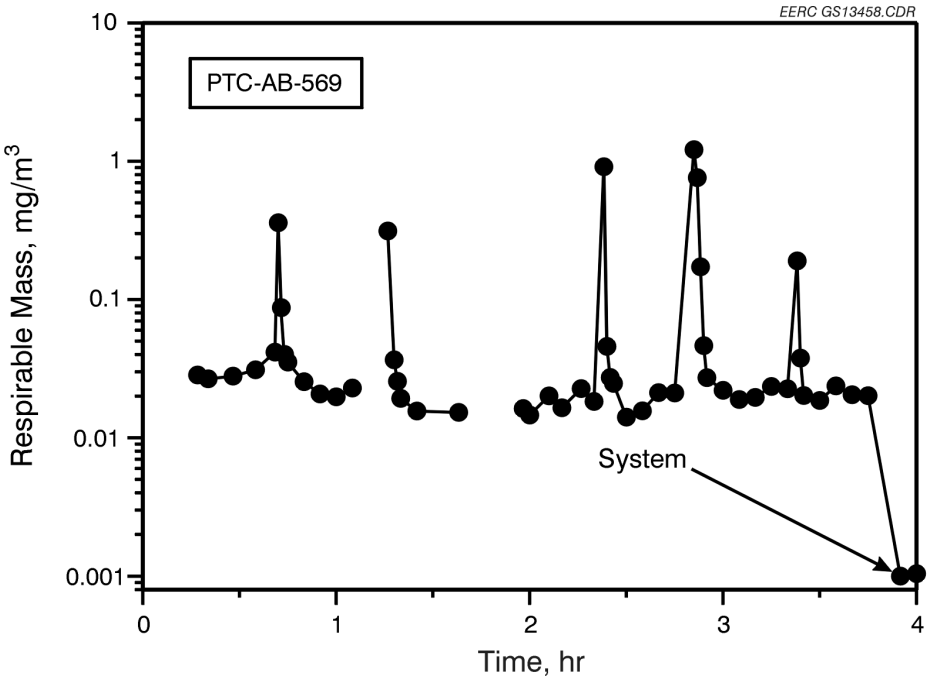

Figure 4.3-5. APS data for Test PTC-AB-569.

Figure 4.3-6 shows the dP over the time of the run. The last two cleaning cycles, shown in Figure 4.3-6, reveal the dP falling from 2.0–1.25 kPa (8–5 in. W.C.) and the pulse interval increasing from an average of 16 to about 20 min. The reason is that for those two cleaning cycles, the bags were each pulsed twice instead of just once. The cleaning cycle dropped the dP from 2.0 kPa (8 in. W.C.) to around 1.5 kPa (6 in. W.C.) on the average. The pulse interval started at about 40 min with clean bags and decreased in time to about 16 min at steady-state conditions. A graph showing pulse interval versus run time is found in Figure 4.3-7.

Particulate sampling data for Run PTC-AB-570 are also presented in Table 4.3-2. Dust loadings from the inlet and outlet of the AHPC were 5.5429 g/m^3 and 0.0016 g/m^3 (2.4225 and 0.00070 gr/scf), respectively. This gives a dust collection efficiency of 99.971%. The filters of the outlet dust-loading samples were again reweighed to establish measurement precision. APS data for PTC-AB-570 are shown in the graph in Figure 4.3-8. The respirable mass integrated average, as shown on the graph, was 0.55 mg/m^3. This emission rate is higher than the emission rate recorded for PTC-AB-569 and corresponds to a lower AHPC dust collection efficiency of

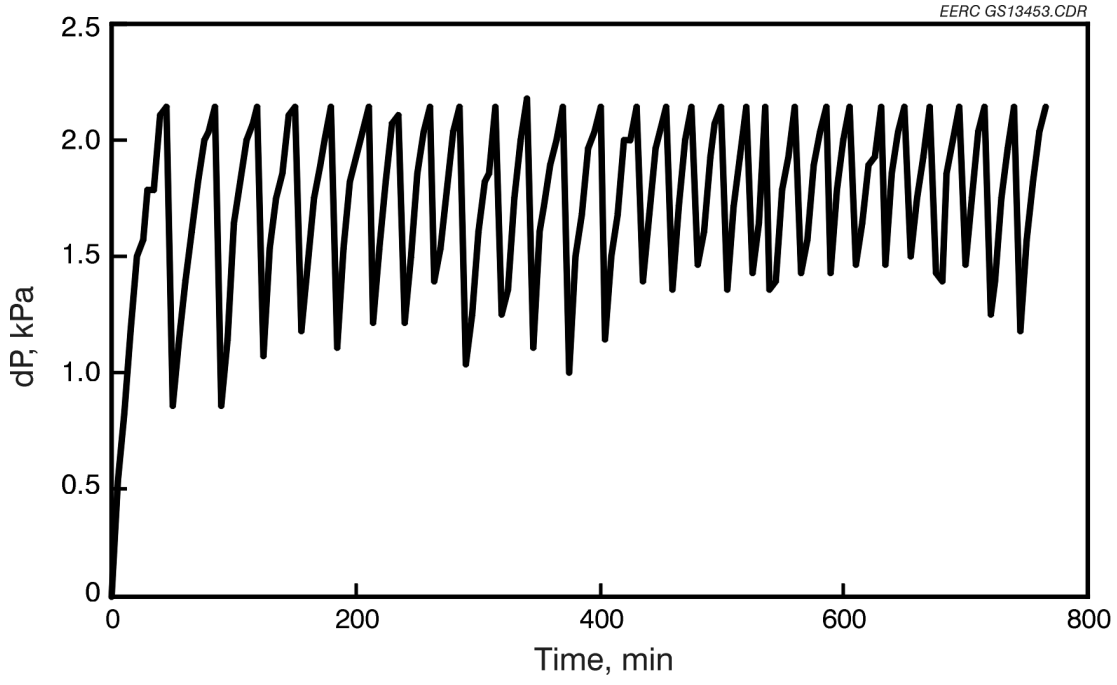

Figure 4.3-6. Pressure drop as a function of time for Test PTC-AB-570 with on-line cleaning using graphite-impregnated PTFE bags.

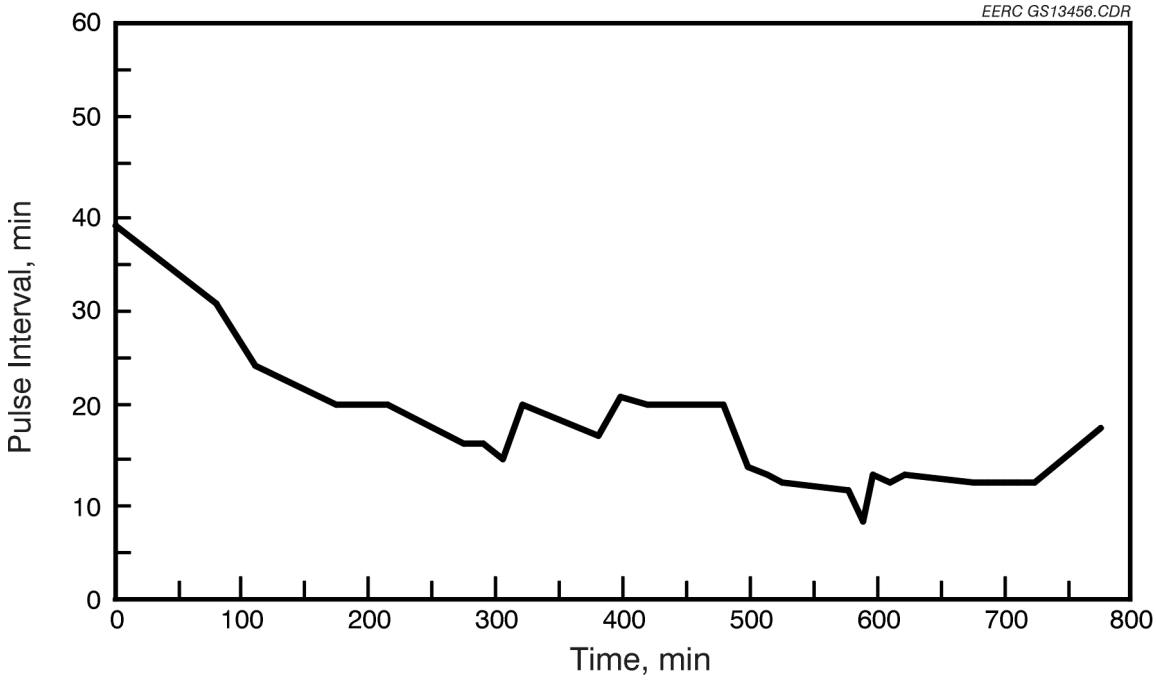

Figure 4.3-7. Pulse interval as a function of time for Test PTC-AB-570 with on-line cleaning using graphite-impregnated PTFE bags.

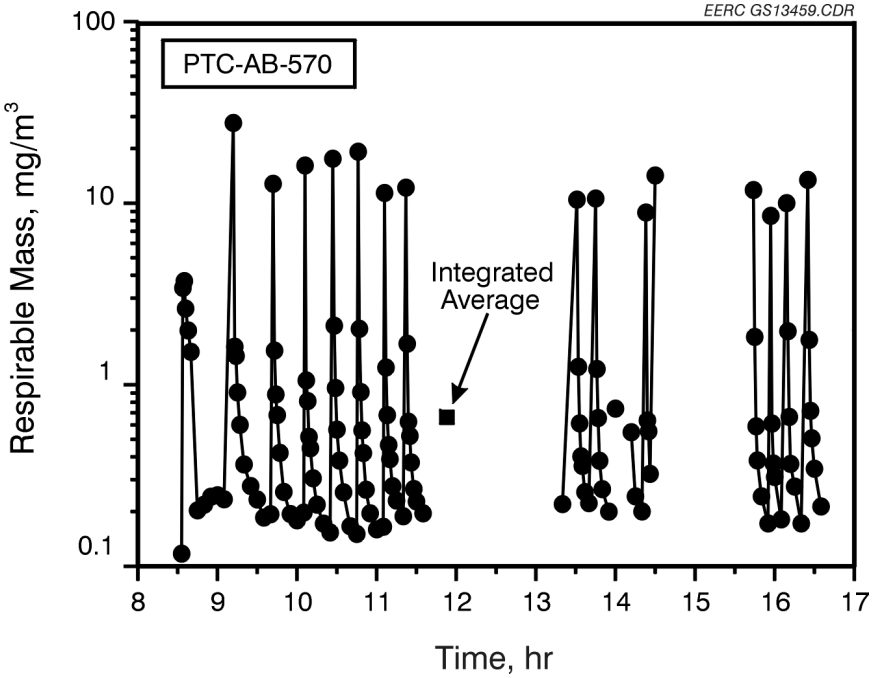

Figure 4.3-8. APS data for Test PTC-AB-570.

99.971%. The higher respirable mass emission data may be due to several nicks in the bag's PTFE membrane, which were discovered after the tests. The nicks may have been caused by the improper handling of the bags during installation.

The purpose of Run PTC-AB-571 was to evaluate the graphite-impregnated PTFE bags in the off-line cleaning mode. The same graphite-impregnated PTFE bags that were used for Test PTC-AB-570 were used again in Test PTC-AB-571. Test parameters remained the same for this run as for those above. The results of this run are shown in Figure 4.3-9. The graphite-impregnated PTFE bags were cleaned before the start of Run PTC-AB-571 by multiple-pulse cycles in the off-line mode. The bags were not removed from the AHPC or cleaned in any other way. At steady-state conditions, the dP dropped from 2.0 kPa (8 in. W.C.) to an average value of 1.25 kPa (5 in. W.C.), and the pulse interval averaged 26 min. The pulse interval data are presented in Figure 4.3-10.

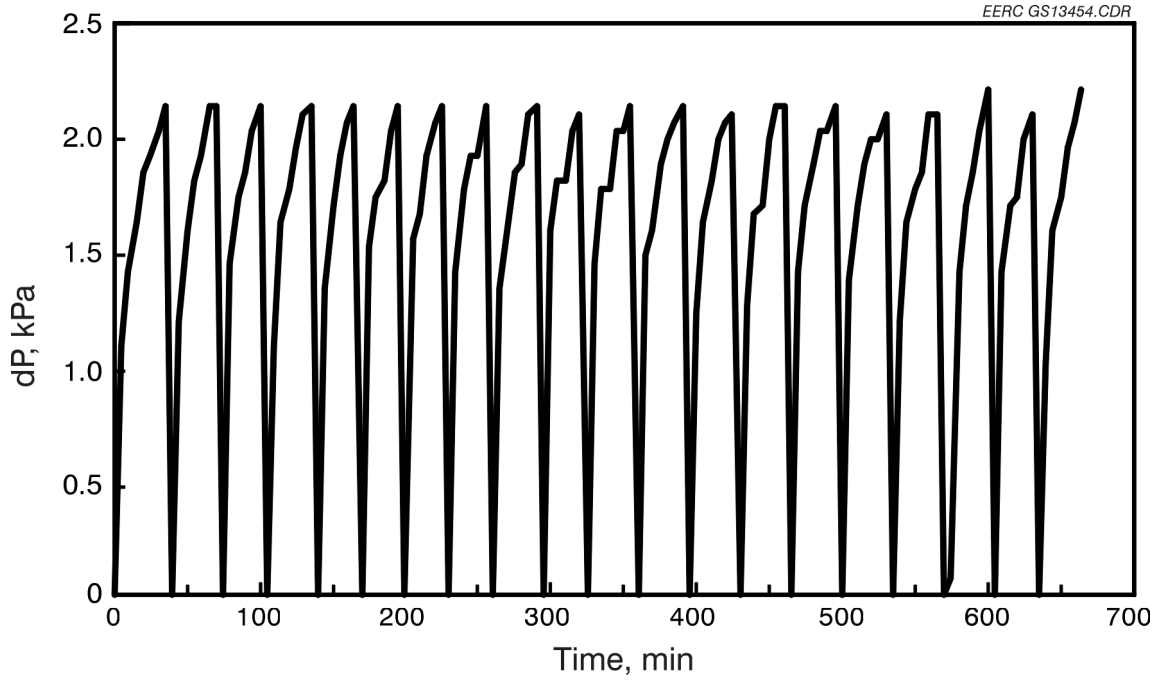

Figure 4.3-9. Pressure drop as a function of time for Test PTC-AB-571 with off-line cleaning using graphite-impregnated PTFE bags.

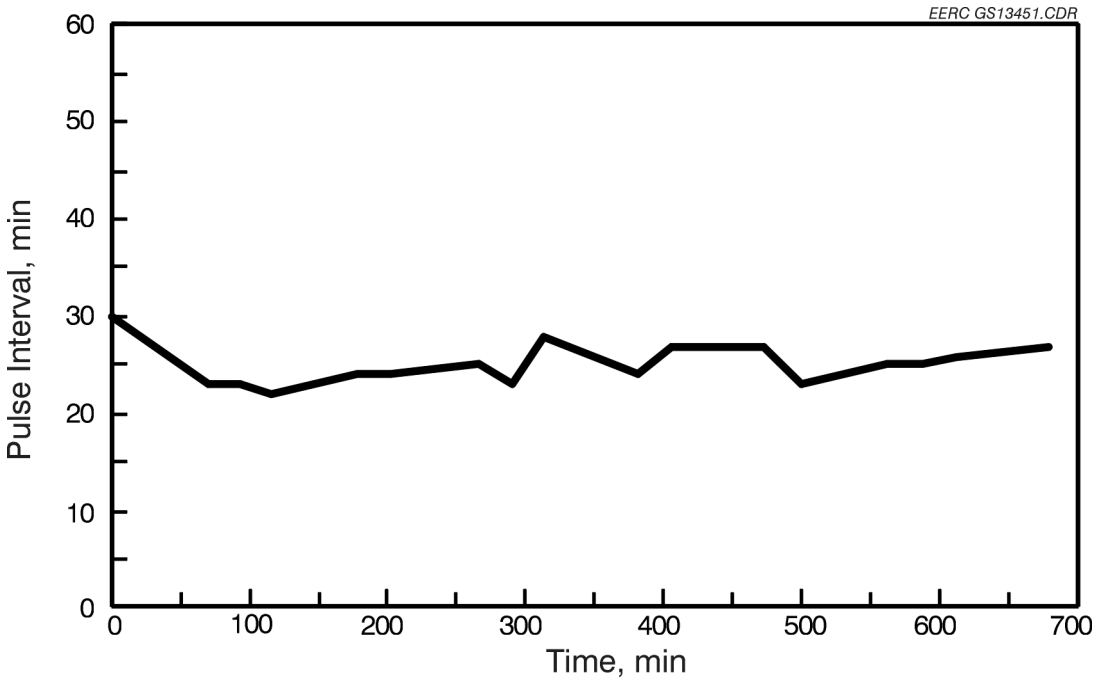

Figure 4.3-10. Pulse interval as a function of time for Test PTC-AB-571 with off-line cleaning using graphite-impregnated PTFE bags.

PTC-AB-571 particulate sampling data are also presented in Table 4.3-2. Dust loadings from the inlet and outlet of the AHPC were 6.6352 g/m^3 and 0.0006 g/m^3 (2.8999 gr/scf and 0.00026 gr/scf), respectively. This gives a dust collection efficiency of 99.991%. The outlet dust loading filter was again re-weighed in order to establish measurement precision. APS data for PTC-AB-571 are shown on the graph in Figure 4.3-11. The respirable mass integrated averages, as shown on the graph, were 0.20 and 0.24 mg/m^3. This corresponds to an AHPC dust collection efficiency of >99.98%. This lower efficiency is attributed to the damaged membrane for this set of bags.

As a check of the validity of the inlet dust-loading data, the fly ash collected in the hopper was weighed and from this weight a dust loading could be calculated. Table 4.3-4 presents the inlet dust-loading data provided by EPA Method 5 and multicyclone sampling for Runs PTC-AB-569, PTC-AB-570, and PTC-AB-571. Dust-loading data calculated using the hopper ash are also presented in Table 4.3-4. The comparison of the gas-sampled dust loadings and the hopper ash dust loadings showed the average hopper ash dust loading to be low by an average of 24%

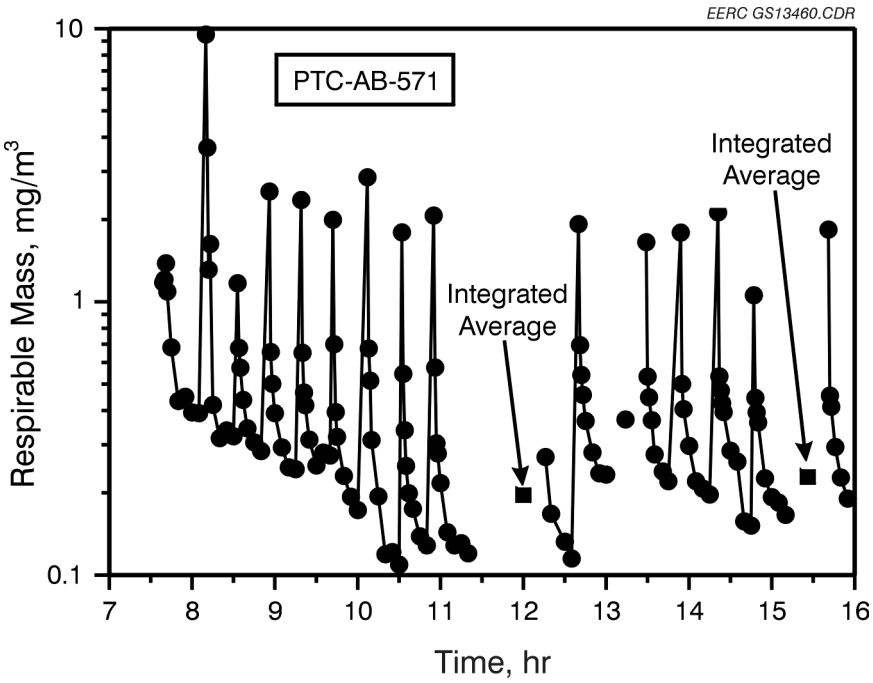

Figure 4.3-11. APS data for Test PTC-AB-571.

TABLE 4.3-4

Mass Balance for Tests PTC-AB-569 to PTC-AB-571

Date	PTC Test No.	Location	Method 5/ Multicyclone Dust Loading, g/m^3	Dust Loading from AHPC Hopper Ash, g/m^3	Difference, %
9/18/96	PTC-AB-569	Inlet	6.6400	4.60	31
9/19/96	PTC-AB-570	Inlet	5.5429	5.15	7
9/20/96	PTC-AB-571	Inlet	6.6352	4.32	35
Average			6.2727	4.69	25
with Weigh-Back			6.2727	6.02	4

throughout the test period. The discrepancy was discovered during cleaning of the baghouse interior, inlet plenum, and inlet piping. A total mass of 10.32 kg (22.76 lb) of fly ash was recovered. The inlet plenum contained the most ash at 6.57 kg (14.48 lb) collected. When the recovered ash was added back to the hopper ash total, the average dust loading calculated from the hopper ash was 6.02 g/m^3 (2.63 gr/scf). This compared well with the 6.2727 g/m^3 (2.74 gr/scf) average derived from the inlet particulate sampling data. The difference between the

gas-sampling dust loadings and the hopper ash dust loadings decreased from 24% to 4% when the recovered ash was added back in to the mass balance. Because of the accumulation of large amounts of ash in the inlet plenum, the plenum was redesigned to minimize the problem.

4.3.1.3 Comparison of the V-Baffle Versus the Butterfly Baffle in On-Line and Off-Line Bag-Cleaning Modes

Tests PTC-AB-572 and PTC-AB-573 were repeats of Tests 568 and 569, respectively. The purpose was to observe operational changes, including on-line versus off-line cleaning modes, using the new butterfly baffle versus the V-baffle design used in Tests PTC-AB-568 to 571.

The dP versus run time for Run 572 is presented in Figure 4.3-12. In this test, the cleaning mode was on-line, with a new set of GORE-TEX® PTFE-only bags installed. During system start-up, flue gas generated by burning natural gas was directed through the AHPC. The AHPC was in contact with this gas for about 500 min before the test. Although not shown in

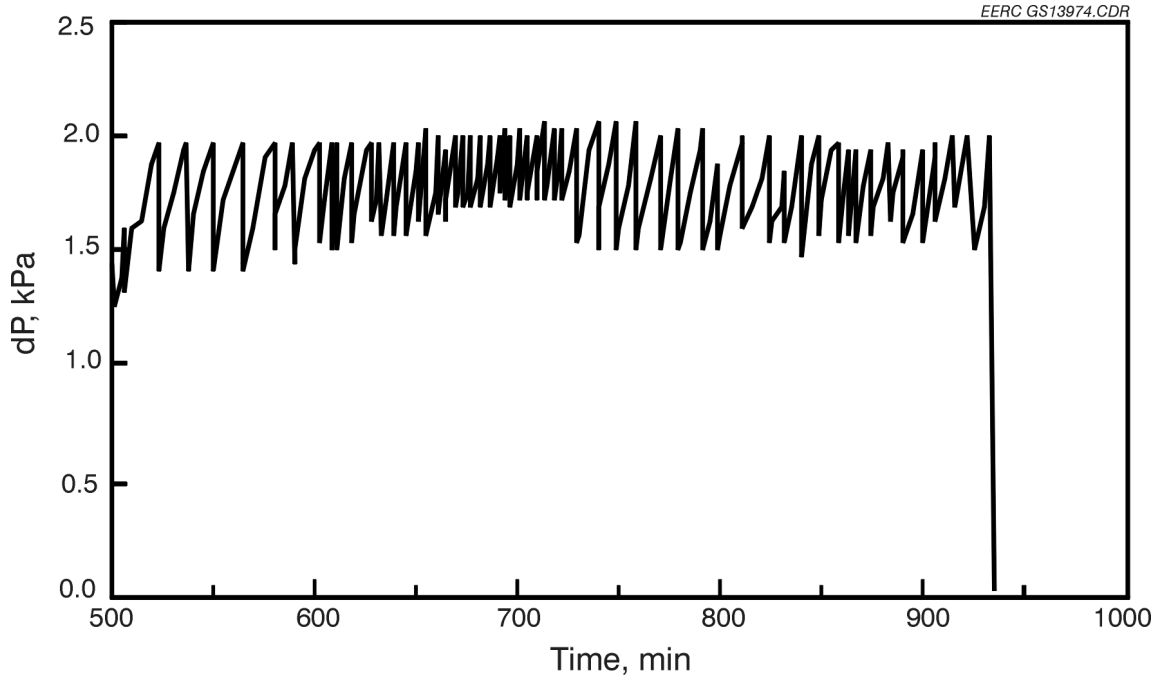

Figure 4.3-12. Pressure drop as a function of time for Test PTC-AB-572 with on-line cleaning using PTFE bags.

Figure 4.3-12, the dP went from 0.5 to 1.3 kPa (2.0 to 5.2 in. W.C.) while the natural gas was fired. Increase in the dP during the heating period was most likely caused by the vaporization and condensation of the residual slag in the combustor. Very fine particles were likely formed that were not easily removed from the bag. Therefore, as shown in Figure 4.3-12, the dP at the start of the test was already 1.3 kPa (5.2 in. W.C.) The initial pulse intervals were 10–15 min, but after about 3 hr, the interval was down to 5 min. The decrease in pulse interval (see Figure 4.3-13) along with the marginal decrease in dP after pulsing indicated problems with bag cleaning. To improve bag cleaning, the pulse pressure was increased from 414 to 621 kPa (60 to 90 psig.) With the pulse pressure increase, the dP became more controllable and the pulse interval increased from 5 to 10 min. The bag-cleaning problem was surprising because in a previous test with this coal (Run 568), the pulse interval was 15 min and the bags cleaned well. The problem was eventually traced to the start-up procedure (discussed in more detail later).

Dust-loading data for Test PTC-AB-572 are tabulated in Table 4.3-2. The sampling data show the inlet and outlet dust concentration to be 8.3791 g/m^3 and 0.0007 g/m^3 (3.6591 gr/scf

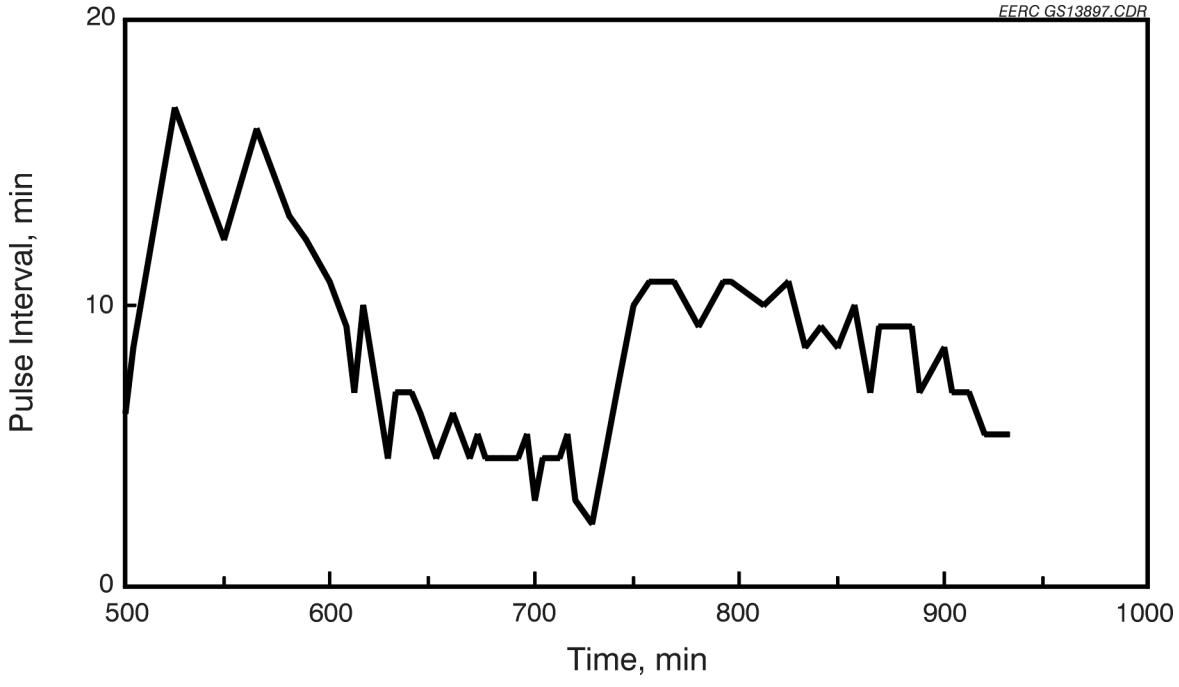

Figure 4.3-13. Pulse interval as a function of time for Test PTC-AB-572 with on-line cleaning using PTFE bags.

and 0.0003 gr/scf), respectively, for a calculated dust removal mass efficiency of 99.992%. Data from the APS are presented in Figure 4.3-14. APS data taken continually over an entire cleaning cycle, including the time just after pulsing, were integrated to produce an average respirable mass value called an integrated average. Three of these integrated averages were done. These values of 0.035, 0.15, and 0.28 mg/m^3 (shown in Figure 4.3-14) correspond to particulate collection efficiencies of ~99.99%. The particulate collection efficiencies calculated from the APS data compare well with the EPA Method 5 dust-loading efficiency of 99.992%.

Test PTC-AB-573 demonstrated off-line cleaning while maintaining an A/C of 3.7 m/min (12 ft/min) and pulse pressure of 621 kPa (90 psig) using a seasoned set of bags from Test PTC-AB-572. Toward the end of the test period, the ESP was turned off and then back on in order to see if there was a clear benefit of the ESP and to see how well the AHPC recovered.

Figure 4.3-15 presents the dP versus time data showing that the difference in dP before and after cleaning was about 0.37 kPa (1.5 in. W.C.). The range of pulse interval reached a steady

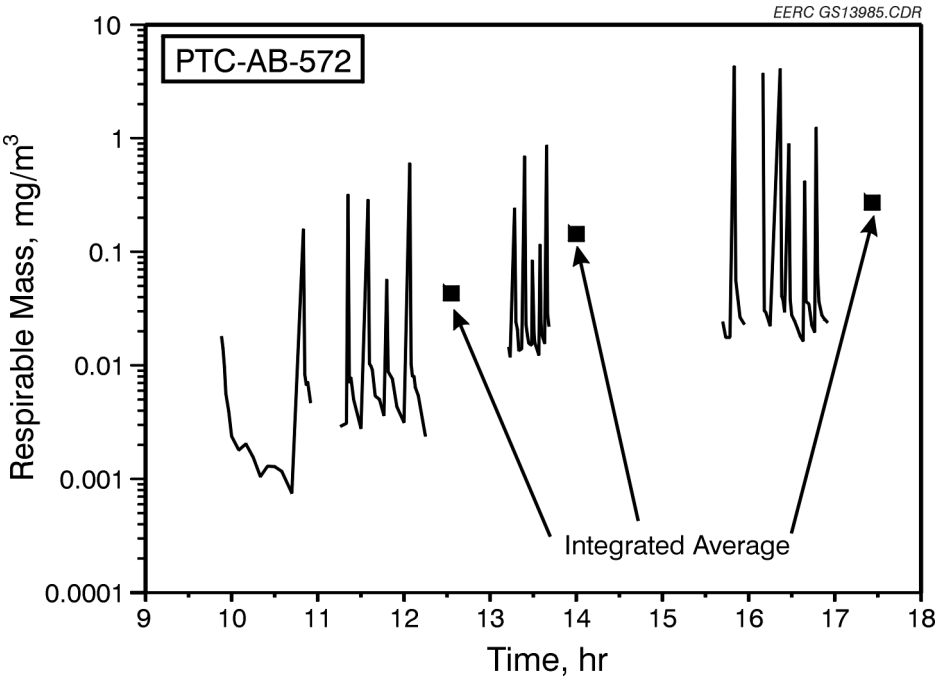

Figure 4.3-14. APS data for Test PTC-AB-572.

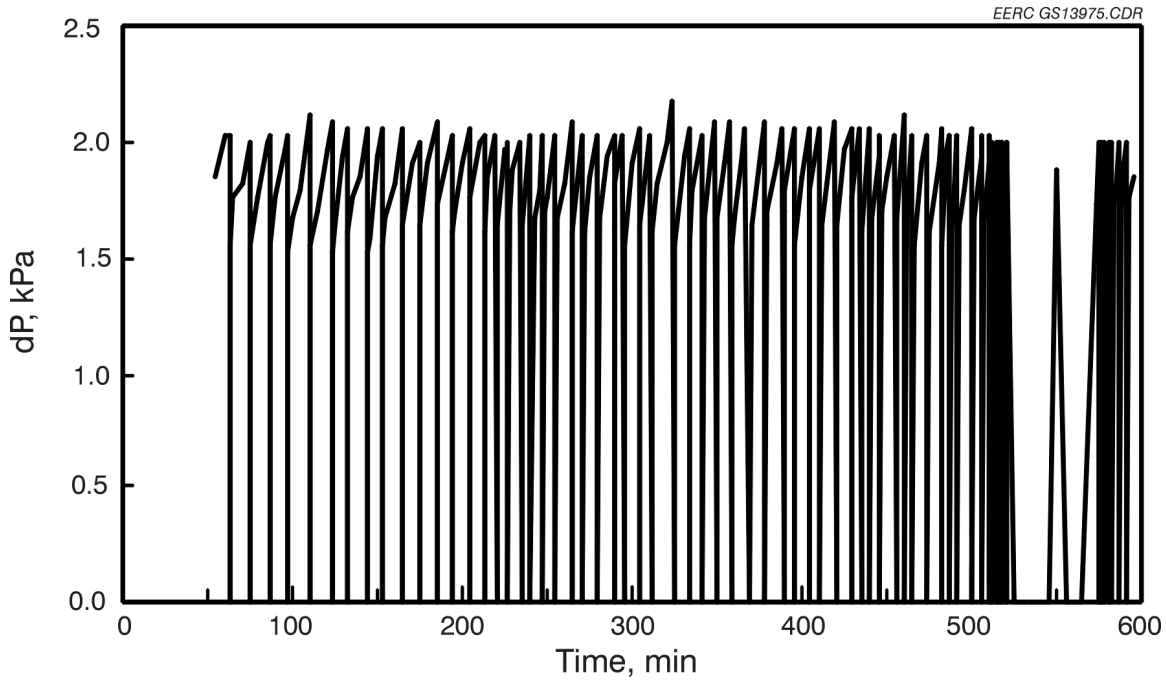

Figure 4.3-15. Pressure drop as a function of time for Test PTC-AB-573 with on-line cleaning using PTFE bags.

state at about 8–12 min as presented in Figure 4.3-16. Again, the bag cleaning was not as good as observed in an earlier run. (As mentioned above, this difficulty was eventually traced to the start-up procedure.) However, at the end of the test when the ESP was turned off, the pressure drop difference from before and after dP was a small 0.08 kPa (0.3 in. W.C.) and pulse interval was 0.75–1.00 min. After the ESP was turned on, the AHPC recovered to the pressure drop and pulse intervals measured before the ESP was turned off. These results indicated that the ESP produced a clear benefit, even though the bag cleaning was not as good as in an earlier run.

The particulate collection efficiency of the AHPC for off-line cleaning was 99.989%, as shown in Table 4.3-2. The inlet and outlet dust loadings were 7.5792 and 0.0009 g/m^3 (3.3097 and 0.0004 gr/scf), respectively. APS data for respirable mass concentrations versus time are shown in Figure 4.3-17. Two integrated averages were done during the test. These average values were 0.03 and 0.07 mg/m^3. The calculated particulate collection efficiencies from the APS data were greater than 99.99%.

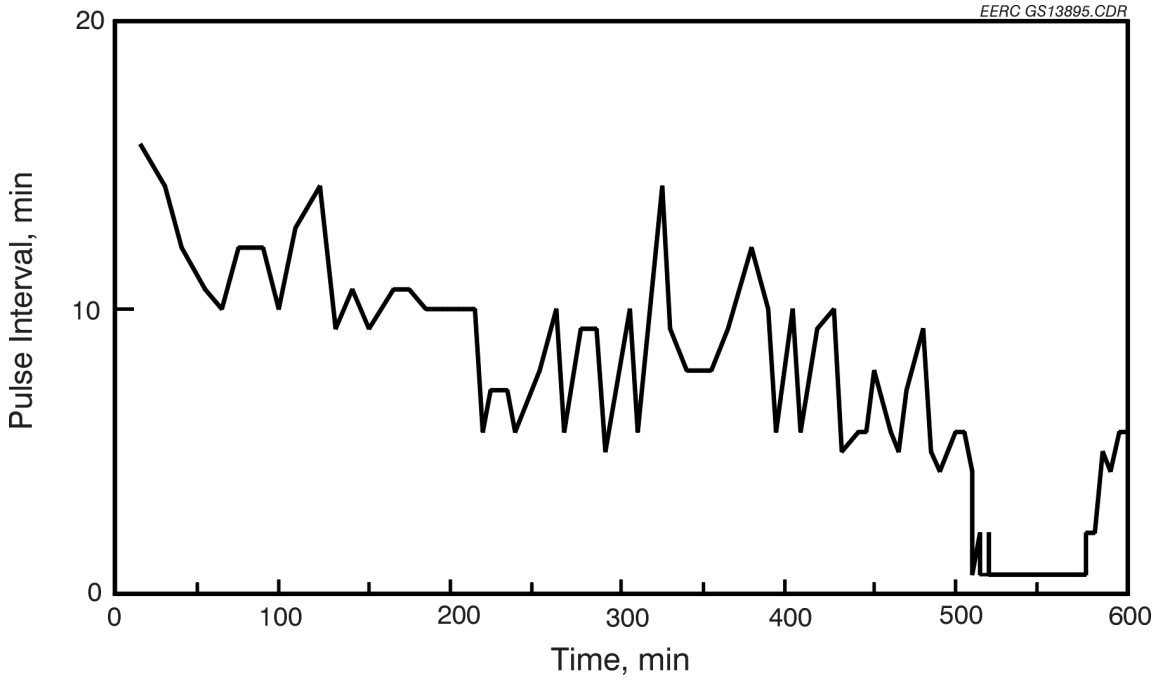

Figure 4.3-16. Pulse interval as a function of time for Test PTC-AB-573 with on-line cleaning using PTFE bags.

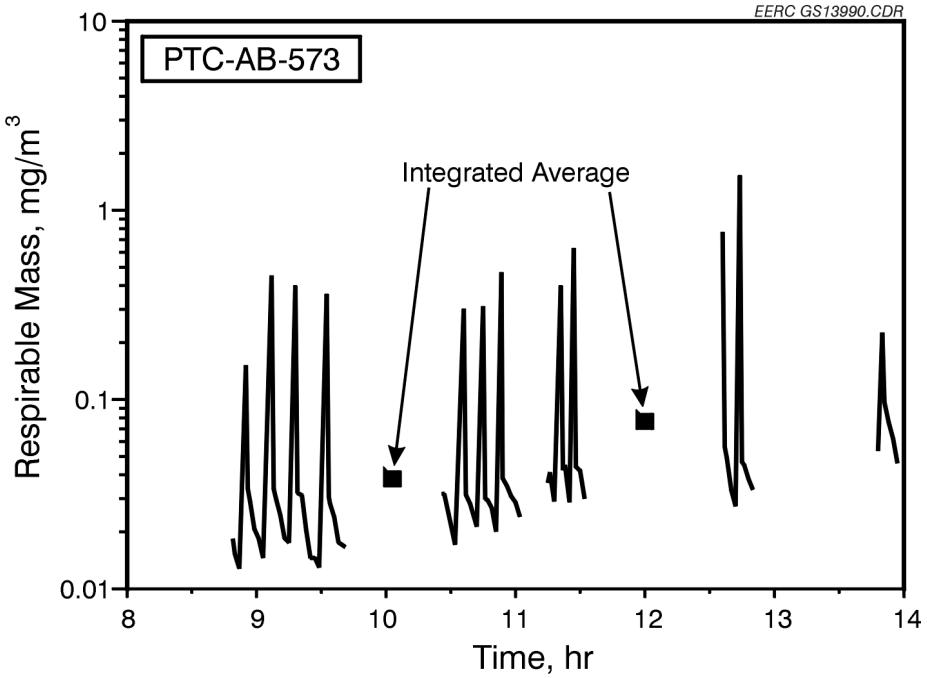

Figure 4.3-17. APS data for Test PTC-AB-573.

The dust loadings calculated from the hopper ash collected after each test agreed within 10% of the inlet dust loadings from EPA Method 5 sampling for both Tests PTC-AB-572 and 573, as shown in Table 4.3-2. The agreement of inlet dust loading confirms the improvement of the butterfly baffle design over the V baffle design.

Since the bags did not clean as well as expected in Tests 572 and 573, a decision was made to evaluate the particulate collection efficiency of the AHPC with the ESP on and off and the bags removed. These tests would determine the collection efficiency of the ESP alone and of the AHPC vessel alone as a knockout chamber.

4.3.1.4 AHPC Performance of the ESP Only

To help evaluate the performance of the ESP and the interaction between the electrostatic and filtration zones, it was desirable to know how much dust the ESP collected and how much dust the bags collected. Since this cannot be determined directly, an approach to determine the ESP performance was to run some tests without bags installed. The ESP was also turned off to observe the AHPC operating as a knockout chamber.

Table 4.3-2 presents the outlet dust loading for Test PTC-AB-574. With the ESP on and bags removed, the particulate emissions ranged between 0.2840 to 0.3728 g/m^3 (0.1240 to 0.1628 gr/scf). Efficiency was calculated using the average of the inlet dust loading of Tests PTC-AB-572 and PTC-AB-573 and the outlet dust loadings of Test PTC-AB-574. The AHPC efficiency with the ESP on without bags was about 95%. This result was encouraging because 90%–95% efficiency for the ESP was the basis for the original concept.

With the ESP off and bags removed, the AHPC outlet dust loadings ranged from 4.0998 to 4.4847 g/m^3 (1.7903 to 1.9584 gr/scf), which corresponds to a collection efficiency of 46%. Again, this result is not surprising considering the dust enters a large chamber and then must exit through the relatively small holes in the tube sheet.

APS respirable mass data, presented in Figure 4.3-18, show the AHPC outlet particulate emission when the ESP was on and when the ESP was off. With the ESP on, the APS showed an average outlet emission of about 220 g/m^3. The average respirable mass emission when the ESP was off was approximately 1300 g/m^3, which is in the range of inlet respirable mass levels measured and indicated that the chamber alone will collect only the larger particles. The ESP by itself, however, achieved 83% collection efficiency of respirable mass. Again, this result is encouraging, because it shows that the ESP removes a substantial portion (83%) of the fine-particle mass, so all of the fine-particle mass will not have to be collected by the bags. These values agree well with theoretical modeling of low-SCA precipitators for fine particles (See Appendix B).

Because of the marginal bag cleaning observed in Tests 573 and 574, several changes were made to the AHPC. First, larger-nozzle pipes were installed to facilitate higher energy pulsing, and, second, the high-voltage electrode was modified to make it directional. The objective of the next tests (Tests PTC-AB-575, 576, 577, and 578) was to study the effects of A/C ratio and off-

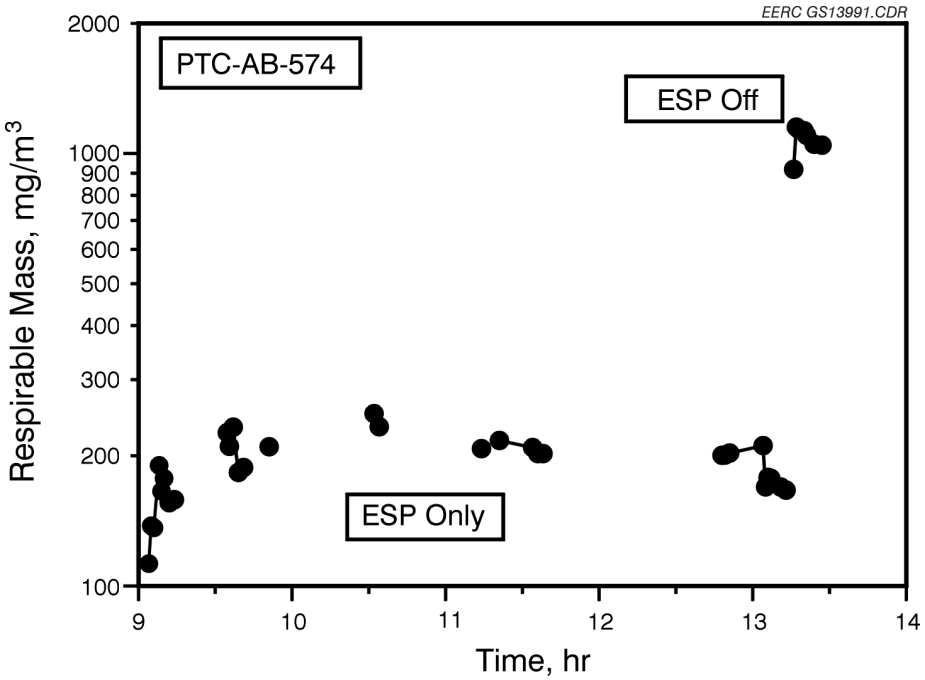

Figure 4.3-18. APS data for Test PTC-AB-574.

line and on-line modes of cleaning after making the modifications. Test parameters are presented in Table 4.3-1. Particulate data are presented in Table 4.3-2.

Test PTC-AB-575 operated at an A/C ratio of 3.7 m/min (12 ft/min) in off-line cleaning mode, and Test PTC-AB-576 operated at an A/C ratio of 3.7 m/min (12 ft/min) in on-line cleaning mode. Tests PTC-AB-577 and 578 operated at an A/C ratio of 4.9 m/min (16 ft/min) in off-line and on-line cleaning modes, respectively. The same set of PTFE bags was used throughout the week of testing. Normally, dP versus time graphs are obtained from the computer-operated data acquisition system. However, the data acquisition system malfunctioned, and so graphs generated during this test period were made by manually inputting the data. Because of this, the graphs appear with a more straight-lined appearance. The graphs, however, still accurately reflect the test data.

4.3.1.5 Effect of On-Line or Off-Line Cleaning After AHPC Modifications

A new set of PTFE-only bags was installed prior to Test PTC-AB-575. The flow from the combustor during start-up on gas was passed through the AHPC. During the heatup period, the dP increased approximately 0.5 kPa (2 in. W.C.), similar to that increase noted in previous observations. When coal is first introduced to the combustor, the AHPC is bypassed until a stable flame is achieved, which normally takes about 10 min. However, the operator forgot to bypass the AHPC when starting coal, which resulted in high-carbon ash reaching the bags. Because of uncertainty over the effect on AHPC operation, the decision was made to install another set of new bags. With the new bags and in the absence of flue gas exhaust, the starting dP was only 0.5 kPa (2 in. W.C.). This led to the conclusion that the start-up procedure on gas might be adversely affecting bag cleanability.

The dP versus time graph for Test PTC-AB-575 is presented in Figure 4.3-19. The change in dP before and after cleaning was 1.25 to 1.40 kPa (5.0 to 5.5 in. W.C.) through 8 hr of testing. This is a dramatic improvement compared with a similar test, PTC-AB-572, in which the change in dP before and after cleaning averaged 0.37 kPa (1.5 in. W.C.) Figure 4.3-20 shows the pulse

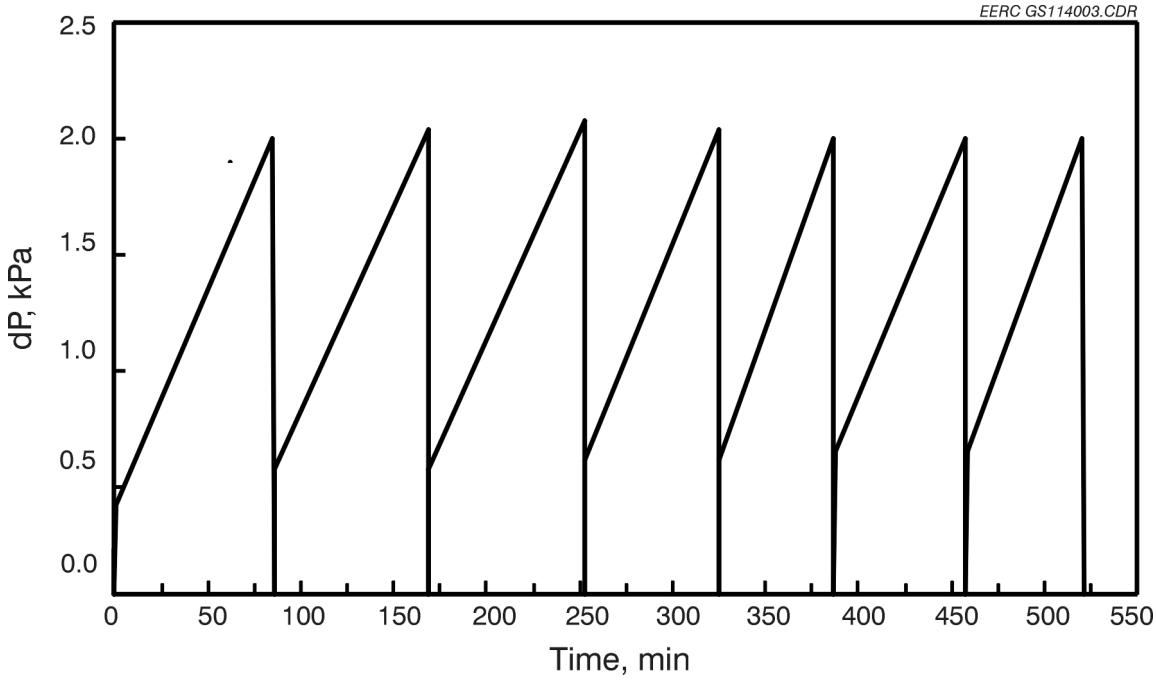

Figure 4.3-19. Pressure drop as a function of time for Test PTC-AB-575 with on-line cleaning using PTFE bags.

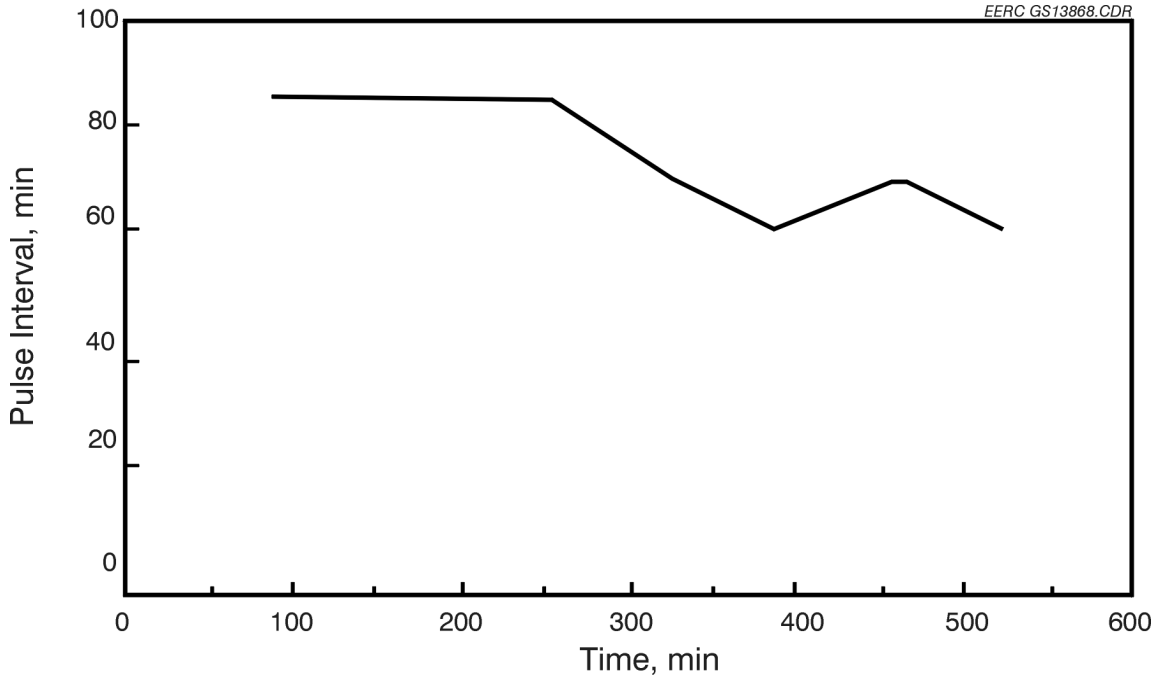

Figure 4.3-20. Pulse interval as a function of time for Test PTC-AB-575 with on-line cleaning using PTFE bags.

interval to be steady at about 70 min. Again, this is a significant improvement over the pulse interval of about 10 min in Test PTC-AB-572. These changes in dP and pulse interval confirmed that the change in start-up procedure improved the operability of the AHPC; however, the addition of a new ESP electrode may have also helped to improve the performance of the AHPC.

The inlet and outlet dust-loading data for the test are presented in Table 4.3-2. Particulate collection efficiency was 99.968%. The somewhat lower particulate efficiencies for this week of tests were traced to insufficiently cleaned AHPC outlet piping and to contamination from pipe-threading paste used on the pulse piping in the outlet plenum. Inspection of the outlet dust-loading filters confirmed the presence of a few large particles that biased the data.

The graph of respirable mass versus time is presented in Figure 4.3-21. The integrated average value for respirable mass was about 0.1 mg/m^3, which equates to a particulate collection efficiency of about 99.99%. These APS results indicate more particle mass in the 5–15-µm range than in previous tests, which further suggests that contamination in the outlet plenum and piping led to the decrease in particulate collection efficiency.

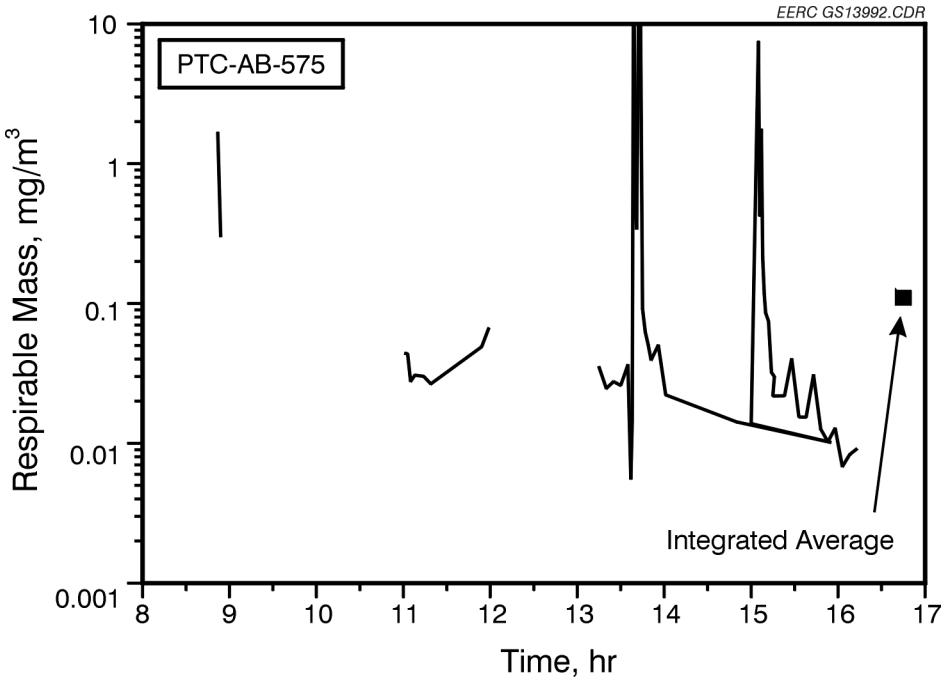

Figure 4.3-21. APS data for Test PTC-AB-575.

In Test PTC-AB-576, the AHPC was set in the on-line cleaning mode. The dP versus time graph is shown in Figure 4.3-22. The change in dP before and after cleaning was at 1.12 to 1.25 kPa (4.5 to 5.0 in. W.C.), with pulse intervals averaging around 70 min (see Figure 4.3-23). Inlet/outlet dust loadings were 9.9274 and 0.0046 g/m^3 (4.3351 and 0.0020 gr/scf), for a collection efficiency of 99.955% (Table 4.3-2). Figure 4.3-24 presents the respirable mass versus time graph for Test PTC-AB-576. Again, both the APS and dust-loading data indicated lower collection efficiencies than previously observed, but this was attributed to the outlet contamination previously mentioned.

4.3.1.6 Air-to-Cloth Ratio Tests

Since Tests 575 and 576 both demonstrated excellent pressure drop control and at least a 70-min bag-cleaning interval, the decision was made to increase the A/C ratio from 3.7 m/min (12 ft/min) to 4.9 m/min (16 ft/min). This was accomplished by disabling the pulse nozzle for one bag and placing a cup over the top of the bag on the clean side of the tube sheet. The cup was

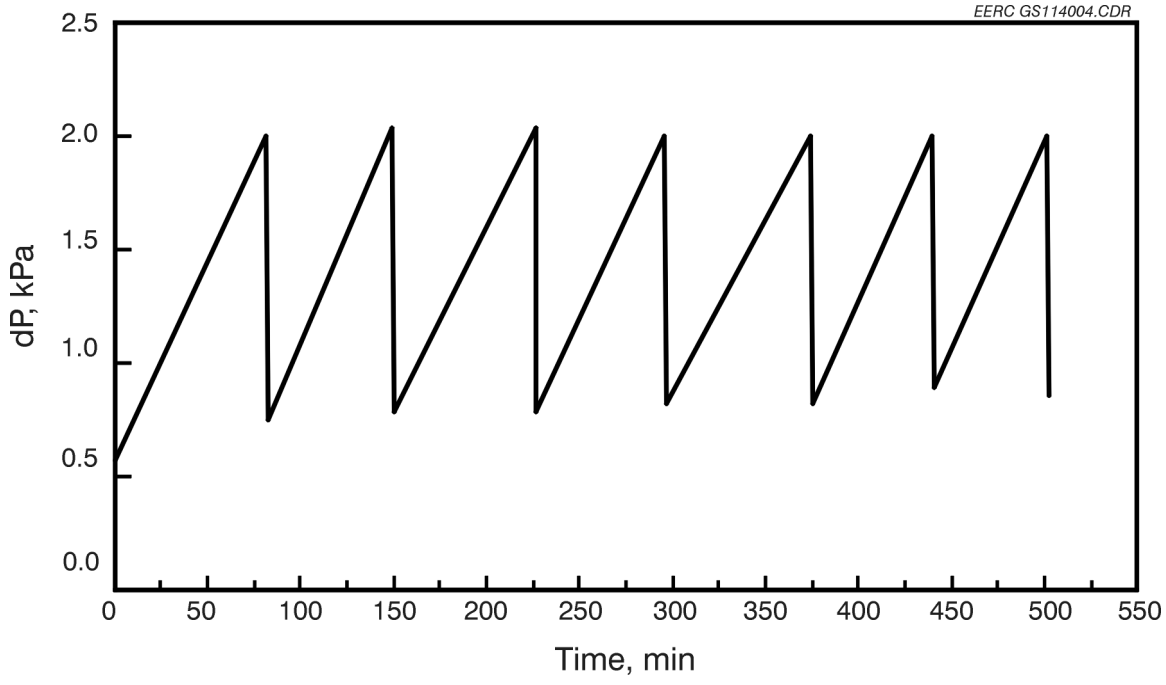

Figure 4.3-22. Pressure drop as a function of time for Test PTC-AB-576 with on-line cleaning using PTFE bags.

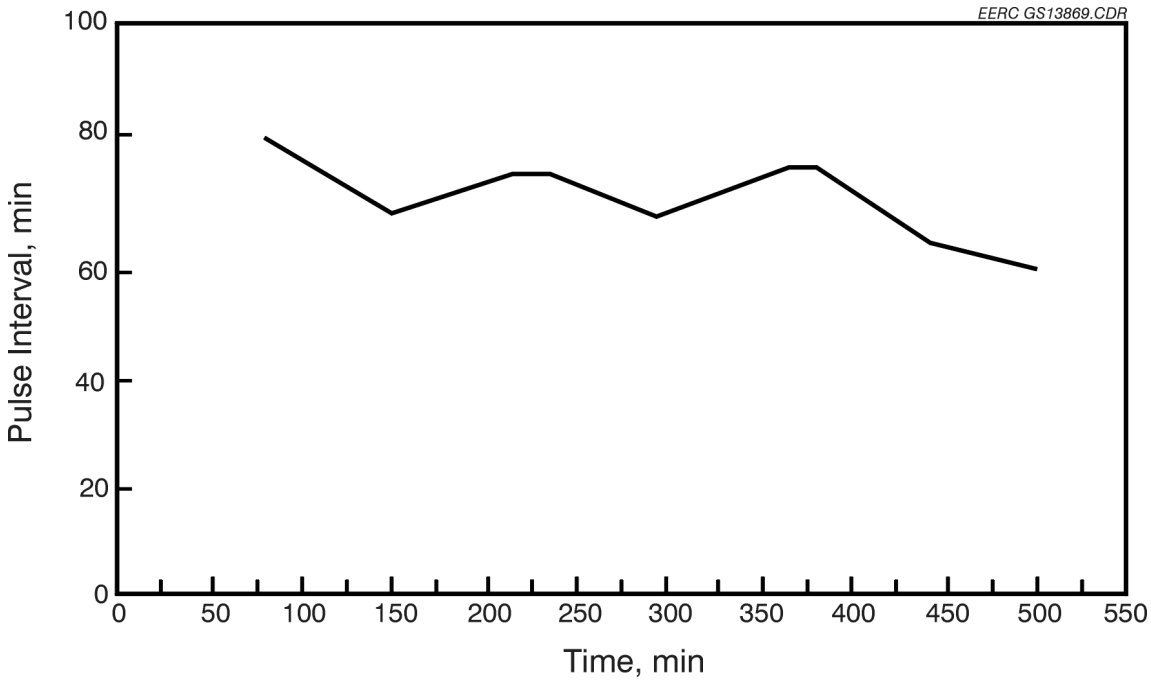

Figure 4.3-23. Pulse interval as a function of time for Test PTC-AB-576 with on-line cleaning using PTFE bags.

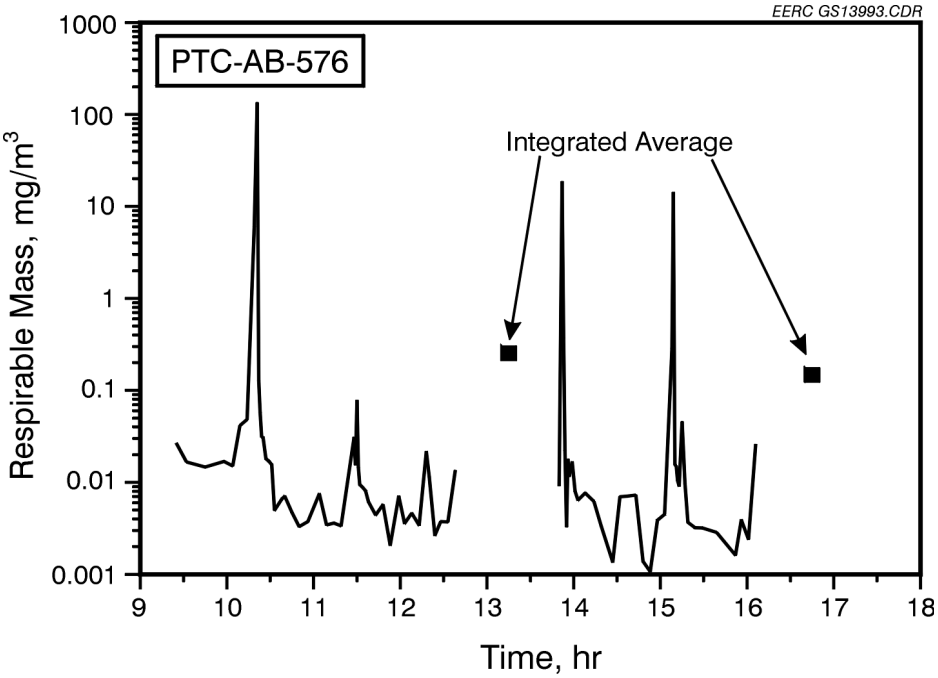

Figure 4.3-24. APS data for Test PTC-AB-576.

sealed against the tube sheet to prevent any flow from going through the bag. For the first test (PTC-AB-577) at 4.9 m/min (16 ft/min), cleaning was off-line. Changes in the dP before and after the cleaning cycle ranged from 0.62 to 0.50 kPa (2.5 to 2.0 in. W.C.) at steady state, as shown in Figure 4.3-25. Pulse intervals decreased from 20 min at the beginning of the test to around 10 min at steady state, as shown in Figure 4.3-26.

Particulate data for Test PTC-AB-577 are found in Table 4.3-2. Inlet and outlet dust loadings and particulate efficiency were 10.5306 g/m^3, 0.0018 g/m^3 (4.5985 gr/scf, 0.0008 gr/scf), and 99.983%, respectively. The integrated average for respirable mass ranged from 0.17 to 0.22 mg/m^3, which also corresponds to an efficiency of 99.98%. The graph for respirable mass versus time is found in Figure 4.3-27. These efficiencies are not quite as high as anticipated, most likely because of outlet contamination, rather than the increase in A/C ratio.

In Test PTC-AB-578, the AHPC was cleaned in the on-line cleaning mode at an A/C ratio of 4.9 m/min (16 ft/min). Similar to off-line cleaning mode, changes in the dP before and after

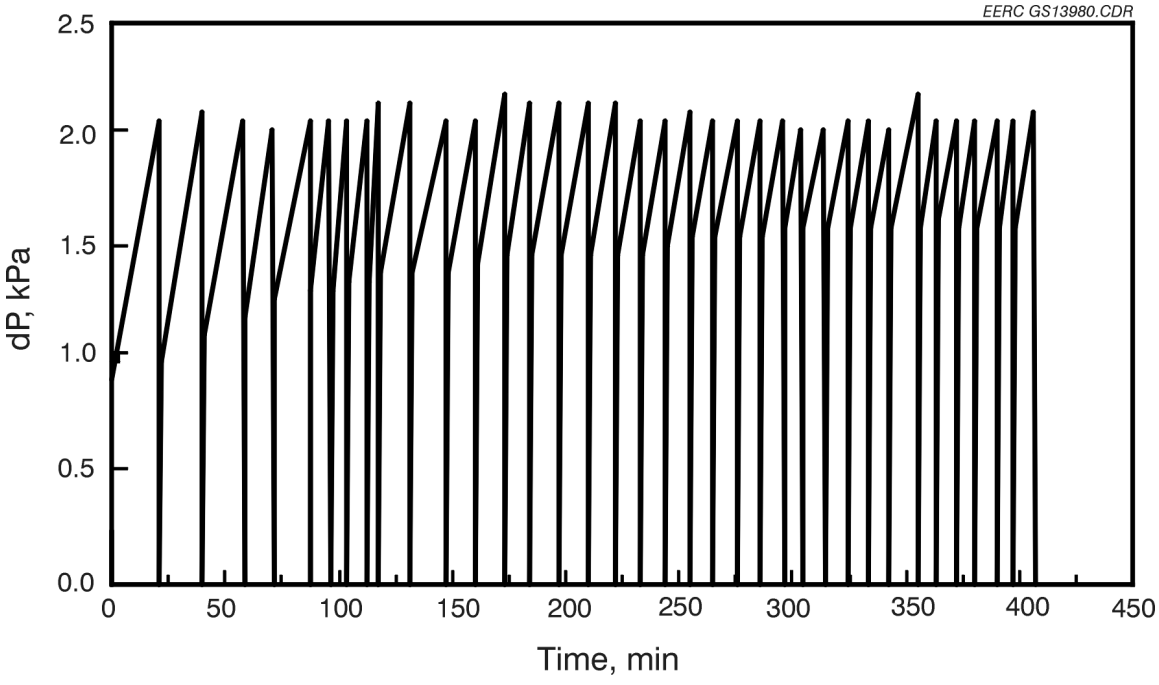

Figure 4.3-25. Pressure drop as a function of time for Test PTC-AB-577 with on-line cleaning using PTFE bags.

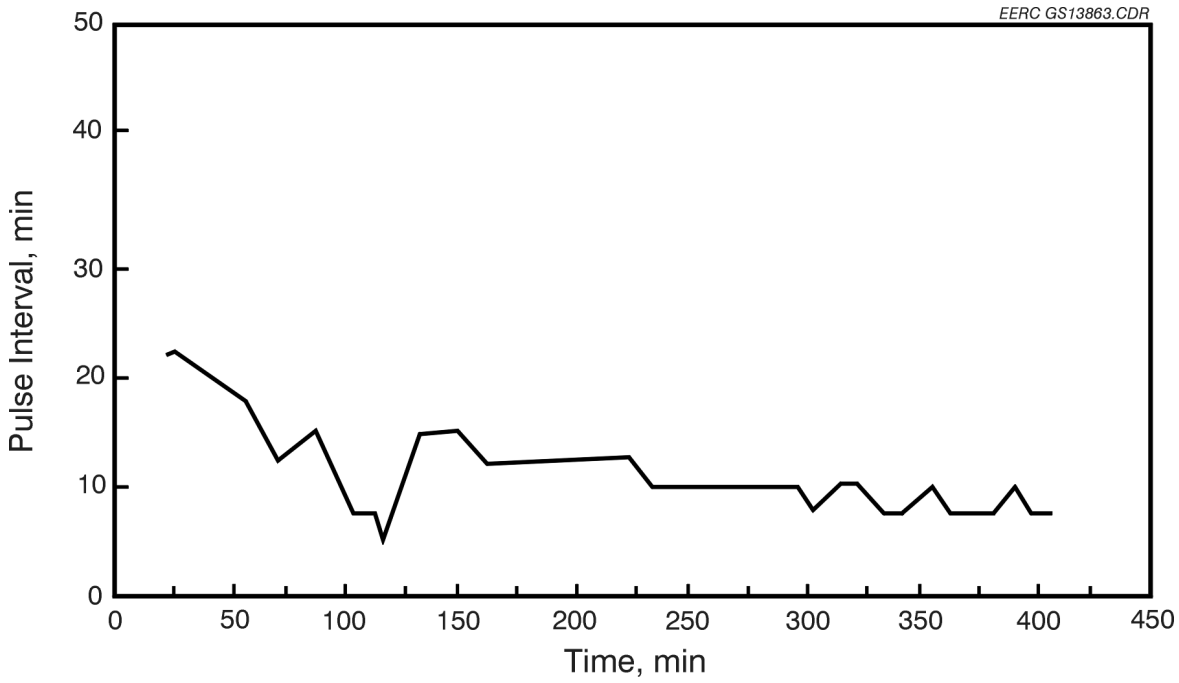

Figure 4.3-26. Pulse interval as a function of time for Test PTC-AB-577 with on-line cleaning using PTFE bags.

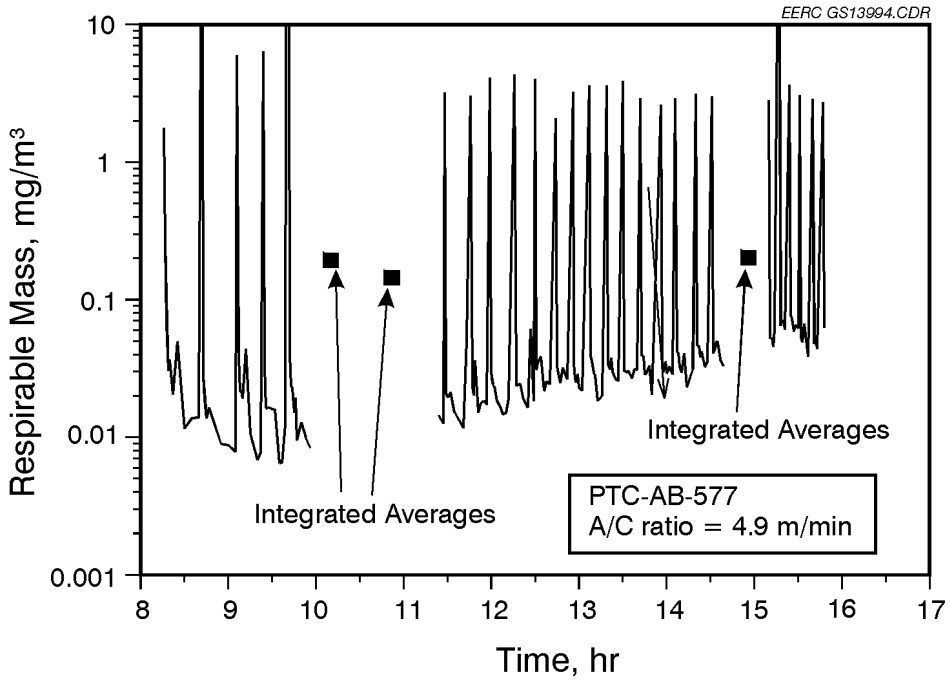

Figure 4.3-27. APS data for Test PTC-AB-577.

the cleaning cycle ranged from 0.62 to 0.50 kPa (2.5 to 2.0 in. W.C.) at steady state. The dP information for the test is shown in Figure 4.3-28. Pulse intervals ranged slightly higher at 10–12 min between cleaning cycles. Figure 4.3-29 presents the pulse interval versus time graph.

Inlet and outlet dust loadings and particulate efficiency were 8.6205 g/m^3, 0.0037 g/m^3 (3.7644 gr/scf, 0.0016 gr/scf) and 99.957%, respectively (Table 4.3-2). Figure 4.3-30 shows the respirable mass versus time of Test PTC-AB-578. The integrated averages were 0.26 and 1.05 mg/m^3. At A/C of 4.9 m/min (16 ft/min), the APS data for on-line cleaning show respirable mass emissions moderately higher than in off-line conditions.

In the postrun evaluation of the last two tests (i.e., Tests PTC-AB-577 and 578), one bag showed mild bag damage due to arcing. The bag was located closest to the inlet baffle. Figure 4.3-31 shows the burn holes and their location along the creases made by the bag cage. The mild damage may have contributed to the observed decrease in particulate collection efficiency. Even though the bag damage was slight, the concern is that it could get worse in

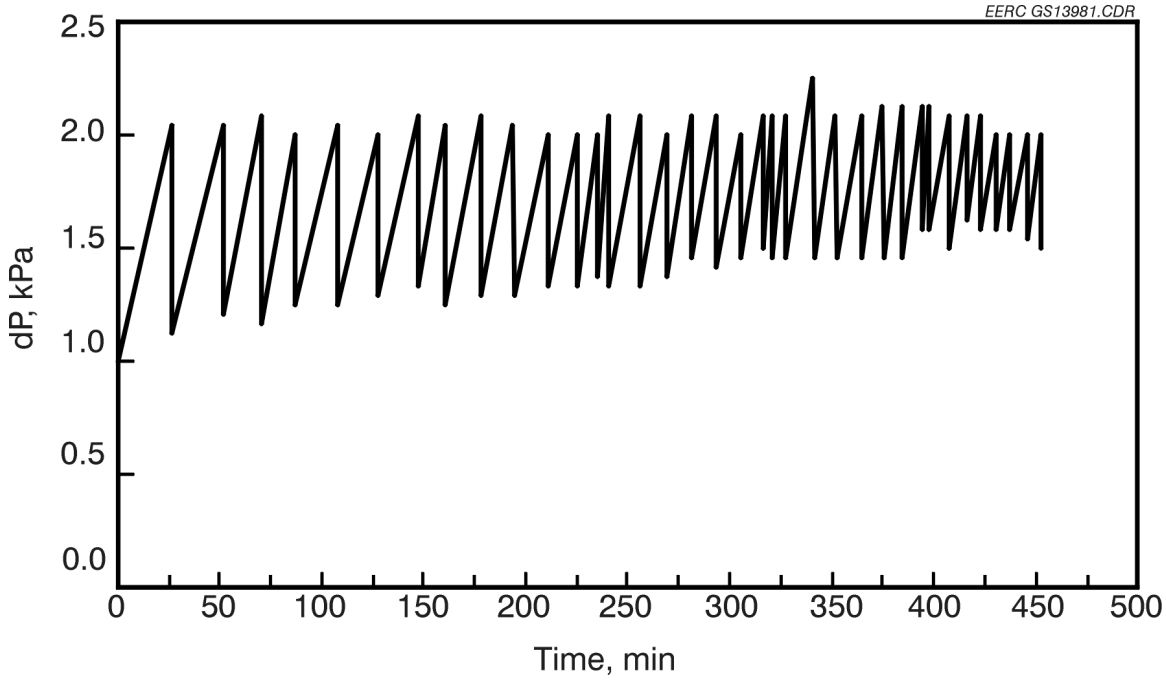

Figure 4.3-28. Pressure drop as a function of time for Test PTC-AB-578 with on-line cleaning using PTFE bags.

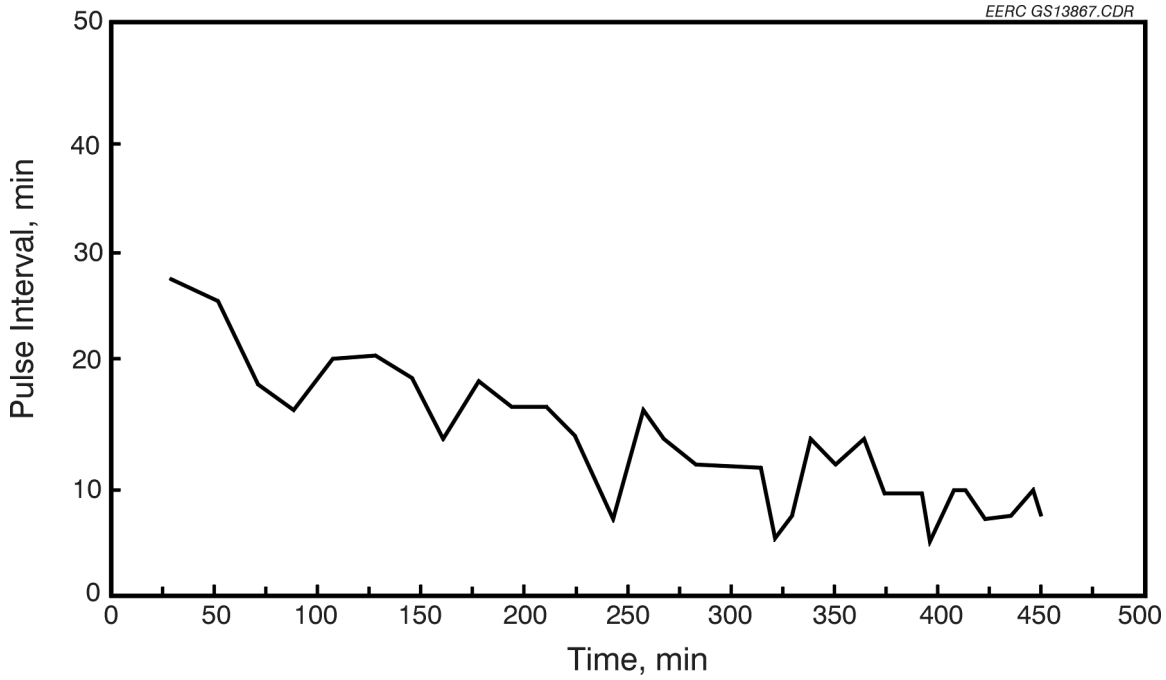

Figure 4.3-29. Pulse interval as a function of time for Test PTC-AB-578 with on-line cleaning using PTFE bags.

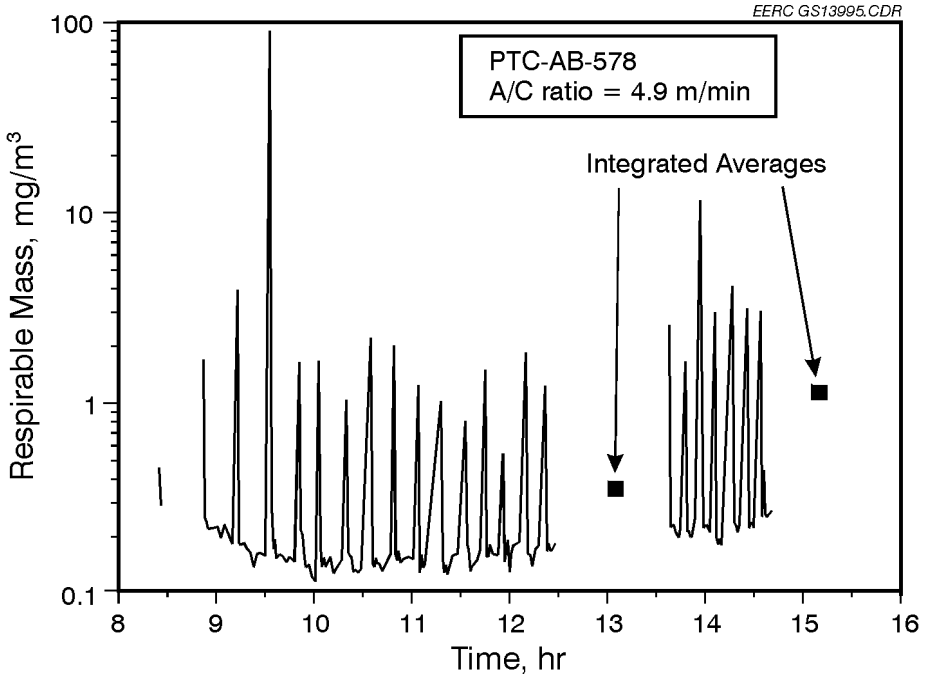

Figure 4.3-30. APS data for Test PTC-AB-578.

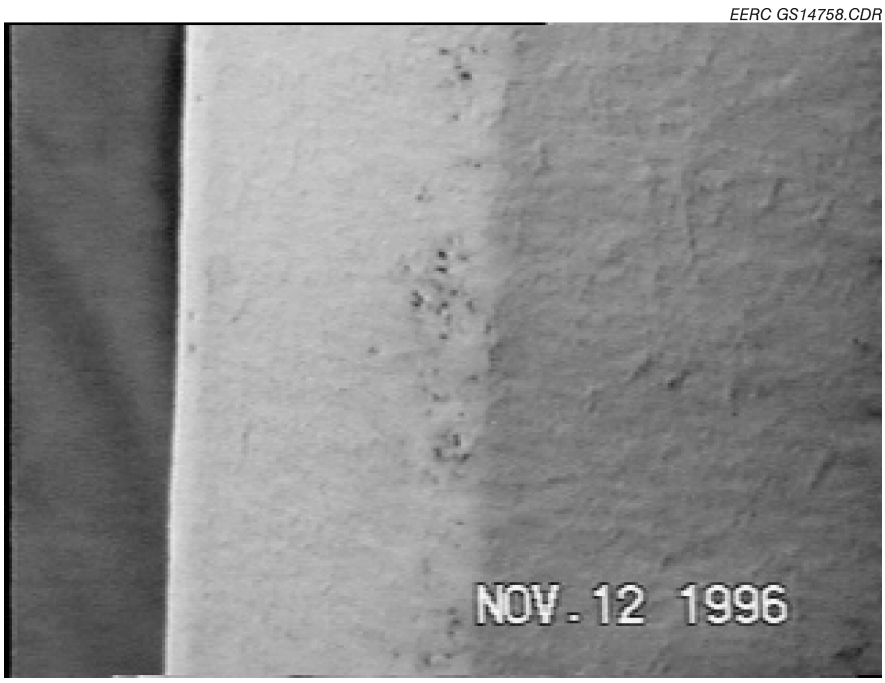

Figure 4.3-31. Close-up view of PTFE Bag A from Tests PTC-AB-577 and 578 showing the burn holes along the crease of the fabric made by the bag cage support.

longer-term operation. No bag damage was observed in the tests at 3.7 m/min (12 ft/min). There is no obvious reason why electrical damage might occur at 4.9 m/min (16 ft/min) and not at 3.7 m/min (12 ft/min). However, there were noticeable differences observed in the gas and dust flow patterns in the AHPC, which could have contributed to the damage. It appeared that there was more turbulence in the area of the baffle exit, first high-voltage electrode, and first bag. Whether this might have resulted in increased ion current to the first bag is unknown. It should be noted that the bags used for these runs were the nonconductive ones. Because of uncertainty over the exact cause of the bag damage, the safest approach for subsequent longer-term tests was to use the conductive bags.

The 4.9 m/min (16-ft/min) tests were successful because the pressure drop was readily controlled, with a pulse-cleaning duration of 10–15 min. However, this is a smaller interval than would be anticipated based on the sole effect of increasing A/C ratio. The theoretical increase in dP as a function of time is proportional to the square of the face velocity, so at 4.9 m/min (16 ft/min), the theoretical cleaning interval should be 0.56 times the interval at 3.7 m/min

(12 ft/min). Based on the 60–70-min pulse interval observed at 3.7 m/min (12 ft/min), the theoretical interval is about 35 min compared to the 10–15-min interval observed. This indicates that additional nonideal effects occurred, such as the change in flow pattern already mentioned. Another effect that could have contributed to the shorter pulse interval is that the three bags were no longer centered front-to-back between the plates. It is possible that removing a different bag or changing the pulse parameters could improve the results. To optimize the results at 4.9 m/min (16 ft/min) would require additional testing of a number of parameters that are beyond the scope of work of the project. The test plan did also call for testing at 7.3 m/min (24 ft/min), but at this point in the development of the AHPC, it was not pursued because there were too many additional questions that needed to be addressed at lower A/C ratios. While operation at 4.9 m/min (16 ft/min) was proven in 8-hr tests, all further testing was conducted at 3.7 m/min (12 ft/min) to facilitate the furthest possible development of the AHPC within the scope of work of the Phase I plan.

4.3.1.7 Particle-Size Distributions and Fractional Efficiency

Figure 4.3-32 plots the combined inlet and outlet particle-size distribution for Test PTC-AB-573. The inlet concentration is a combination of data from the SMPS, multicyclone sampling, and Coulter counter analysis of the first cyclone catch.

While the multicyclone collects all of the inlet ash, it divides it into only six fractions: the five cyclones and a backup filter. The cut point of the first cyclone is typically about 7 μm (depending on temperature and sampling flow rate), and the cut point of the last cyclone is typically about 0.7 μm. To obtain more information about the entire particle-size distribution requires further resolution of the first cyclone catch (which usually contains about 80% of the total mass) and the particles collected on the backup filter. A convenient method to expand the resolution of the first cyclone catch is to perform a Coulter counter analysis on it and to combine the data. Since no instrument is available to accurately determine the distribution of the multicyclone filter catch, the submicron distribution is most conveniently determined by direct sampling of the flue gas with the SMPS. At the outlet, the dust concentration is too low to use

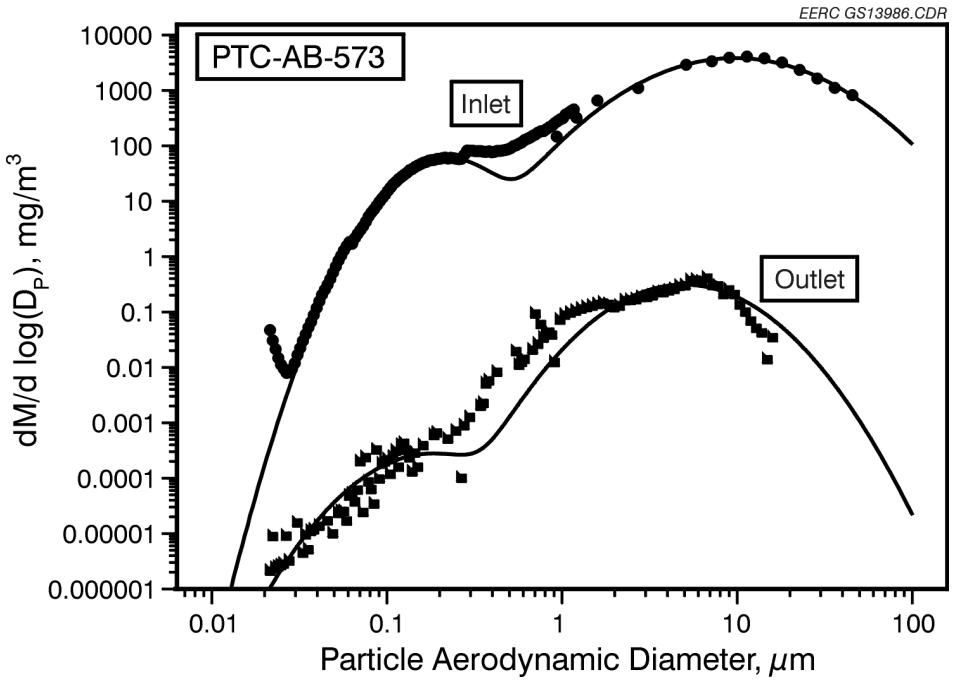

4.3-32. Inlet and outlet particle-size distribution for Test PTC-AB-573.

multicyclones or the Coulter counter, so the distribution is obtained by combining data from the SMPS and APS.

A number of assumptions and conversions were made to combine the data into single particle-size distributions. First, the particle sizes for the SMPS and Coulter data were converted to aerodynamic diameters, which is a function of the geometric particle diameter and the particle density. It was assumed that the SMPS diameter was roughly equal to the geometric diameter, and the density for all particles was 2.5 g/cm^3. Once the particle size was represented in terms of aerodynamic diameter, the mass concentration (mg/m^3) for each channel (size) was calculated. The Coulter counter data represent the first cyclone catch of the multicyclone, which is the upper end of the particle-size distribution. The Coulter counter data are provided in two forms: number of particles counted in each channel and percent of total mass in each channel. The mass concentration was calculated based on the percentage of total mass in each channel, the total mass in the cyclone catch, and the volume of gas sampled. The results are in mg/m^3. The SMPS mass concentration is calculated from the particle geometric diameter, assumed density, and the dilution-corrected number concentration for each channel. The mass distribution for the

multicyclone sample is calculated directly from the data. Once the mass concentration was calculated, it was plotted (on a dM/d log [Dp] basis) as a function of particle size. This convention is used to ensure the data are presented in terms of equal differences in the logarithms of the channel intervals for each sampling method.

The outlet concentration is a combination of the SMPS and APS data collected at the outlet of the AHPC under various operating conditions. The outlet SMPS data are processed the same as the inlet data. The APS mass concentration can be downloaded as a function of aerodynamic diameter. The APS software automatically corrects for dilution and requires an input value for density, which is measured with a helium–air pycnometer. The APS samples represent the particulate emissions for an entire cleaning cycle or multiple cycles. This gives a representation of the true collection efficiency for the AHPC. The SMPS software does not allow samples longer than 5 min. Therefore, samples were taken immediately after a pulse and prior to pulsing to get a full range of the submicron particle collection efficiency.

Both the inlet and outlet distributions can be represented by bimodal log-normal equations (see Figure 4.3-32). From these equations, the fractional efficiencies for each set of AHPC operating conditions can be determined. Figure 4.3-33 represents a test condition, burning Absaloka subbituminous coal, where there was contamination in the outlet gas stream. Note the significantly greater mass measured in the 5–20-μm range in Figure 4.3-33 compared to Figure 4.3-32. This contamination was confirmed by the EPA Method 5 dust loadings.

4.3.1.8 Conclusions from 8-hr Tests Firing Absaloka Coal

The AHPC demonstrated good bag cleanability and operability, with particulate collection efficiencies of 99.99% achieved.

- For the initial tests, off-line bag cleaning produced pulse intervals of 20–30 min, while the pulse interval for on-line cleaning was about 15 min.

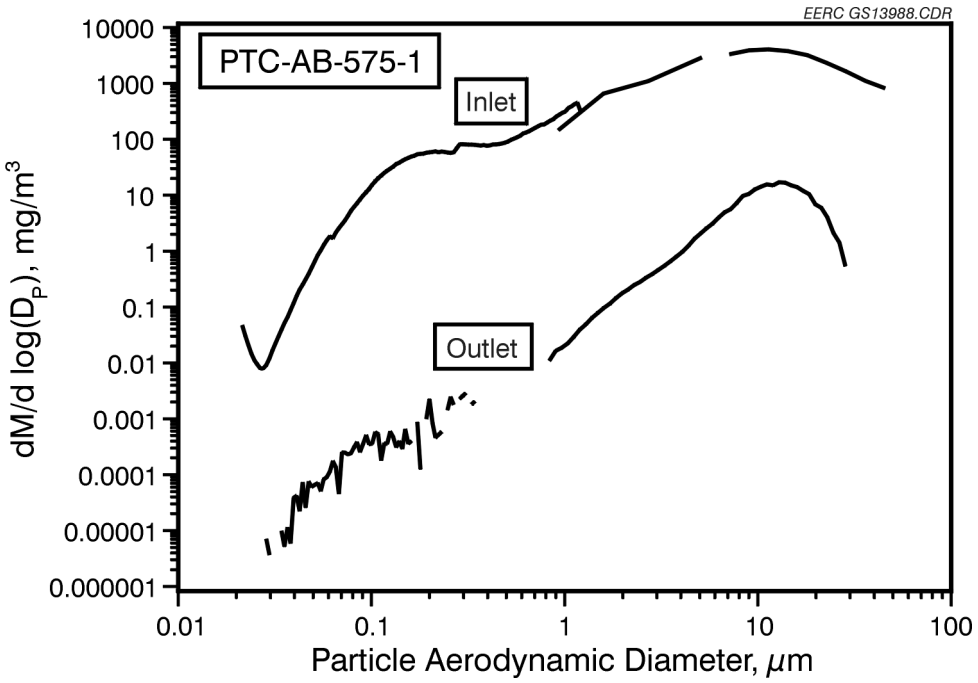

4.3-33. Contamination in the outlet gas stream from sources other than the emission from the AHPC can be seen in this figure.

- No significant differences were observed between the PTFE-only bags and the graphite-impregnated PTFE bags in collector efficiency or pressure drop.

- The change in the start-up procedure made a dramatic improvement in performance. The new butterfly baffle corrected the problem of ash dropout in the inlet plenum.

- Without bags, the total mass ESP particle collection efficiency in the AHPC was 95%, and the respirable mass efficiency was 83%.

- The collection efficiency of the AHPC shell with no bags and the ESP off was 48%.

- The new electrode modification to the ESP grid increased current flow and improved the pulse-cleaning interval to 70 min.

- Successful operation was achieved at 4.9 m/min (16 ft/min) with a pulse interval of 10–15 min.

4.3.2 8-hr Test Results Firing Blacksville Bituminous Coal

Six 8-hr tests of the AHPC firing Blacksville bituminous coal were completed. The objectives of these tests were as follows:

- Test operability with real flue gas firing a bituminous coal
- Test on-line versus off-line cleaning
- Test system recovery with the ESP off and then back on
- Test bag type
- Test the effects of NH_3/SO_3 conditioning

Operation variables for all of the Blacksville bituminous-fired tests are found in Table 4.3-5; the particulate information is listed in Table 4.3-6; and average concentrations of flue gas constituents are presented in Table 4.3-7. Operating the AHPC using Blacksville bituminous was somewhat more difficult because of the higher carbon content of the ash. The loss-on-ignition value for the ash was 2.3% by weight. The unburned carbon in the ash tended to accumulate on the surface of electrical insulators, forming a conductive path that led to arcing between the high-voltage electrode and ground. There were also problems with the coal feed, which resulted in occasional higher levels of carbon carryover into the AHPC. A very high submicron mass loading observed with the SMPS at the outlet of the AHPC was caused by high SO_3 in the flue gas (11.1 ppm).

4.3.2.1 Effect of On-Line or Off-Line Bag Cleaning

The first test with Blacksville coal, PTC-BV-579, was at an A/C of 3.7 m/min (12 ft/min), and bag cleaning was done off-line. New graphite-impregnated bags were installed at the beginning of the test. Figure 4.3-34 gives the dP versus time graph showing the change in dP

TABLE 4.3-5

Test Parameters for Blacksville Coal

Date:	11-18-96	11-19-96	12-16-96	12-17-96	12-18-96	12-19-96
PTC Test No.	PTC-BV-579	PTC-BV580	PTC-BV-581	PTC-BV-582	PTC-BV-583	PTC-BV-584
A/C Ratio, m/min (ft/min)	3.7 (12)	3.7 (12)	3.7 (12)	3.7 (12)	3.7 (12)	3.7 (12)
Inlet Temp., °C (°F)	149 (300)	149 (300)	149 (300)	149 (300)	149 (300)	149 (300)
On-Line and Off-Line Cleaning	Off	On	Off	On	Off	On
Baffling	Butterfly	Butterfly	Butterfly	Butterfly	Butterfly	Butterfly
Voltage, kV	50	50	50	50	50	50
Type of Bag	Graphite–PTFE Set 7	Graphite–PTFE Set 7	PTFE Set 8	PTFE Set 8	PTFE Set 8	PTFE Set 8
No. of Bags in Use	4	4	0	4	4	4
Pulse Pressure, kPa (psig)	621 (90)	621 (90)	621 (90)	621 (90)	621 (90)	621 (90)
Pulse Duration, s	0.2	0.2	0.2	0.2	0.2	0.2
Pulsing Initiation Pressure, kPa (in. W.C.)	2.0 (8.0)	2.0 (8.0)	2.0 (8.0)	2.0 (8.0)	2.0 (8.0)	2.0 (8.0)

TABLE 4.3-6

Dust-Loading Data for Blacksville Coal

Date	PTC Test No.	Hopper Ash, g/m^3	Inlet, g/m^3	Outlet, g/m^3	Percent Collection Efficiency
11-18-96	PTC-BV-579	3.98	5.7779	0.0014	99.976[1]
11-19-96	PTC-BV-580	5.43	5.9350	0.0000	100.000
12-16-96	PTC-BV-581	5.91	7.4072	0.0021	99.973
12-17-96	PTC-BV-582	4.99	4.4376	0.0005	99.992
12-18-96	PTC-BV-583	4.81	4.3366	0.0005	99.992
12-19-96	PTC-BV-584	4.76	4.9311	0.0055	99.887[2]

[1] SO_3 on filter.

[2] Gasket degradation observed as a source of outlet contamination.

TABLE 4.3-7

Average Flue Gas Concentrations for Tests PTC-BV-579 to PTC-BV-584[1]

O_2, % by volume	CO_2, % by volume	H_2O, % by volume	SO_2, ppm	SO_3, ppm	NO_x, ppm
4–4.5	13–14.5	8	1650–1800	11.1	525–600

[1] Dry basis except for H_2O.

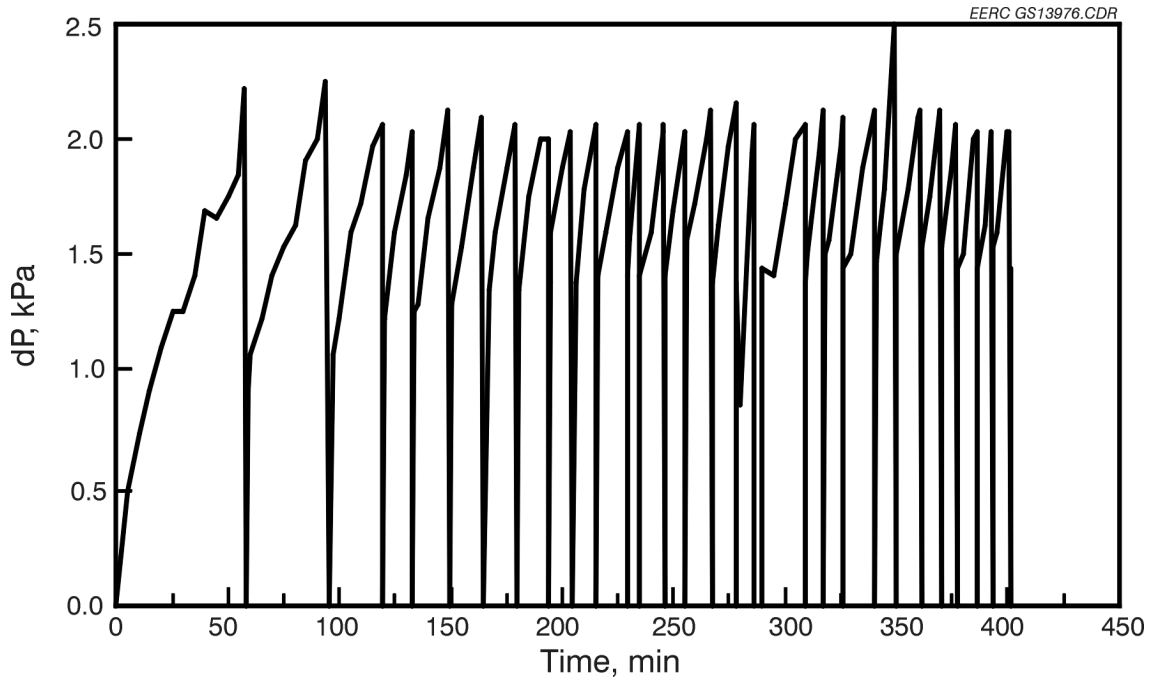

4.3-34. Pressure drop as a function of time for Test PTC-BV-579 with on-line cleaning using PTFE bags.

before and after a cleaning cycle to average about 0.5 kPa (2.0 in. W.C.) The pulse interval reached a steady state of approximately 10–15 min. The pulse interval versus time graph is found in Figure 4.3-35.

The dust-loading data in Table 4.3-6 show the inlet particulate loading to be 5.7779 g/m^3 (2.5231 gr/scf) and the outlet loading to be 0.0014 g/m^3 (0.0006 gr/scf). The particulate collection efficiency was calculated at 99.976%. The somewhat low apparent collection efficiency was primarily caused by SO_3 accumulation on the dust-loading filter. The filter was kept at 121°C (250°F), which is well below the acid dew point for 11.1 ppm SO_3. For later tests

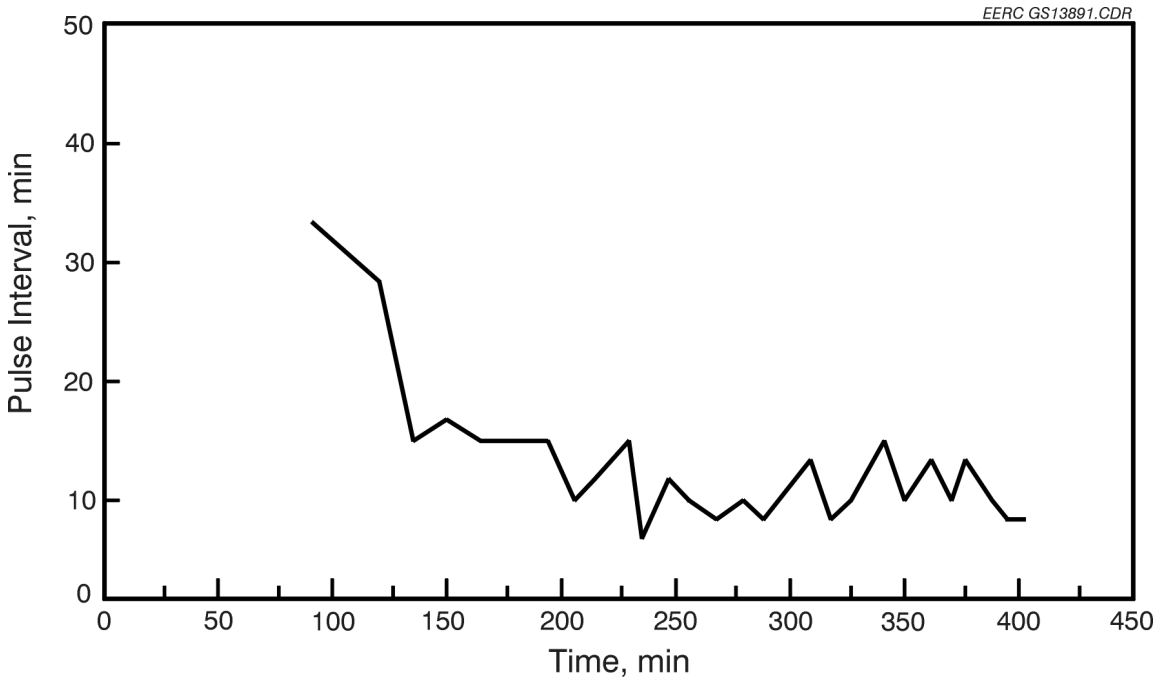

Figure 4.3-35. Pulse interval as a function of time for Test PTC-BV-579 with on-line cleaning using PTFE bags.

with Blacksville coal, the filter temperature was increased to 177°C (350°F) to prevent acid condensation on the sampling filter. The graph of respirable mass versus time is presented in Figure 4.3-36. Two integrated averages were done in this test. The integrated average values were 0.02 and 0.03 mg/m^3. The APS data indicate particulate efficiencies of >99.99%.

Based on stack sampling for SO_3 by the controlled condensation method, the concentration of SO_3 in the flue gas was found to be 11.1 ppm. Based on the SMPS mass concentration, the SO_3 concentration was calculated to be approximately 8 ppm.

Run PTC-BV-580 was done using the same GORE-TEX® graphite-impregnated bags as used in PTC-BV-579, but the mode of cleaning was on-line, as shown in Figure 4.3-37. The changes in dP before and after a cleaning cycle averaged about 0.42 kPa (1.7 in. W.C.) Pulse interval ranged from 5 to 8 min at steady state. Figure 4.3-38 presents a graph of the pulse interval versus time.

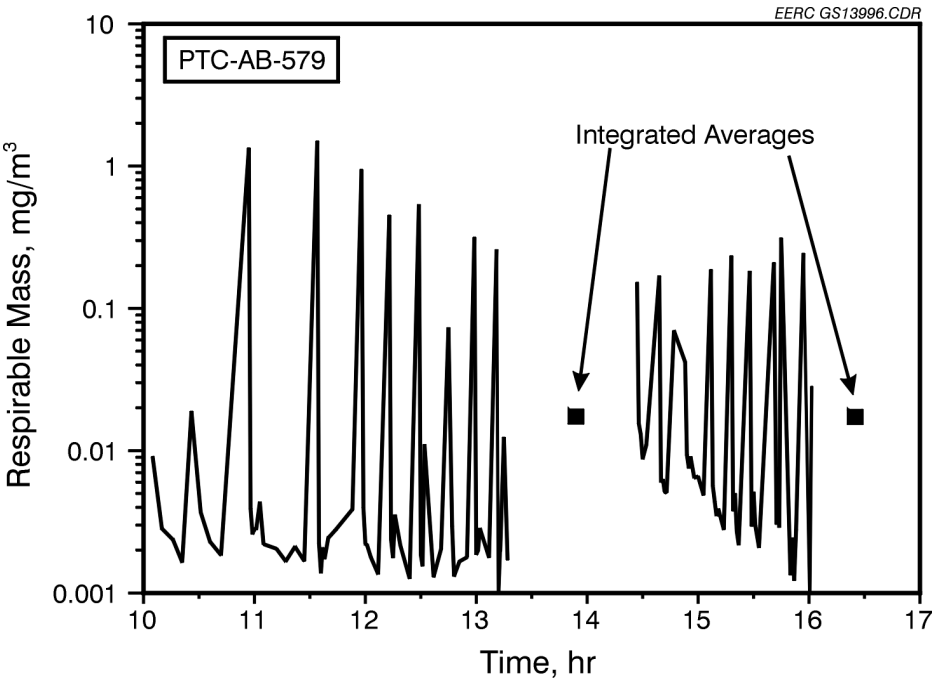

Figure 4.3-36. APS data for Test PTC-BV-579.

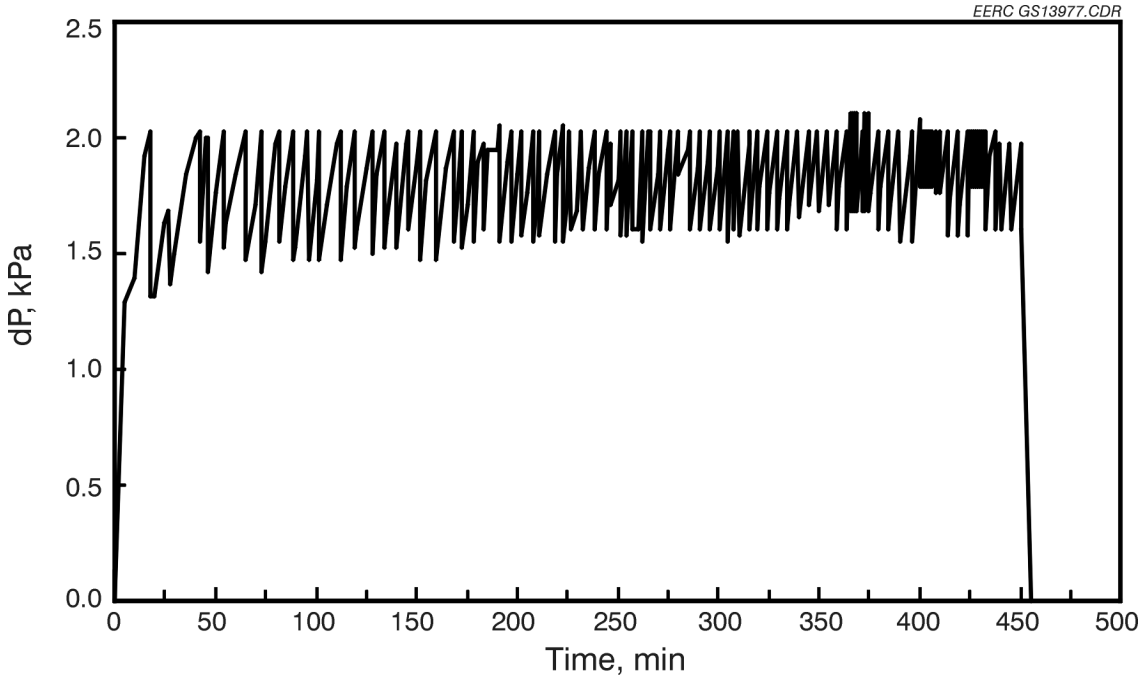

Figure 4.3-37. Pressure drop as a function of time for Test PTC-BV-580 with on-line cleaning using PTFE bags.

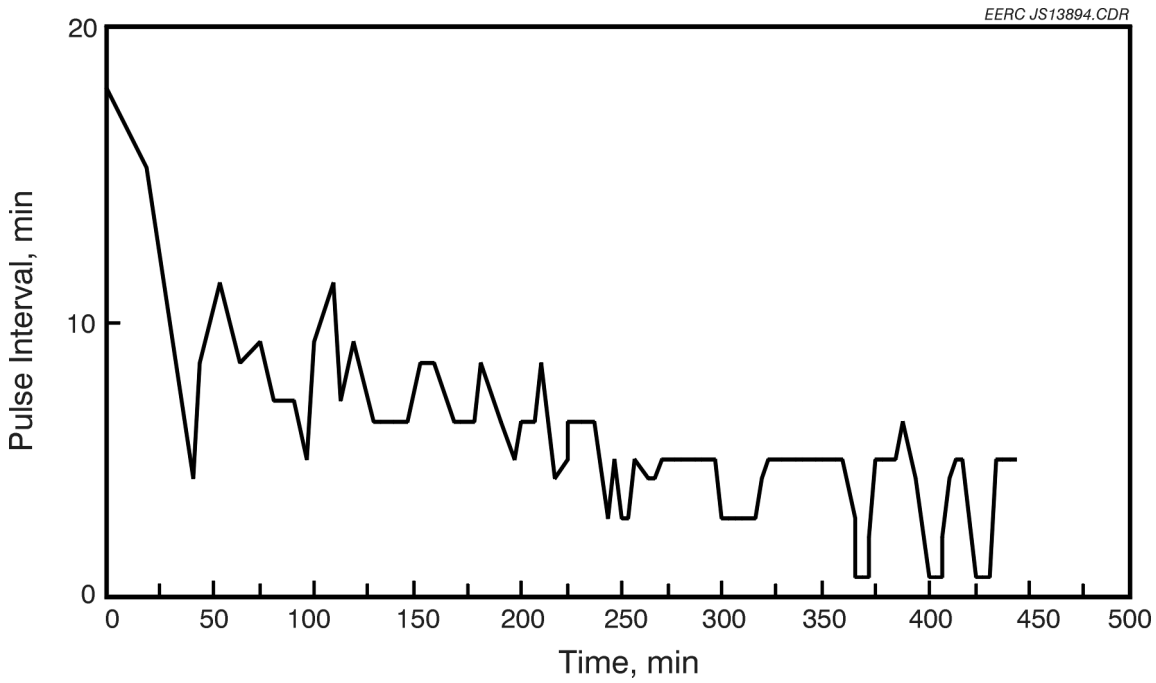

Figure 4.3-38. Pulse interval as a function of time for Test PTC-BV-580 with on-line cleaning using PTFE bags.

Inlet dust loading (Table 4.3-6) was 5.9350 g/m^3 (2.5045 gr/scf). Because of a weighing error, the outlet dust loading was erroneous. Therefore, no total mass particulate collection efficiency was calculated for this test. APS data are presented in Figure 4.3-39. Three integrated average APS measurements range from 0.009 to 0.02 mg/m^3, indicating the respirable mass collection efficiency was >99.99%.

Since there were arcing problems with the ESP and the pulse interval was from 5 to 8 min, the ESP was turned off and then back on three times at the end of this test period to determine if the ESP was providing any benefit. With the ESP off, the dP before and after bag cleaning ranged from about 0.25 to 0.12 kPa (1.0–0.5 in. W.C.), with a pulse interval between 45 and 60 s. Figure 4.3-37 shows the recovery of the AHPC cleaning performance after the ESP was turned back on. These results show that the ESP was still providing a significant benefit, even though the ESP performance was severely compromised by arcing over the insulators. It should be noted that these arcing problems should not be considered chronic, because much larger insulators would be used in a full-scale unit. For the 5.7-m^3/min (200-acfm) model, smaller insulators were

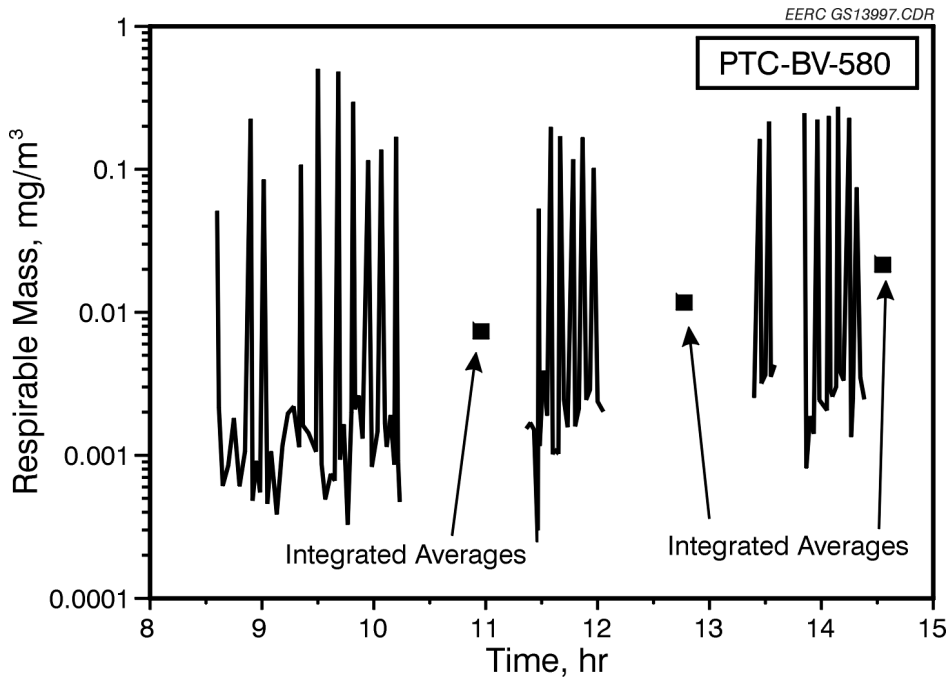

Figure 4.3-39. APS data for Test PTC-BV-580.

used because of space considerations. Prior to the next tests, the insulators were improved to minimize the arcing.

After these improvements were made, Tests 579 and 580 were repeated as Tests 581 and 582 with a new set of graphite-impregnated bags.

4.3.2.2 Repeat 8-hr Tests Firing Blacksville Coal

For Test PTC-BV-581, the bag-cleaning mode was set for off-line. Figure 4.3-40 shows the dP versus time graph of the test. During the first cleaning cycle, the dP jumped from 1.25 to 2.50 kPa (5 to >10 in. W.C.). This was due to a slug of ash and unburned carbon flooding the AHPC compartment. During this upset, the ESP current went up from 3.5 mA to the set upper limit of 4.25 mA. Visual inspection in the AHPC revealed arcing occurring across various places on the grid. This occasional slugging continued until 320 min into the test. At that point, it was determined that the fuel gun supplying the mix of air and coal into the combustor was obstructed. After the gun was cleaned, the dP versus time graph shows more consistent steady-state

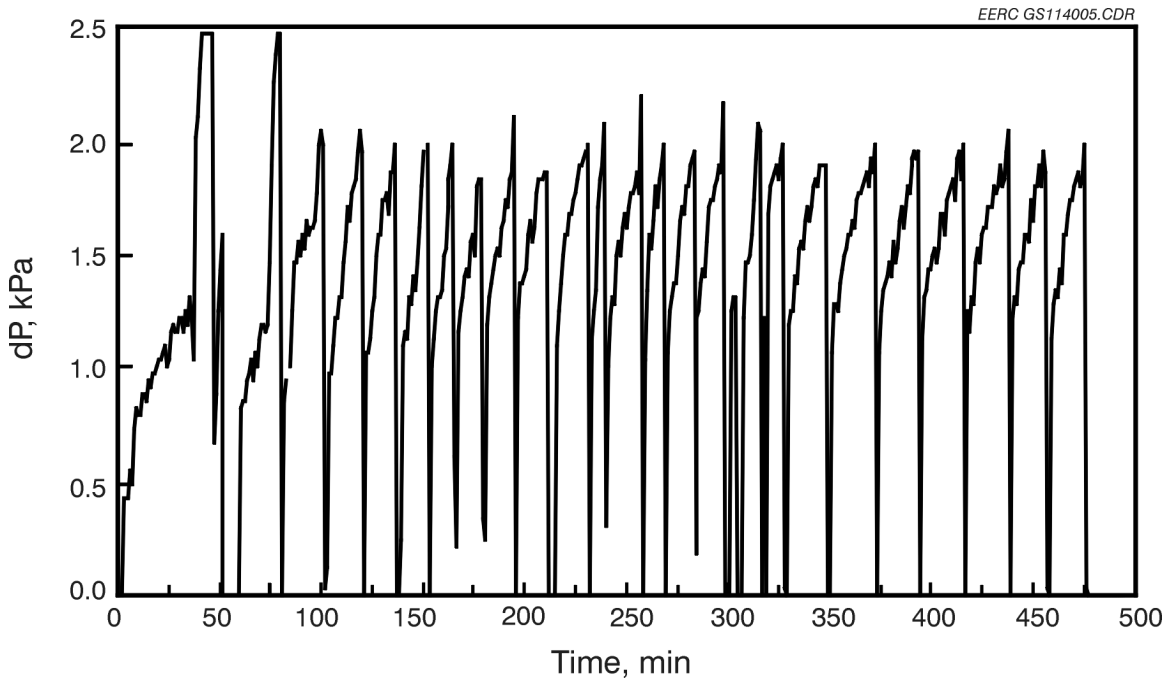

Figure 4.3-40. Pressure drop as a function of time for Test PTC-BV-581 with on-line cleaning using PTFE bags.

performance. The before and after changes in dP were about 0.82 to 0.87 kPa (3.3 to 3.5 in. W.C.) The pulse interval versus time information is found in Figure 4.3-41. During the steady-state period, the pulse interval ranged from 20 to 25 min, which was an improvement over the 10-min interval observed in the first test.

Inlet and outlet dust loadings were 7.4072 and 0.0021 g/m^3 (3.2346 and 0.0009 gr/scf), respectively (Table 4.3-6). The particulate efficiency was 99.973%. The indicated efficiency would likely have been higher, but there were traces of contamination of silicone gasket particles on the filter. After the run, the outlet plenum cover gasket showed signs of acid attack and was the likely source of this contamination. The graph of respirable mass versus time is presented in Figure 4.3-42. APS integrated averages for this test were 0.045 and 0.047 mg/m^3, corresponding to a respirable mass collection efficiency of >99.99%.

Test PTC-BV-582 was performed using the same bags, but bag cleaning was on-line. The change in dP before and after a cleaning cycle ranged from 0.50 to 0.62 kPa (2.0 to 2.5 in. W.C.)

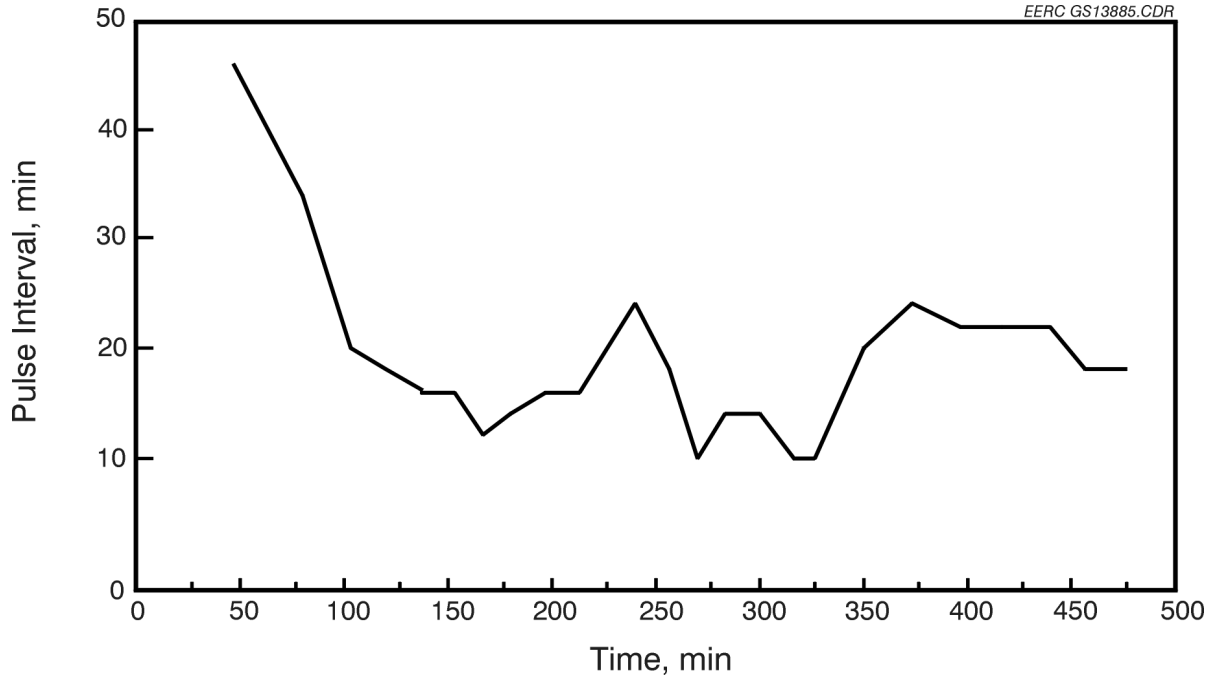

Figure 4.3-41. Pulse interval as a function of time for Test PTC-BV-581 with on-line cleaning using PTFE bags.

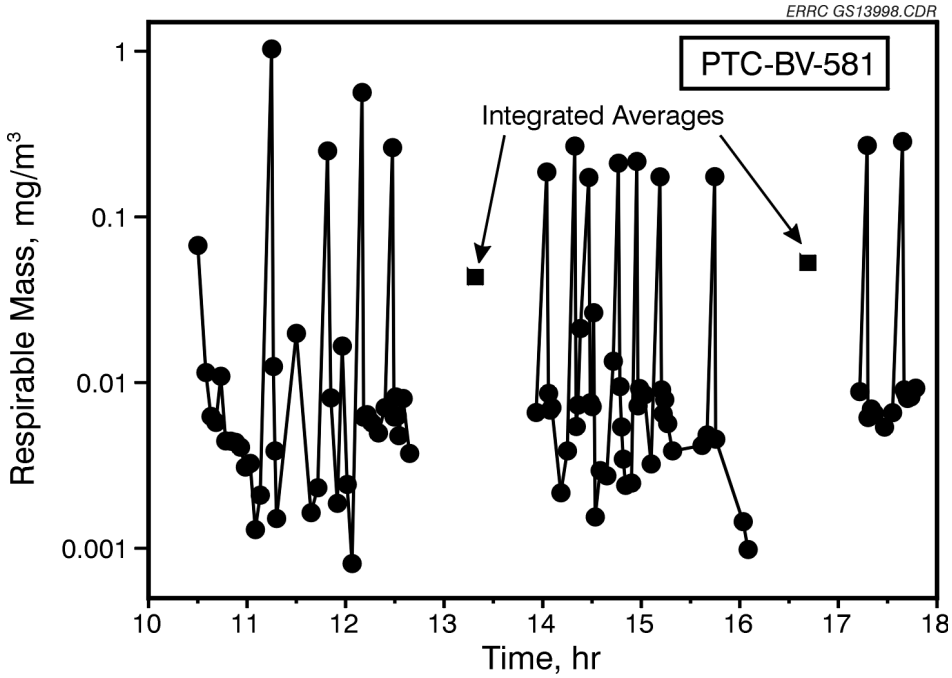

Figure 4.3-42. APS data for Test PTC-BV-581.

A graph showing the dP versus time is found in Figure 4.3-43. The pulse interval averaged about 15–20 min. Figure 4.3-44 presents the pulse interval versus time graph.

Inlet and outlet dust loadings were 4.4376 and 0.0005 g/m^3 (1.9378 and 0.0002 gr/scf), respectively (Table 4.3-6). The low particulate collection efficiency of 99.92% is attributed to gasket contamination. However, the APS data (integrated averages of 0.030, 0.032, and 0.030 mg/m^3) show that respirable mass collection efficiency was >99.99% (see Figure 4.3-45).

4.3.2.3 Flue Gas Conditioning Firing Blacksville Coal

The purpose of the next two tests, BV-583 and 584, was to evaluate the effect of NH_3/SO_3 conditioning on AHPC performance. A new set of GORE-TEX® PTFE bags was installed. Flue gas-conditioning agents of NH_3/SO_3 were added to the inlet gas stream of the AHPC. A concentration ratio of NH_3/SO_3 was set at 24 ppm/12 ppm, respectively, and injected upstream of the AHPC. The dramatic effect of conditioning is shown in Figure 4.3-46. The pulse interval was

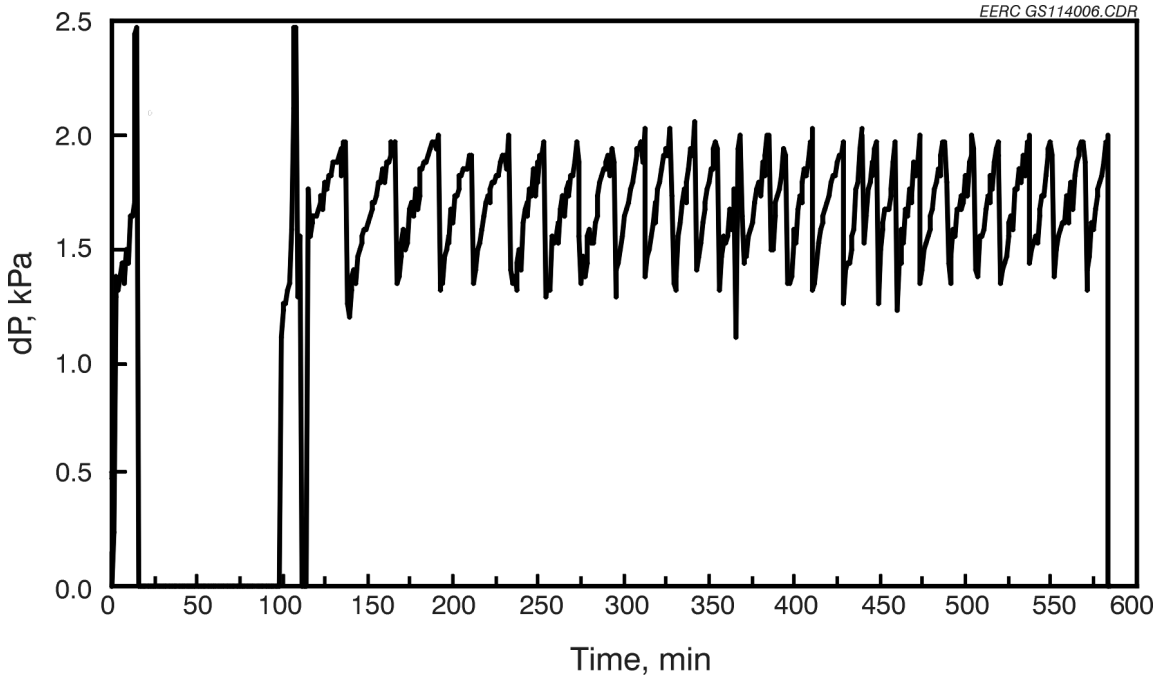

Figure 4.3-43. Pressure drop as a function of time for Test PTC-BV-582 with on-line cleaning using PTFE bags.

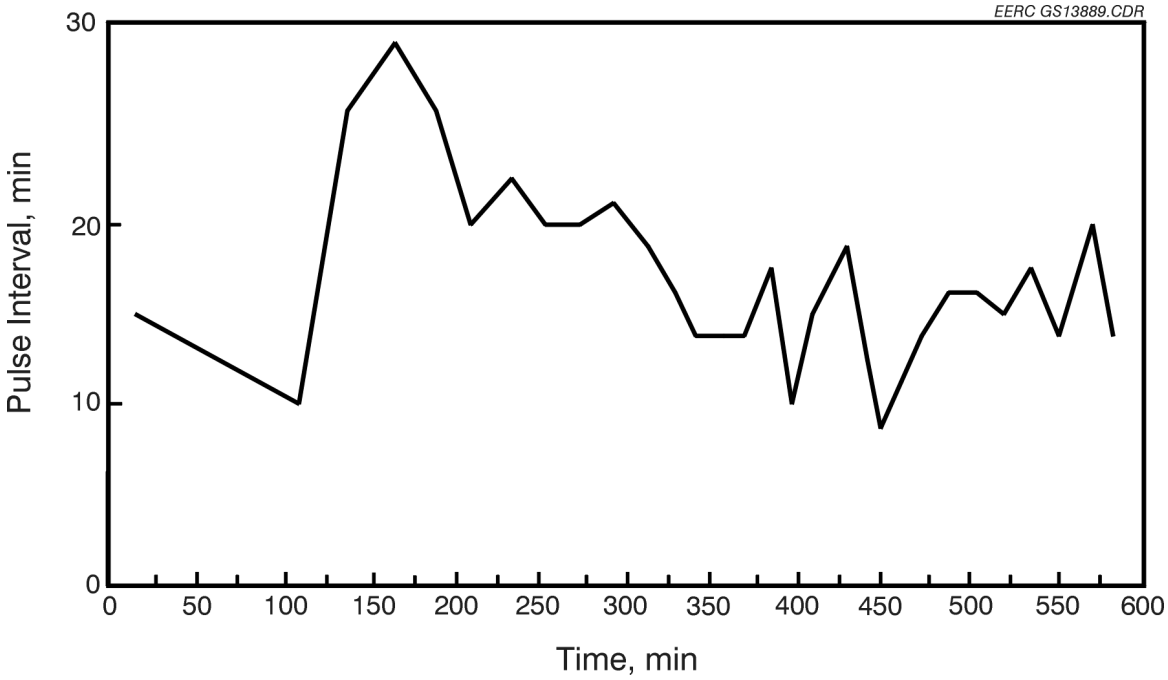

Figure 4.3-44. Pulse interval as a function of time for Test PVC-BV-582 with on-line cleaning using PTFE bags.

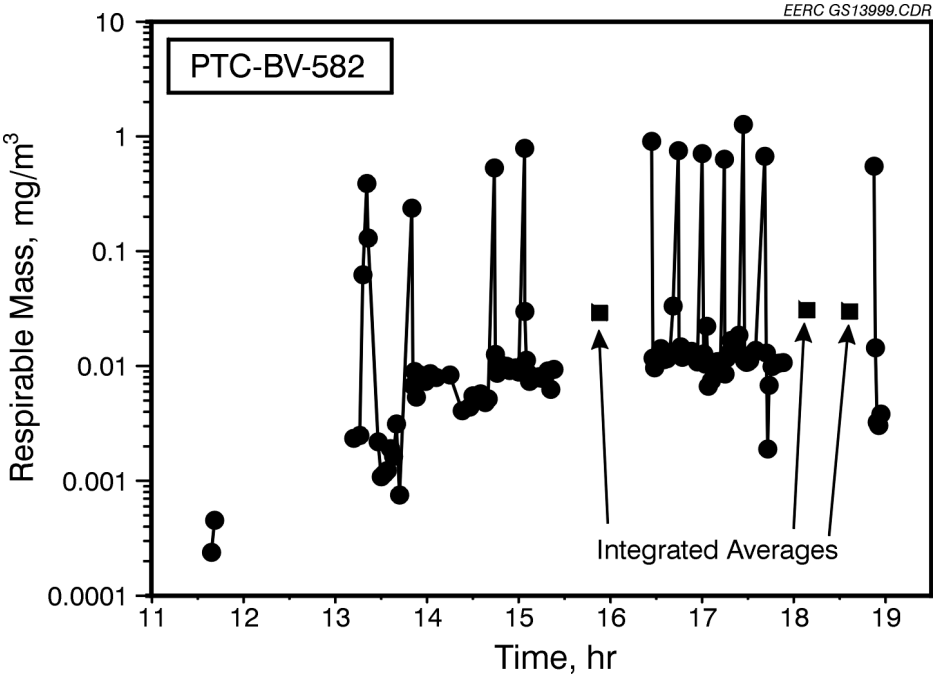

Figure 4.3-45. APS data for Test PTC-BV-582.

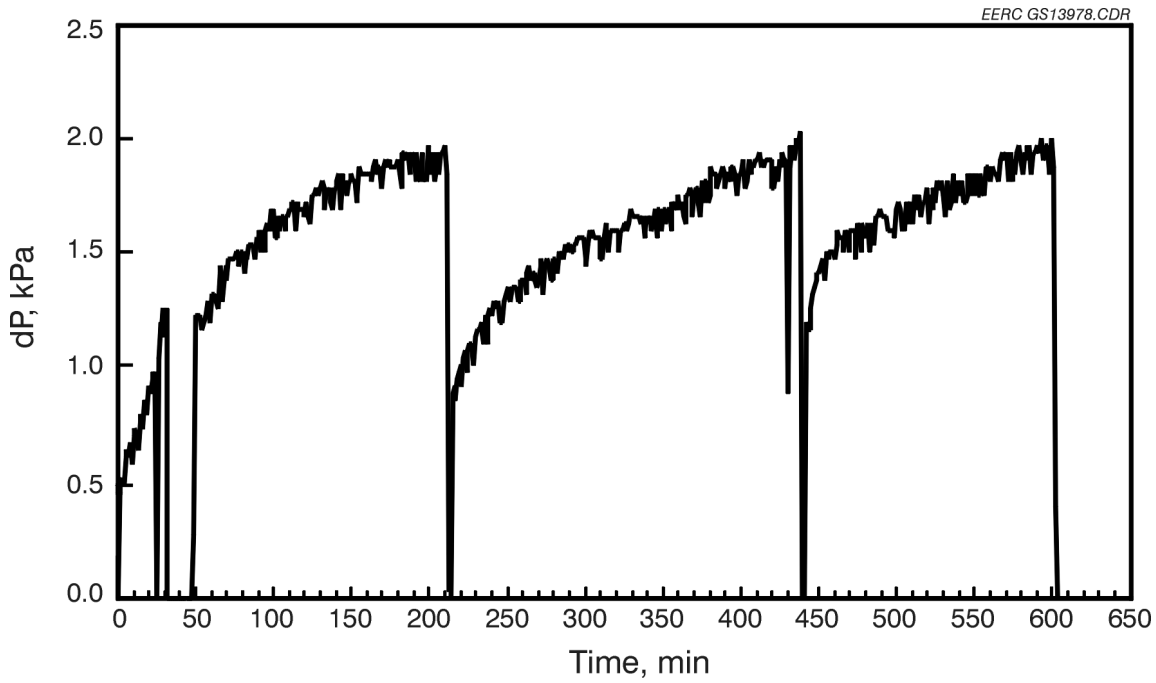

Figure 4.3-46. Pressure drop as a function of time for Test PTC-BV-583 with off-line cleaning using PTFE bags.

200 min compared to 20 min without conditioning in Test 581. The graph of pulse cycles versus time is shown in Figure 4.3-47.

The inlet and outlet particulate emissions were 4.3366 and 0.0005 g/m^3 (1.8937 and 0.0002 gr/scf), respectively, for a removal efficiency of 99.992%. The graph of respirable mass versus time is presented in Figure 4.3-48. No integrated averages were performed during this test. However, except during cleaning cycles, the respirable mass data were below 0.01 mg/m^3, indicating a collection efficiency of much greater than >99.99%.

Test BV-584 had the same conditions as Test PTC-BV-583, changing only the mode of bag cleaning to on-line. Figure 4.3-49 presents the dP versus time graph of PTC-BV-584. At the start of the test, flue gas-conditioning agents of NH_3/SO_3 were not set at the correct addition rates, and performance did not improve as in the previous test. At 250 min into the test, the ratio of conditioning agents NH_3/SO_3 was adjusted to ensure it was set at 24/12 ppm. At this point, the dP began to decrease even though dust continued to flow into the AHPC. After about 40 min, the dP

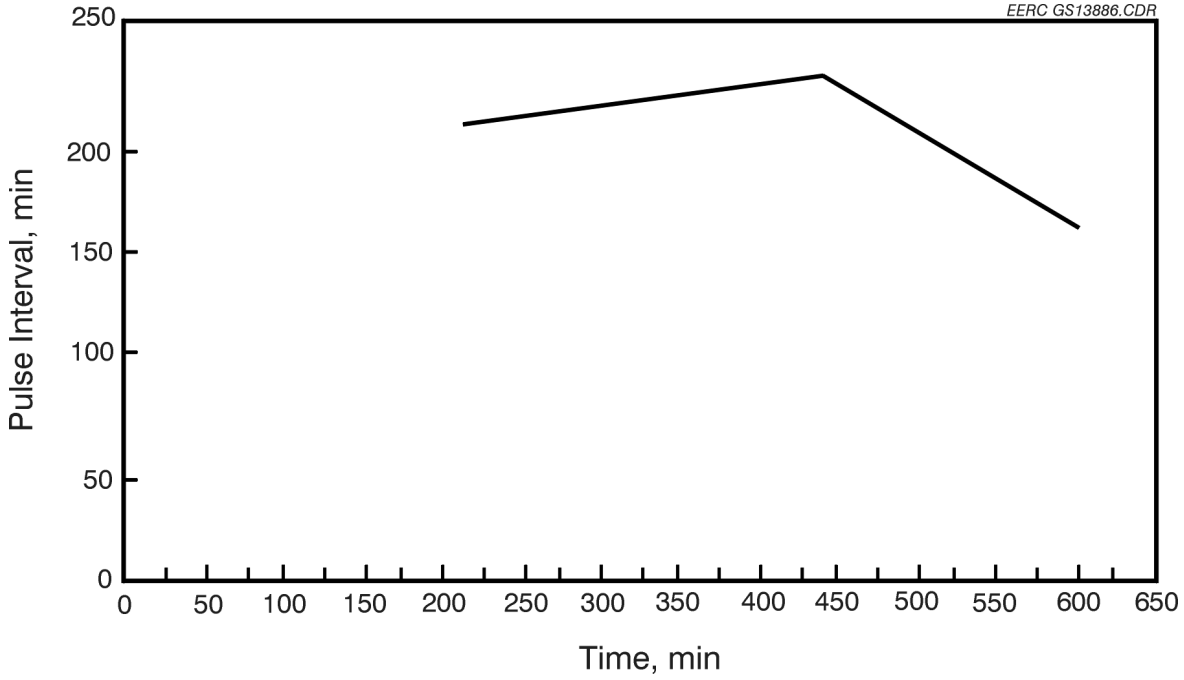

Figure 4.3-47. Pulse interval as a function of time for Test PTC-BV-583 with on-line cleaning using PTFE bags.

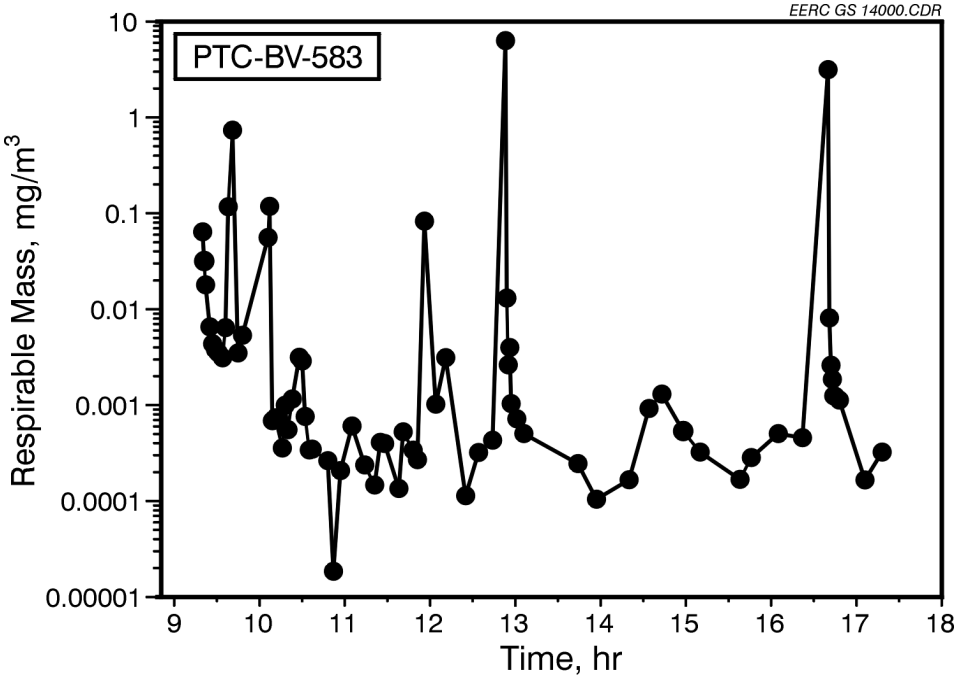

Figure 4.3-48. APS data for Test PTC-BV-583.

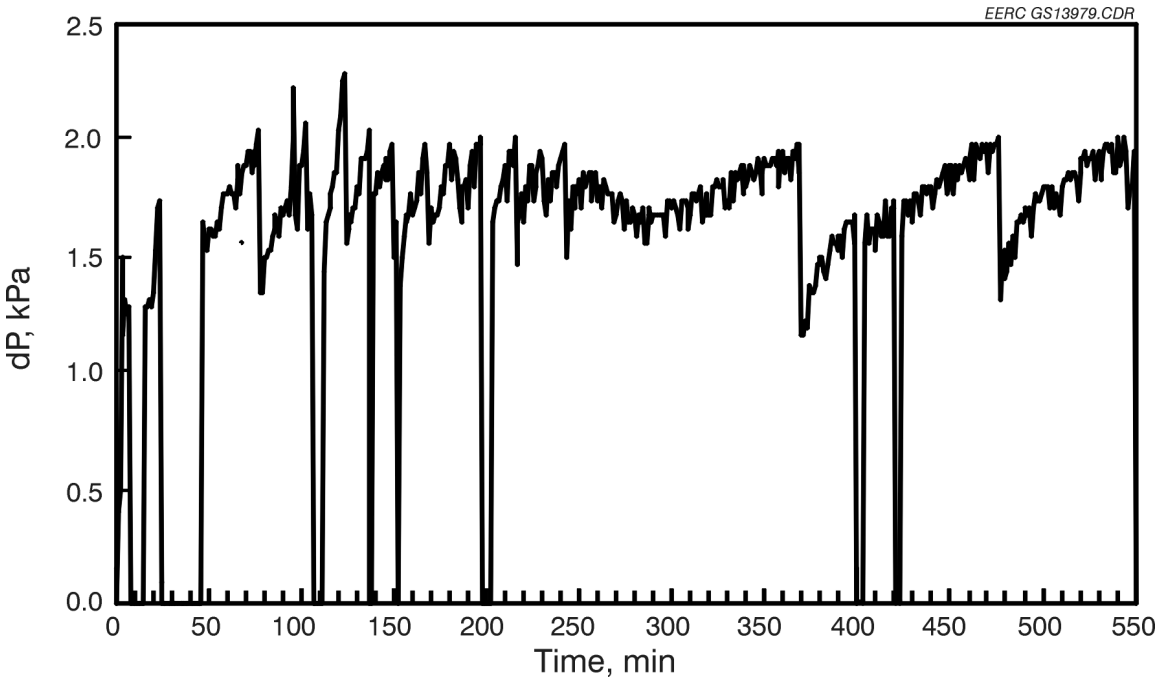

Figure 4.3-49. Pressure drop as a function of time for Test PTC-BV-584 with on-line cleaning using PTFE bags.

began to increase, but at a far slower rate. The pulse interval went from 10 to 20 min during the first part of the test to an average of 100 min after the change in the conditioning agent ratio. Figure 4.3-50 presents the graph of pulse interval versus time.

The inlet and outlet dust loadings were 4.9311 and 0.0055 g/m^3 (2.1533 and 0.0024 gr/scf), respectively. Particulate efficiency was 99.887%. The removal efficiencies for these tests are biased low because of the particulate added to the outlet of the AHPC by SO_3 attack on the silicone gasketing material. Figure 4.3-51 presents the graph of respirable mass versus time. No integrated average was done. The APS data show the decreasing concentration of respirable mass during the course of the test. The improvements in particulate collection may be due to the changes in the ratio of gas-conditioning agents. At the end of the test, the respirable mass emissions were less than 0.01 mg/m^3, corresponding to a respirable mass collection efficiency of 99.999%.

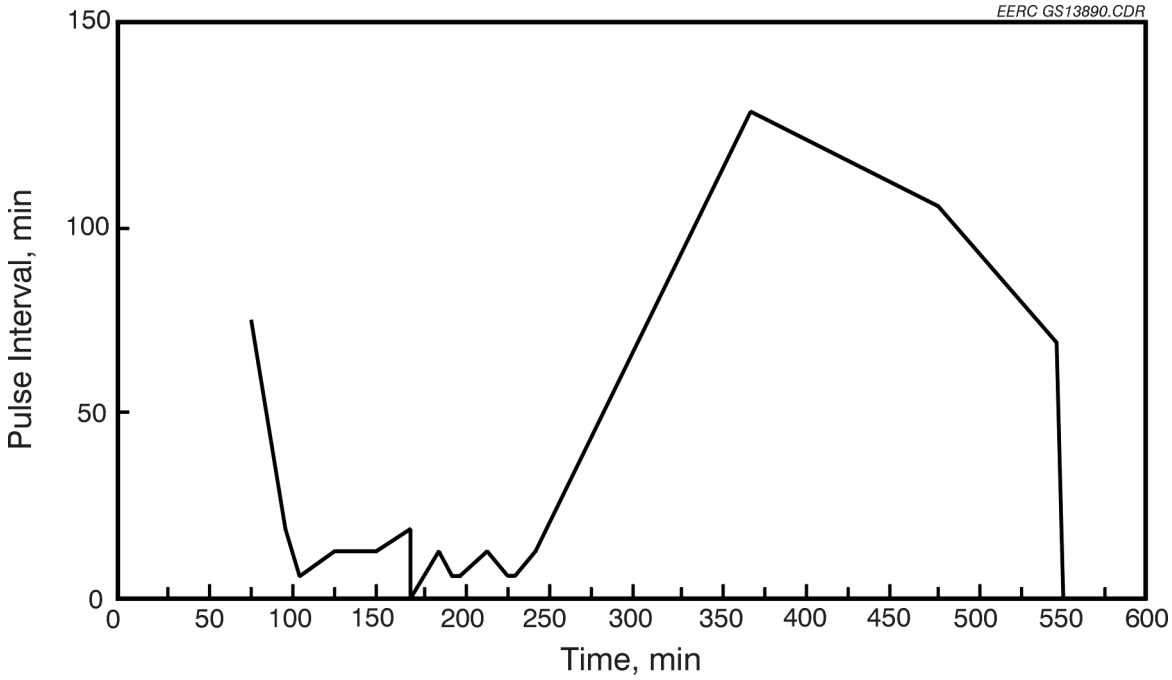

Figure 4.3-50. Pulse interval as a function of time for Test PTC-BV-584 with on-line cleaning using PTFE bags.

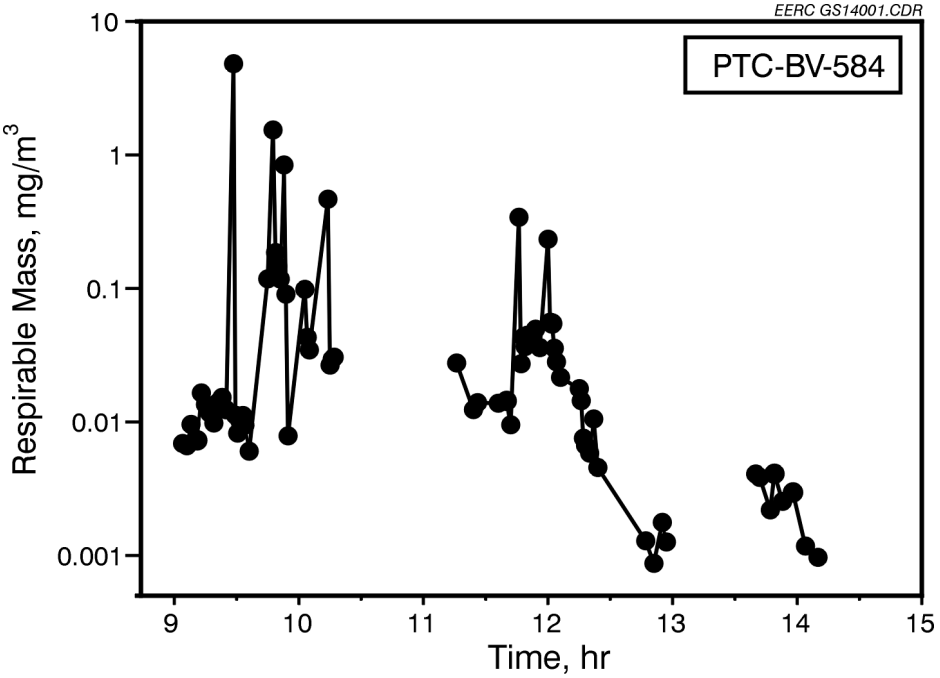

Figure 4.3-51. APS data for Test PTC-BV-584.

4.3.2.4 Conclusions from 8-hr Tests Firing Blacksville Coal

- Successful operation of the AHPC firing Blacksville bituminous was accomplished.
- Particulate collection efficiency of >99.99% was achieved.
- Off-line cleaning produced pulse intervals of about 20 min, while pulse intervals for on-line cleaning were about 15 min.
- Injection of NH_3/SO_3 dramatically improved AHPC performance both in pressure drop and pulse interval.

4.3.3 Summary of 8-hr Test Results

- The AHPC demonstrated good bag cleanability and operability at an A/C of 3.7 m/min, firing both Absaloka and Blacksville coals.
- Particulate collection efficiencies of >99.99% were achieved for all test parameters studied.
- Without bags, the total mass ESP particle collection efficiency in the AHPC was 95% and the respirable mass efficiency was 83%.
- The collection efficiency of the AHPC shell with no bags and the ESP off was 48%.
- Successful operation was achieved at 4.9 m/min (16 ft/min) with a pulse interval of 10–15 min.
- Injection of NH_3/SO_3 dramatically improved AHPC performance both in pressure drop and pulse interval.

- Under different bag cleaning modes and different coals, the AHPC demonstrated the ability to recover after interrupt to the ESP power.

4.4 100-hr Tests Firing Coal

Absaloka subbituminous and Blacksville bituminous coals were fired for the 100-hr tests. The objectives of those tests were as follows:

- Determine operability of AHPC for an extended period at steady-state conditions firing two types of coal

- Determine baseline information of the fate of seven trace metals using the AHPC system

- Determine trace metal control using sorbent injection

- Determine the effects of the flue gas conditioning over an extended Test period

4.4.1 100-hr Baseline Tests Firing Absaloka Subbituminous Coal (PTC-AB-585)

The operational parameters for the coal-fired 100-hr test are presented in Table 4.4-1. The AHPC was operated at an A/C of 3.7 m/min (12 ft/min) using graphite-impregnated PTFE bags supplied by W.L. Gore. The ESP was set to operate at 50 kV. The temperature of the AHPC was maintained at 149°C (300°F) throughout the test. EPA Method 29 multimetals sampling train was used to determine trace metal concentrations for As, Cd, Cr, Hg, Ni, Pb, and Se as well as the particulate loading of the gas stream. Sampling of the inlet and outlet flue gas from the AHPC was performed simultaneously. The duration for inlet sampling was 1 hr, while it was 4 hr for the outlet sampling and, in some cases, 24 hr. A multicyclone sampling system was used to collect a size-fractionated dust sample from the inlet of the AHPC. An APS and a SMPS–CPC were used to get real-time particulate concentration and size distribution data.

TABLE 4.4-1

Test Parameters for PTC-AB-585

Week of February 3, 1997	
Air/Cloth Ratio, m/min (ft/min)	3.7 (12)
Inlet Temperature, °C (°F)	149 (300)
On-Line and Off-Line Cleaning	On
Baffling	Butterfly
Voltage, kV	50
Type of Bag	Graphite-impregnated PTFE
Bag Identification	Set 10
No. of Bags in Use	4
Pulse Pressure, kPa (psig)	612 (90)
Pulse Duration, s	0.20
Pulsing Initiation Pressure, kPa (in. W.C.)	2.0 (8.0)

4.4.1.1 Results for Test PTC-AB-585 – Day 1

The PTC combustor was heated on natural gas to reach the specified operating temperatures within the system. The AHPC was heated by resistance heating to the specified 149°C (300°F). The inlet and outlet piping to the AHPC were also heated by electric-resistive heaters. No flue gas generated by natural gas was allowed to enter the AHPC. Past experience has shown that a fine-particle fume, generated by firing natural gas, may lead to bag-cleaning problems. Therefore, the AHPC was bypassed during system heatup. After the system equilibrated, the flue gas was directed into the AHPC. The average concentrations of the flue gas constituents are listed in Table 4.4-2. Figure 4.4-1 presents the change in pressure (dP) of the bags versus run time. The initial dP on the clean bags was 0.52 kPa (2.1 in. W.C.). The change in dP before and after cleaning decreased during the first day of testing, starting with a change in dP of 1.3 kPa at a run time of about 1.5 hr to a change in dP of 0.9 kPa at 24 hr. The ESP current is also displayed in Figure 4.4-1. The ESP current was at about 4.00 mA at the beginning of the test and rose slightly to 4.25 mA and then decreased to a steady state ranging from 3.30 to 3.50 mA. The pulse interval decreased also from about 75 min on the first pulse interval to about 40 min by the end of the day. The pulse interval information is plotted in Figure 4.4-2.

TABLE 4.4-2

Average Flue Gas Concentrations for Test PTC-AB-585[1]

O_2, % by volume	CO_2, % by volume	H_2O, % by volume	SO_2, ppm	NO_x, ppm
4.0–4.5	14–16	9.5–10.0	720	700

[1] Dry basis except for H_2O.

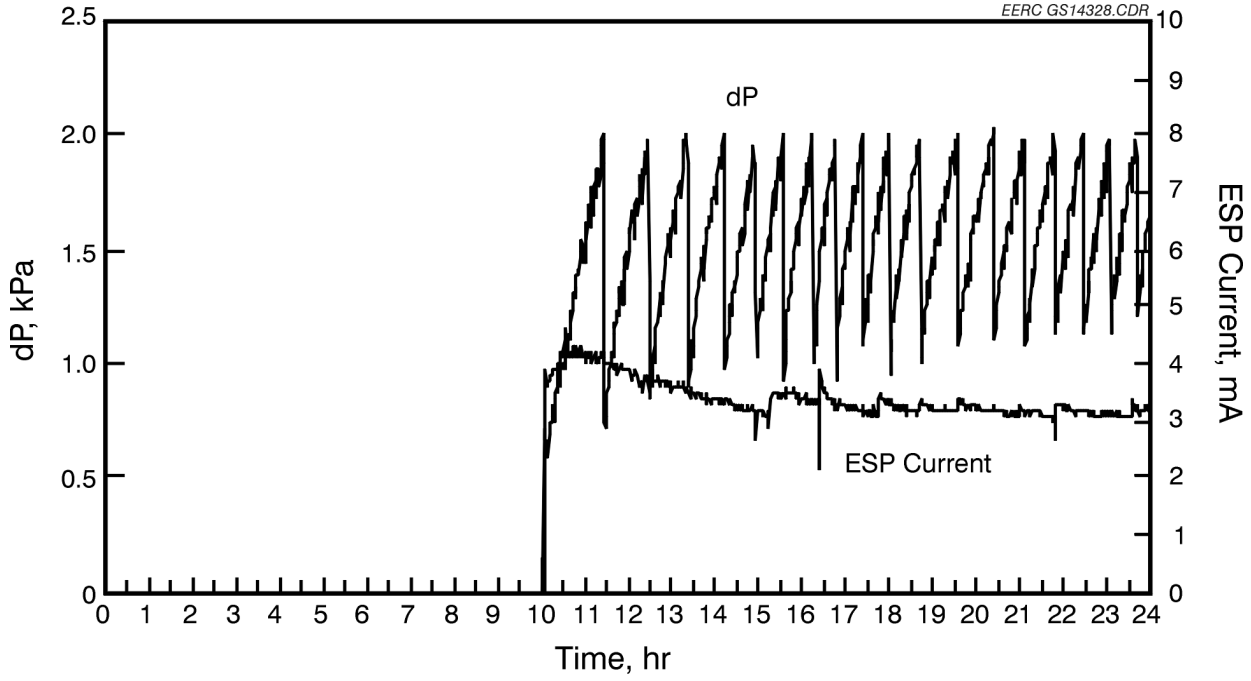

Figure 4.4-1. Pressure drop as a function of time for Day 1, February 3, 1997, Test PTC-AB-585 with on-line cleaning using graphite-impregnated PTFE bags.

Dust-loading data for Test PTC-AB-585 are presented in Table 4.4-3. One inlet and one outlet particulate sample were taken on the first day (February 3, 1997). The dust loading calculated from the ash collected in the AHPC hopper bottom of 6.84 g/m^3 (2.99 gr/scf) compared favorably with the inlet particulate dust loading sample of 6.4268 g/m^3 (2.8088 gr/scf). The outlet dust loading for the first day was 0.00008 g/m^3 (0.00037 gr/scf). The AHPC efficiency was calculated at 99.99987%. APS data confirmed the outlet dust-loading data with integrated averages of <0.01 mg/m^3, which corresponds to an efficiency of >99.999%. Figure 4.4-3 presents the graph of particulate concentration versus run time.

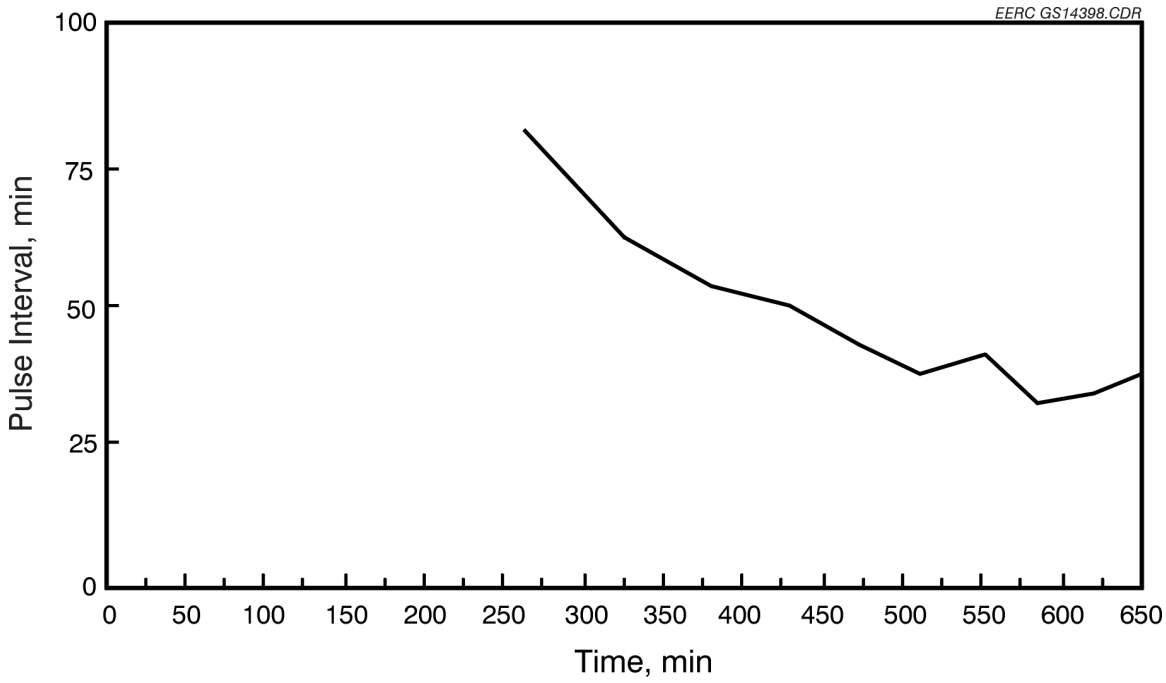

Figure 4.4-2. Pulse interval as a function of time for Day 1, February 3, 1997, Test PTC-AB-585 with on-line cleaning using graphite-impregnated PTFE bags.

TABLE 4.4-3

Dust-Loading Data for Test PTC-AB-585

Date	PTC Test No.	Hopper Ash, g/m^3	Inlet, g/m^3	Outlet, g/m^3	Percent Collection Efficiency
2-3-97	PTC-AB-585	6.84	6.4268	0.0008	99.999987
2-4-97	PTC-AB-585	6.13	6.1515	<0.000003	>99.99998
2-4-97	PTC-AB-585		6.3478[2]		
2-5-97	PTC-AB-585	5.81	6.1172	<0.000003[1]	>99.99998
2-6-97	PTC-AB-586	6.04	6.0682	0.000003[1]	99.99998

[1] Sampling time of 24 hr.
[2] Multicyclone.

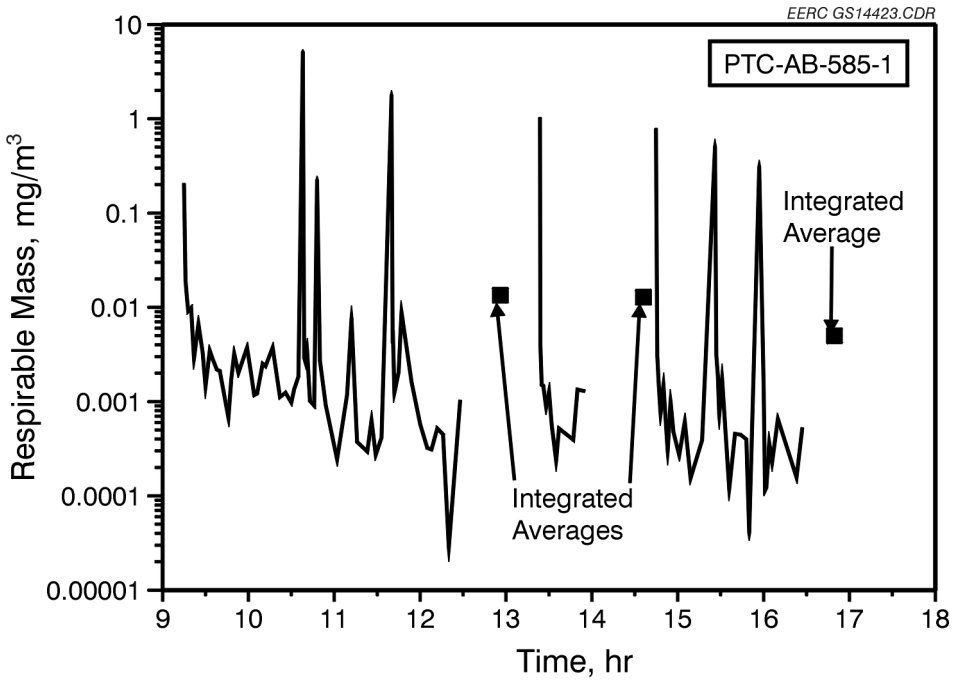

Figure 4.4-3. APS data for Day 1, February 3, 1997, Test PTC-AB-585.

4.4.1.2 Results for Test PTC-AB-585 – Day 2

The specified operational parameters remained unchanged during Day 2. The graph of dP versus time is plotted in Figure 4.4-4. The graph shows the change in dP before and after a cleaning cycle decreasing from 0.9 to 0.7 kPa. Pulse intervals went from about 40 min between cleaning cycles to about 26 min. Figure 4.4-5 presents the plot of pulse interval versus time for Day 2.

The AHPC was taken off-line from 33.2 to 33.6 hr to clean the ESP grid and the sight ports. Automatic rappers were not installed on the high-voltage electrode, so in longer-term operations, manual cleaning was required. The ESP current was 3.3 mA at 25 hr and decreased to 2.6 mA at 33.2 hr. The ESP current is shown in Figure 4.4-4. After the grid was cleaned, the ESP current jumped to a start-up level of 4.2 mA. ESP current continued to decrease to 3.1 mA at 48 hr. The decrease in ESP current did not seem to affect the time between pulse intervals.

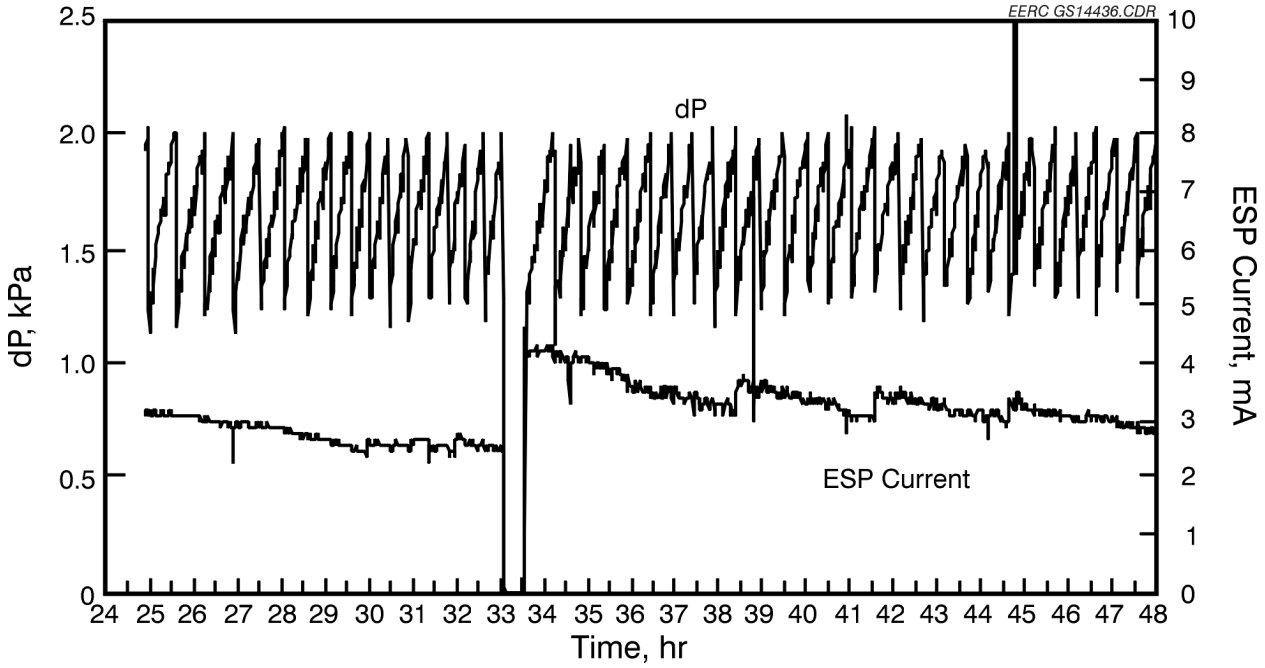

Figure 4.4-4. Pressure drop as a function of time for Day 2, February 4, 1997, Test PTC-AB-585 with on-line cleaning using graphite-impregnated PTFE bags.

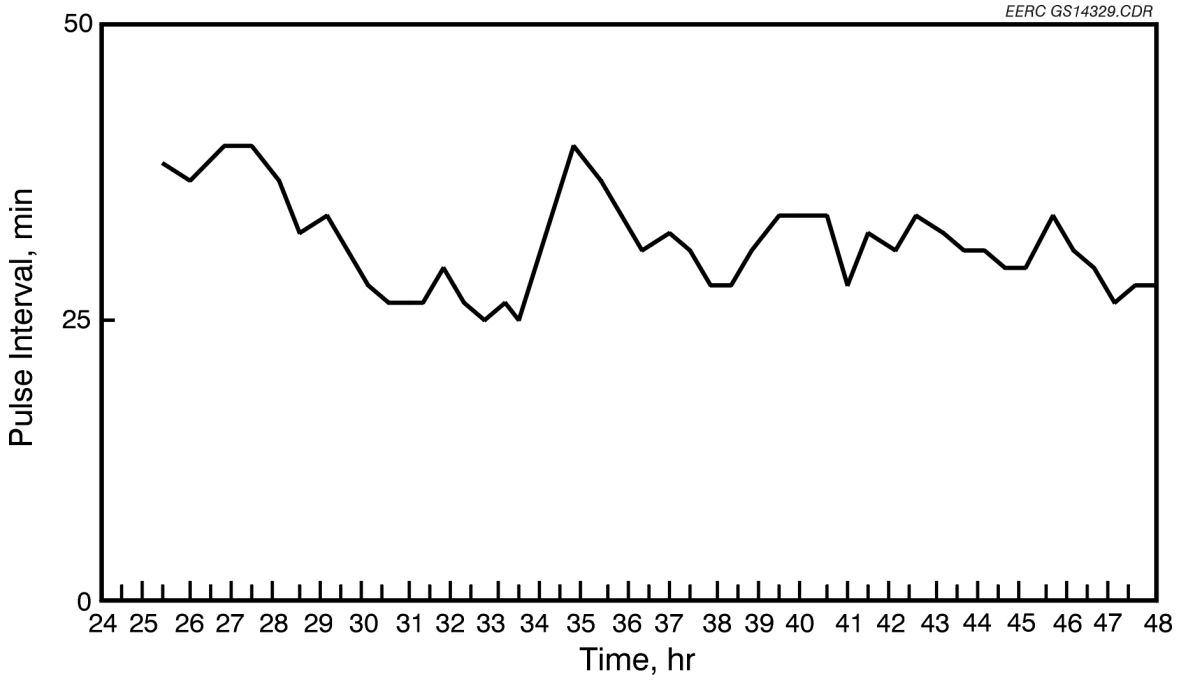

Figure 4.4-5. Pulse interval as a function of time for Day 2, February 4, 1997, Test PTC-AB-585 with on-line cleaning using graphite-impregnated PTFE bags.

The dust-loading data for Day 2 of Test PTC-AB-585 are listed in Table 4.4-3. Inlet and outlet dust loadings were 6.1515 g/m^3 (2.6865 gr/scf) and <0.000003 g/m^3 (<0.000001 gr/scf). Inlet dust loading calculated from the AHPC ash hopper of 6.13 g/m^3 (2.69 gr/scf) confirms the inlet dust loading. A multicyclone sample was taken at the inlet of the AHPC. The dust loading calculated from the multicyclone sampling was 6.3478 g/m^3 (2.7743 gr/m^3). The APS data are presented in Figure 4.4-6. Three integrated averages for respirable mass were taken. All three integrated averages, 0.0023, 0.0025, and 0.0035 mg/m^3, were below 0.01 mg/m^3 in respirable mass concentration, which indicates a >99.999% particulate collection efficiency. A plot of the combined inlet particulate concentration and combined outlet concentration versus particle size is presented in Figure 4.4-7. The inlet concentration curve was constructed using data from the SMPS, multicyclone sampling, and Coulter counter analysis of the first cyclone catch. Thus this plot confirms the collection efficiency results from EPA in-stack sampling methods for each range of aerodynamic particle size. As seen in Figure 4.4-7, the collection efficiency is >99.99% over the entire range of particle sizes, from 0.01 to 10 μm in aerodynamic diameter.

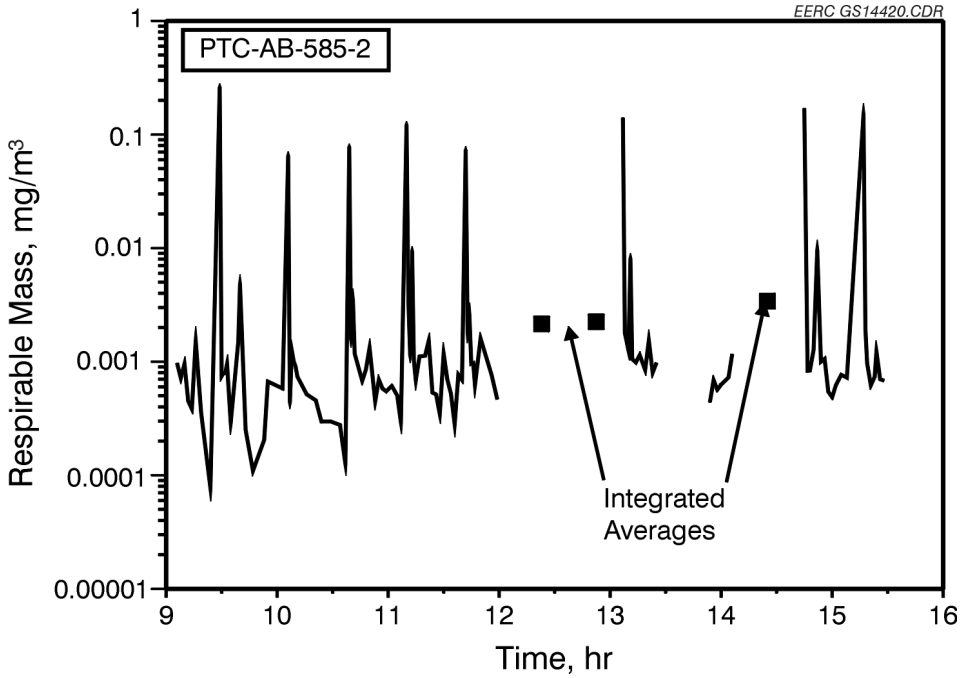

Figure 4.4-6. APS data for Day 2, February 4, 1997, Test PTC-AB-585.

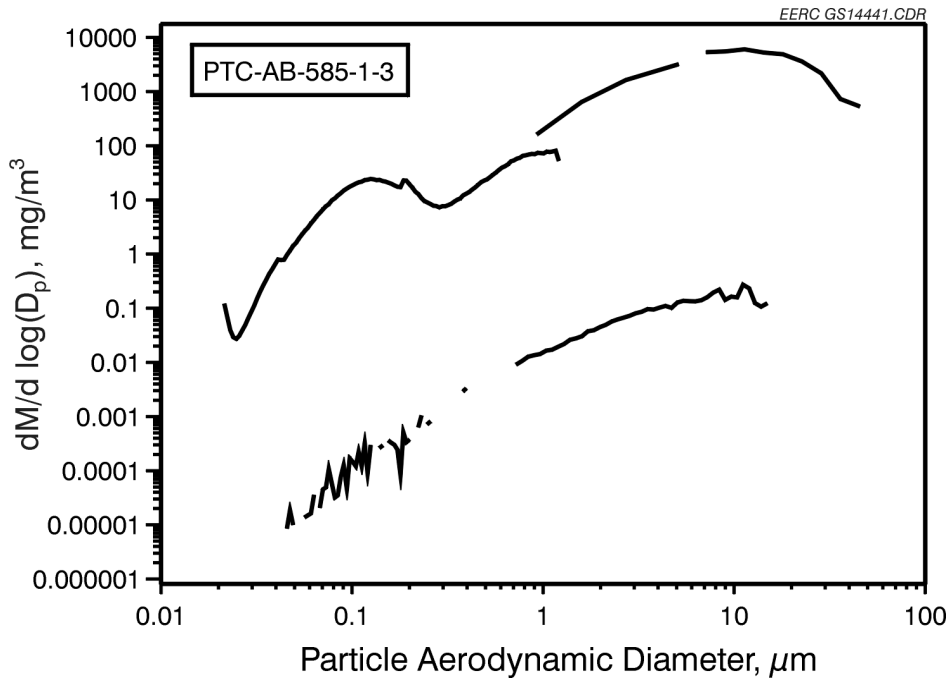

Figure 4.4-7. The combined inlet and outlet particulate concentration versus aerodynamic particle-size data for Day 2, February 4, 1997, Test PTC-AB-585.

4.4.1.3 Results for Test PTC-AB-585 – Day 3

Day 3 of PTC-AB-585 showed the AHPC operating at steady-state conditions. There were no unscheduled upsets in operation of the PTC or the AHPC. The graph of dP versus time is plotted in Figure 4.4-8. The change in dP from before to after bag cleaning remained fairly consistent, ranging between 0.75 and 0.62 kPa (3.0 to 2.5 in. W.C.). Also plotted in Figure 4.4-8 is the ESP current versus run time. The ESP current is located on the second y axis. The plot shows a steady decline in ESP current from 49 hr and 57 hr. Pulse interval, plotted in Figure 4.4-9, shows no significant decrease in time between 49 to 57 hr. At 57 hr, the AHPC was taken off-line for scheduled cleaning of electrodes and view ports. When the AHPC resumed operation, the pulse interval went from 25 min before cleaning to about 35 min after cleaning. The ESP current also jumped up from 2.2 mA before cleaning to 3.9 mA after cleaning. However, within 1.5 hr after going on-line, the AHPC appeared to reach a steady-state pulse

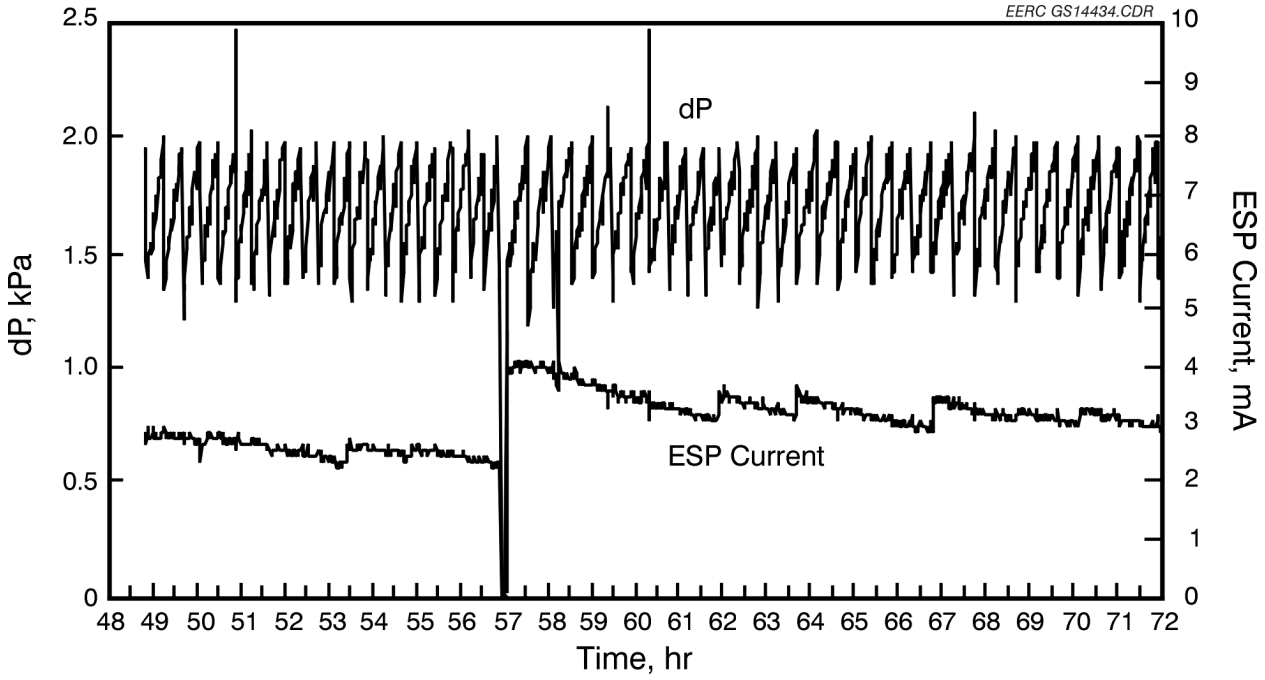

Figure 4.4-8. Pressure drop as a function of time for Day 3, February 5, 1997, Test PTC-AB-585 with on-line cleaning using graphite-impregnated PTFE bags.

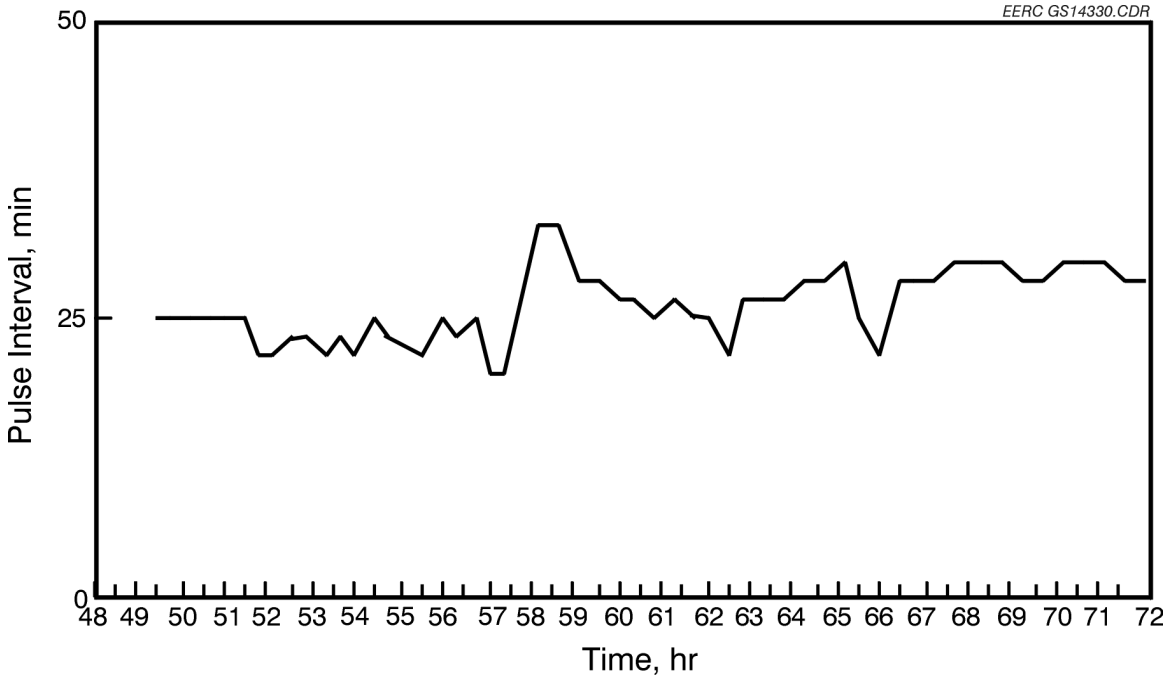

Figure 4.4-9. Pulse interval as a function of time for Day 3, February 5, 1997, Test PTC-AB-585 with on-line cleaning using graphite-impregnated PTFE bags.

interval of about 25 to 28 min. In Figure 4.4-8 (ESP current versus run time), the ESP current takes periodic small jumps upward. These jumps can be seen at 62, 63.7, 66.8, and 70.3 hr. These current jumps correspond to rapping of the ESP plates. Notice that the jump in current decreases with time. However, these small fluctuations in ESP current did not seem to affect the pulse interval times.

Dust loading performed on Day 3 is presented in Table 4.4-3. Inlet dust loading was measured at 6.1172 g/m^3 (2.6735 gr/scf). The dust loading sampled from the inlet duct compared well to the inlet dust loading calculated from the mass of ash collected from the AHPC ash hopper. The calculated dust loading was 5.81 g/m^3 (2.54 gr/scf). The outlet dust loading was <0.000003 g/m^3 (<0.000001 gr/scf), giving a dust-loading efficiency of >99.99998%. The outlet sample was obtained after sampling the outlet duct for 24 continuous hours. Figure 4.4-10 presents the respirable mass data taken for Day 3. Four integrated averages taken during Day 3 were 0.0029, 0.0037, 0.0027, and 0.0036 mg/m^3. All the average values for respirable mass fell below the 0.01-mg/m^3 particulate concentration, which signifies a >99.999% particulate

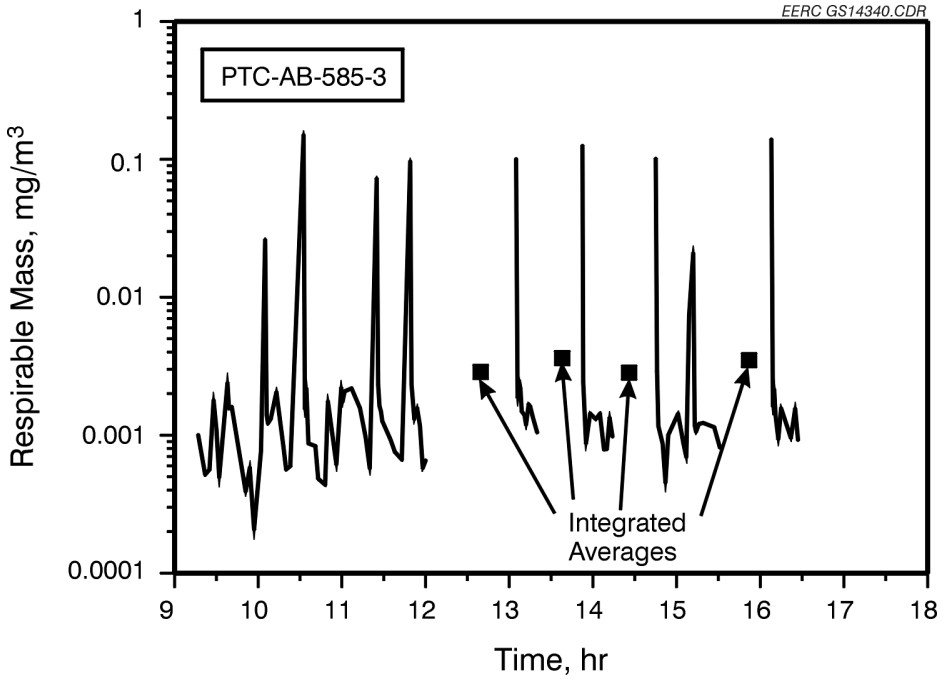

Figure 4.4-10. APS data for Day 3, February 5, 1997, Test PTC-AB-585.

collection efficiency. In the plot shown in Figure 4.4-11, the collection efficiency of >99.99% is confirmed over the entire range of particle sizes, from 0.01 to 10 μm in aerodynamic diameter.

4.4.1.4 Results for Test PTC-AB-585 – Day 4

Day 4 had no unscheduled system upsets. Pressure drop versus time, presented in Figure 4.4-12, shows consistent change in dP from before to after bag-cleaning cycles. This dP change averaged 0.62 kPa (2.5 in. W.C.). The pulse interval for Day 4, shown in Figure 4.4-13, ranged from 25 to 28 min. Again, as in Day 3, the pulse interval and ESP current jump up after the scheduled off-line cleaning of the AHPC. However, steady-state operation of the AHPC is achieved within 1.5 hr after returning to operation.

Dust-loading data for Day 4 are presented on Table 4.4-3. Inlet dust loading was measured at 6.0682 g/m^3 (2.6521 gr/scf). The inlet dust loading, calculated from the mass of ash collected from the AHPC ash hopper, was 6.04 g/m^3 (2.64 gr/scf). This agreed well with the dust loading

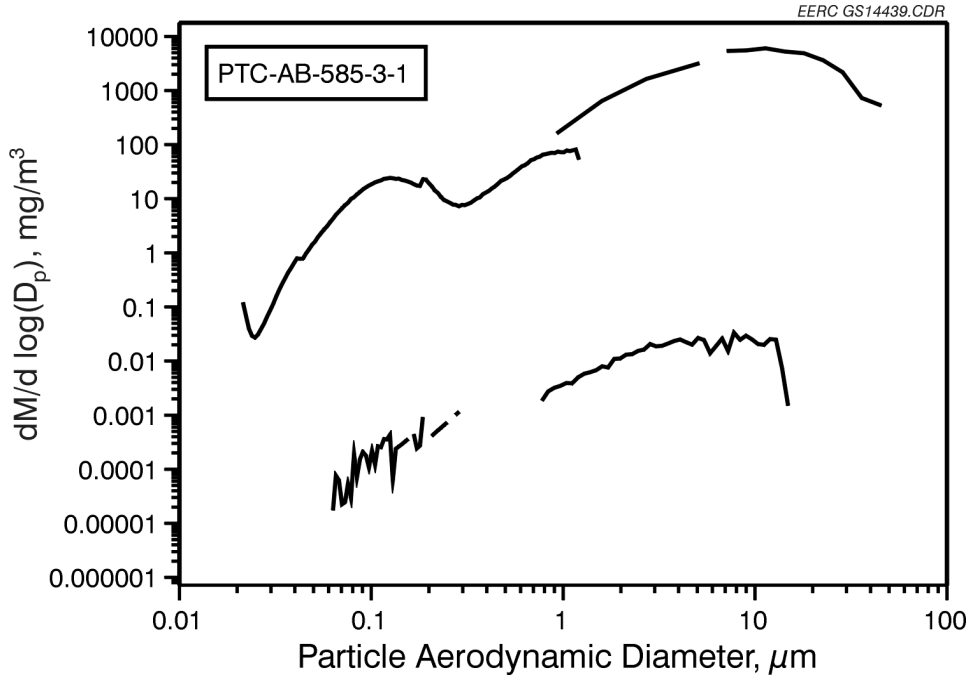

Figure 4.4-11. The combined inlet and outlet particulate concentration versus aerodynamic particle-size data for Day 3, February 5, 1997, Test PTC-AB-585.

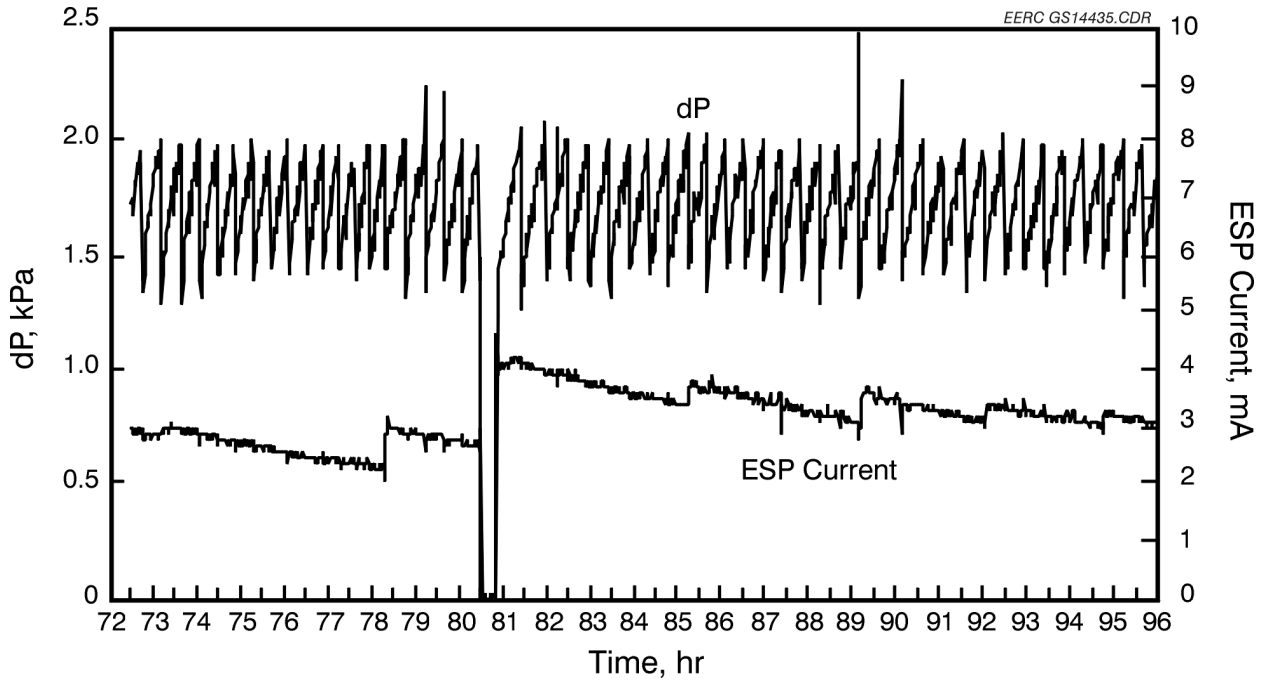

Figure 4.4-12. Pressure drop as a function of time for Day 4, February 6, 1997, Test PTC-AB-585 with on-line cleaning using graphite-impregnated PTFE bags.

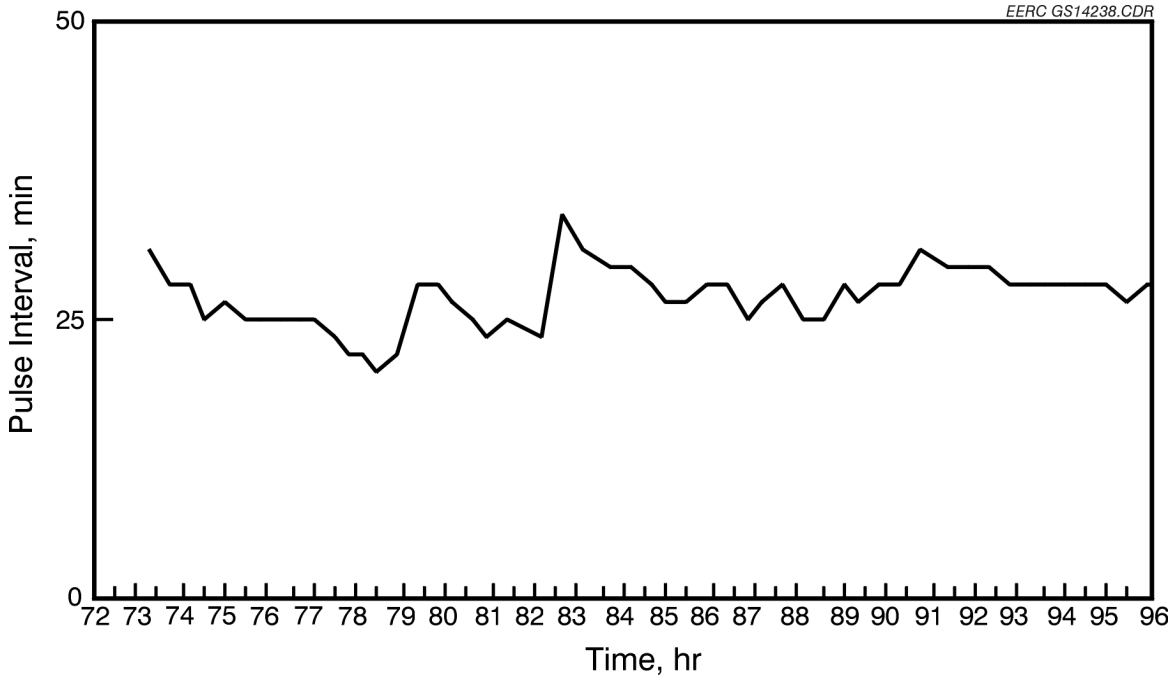

Figure 4.4-13. Pulse interval as a function of time for Day 4, February 6, 1997, Test PTC-AB-585 with on-line cleaning using graphite-impregnated PTFE bags.

sampled 24 continuous hours. The APS data are presented in Figure 4.4-14. Three integrated averages for respirable mass were taken. All three integrated averages, 0.0023, 0.0025, and 0.0035 mg/m^3, were below 0.01 mg/m^3 respirable mass concentration, which indicates a >99.999% particulate collection efficiency. In the plot shown in Figure 4.4-15, the collection efficiency of >99.99% is confirmed over the entire range of particle sizes, from 0.01 to 10 μm in aerodynamic diameter.

4.4.1.5 Results for Test PTC-AB-585 – Day 5

Day 5 showed the AHPC operating at steady-state conditions. There were no unscheduled upsets in operation of the PTC or the AHPC. The graph of dP versus time is plotted in Figure 4.4-16. The change in dP from before to after bag cleaning remained fairly consistent, ranging between 0.75 and 0.62 kPa (3.0–2.5 in. W.C.). Also plotted in Figure 4.4-16 is the ESP current versus run time. Pulse interval, plotted in Figure 4.4-17, shows no significant decrease, but remained steady at about 25 min.

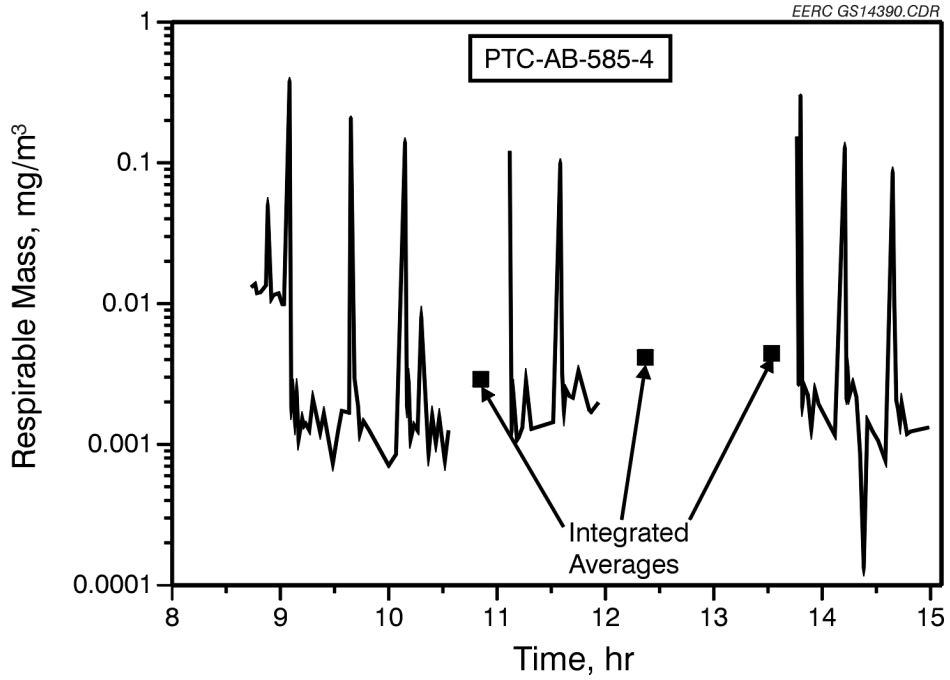

Figure 4.4-14. APS data for Day 4, February 6, 1997, Test PTC-AB-585.

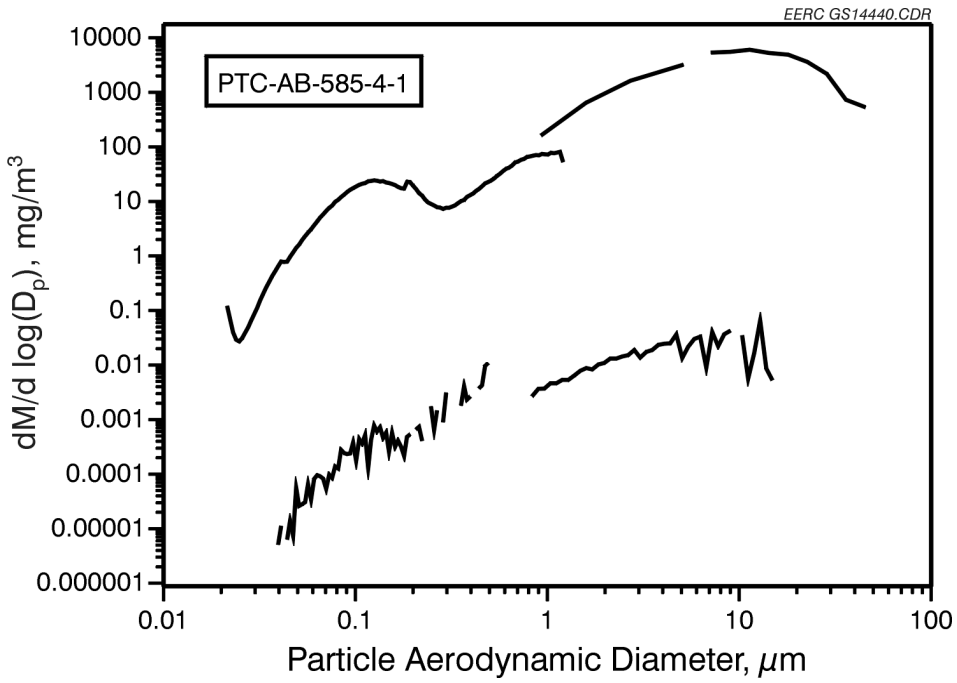

Figure 4.4-15. The combined inlet and outlet particulate concentration versus aerodynamic particle-size data for Day 4, February 6, 1997, Test PTC-AB-585.

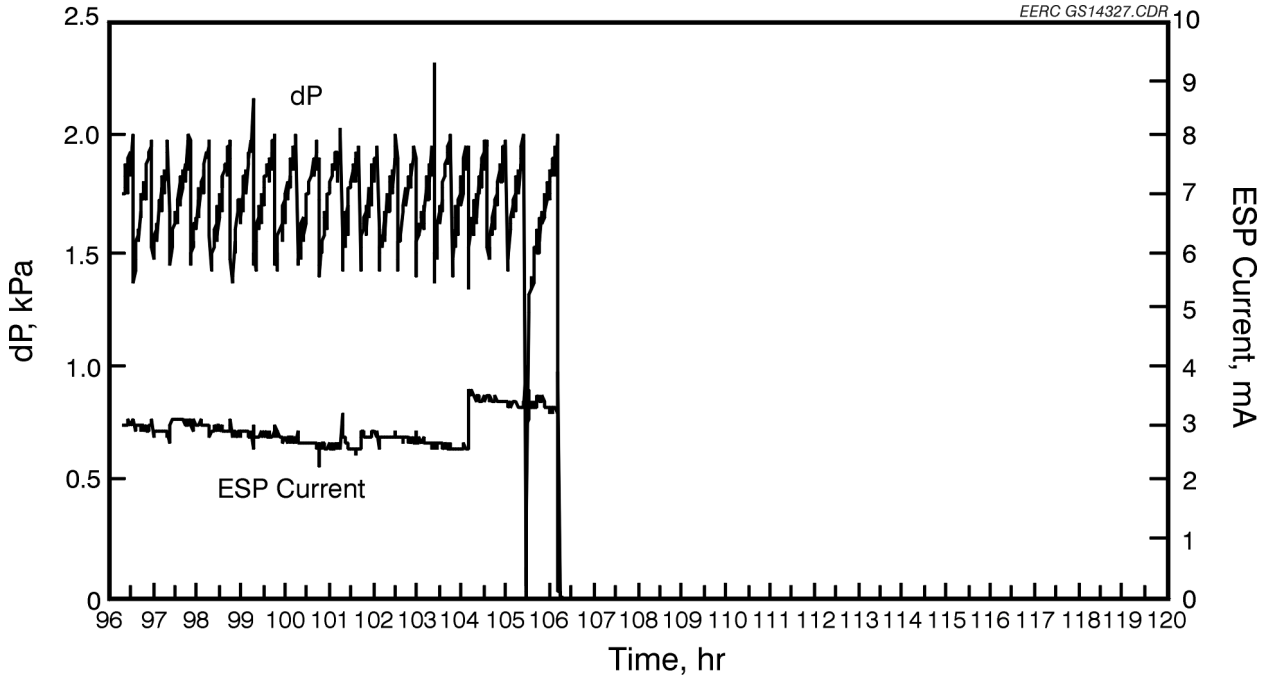

Figure 4.4-16. Pressure drop as a function of time for Day 5, February 7, 1997, Test PTC-AB-585 with on-line cleaning using graphite-impregnated PTFE bags.

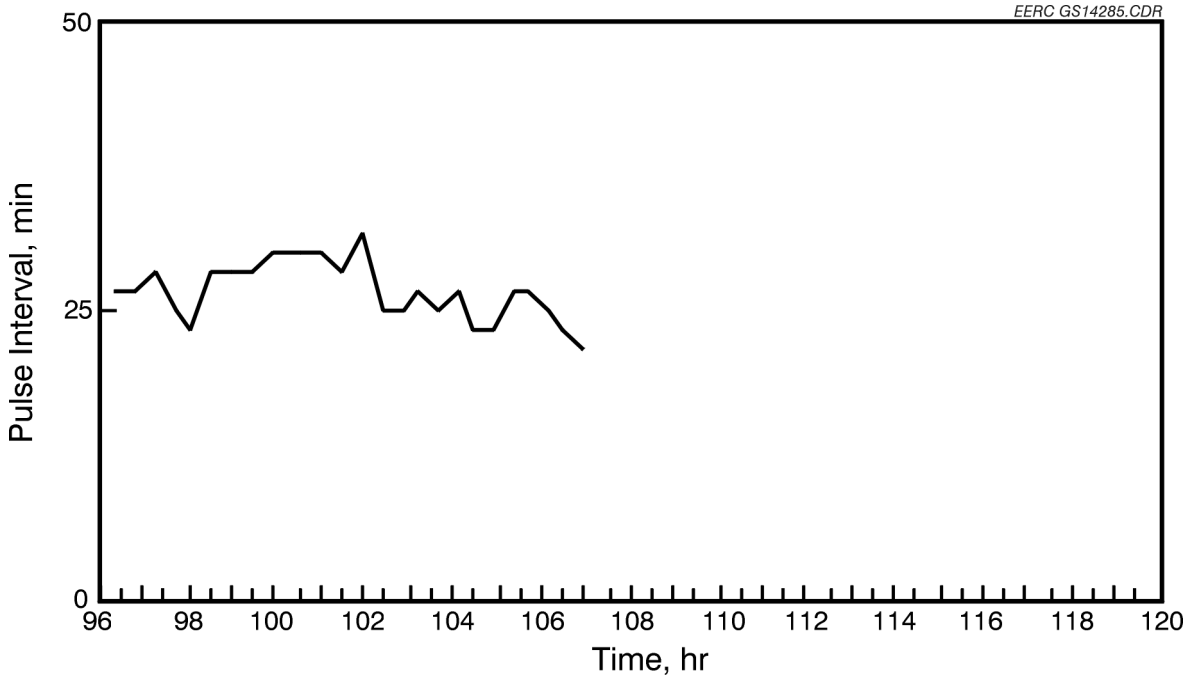

Figure 4.4-17. Pulse interval as a function of time for Day 5, February 7, 1997, Test PTC-AB-585 with on-line cleaning using graphite-impregnated PTFE bags and 50-kV applied voltage.

4.4.1.6 Particulate Collection Efficiency for Test PTC-AB-585

Table 4.4-4 gives the particulate collection efficiency of the AHPC for Test PTC-AB-585. The collection efficiency was determined over a particle-size range of 0.01 to 50 microns. Three sampling methods, EPA-5, APS, and the CPC, were used to determine the concentration of particles according to size. The correlation of the three sampling methods confirms the collection efficiency of the AHPC for all size fractions of particulate to be >99.999%. The EPA-5 sampling demonstrated >99.9999% collection efficiency over a 24-hr period of sampling at the outlet of the AHPC. The 24-hour sampling time was necessary in order to accumulate enough dust on the filter to weigh accurately. The outlet particulate concentration was calculated at 3 $\mu g/m^3$. Particle outlet concentrations for the APS and the CPC were determined to be 2.5 $\mu g/m^3$ and 500 particles/cm^3, respectively.

TABLE 4.4-4

Particulate Collection Efficiency for Test PTC-AB-585, 100-hr test

Method	Particle Size, μm	Outlet Concentration	Collection Efficiency, %
EPA-5 (24 hr)	0.01–50	3 $\mu g/m^3$	>99.9999
APS (30 min average)	0.5–5	2.5 $\mu g/m^3$	>99.999
CPC (real time)	0.01–1	500 particles/cm^3	>99.999

4.4.1.7 Trace Metal Concentrations from Duct Sampling

Flue gas was taken from inlet and outlet locations of the AHPC using the EPA Method 29 multimetals sampling method. Also, ash samples were taken each day from the ash hopper of the AHPC. Seven trace metals analyzed for were As, Cd, Cr, Pb, Ni, Se, and Hg. Table 4.4-5 presents the trace metal data for the Method 29 samples, the hopper ash samples, and the composite coal sample. All hopper ash samples were analyzed for mercury. Method 29 was not designed to differentiate between oxidized and elemental forms of mercury vapor; however, it provides some speciation information. The oxidized form of mercury is primarily collected in the H_2O_2 impingers, while the elemental vapor is collected primarily in the last two $KMn0_4$ impingers.

As Table 4.4-5 shows, all seven trace elements were detected in the inlet filter cake of the Method 29 sample. Except for selenium at 21.41% RSD (relative standard deviation), the %RSD was <20% for the other six elements. However, the outlet filter, after 24 hr of dust collection, showed all seven trace elements near or below detection limits. This is another indication of the AHPC's ability to remove, with a high degree of efficiency, a full range of particle sizes. Of the seven elements, only three (Hg, Se, and Cr) appear in detectable quantities in the vapor form.

Table 4.4-6 summarizes the trace element data for baseline Test PTC-AB-585, showing the inlet and outlet averages for the seven trace elements. Five trace metals (As, Cd, Cr, Pb, and Ni)

TABLE 4.4-5

Trace Metal Data for Test PTC-AB-585

	Inlet 1				Inlet 3				Inlet 6				Inlet 8				Statistics		
Sample Type	Filter	H_2O_2	$KMnO_4$	Total	Filter	H_2O_2	$KMnO_4$	Total	Filter	H_2O_2	$KMnO_4$	Total	Filter	H_2O_2	$KMnO_4$	Total	Average	STDV	%RSD
Mercury, µg/m³	1.36	1.61	3.45	6.42	1.35	0.93	3.53	5.81	0.65	1.47	3.1	5.2	0.56	1.09	2.91	4.56	5.50	0.69	12.54
Arsenic, µg/m³	83.6	1.01	NA[1]	84.6	86.2	1.03	NA	87.21	734	1.01	NA	74.47	85.0	0.99	NA	86.0	83.1	5.05	6.08
Cadmium, µg/m³	1.09	0.08	NA	1.17	1.85	0.08	NA	1.93	1.9	0.08	NA	1.98	1.52	0.07	NA	1.59	1.67	0.32	19.43
Chromium, µg/m³	464	0.75	NA	465	539	0.88	NA	540	463	0.91	NA	463.71	383	0.94	NA	384	463	55.18	11.92
Lead, µg/m³	317	0.5	NA	317.5	337	0.52	NA	338	322	0.5	NA	322.5	297	0.5	NA	297	319	14.24	4.47
Nickel, µg/m³	225	2.01	NA	227	222	2.06	NA	224	214	2.02	NA	216.28	225	1.98	NA	227	223	4.34	1.94
Selenium, µg/m³	26.4	16.1	NA	42.4	23.4	7.73	NA	31.1	25.1	6.05	NA	31.15	21.2	1.98	NA	23	32.0	6.85	21.41

	Outlet 2			Outlet 4			Outlet 7				Outlet 9			Statistics		
Sample Type	H_2O_2	$KMnO_4$	Total	H_2O_2	$KMnO_4$	Total	Filter	H_2O_2	$KMnO_4$	Total	H_2O_2	$KMnO_4$	Total	Average	STDV	%RSD
Mercury, µg/m³	0.68	2.55	3.23	3.05	1.8	4.85	0.01	3.16	1.64	4.81	2.91	1.35	4.26	4.29	0.65	18.36
Arsenic, µg/m³	NA	NA	NA	NA	NA	NA	0.01	0.28	NA	0.29	NA	NA	NA	NA	NA	NA
Cadmium, µg/m³	NA	NA	NA	NA	NA	NA	0.001	0.02	NA	0.021	NA	NA	NA	NA	NA	NA
Chromium, µg/m³	NA	NA	NA	NA	NA	NA	0.06	0.51	NA	0.57	NA	NA	NA	NA	NA	NA
Lead, µg/m³	NA	NA	NA	NA	NA	NA	0.02	0.14	NA	0.16	NA	NA	NA	NA	NA	NA
Nickel, µg/m³	NA	NA	NA	NA	NA	NA	0.06	0.57	NA	0.63	NA	NA	NA	NA	NA	NA
Selenium, µg/m³	NA	NA	NA	NA	NA	NA	0.1	15.58	NA	15.68	NA	NA	NA	NA	NA	NA

	Coal and Hopper Ash				
Sample Type	Coal, µg/g	Ash 1, µg/m³	Ash 2, µg/m³	Ash 3, µg/m³	Ash 4, µg/m³
Mercury	0.080	0.36	0.35	1.00	0.37
Arsenic	1.16			65	
Cadmium	0.057			<0.1	
Chromium	9.4			349	
Lead,	4.4			252	
Nickel	4.6			160	
Selenium	0.54			15	

[1] Not applicable.

TABLE 4.4-6

Trace Element Data for Test PTC-AB-585, μg/m^3

	Hg	As	Cd	Cr	Pb	Ni	Se
Average Inlet	5.5	83.0	1.7	463.0	319.0	223.0	32.0
Average Outlet	3.6	<10	<0.08	0.57	<0.50	<2.0	16.0
Percent Removal	34.5	>99.8	>95.3	99.9	>99.8	>99.1	50.0

showed good percent removals. The AHPC removed 34.5% of mercury from the gas stream, and 50.0% of the Se was removed.

Total inlet mercury concentrations ranged from 6.42 to 4.56 μg/m^3, averaging 5.50 μg/m^3. The %RSD was 12.54%. Figure 4.4-18 shows the distribution of mercury species in the Method 29 inlet sampling. One inlet and outlet sample were taken each day of PTC-AB-585. The total mercury concentration for gas and solid samples paralleled values measured in previous tests firing Absaloka subbituminous. In this figure, the concentration of mercury in the solid sample (filter ash) is compared with the concentration of mercury (Hg^0 and Hg^{2+}) sampled in the vapor phase. The mercury collected on the inlet filter ranged from 1.36 to 0.56 μg/m^3, averaging 0.98 μg/m^3.

The percent removal of Hg^0 calculated is presented in Figure 4.4-19. The percent removal of Hg^0 increased during the first day of testing and then leveled out. The ratio of oxidized to elemental mercury vapor that passes the filter is defined as the concentration of oxidized mercury analyzed from the H_2O_2 impingers divided by the concentration of elemental mercury analyzed from the $KMnO_4$ impingers. Table 4.4-7 presents the calculated ratios of oxidized to elemental mercury for both inlet and outlet mercury samples.

Distribution of mercury species for Method 29 outlet sampling is shown in Figure 4.4-20. The outlet mercury concentration averaged 3.56 μg/m^3 with a RSD of 18.36%. No outlet filters were submitted for trace metal analysis except Outlet Sample 7 because of the very low mass

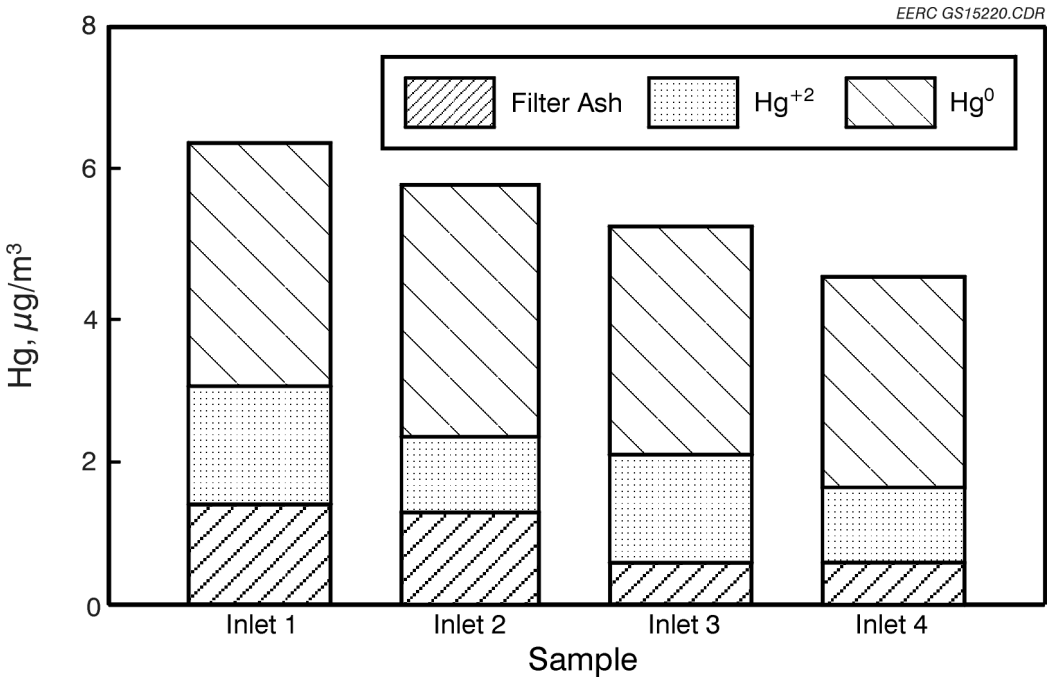

Figure 4.4-18. Distribution of inlet mercury species according to EPA Method 29.

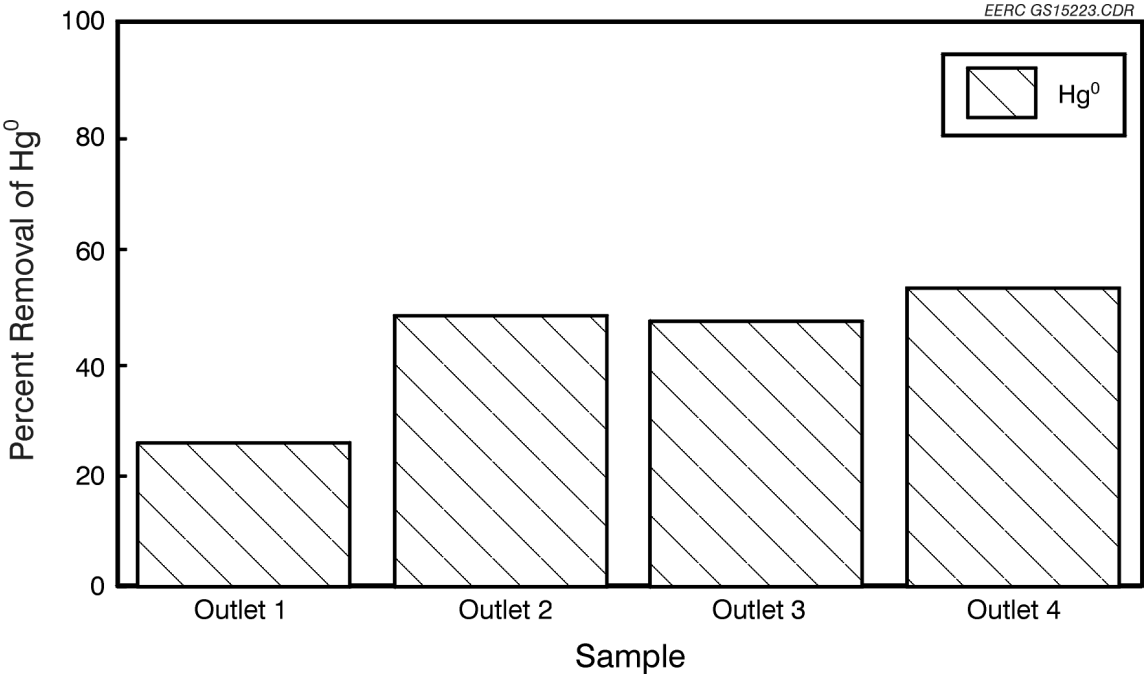

Figure 4.4-19. Percent removal of Hg^0 at the outlet filters for Test PTC-AB-585.

TABLE 4.4-7

Ratio of Oxidized Mercury to Elemental Mercury, Test PTC-AB-585

	Inlet	Outlet
	Hg/Hg^{2+}	Hg/Hg^{2+}
	0.47	0.27
	0.26	1.69
	0.47	2.21
	0.37	2.16
Average	0.39	2.02[1]

[1]Average of the last three values.

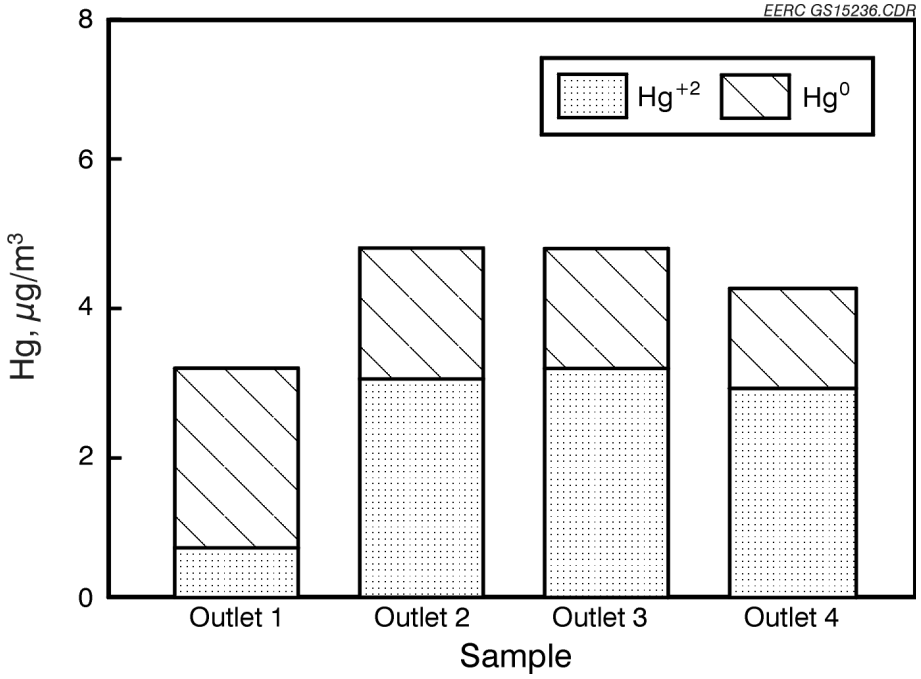

Figure 4.4-20. Distribution of mercury between the solid ash and gas samples as well as the speciation of mercury in the gas sample.

collected on the filter. Outlet Sample 7 confirmed that trace metal concentrations for the filter were very near detection or below detection limits for all seven trace metals. The average reduction of total mercury concentration across the AHPC was 1.94 µg/m^3. As shown on Table 4.4-7, the ratio of oxidized to elemental mercury for inlet samples averaged 0.39. Figure 4.4-20 shows the change in the proportion of Hg^0 and Hg^{2+} in the outlet samples from

Day 1 to Day 2 and continues through the test duration. The ratio of Hg^0 and Hg^{2+} of 0.27 in the Day 1 Outlet Sample compares well with the average ratio of Hg^0 and Hg^{2+} in the inlet samples of 0.39. Excluding the first day's sampling of the outlet, the average ratio of oxidized to elemental mercury was reversed at 2.02.

Figure 4.4-21 shows the percent removal of Hg^{2+} versus outlet samples. The percent removal values were all negative except for the first outlet sample. The negative percent removal values demonstrate the generation Hg^{2+} by converting Hg^0 to Hg^{2+}. This may indicate that a combination of the ash, electrical field, or filter may be catalyzing the conversion of elemental mercury to oxidized mercury. This observation could be significant in determining a mercury control technology for this filtration system.

The two other elements behaving like a vapor were chromium and selenium. The analysis of chromium and selenium vapor may be done only on the H_2O_2 impingers. The $KMnO_4$ in the following impingers is present in too high a concentration for trace metal evaluations other than

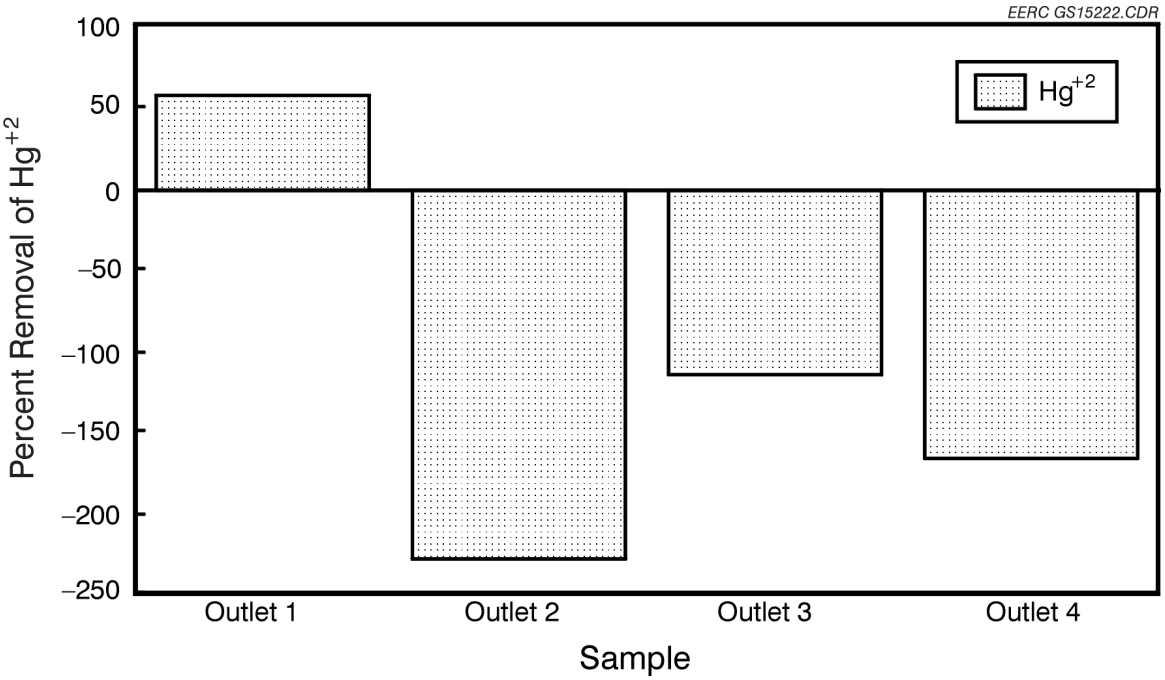

Figure 4.4-21. Percent removal of Hg2$^+$ at the outlet filters for Test PTC-AB-585.

elemental mercury. The average inlet chromium vapor concentration was 0.87 μg/m^3. The outlet chromium concentration 0.51 μg/m^3. With the concentration this low for chromium, it is difficult to draw any conclusions as to the effect the AHPC may have on the fate of vapor-phase chromium. However, all of the particulate-phase chromium is effectively removed.

The total inlet selenium concentration collected in all forms was 31.99 μg/m^3 with 21.41% RSD. The total inlet selenium concentration in vapor form ranged from 16.08 to 1.98 μg/m^3. Total outlet selenium concentration in all forms was measured at 15.68 μg/m^3. Only 0.1 μg/m^3 was found on the filter, indicating that >99% of the selenium in the outlet sample was in vapor form.

4.4.1.8 Conclusions from Baseline Test PTC-AB-585 Firing Absaloka Coal

- The AHPC operated successfully on Absaloka subbituminous for approximately 100 hr.
- Pressure drop was controlled, and pulse intervals ranged between 25 and 35 min.
- Particulate efficiency of >99.999% was achieved throughout the test period.
- All seven trace elements (As, Cd, Cr, Pb, Ni, Se, and Hg) were found in the filter ash.
- Of the seven elements, only three (Hg, Se, and Cr) appeared in detectable quantities in vapor form.
- The ratio of oxidized mercury to elemental mercury sampled at the inlet was 0.27 and at the outlet 2.02, indicating that mercury was oxidized across the AHPC.

4.4.2 100-hr Sorbent Injection Tests Firing Absaloka Subbituminous Coal (PTC-AB-586)

The purpose of this test was to evaluate the AHPC while injecting a mixture of activated carbons for mercury control. Therefore, the second 100-hr test was to repeat the first 100-hr test with the addition of duct injection of a sorbent for trace metal emission control. The AHPC operating temperature was lowered from 149°C (300°F) to 135°C (275°F). The lower temperature was used in an attempt to improve the absorption characteristics of the sorbents. A new set of GORE-TEX® graphite-impregnated bags was used for this test. A complete list of test specifications is presented in Table 4.4-8.

TABLE 4.4-8

Test Parameters for PTC-AB-586

Week of March 3–7, 1997	
Air/Cloth Ratio, m/min (ft/min)	3.7 (12)
Inlet Temp., °C (°F)	135 (275)
On-Line and Off-Line Cleaning	On
Baffling	Butterfly
Voltage, kV	50
Type of Bag	Graphite-impregnated PTFE
Bag Identification	Sets 11 and 12
No. of Bags in Use	4
Pulse Pressure, kPa (psig)	612 (90)
Pulse Duration, s	0.2
Pulsing Initiation Pressure, kPa (in. of W.C.)	2.0 (8.0)

Two sorbents were used for this test. A lignite-based activated carbon (LAC) and an iodine-impregnated activated carbon (IAC). These two activated carbons were mixed in a ratio of 4:1 LAC to IAC, respectively. The sorbent addition rate was adjusted to achieve a sorbent-to-mercury ratio of 3000:1. For Absaloka coal, the sorbent addition feed rate was 5.34 g/hr. The sorbent injection device is called a dry powder disperser (DPD). The DPD operates using a hollow cylinder to store the sorbent with a movable piston at the bottom of the hollow cylinder. A sketch of the device is shown in Figure 4.4-22. As the piston moves upward in the cylinder, it

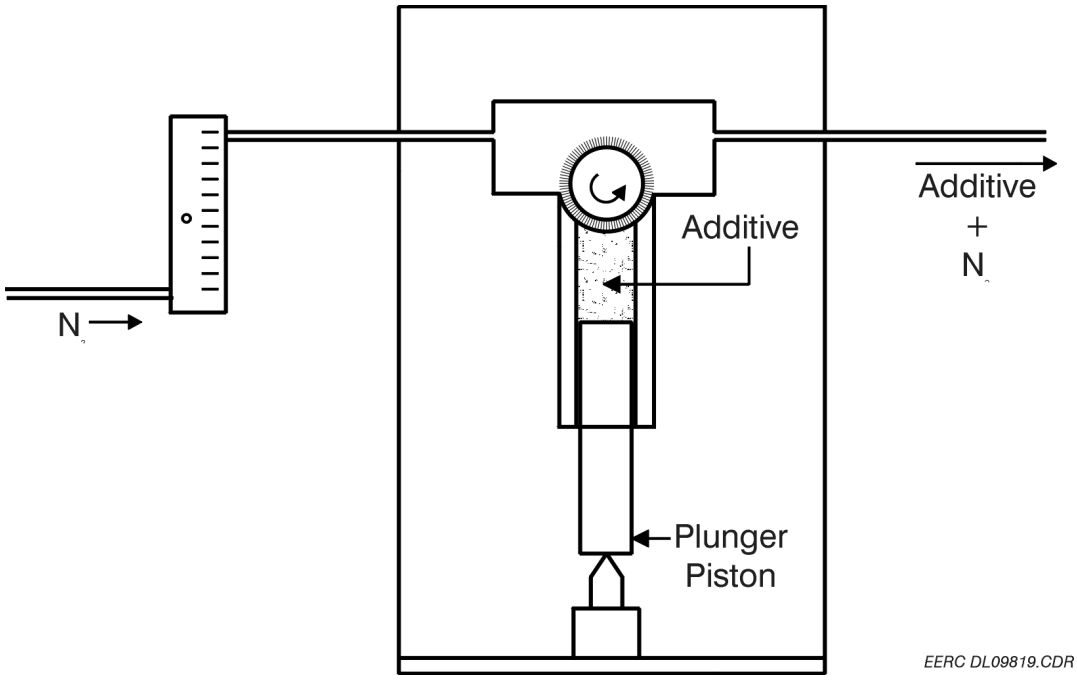

Figure 4.4-22. Dry powder disperser used to inject mercury sorbent into the flue gas stream.

moves the sorbent into contact with a rapidly spinning wheel brush. As the spinning wheel brush scrapes the sorbent from the cylinder, a stream of N_2 gas flows around the wheel brush and elutreates the now-dispersed dust into the injection line. The N_2 gas carries the dust through a 0.3-cm (⅛-in.)-OD tube to the flue gas piping. Adjusting the upward speed of the piston allowed a constant and consistent feed rate to be maintained.

Trace metal sampling using Method 29 was performed for the determination of seven trace metals. Since there is greater interest in mercury, a Semtech mercury analyzer was set up to monitor on-line the elemental and oxidized mercury concentrations at both the inlet and outlet of the AHPC. A $SnCl_2$ pretreatment process was used in conjunction with the Semtech mercury analyzer for determining the concentration of oxidized mercury in the flue gas stream.

The PTC was started up on natural gas and the AHPC inlet/outlet flue gas piping was preheated by electrical resistance heaters. No flue gas generated by the natural gas from the PTC was allowed into the AHPC. Once the PTC stabilized at 982°C (1800°F), the combustor was

switched to coal. The PTC remained on coal throughout the remainder of Test PTC-AB-586. The analysis of the flue gas is found in Table 4.4-9.

TABLE 4.4-9

Average Flue Gas Concentrations for Test PTC-AB-586[1]

O_2, % by volume	CO_2, % by volume	H_2O, % by volume	SO_2, ppm	NO_x, ppm
4–4.5	14–16	9.5–10.0	750–700	700

[1] Dry basis except for H_2O.

4.4.2.1 Results for Test PTC-AB-586 – Day 1

The purpose of Day 1 of Test PT-AB-586 was to provide a baseline of operation for the AHPC at a temperature of 135°C (275°F) and to provide time to install and shake down the mercury analyzer for on-line analysis.

Once the combustor stabilized on coal, the flue gas was directed into the AHPC. However, when the flue gas was directed into the AHPC, the combustor experienced an upset condition, causing a slug of unburned coal to reach the AHPC. The upset resulted in a degradation in the operation of the ESP in the AHPC. With the ESP dysfunction, the bags were quickly blinded by the incoming unburned carbon. After an attempt to clean the bags off-line, it was decided that a new set of bags should replace the carbon-coated bags before the AHPC was restarted. The cause of the upset was found to be an open 3.8-cm (1½-in.) valve located on a section of the inlet piping to the AHPC. Also, during the installation and testing of the new bags, it was observed that the bag cage supports tended to "bounce" up during the pulse of air. Previous testing did not show this bounce in the bag cage during pulsing. After the outlet plenum was modified slightly to hold the bag cages in place during the cleaning cycle, the AHPC was returned to normal operation.

The graph in Figure 4.4-23 shows the dP versus time and ESP current versus time for Day 1 of Test PTC-AB-586. The change in dP before and after the cleaning cycle decreased throughout the day. The change in dP began at 1.27 kPa (5.1 in. W.C.) and ended at 0.90 kPa (3.6 in. W.C.). ESP current declined steadily between each electrode-cleaning sequence. The ESP current started at 3.8 mA and ended the day at 3.2 mA. The pulse interval versus time graph is shown in Figure 4.4-24. The pulse interval remained steady at about 75 minutes between cleaning cycles.

Dust-loading data for Day 1 are presented in Table 4.4-10. Inlet dust loading measured at 6.6514 g/m^3 (2.9072 gr/scf). The inlet dust loading, calculated from the mass of ash collected from the AHPC ash hopper, was 4.83 g/m^3 (2.64 gr/scf). The outlet dust loading was 0.0001 g/m^3 (0.000228 gr/scf), giving a collection efficiency of 99.996%. Respirable mass measurements by APS are shown in Figure 4.4-25, and indicate very high efficiency of the AHPC, with an integrated respirable mass value of less than 0.01 mg/m^3. The integrated average for Day 1 of Test PTC-AB-586 was 0.002 mg/m^3. In the plot shown in Figure 4.4-26, the collection efficiency

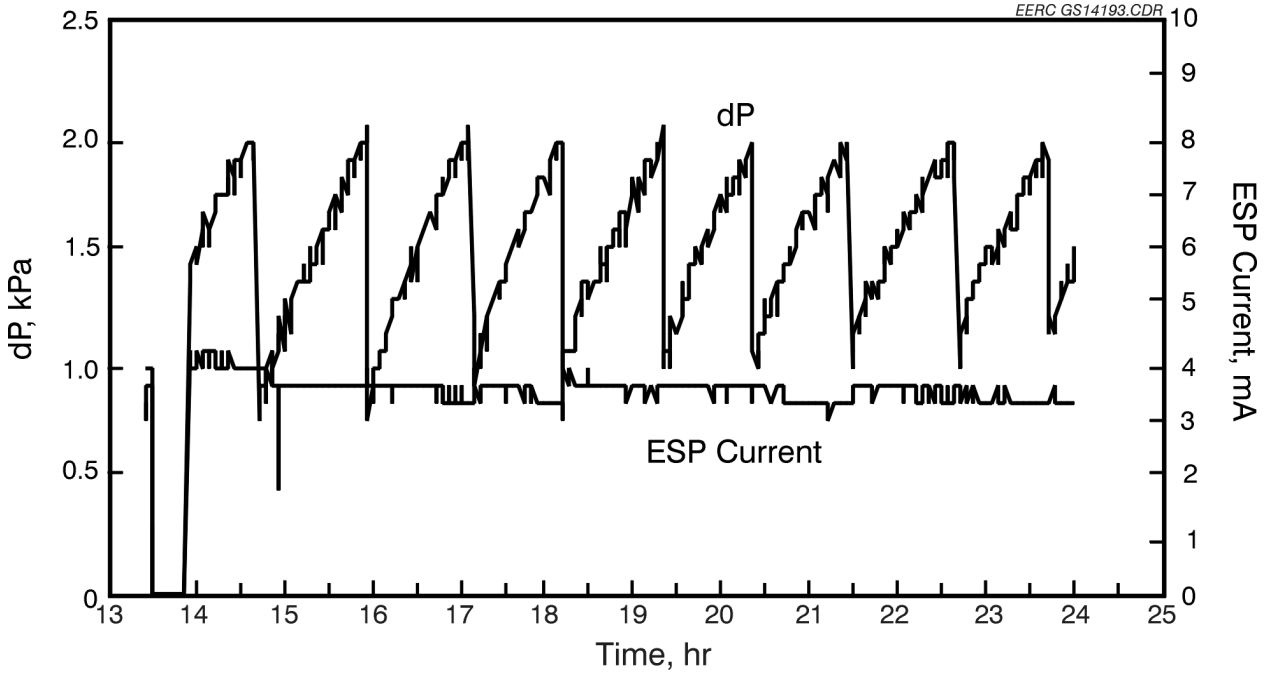

Figure 4.4-23. Pressure drop as a function of time for Day 1, March 3, 1997, Test PTC-AB-586 with on-line cleaning using graphite-impregnated PTFE bags.

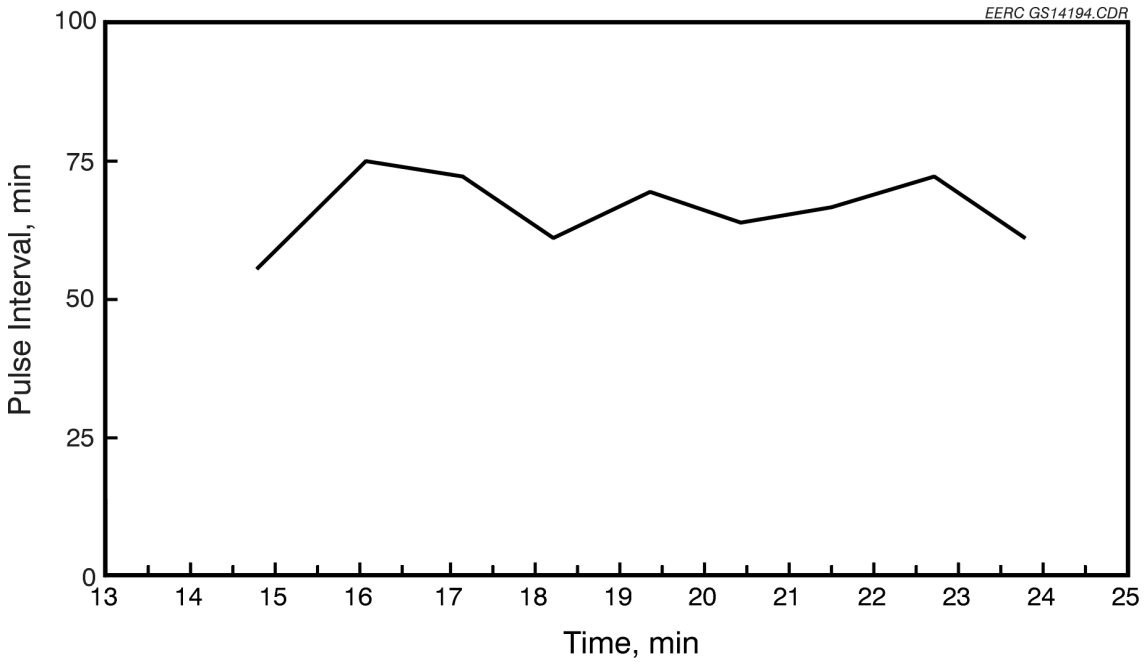

Figure 4.4-24. Pulse interval as a function of time for Day 1, March 3, 1997, Test PTC-AB-586 with on-line cleaning using graphite-impregnated PTFE bags.

TABLE 4.4-10

Dust-Loading Data for Test PTC-AB-586

Date	PTC Test No.	Hopper Ash, g/m^3	Inlet, g/m^3	Outlet, g/m^3	Percent Collection Efficiency
3-3-97	PTC-AB-586	4.83	6.6514	0.000228	99.99656
3-4-97	PTC-AB-586	6.86	7.6285	0.000068[1]	99.99910
3-5-97	PTC-AB-586	7.57	7.3683	0.000113[1]	99.99845
3-6-97	PTC-AB-586		7.1629[2]		
3-6-97	PTC-AB-586	7.25	7.2491	0.000045[1]	99.99937
3-7-97	PTC-AB-586	7.50	7.4280	0.000048[1]	99.99935

[1] Sampling time of 24 hr.
[2] Multicyclone.

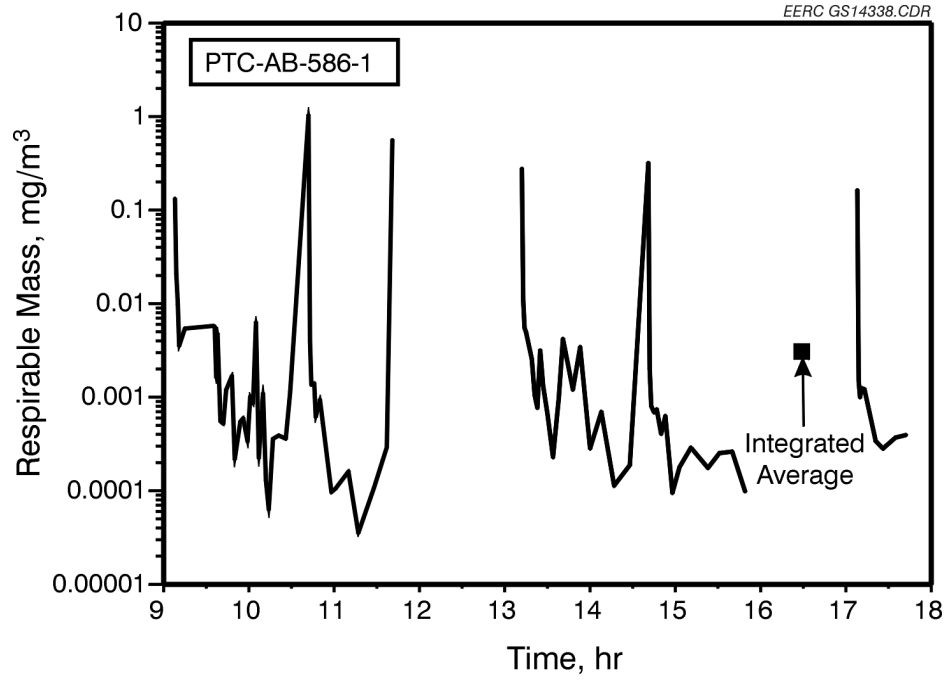

Figure 4.4-25. APS data for Day 1, March 3, 1997, Test PTC-AB-586.

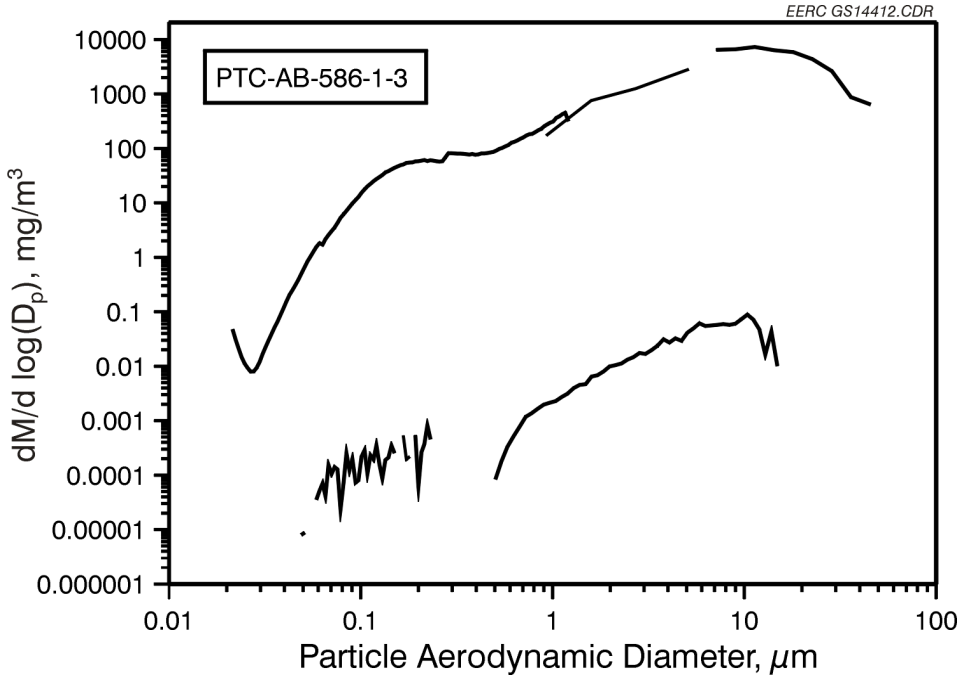

Figure 4.4-26. The combined inlet and outlet particulate concentration versus aerodynamic particle-size data for Day 1, March 3, 1997, Test PTC-AB-586.

of >99.99% is confirmed over the entire range of particle sizes, from 0.01 to 10 μm in aerodynamic diameter.

Figure 4.4-27 displays the graph of mercury concentration versus time. A mercury analyzer that was installed at the AHPC outlet was set up to monitor only elemental mercury vapor. Flue gas sampling began at 8:48 p.m. The outlet mercury vapor concentrations measured between 8:48 and 10:15 p.m. by the analyzer seem to correspond to the outlet elemental mercury vapor values from Method 29 testing. Table 4.4-11 contains the Method 29 mercury analyses for Test PTC-AB-586. The Method 29 values for elemental mercury and oxidized mercury presented in Figure 4.4-27 with the on-line mercury versus time graphs show the on-line mercury analyzer remaining fairly steady at about 1.5 μg/m^3 from 12:00 midnight to 4:35 a.m. in the morning. At that point, the elemental mercury concentration dropped with the corresponding combustor upset that slugged coal into the AHPC. The elemental mercury emission fluctuated as the AHPC recovered from the upset. After the scheduled maintenance of the AHPC from 8:53 to 10:03 a.m., the mercury analyzer continued to measure elemental mercury vapor at about 2.0 μg/m^3.

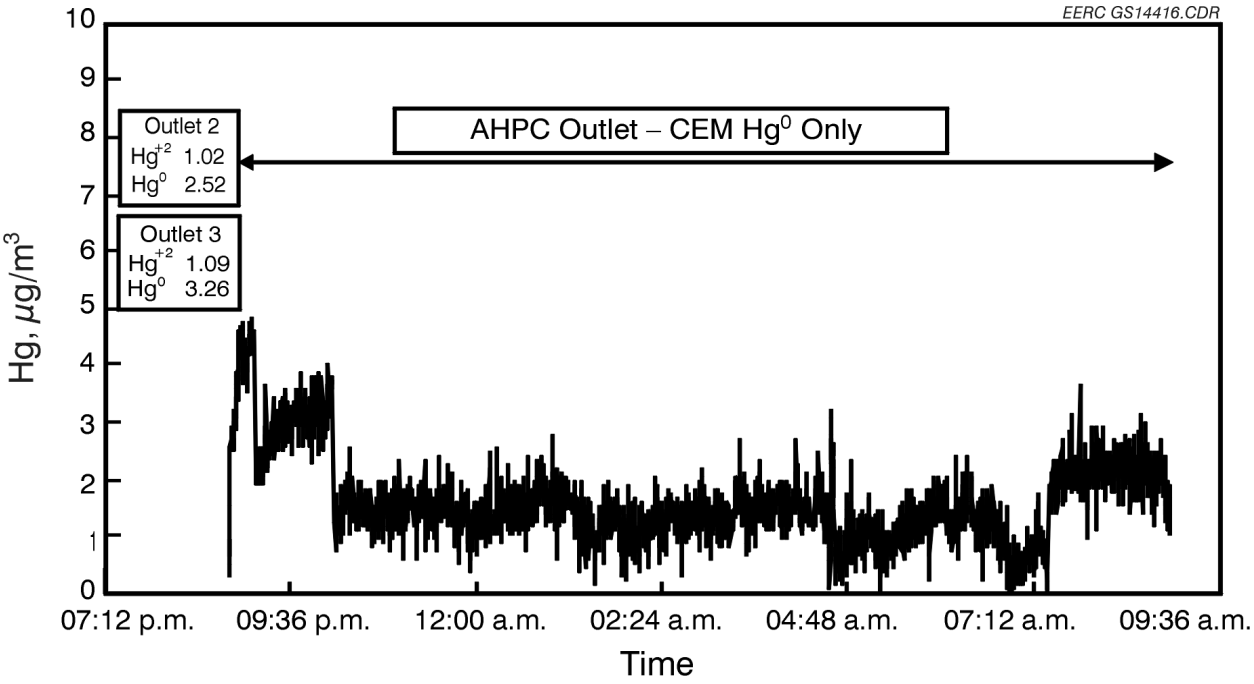

Figure 4.4-27. Mercury concentration versus time for Day 1, March 3, 1997, Test PTC-AB-585.

TABLE 4.4-11

Trace Metal Data for Test PTC-AB-586

	Inlet 1				Inlet 3				Inlet 5				Inlet 8				Inlet 10				Statistics		
Sample Type	Filter	H_2O_2	$KMnO_4$	Total	Filter	H_2O_2	$KMnO_4$	Total	Filter	H_2O_2	$KMnO_4$	Total	Filter	H_2O_2	$KMnO_4$	Total	Filter	H_2O_2	$KMnO_4$	Total	Average	STDV	%RSD
Mercury, µg/m³	0.93	1.09	3.26	5.28	0.61	1.95	4.92	7.38	0.66	2.53	3.9	7.09	0.73	2.38	4.5	7.61	0.52	2.14	4.37	7.03	6.84	0.83	12.07
Arsenic, µg/m³	93.2	0.81		94				0	103	1.01		104				0				0	99.0		
Cadmium, µg/m³	2.26	0.06		2.32				0	1.25	0.08		1.33				0				0	1.82		
Chromium, µg/m³	510	0.97		510				0	555	1.47		557				0				0	532		
Lead, µg/m³	293	0.4		293				0	288	0.51		288				0				0	290		
Nickel, µg/m³	226	1.61		227				0	229	2.02		231				0				0	228		
Selenium, µg/m³	14.0	3.74		17	28.2	2.05		30.3	26.5	1.01		27.5	21.8	1.01		22.8	31.22	0.95		32.2	25	5.25	21.4

	Outlet 2				Outlet 4				Outlet 6				Outlet 9				Outlet 11				Statistics		
Sample Type	Filter	H_2O_2	$KMnO_4$	Total	Filter	H_2O_2	$KMnO_4$	Total	Filter	H_2O_2	$KMnO_4$	Total	Filter	H_2O_2	KMnO4	Total	Filter	H_2O_2	$KMnO_4$	Total	Average	STDV	%RSD
Mercury, µg/m³	0.00	1.02	2.52	3.54	NA	2.23	0.36	2.59	0.00	2.25	0.27	2.52	NA	2.79	0.25	3.04	NA	2.26	0.21	2.47	2.83	0.41	14.40
Arsenic, µg/m³	0.00	0.47	NA	0.47	NA	NA	NA	NA	0.28	0.35	NA	0.63	NA	NA	NA	NA	NA	NA	NA	NA	NA	NA	NA
Cadmium, µg/m³	0.00	0.04	NA	0.04	NA	NA	NA	NA	0.07	0.03	NA	0.1	NA	NA	NA	NA	NA	NA	NA	NA	NA	NA	NA
Chromium, µg/m³	0.00	0.52	NA	0.52	NA	NA	NA	NA	3.02	0.27	NA	3.29	NA	NA	NA	NA	NA	NA	NA	NA	NA	NA	NA
Lead, µg/m³	0.00	0.24	NA	0.24	NA	NA	NA	NA	0.63	0.17	NA	0.8	NA	NA	NA	NA	NA	NA	NA	NA	NA	NA	NA
Nickel, µg/m³	0.00	0.95	NA	0.95	NA	NA	NA	NA	1.02	0.7	NA	1.72	NA	NA	NA	NA	NA	NA	NA	NA	NA	NA	NA
Selenium, µg/m³	0.00	20.8	NA	20.8	NA	3.88	NA	3.88	0.23	3.37	NA	3.9	NA	3.69	NA	3.69	NA	4.76	NA	4.76	7.35	6.74	91.77

	Coal and Hopper Ash						Blanks for Inlet, µg/m³			Blanks for Outlet, µg/m³		
Sample Type	Coal, µg/g	Ash 1, µg/m³	Ash 2, µg/m³	Ash 3, µg/m³	Ash 4, µg/m³	Ash 5, µg/m³	Filter	H_2O_2	$KMnO_4$	Filter	H_2O_2	$KMnO_4$
Mercury	0.080	1.13	1.03	1.98	1.8	3.8	<0.004	<0.177	<0.088	<0.001	<0.050	
Arsenic	1.16	93		106			<0.177	<3.351		<0.050	<1.009	
Cadmium	0.057	1.4		0.33			<0.071	<0.265		<0.020	<0.076	
Chromium	9.4	477		460			<0.068	<0.883		<0.019	<0.252	
Lead	4.4	279		263			<0.088	<1.766		<0.025	<0.504	
Nickel	4.6	225		210			<0.353	<7.062		<0.101	<2.018	
Selenium	0.54	19.9	26.9	29.0	24.0	52.5	<0.353	<3.531		<0.101	<1.009	

4.4.2.2 Results for Test PTC-AB-586 – Day 2

The objective for Day 2 to the end of the test was to evaluate particulate and trace metal collection in the AHPC while injecting a mixture of activated carbon. The dP versus time graph for Day 2 is given in Figure 4.4-28. The change in dP before and after cleaning remained fairly stable, ranging from 0.90 to 0.80 kPa (3.6 to 3.2 in. W.C.). Pulse intervals (Figure 4.4-29) maintained at about 75 min between pulse cycles until about 28.2 hr (4:35 a.m.). At that time, a plug in the coal gun of the PTC caused a slug of coal to reach the AHPC. The upset dramatically shortened the pulse interval time from 75 to 45 min between cleaning cycles. The AHPC came off-line at 32.9 hr (8:53 a.m.) into the run for routine maintenance of the ESP grid and cleaning of AHPC view ports. Additional adjustments were made to the bag cage supports at this time. The AHPC returned to on-line status at 34.2 hr (10:07 a.m.). The pulse interval started at 50 min but quickly reached steady state at about 38 min for the rest of Day 2.

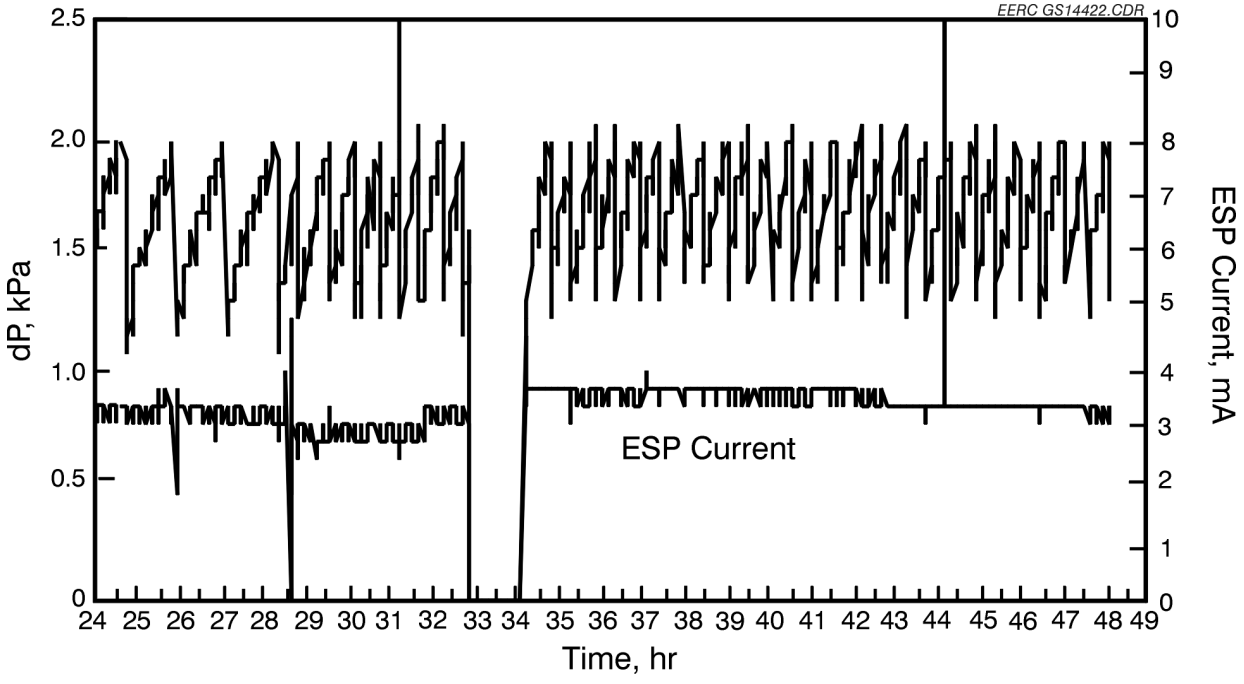

Figure 4.4-28. Pressure drop as a function of time for Day 2, March 4, 1997, Test PTC-AB-586 with on-line cleaning using graphite-impregnated PTFE bags.

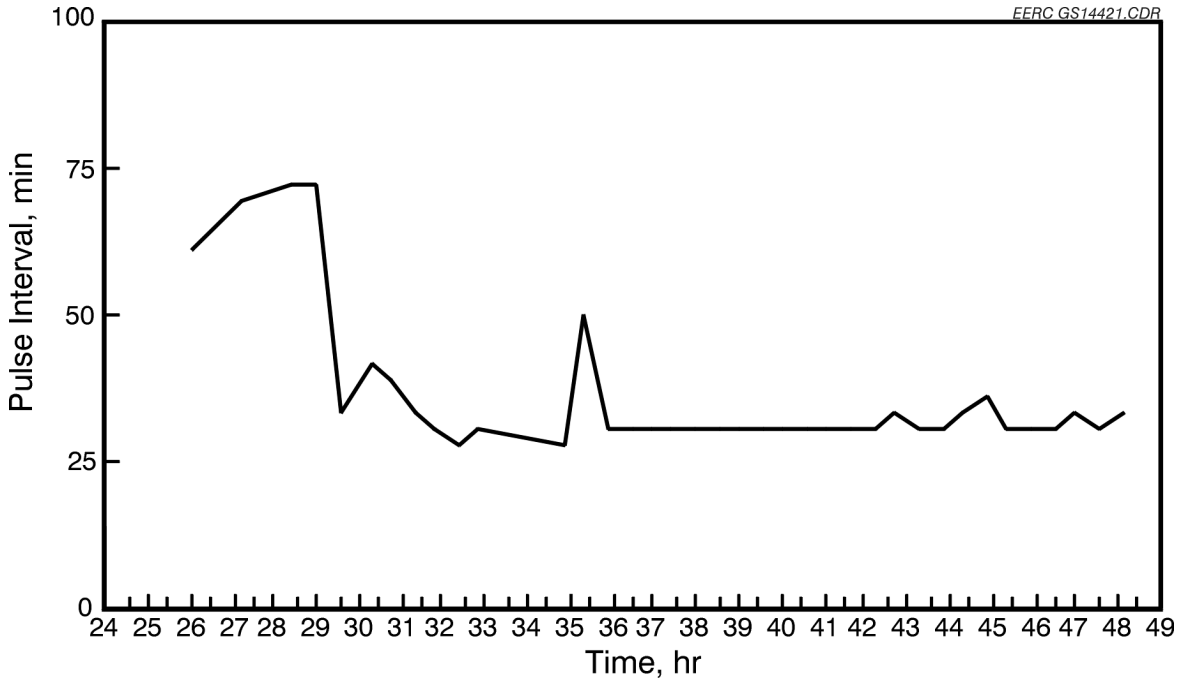

Figure 4.4-29. Pulse interval as a function of time for Day 2, March 4, 1997, Test PTC-AB-586 with on-line cleaning using graphite-impregnated PTFE bags.

Sorbent injection started at 37.5 hr (1:24 p.m.), on March 4. Over the entire length of Test PTC-AB-586, the sorbent feed rate averaged 5.24 g/hr and represented an average sorbent-to-mercury ratio of 3034. The addition of sorbent did not seem to affect the pulse interval of the AHPC.

Dust-loading data for Day 2 are presented in Table 4.4-10. Inlet dust loading measured at 7.6285 g/m^3 (3.3340 gr/scf). The inlet dust loading, calculated from the mass of ash collected from the AHPC ash hopper, was 6.86 g/m^3 (3.00 gr/scf). Fair agreement exists between the two inlet dust-loading values. The outlet dust loading was 0.000068 g/m^3 (0.000030 gr/scf), giving a collection efficiency of 99.9991%. The outlet particulate sample was collected over a period of 24 hr. Respirable mass measurements by the APS are presented in Figure 4.4-30. The APS data confirm better than 99.99% collection efficiency of the AHPC, with an integrated respirable mass value of less than 0.01 mg/m^3. The two integrated average APS results for Day 2 were 0.0075 and 0.002 mg/m^3. The injection of sorbent did not degrade the AHPC collection efficiency. In the

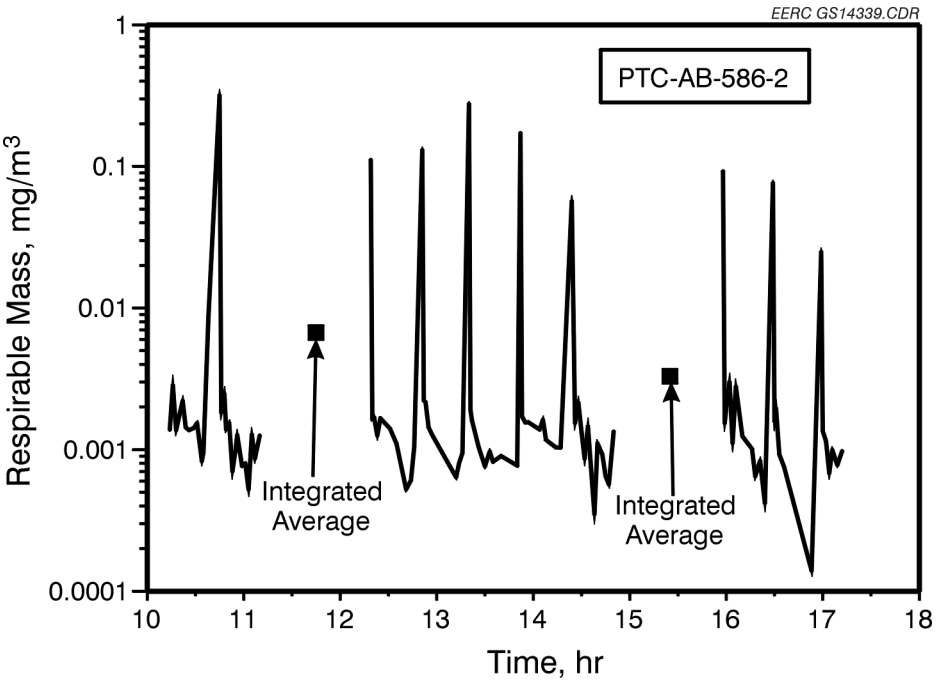

Figure 4.4-30. APS data for Day 2, March 4, 1997, Test PTC-AB-586.

plot shown in Figure 4.4-31, the collection efficiency of >99.99% is confirmed over the entire range of particle sizes, from 0.01 to 10 μm in aerodynamic diameter.

The graph showing the relationship of elemental mercury concentration in the AHPC outlet piping versus time is found in Figure 4.4-32. Sorbent injection began at 1:24 p.m. on Day 2, March 4. The mercury continuous emission monitor (CEM) showed a continuous decrease in elemental mercury concentration after sorbent injection began. Periodic increases in elemental mercury emissions correspond to the discontinuation of sorbent feed for cartridge replacement in the DPD.

An EPA Method 29 sample of the outlet confirmed the low elemental mercury values. The outlet Method 29 data are shown in Figure 4.4-32 and in Table 4.4-11 labeled Outlet 4. The elemental mercury concentration of the outlet measured 0.36 μg/m^3, and the oxidized mercury concentration measured 2.23 μg/m^3. The inlet mercury values, labeled Inlet 3, measured 4.92 μg/m^3 for elemental mercury and 1.95 μg/m^3 for oxidized mercury.

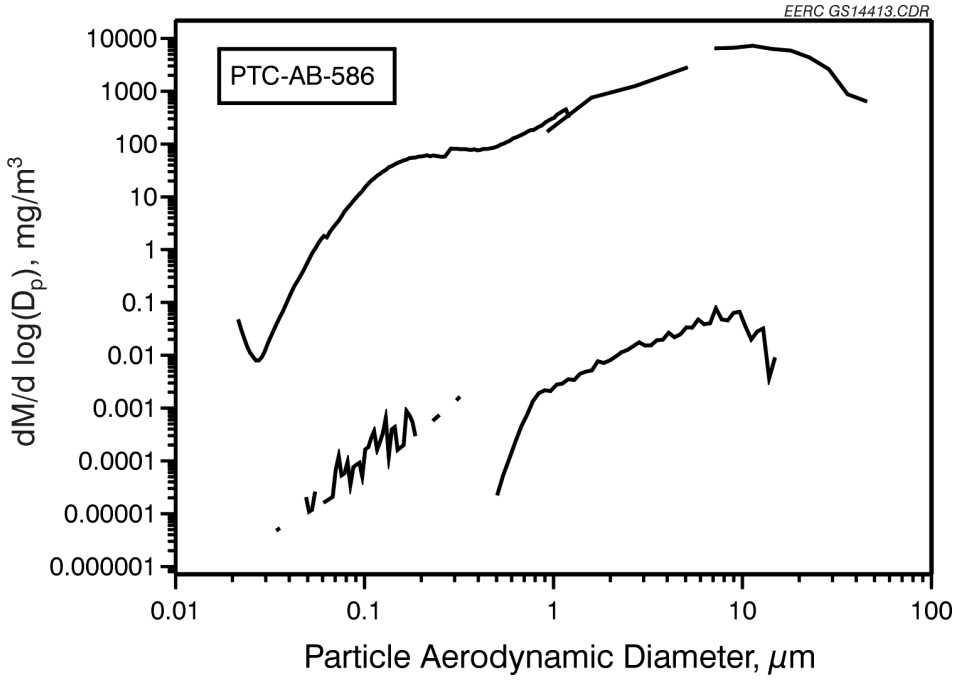

Figure 4.4-31. The combined inlet and outlet particulate concentration versus aerodynamic particle-size data for Day 2, March 4, 1997, Test PTC-AB-586.

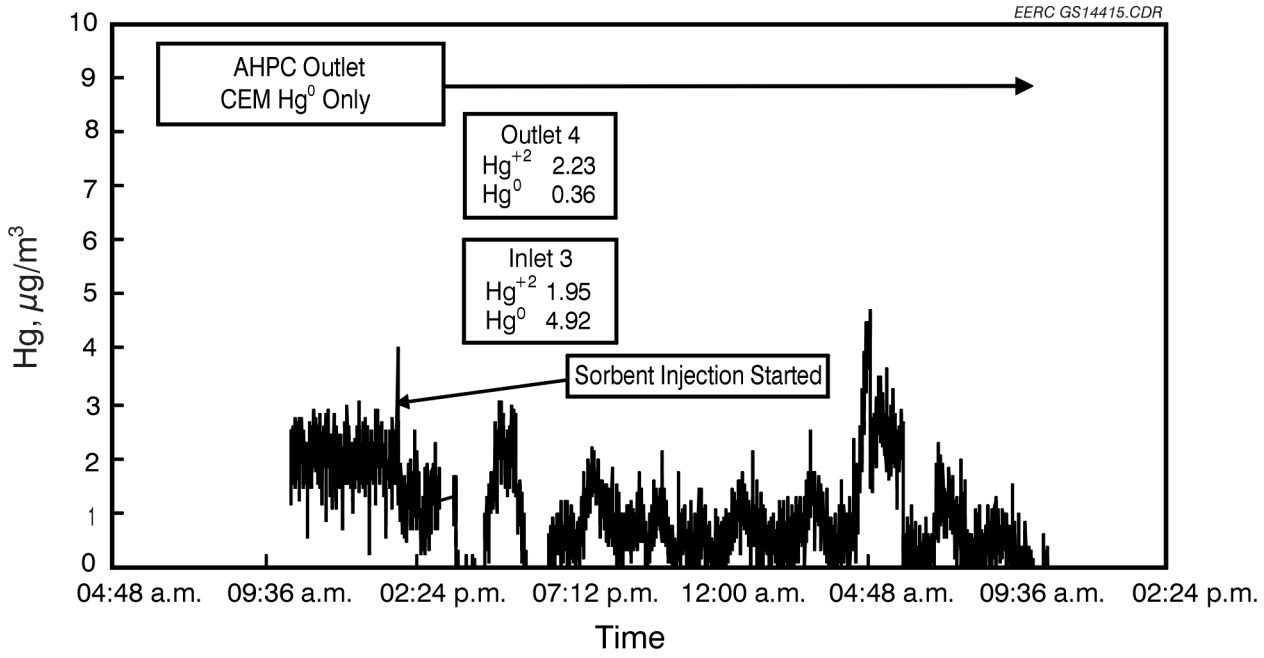

Figure 4.4-32. Mercury concentration versus time for Day 2, March 4, 1997, Test PTC-AB-586.

4.4.2.3 Results for Test PTC-AB-586 – Day 3

The dP versus time graph for Day 3 is found in Figure 4.4-33. The change in dP before and after cleaning was about 0.80 kPa (3.2 in. W.C.) throughout the day. The pulse interval fluctuated between 30 and 40 min. The graph of pulse interval versus time is given in Figure 4.4-34. The AHPC came off-line at 57.1 hr (9:00 a.m.) into the run for routine maintenance of the ESP grid and cleaning of AHPC view ports. The AHPC returned to on-line status at 57.6 hr (9:36 a.m.). A slight increase in pulse interval was noted after baghouse maintenance, but quickly reached steady state for the rest of Day 3.

The dust-loading data for Day 3 are presented in Table 4.4-10. The EPA Method 29 inlet dust loading measured at 7.3683 g/m^3 (3.2203 gr/scf). The inlet dust loading, calculated from the mass of ash collected from the AHPC ash hopper, was 7.57 g/m^3 (3.31 gr/scf). A multicyclone sample was also collected at the inlet. The inlet multicyclone dust loading was 7.1629 g/m^3 (3.1305 gr/scf). The three inlet dust-loading values agree well enough to give confidence in the

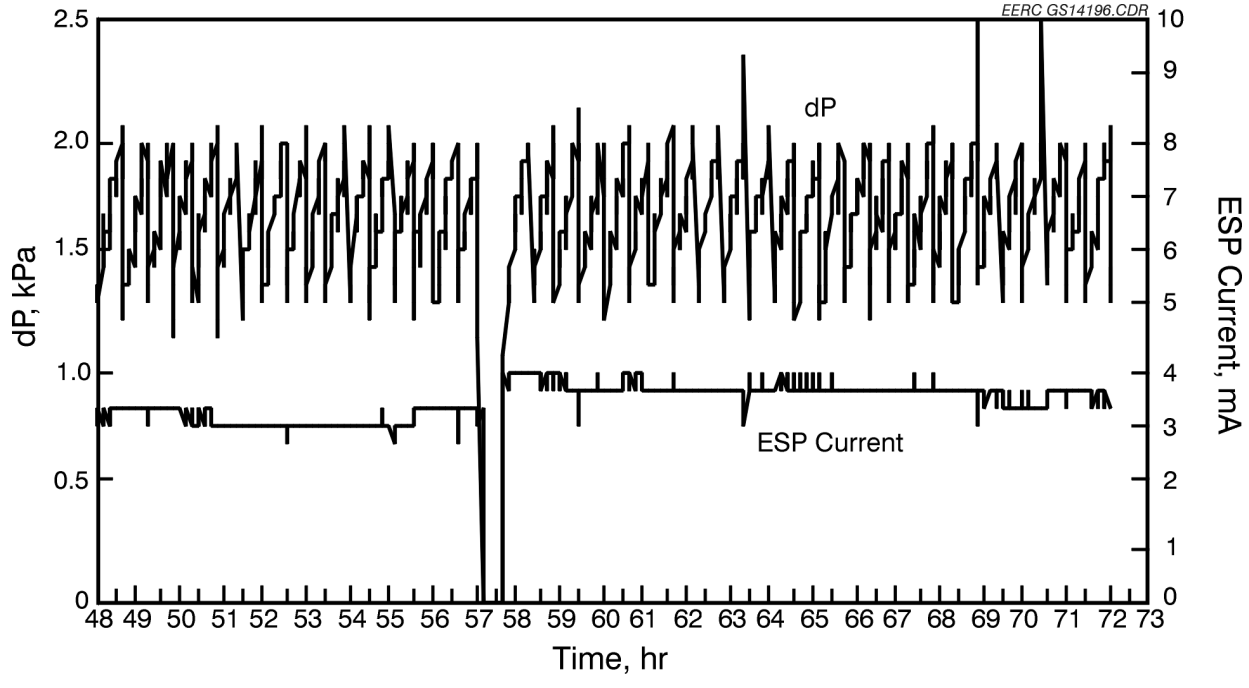

Figure 4.4-33. Pressure drop as a function of time for Day 3, March 5, 1997, Test PTC-AB-586 with on-line cleaning using graphite-impregnated PTFE bags.

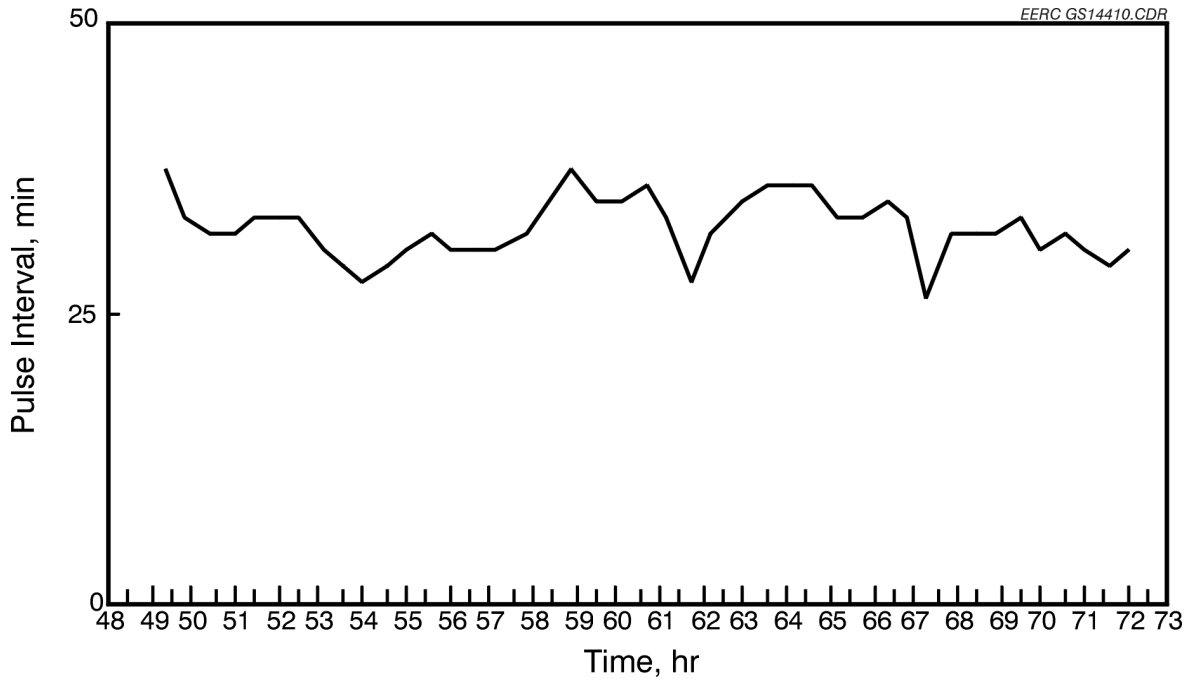

Figure 4.4-34. Pulse interval as a function of time for Day 3, March 5, 1997, Test PTC-AB-586 with on-line cleaning using graphite-impregnated PTFE bags.

inlet particulate data. The outlet dust loading was 0.000113 g/m^3 (0.00005 gr/scf), giving a dust-loading efficiency of 99.9985%. The outlet particulate sample was collected over a period of 24 hr. Respirable mass measurements by the APS are presented in Figure 4.4-35. The three integrated averages all less than 0.01 mg/m^3 confirm >99.999% collection efficiency of the AHPC. The injection of sorbent did not seem to degrade the AHPC collection efficiency. In the plot found in Figure 4.4-36, the particulate collection efficiency of >99.99% is confirmed over the entire range of particle sizes, from 0.01 to 10 μm in aerodynamic diameter.

The mercury analyzer readout for Day 3 is presented in Figure 4.4-37. The mercury analyzer continued to monitor the elemental mercury concentration on the outlet of the AHPC from 12:00 midnight to 1:30 p.m. on Day 3. The elemental mercury concentration was below the 0.5-μg/m^3 detection limit. Outlet Method 29 sampling, labeled Outlet 6 on Table 4.4-11, confirms the low elemental mercury levels with a measured value of 0.27 μg/m^3. The oxidized mercury concentration of the outlet sample was 2.25 μg/m^3. The mercury inlet concentration,

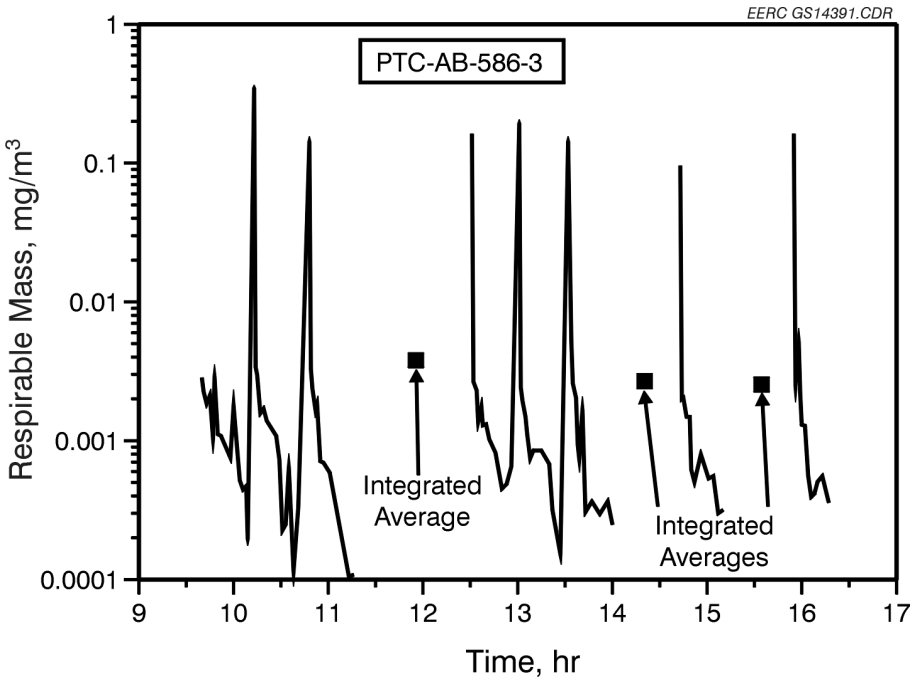

Figure 4.4-35. APS data for Day 3, March 5, 1997, Test PTC-AB-586.

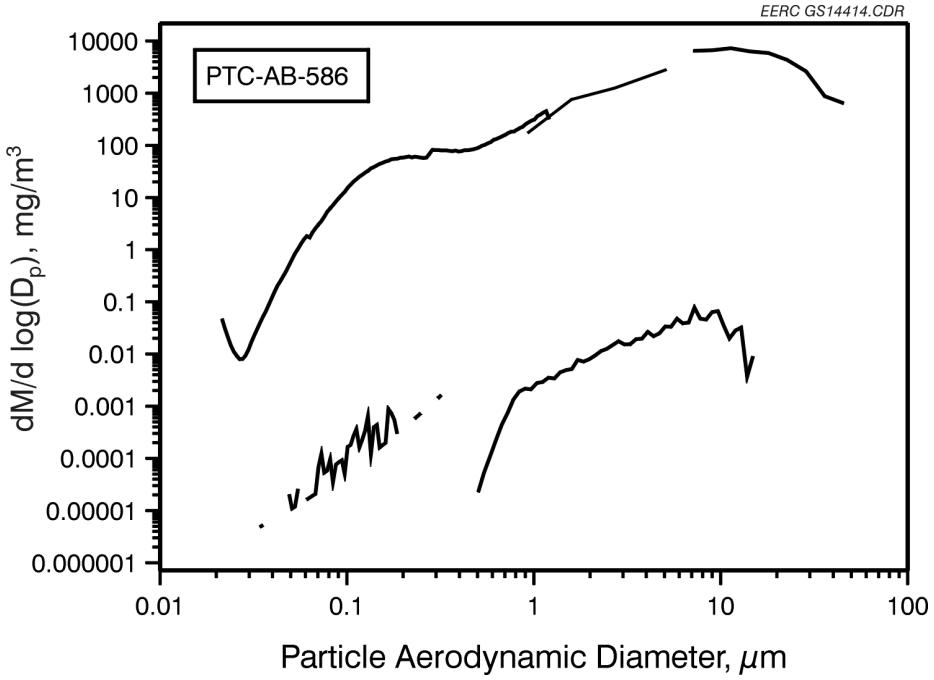

Figure 4.4-36. The combined inlet and outlet particulate concentration versus aerodynamic particle-size data for Day 3, March 5, 1997, Test PTC-AB-586.

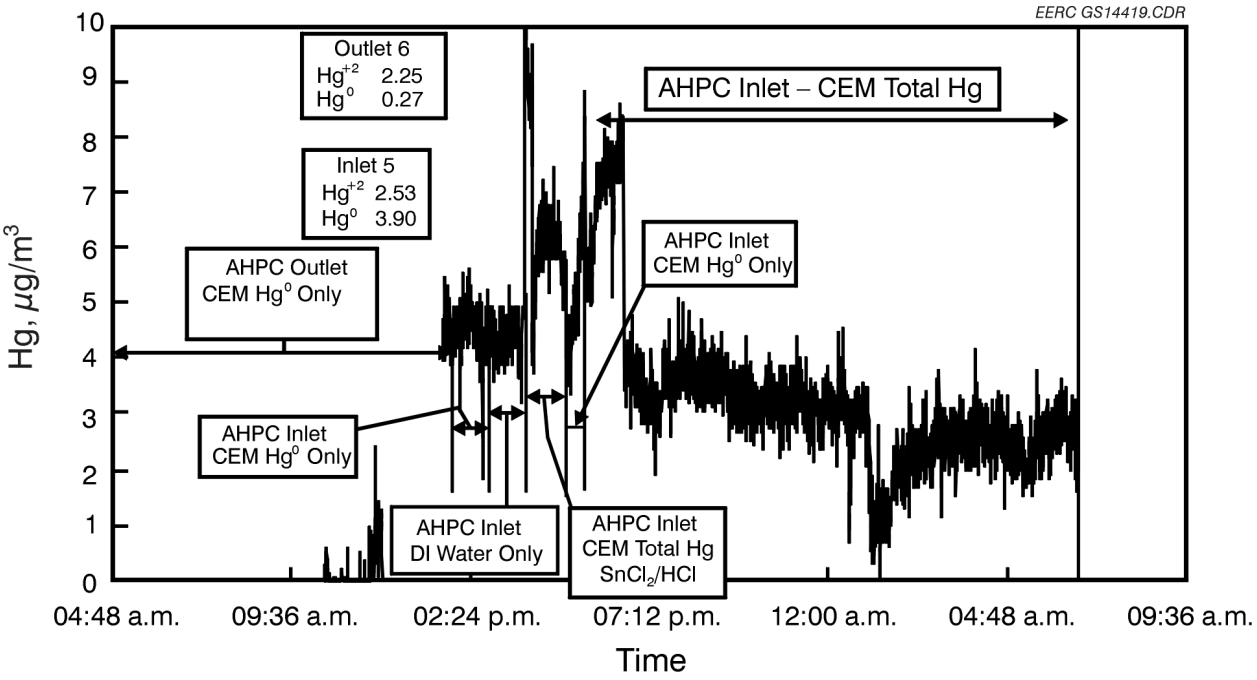

Figure 4.4-37. Mercury concentration versus time for Day 3, March 5, 1997, Test PTC-AB-586.

labeled Inlet 5 on Table 4.4-11, was measured at 3.90 and 2.53 µg/m^3 for elemental and oxidized mercury, respectively. At 1:30 p.m., the mercury analyzer changed locations from sampling outlet elemental mercury to inlet elemental mercury. The graph of mercury versus time in Figure 4.4-37 shows the mercury concentration increasing from <0.5 to about 4.6 µg/m^3. At 3:03 p.m., the mercury CEM started using a pretreatment cell prior to analysis. The pretreatment cell normally would operate with a $SnCl_2$ solution; however, deionized water (DI) was substituted for start-up purposes. Because the $SnCl_2$ was absent, no reduction of Hg^{2+} occurred. Therefore, at 3:03 p.m., no change in elemental mercury concentration was observed. At 3:27 p.m., the DI water was replaced with the $SnCl_2$ solution for the analysis of total mercury vapor in the inlet flue gas stream. The mercury concentration spiked when the CEM switched to bypass. At 3:51 p.m., the CEM began to analyze for total mercury in the inlet flue gas. The CEM values averaged about 6.5 µg/m^3. From 4:59 p.m. to 5:26 p.m., the mercury CEM sampled for elemental mercury. The average mercury concentration was about 4.5 µg/m^3. At 5:27 p.m., the mercury CEM switched to total mercury. The mercury analyzer read 8.5 µg/m^3 and then was rezeroed, dropping the mercury reading to 5.5 µg/m^3. The mercury concentration rose

dramatically from 5.5 to 8.5 μg/m^3. Then, at 6:45 p.m., about the same time the coal feeder was being refilled, the total mercury concentration dropped quickly to 4.5 μg/m^3. Speculation is that a small upset in combustor conditions may have contaminated the inlet sampling filter with unburned coal. Later examination of the filter did show the presence of carbon particles. The concentration of total mercury continued to decrease throughout Day 3 (March 5) and into the morning of Day 4 (March 6).

4.4.2.4 Results for Test PTC-AB-586 – Day 4

The dP versus time graph for Day 4 is found in Figure 4.4-38. The change in dP before and after the cleaning cycle remained at about 0.80 kPa (3.2 in. W.C.) throughout the day. The pulse interval fluctuated between 30 and 40 min. The graph of pulse interval versus time is found in Figure 4.4-39. The AHPC came off-line at 80 hr (8:06 a.m.) into the run for routine maintenance of the ESP grid and cleaning of AHPC view ports. Also, a minor repair to the ESP high-voltage interface to the grid was performed. The AHPC returned to on-line status at 81 hr (9:06 a.m.). A

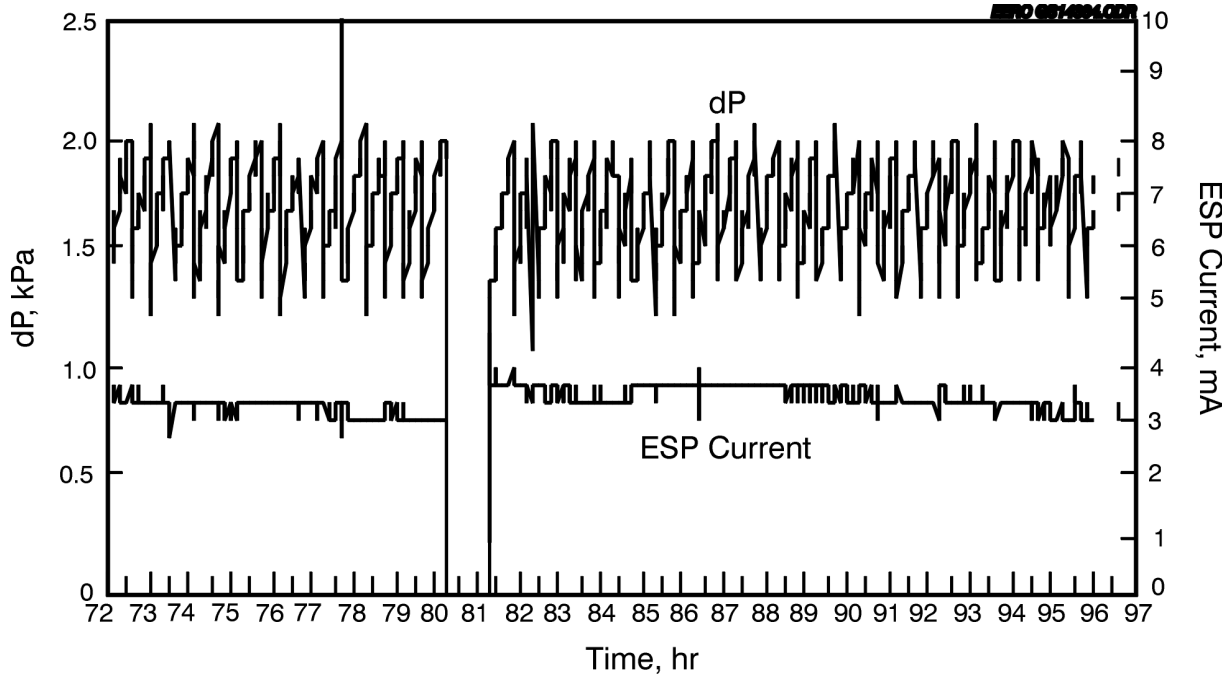

Figure 4.4-38. Pressure drop as a function of time for Day 4, March 6, 1997, Test PTC-AB-586 with on-line cleaning using graphite-impregnated PTFE bags.

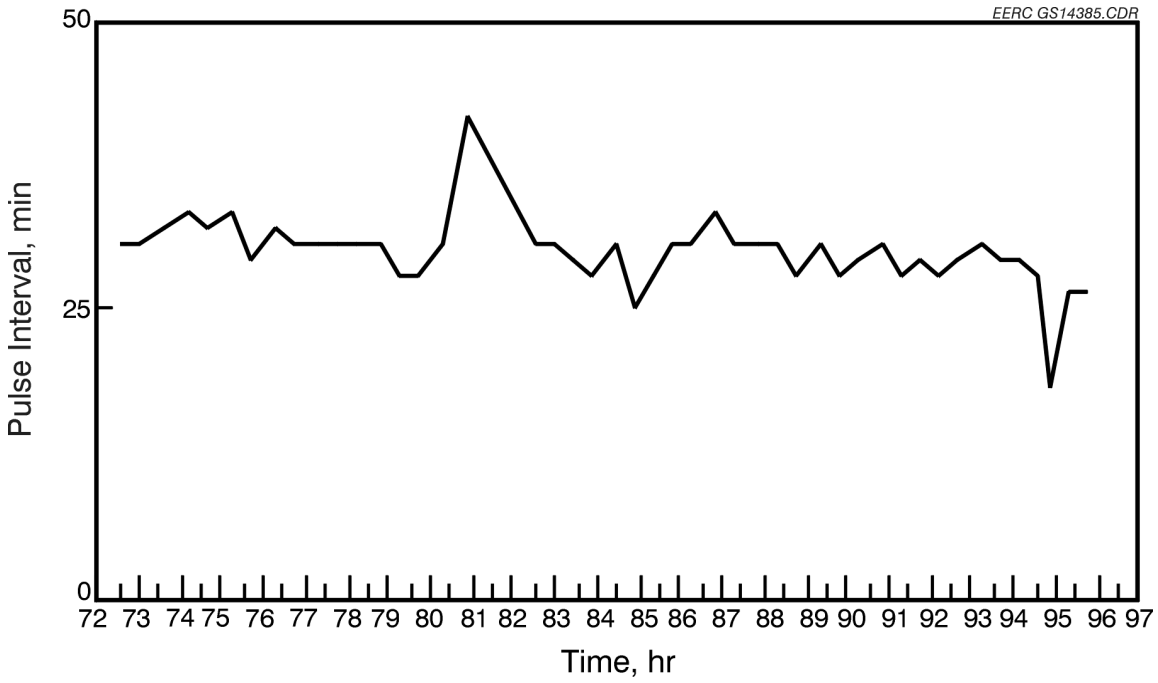

Figure 4.4-39. Pulse interval as a function of time for Day 4, March 6, 1997, Test PTC-AB-586 with on-line cleaning using graphite-impregnated PTFE bags.

slight increase in pulse interval was noted after maintenance, but the AHPC quickly reached steady state for the rest of Day 4.

The dust-loading data for Day 4 are presented in Table 4.4-10. The EPA Method 29 inlet dust loading measured was 7.2491 g/m^3 (3.1682 gr/scf), and the inlet dust loading, calculated from the mass of ash collected from the AHPC ash hopper, was 7.25 g/m^3 (3.17 gr/scf). The outlet dust loading was 0.000045 g/m^3 (0.000020 gr/scf), giving a collection efficiency of 99.9994%. The outlet particulate sample was collected over a period of 24 hr. Respirable mass measurements by the APS are presented in Figure 4.4-40. The respirable mass integrated averages for Day 4 were 0.0033, 0.0031, and 0.0024 mg/m^3. The three integrated averages of all less than 0.01 mg/m^3 confirm >99.999% collection efficiency of the AHPC. The injection of sorbent did not seem to degrade the AHPC collection efficiency. In the plot given in Figure 4.4-41, the collection efficiency of >99.99% is confirmed over the entire range of particle sizes, from 0.01 to 10 μm in aerodynamic diameter.

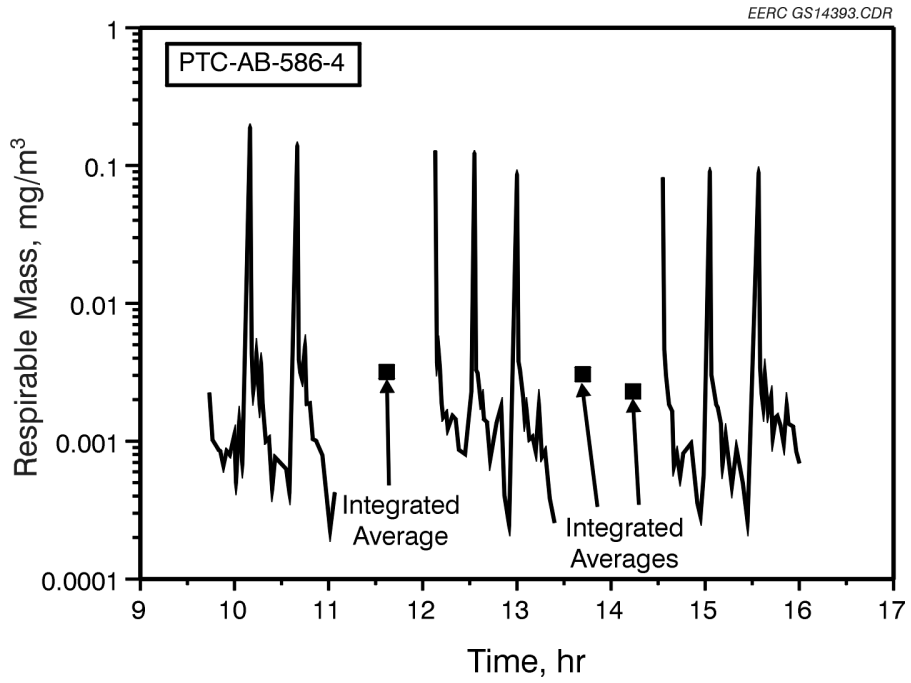

Figure 4.4-40. APS data for Day 4, March 6, 1997, Test PTC-AB-586.

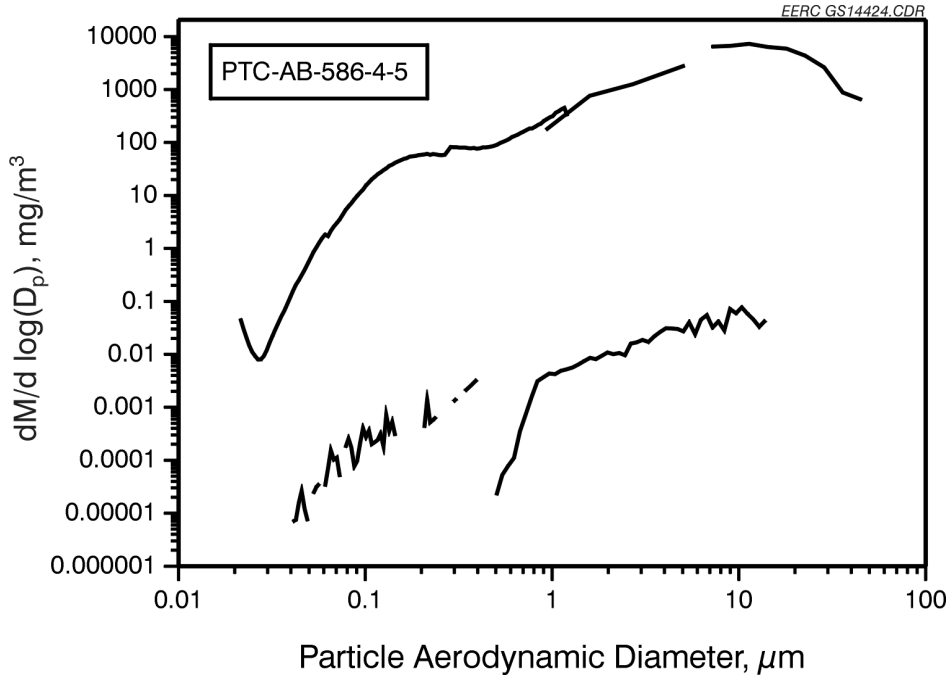

Figure 4.4-41. The combined inlet and outlet particulate concentration versus aerodynamic particle-size data for Day 4, March 6, 1997, Test PTC-AB-586.

The mercury analyzer readout for Day 4 is presented in Figure 4.4-42. The mercury analyzer continued to monitor total mercury concentration on the inlet of the AHPC from midnight to 6:30 a.m. on Day 4. The total mercury concentration was about 3.5 μg/m^3 at midnight and dropped to 0.5 μg/m^3 around 1:15 a.m. No explanation can be given at this time. However, there may have been a problem with the sampling pretreatment system. Total mercury values climbed and leveled off at about 2.5 μg/m^3 until a maintenance shutdown at 6:30 a.m. The mercury analyzer was rezeroed and the sampling point changed from the inlet to the outlet of the AHPC. Preliminary start-up sampling was done between 7:00 and 9:30 a.m. Real-time sampling of the outlet began at 9:30 a.m., sampling for elemental mercury only. The elemental mercury measured about 0.75 μg/m^3. During this time period, outlet Method 29 sampling (Outlet 9 on Table 4.4-11) confirmed the low elemental mercury levels with a measured value 0.25 μg/m^3. The oxidized mercury concentration was 2.79 μg/m^3. The mercury inlet concentration (Inlet 8 on Table 4.4-11), was measured at 4.50 and 2.38 μg/m^3 for elemental and oxidized mercury, respectively. The efficiency capture of total mercury by the sorbent was 56%, as derived from the Method 29 analysis. At 1:20 p.m., the mercury analyzer switched from elemental to total mercury

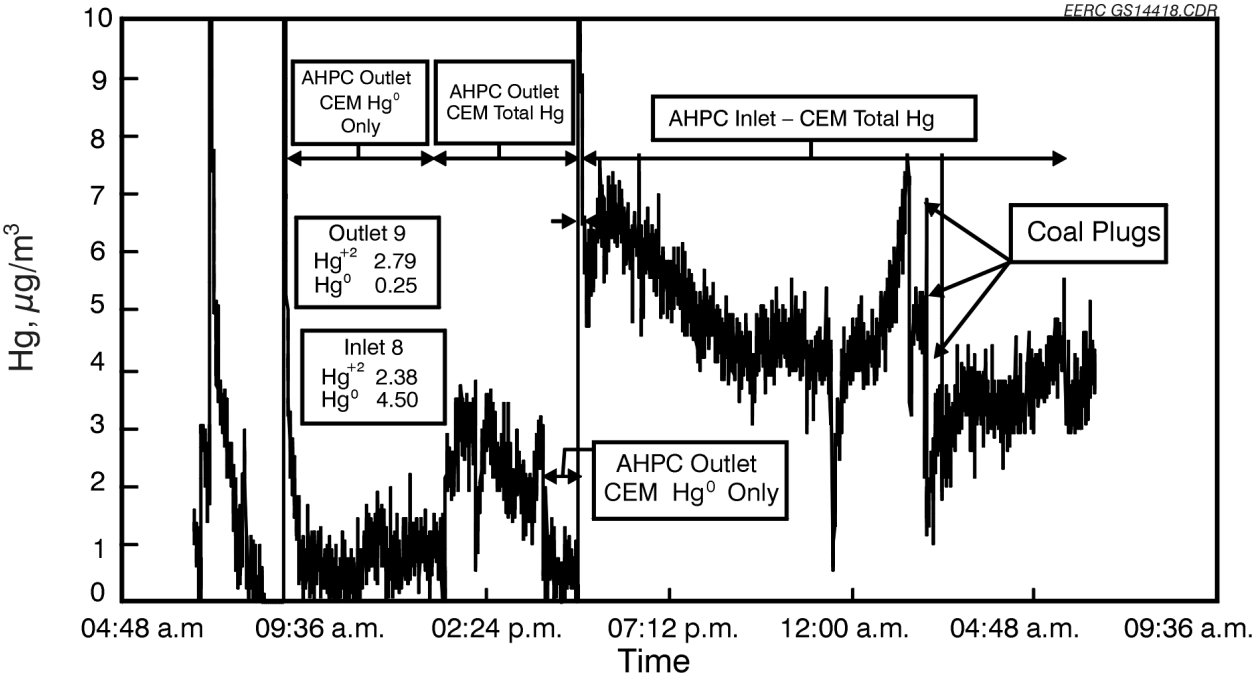

Figure 4.4-42. Mercury concentration versus time for Day 4, March 6, 1997, Test PTC-AB-586.

on the outlet. The total mercury concentration measured about 3.0 μg/m^3, agreeing well with the Method 29 analysis. The total mercury concentration ranged between 2.0 and 3.0 μg/m^3 from 1:20 to 3:20 p.m. At 3:20 p.m., the mercury analyzer was switched from total mercury to elemental mercury. The mercury concentration dropped to 0.5 μg/m^3. At 4:43 p.m., the sampling location was switched from outlet to inlet. The mercury analyzer started sampling for total mercury at 4:51 p.m. The mercury analyzer continued to measure total mercury from 4:51 p.m. to 7:00 a.m. on Day 5, March 7. The total mercury concentration seemed to stabilize around 4.5 μg/m^3 until 12:00 midnight.

4.4.2.5 Results for Test PTC-AB-586 – Day 5

The dP versus time graph for Day 5 is found in Figure 4.4-43. The change in dP before and after the cleaning cycle remained at about 0.80 kPa (3.2 in. W.C.) throughout the day. The pulse interval fluctuated between 30 and 35 min (Figure 4.4-44). At 98 hr (1:57 a.m.), the coal gun plugged, sending unburned carbon into the AHPC. Two more coal plugs occurred within 30 min

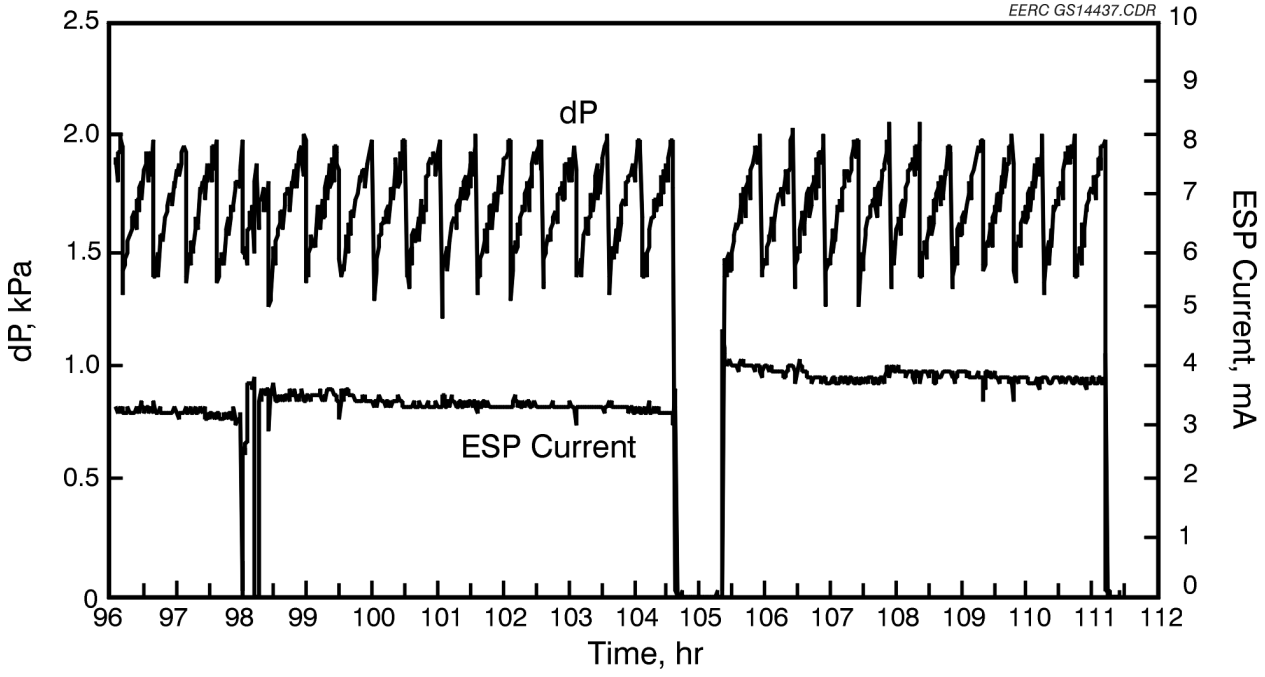

Figure 4.4-43. Pressure drop as a function of time for Day 5, March 7, 1997, Test PTC-AB-586 with on-line cleaning using graphite-impregnated PTFE bags.

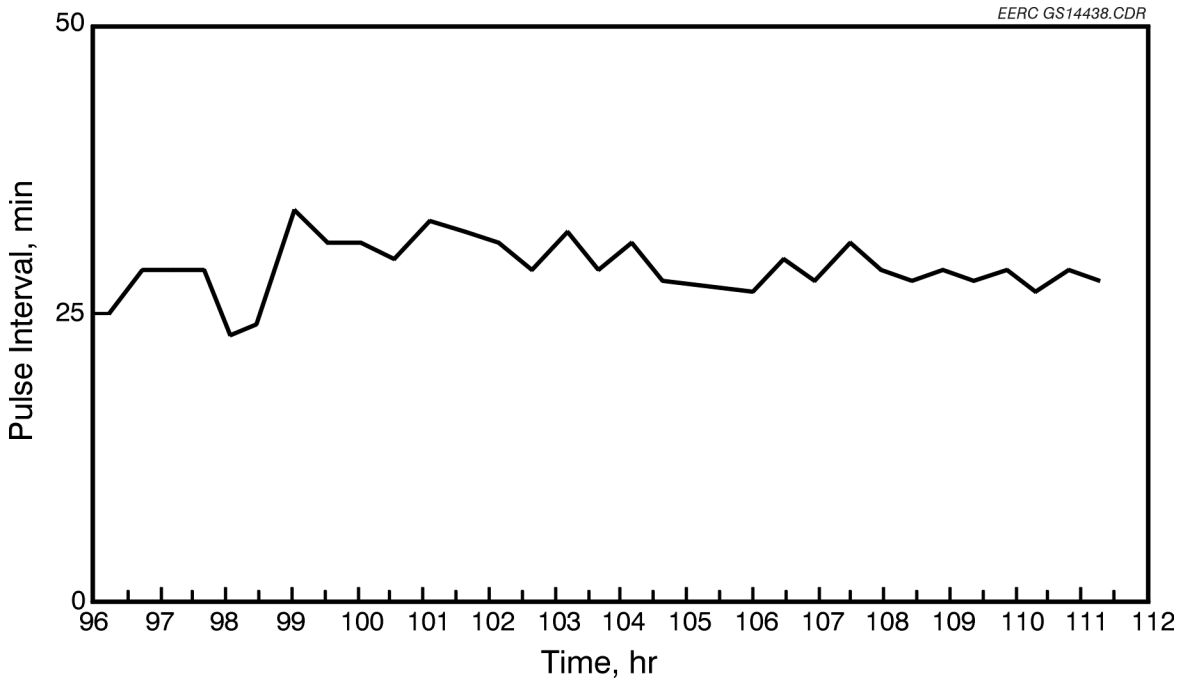

Figure 4.4-44. Pulse interval as a function of time for Day 5, March 7, 1997, Test PTC-AB-586 with on-line cleaning using graphite-impregnated PTFE bags.

of the first. The AHPC operation was affected, as seen in the dP versus time graph (Figure 4.4-43) at 98 to 98.6 hr. The coal plugs disrupted the ESP, causing a minor upset in the operation of the AHPC. The AHPC came off-line at 104 hr (8:33 a.m.) into the run for routine maintenance of the ESP grid and cleaning of AHPC view ports. The AHPC returned to on-line status at 105 hr (9:10 a.m.). No increase in pulse interval was noted after baghouse maintenance.

The dust-loading data for Day 5 are presented in Table 4.4-10. Respirable mass measurements by the APS are presented in Figure 4.4-45. The three integrated averages of all less than 0.01 mg/m^3 confirm a >99.999% collection efficiency of the AHPC. The injection of sorbent did not seem to degrade the AHPC collection efficiency. In the plot given in Figure 4.4-46, the collection efficiency of >99.99% is confirmed over the entire range of particle sizes, from 0.01 to 10 μm in aerodynamic diameter.

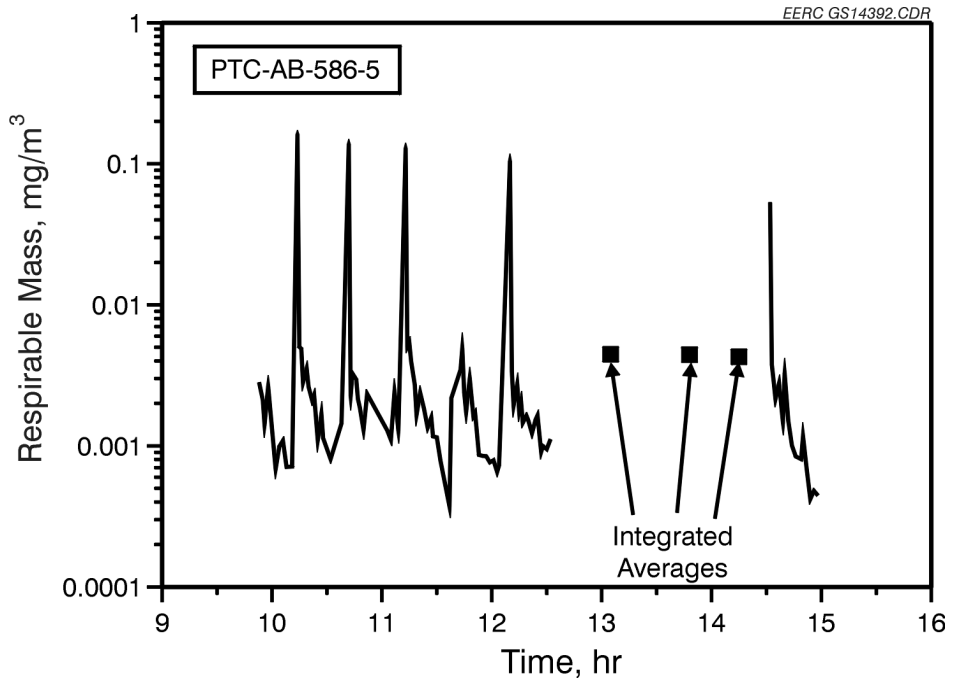

Figure 4.4-45. APS data for Day 5, March 7, 1997, Test PTC-AB-586.

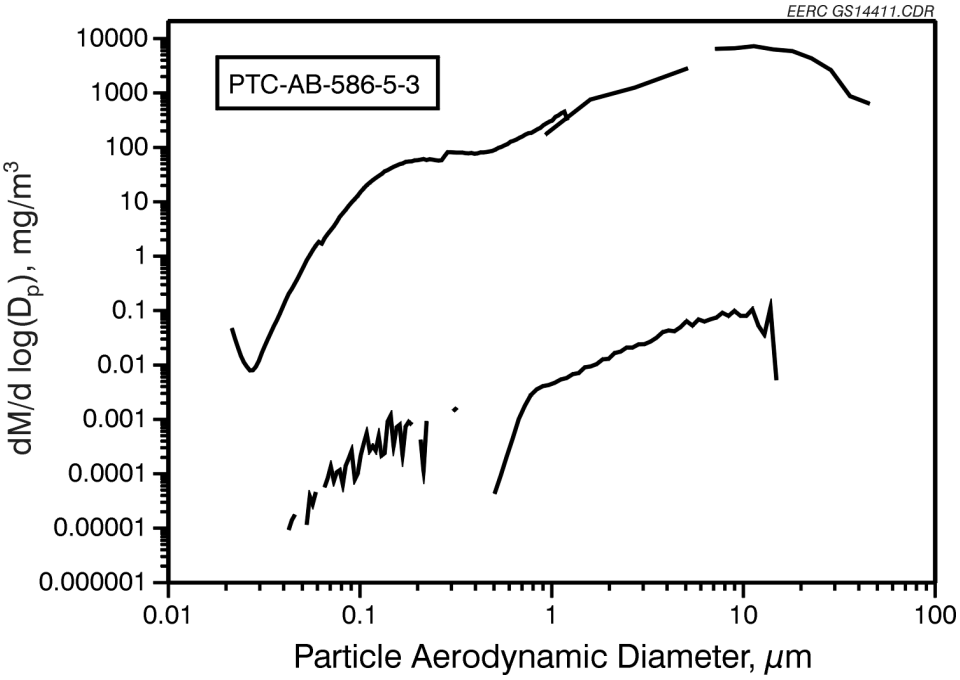

Figure 4.4-46. The combined inlet and outlet particulate concentration versus aerodynamic particle-size data for Day 5, March 7, 1997, Test PTC-AB-586.

The mercury analyzer readout for Day 5 is presented in Figure 4.4-47. The mercury analyzer continued to monitor total mercury concentration on the inlet of the AHPC from midnight to 6:30 a.m. on Day 5. The total mercury concentration was about 4.2 μg/m^3 at midnight and increased to 7.5 μg/m^3 around 1:56 a.m. No explanation can be given at this time for the increase in mercury. However, this increase in mercury may indicate a change in firing environment inside the combustor. As mentioned above, at 1:57 a.m., the PTC experienced three coal plugs. The total mercury values measured during this time decreased with each coal plug. The coal accumulated on the sample filter adversely affected the mercury concentration into the mercury analyzer. Figure 4.4-47 shows the time of occurrence of the coal plugs on the mercury versus time graph. The analyzer was shut down for maintenance from 6:30 to 7:10 a.m. The mercury analyzer was rezeroed and the sampling point changed from inlet to outlet of the AHPC. The total mercury concentration at the outlet measured about 4.0 μg/m^3. From 8:33 to 9:10 a.m., AHPC went off-line. Therefore, the mercury concentration at that time read very close to zero. After the AHPC came back on-line, the total mercury concentration ranged from 2.0 to 2.5 μg/m^3. During this time period, outlet Method 29 sampling (Outlet 11, Table 4.4-11)

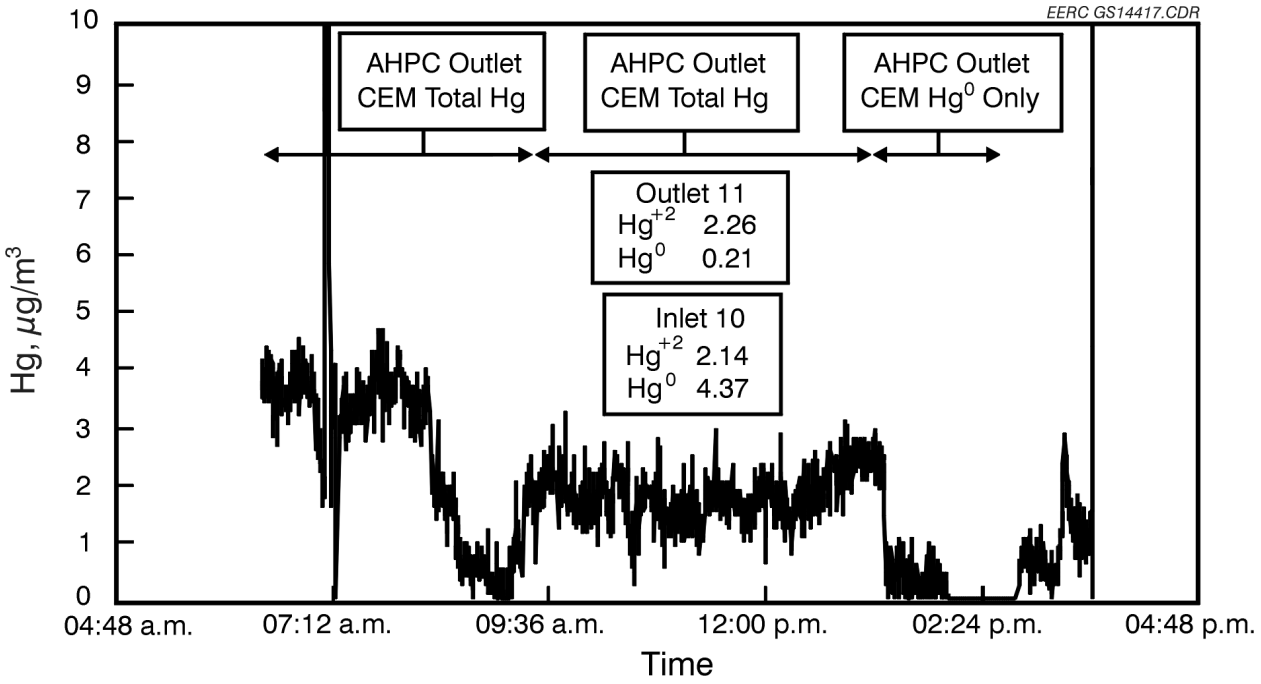

Figure 4.4-47. Mercury concentration versus time for Day 5, March 7, 1997, Test PTC-AB-586.

presented a low elemental mercury concentration of 0.21 μg/m^3. The oxidized mercury concentration of the outlet was 2.26 μg/m^3. The Method 29 mercury inlet concentration (Inlet 10, Table 4.4-11) was measured at 4.37 and 2.14 μg/m^3 for elemental and oxidized mercury, respectively. The efficiency of total mercury captured by the sorbent was 62%, as determined from the Method 29 analysis. At 1:19 p.m., outlet sampling was switched from total mercury mode to elemental mercury only. The elemental mercury quickly dropped to below 0.5 μg/m^3. Shutdown of the analyzer was at 3:37 p.m.

4.4.2.6 Trace Metal Concentrations from Duct Sampling

Flue gas was taken from inlet and outlet locations of the AHPC using the EPA Method 29 multimetals sampling method. The inlet and outlet Method 29 samples were performed simultaneously. Seven trace metals analyzed for were As, Cd, Cr, Pb, Ni, Se, and Hg. Table 4.4-11 presents the trace metal data for inlet and outlet sampling, coal, baghouse ash, and blanks.

All seven elements were present in measurable quantities in the ash found on the inlet Method 29 filter. Only Cr and Ni show up in Outlet 6 filter, suggesting that a small amount of contamination may be coming from the stainless steel on the clean side of the AHPC. As in Test PTC-AB-585, only three trace metals (Cr, Hg and Se) were found in detectable quantities in both the inlet and outlet H_2O_2 impingers of the Method 29 sampling train.

Total inlet selenium concentrations averaged 24.59 μg/m^3, with a standard deviation (STDV) of 5.25 g/m^3 and %RSD of 21.36%. Total outlet selenium concentrations averaged 7.35 μg/m^3, with a STDV of 6.74 g/m^3 and %RSD of 91.77%. The high %RSD was due to the analysis of only selenium in the two outlet samples. Selenium concentration in the vapor form was measured as 20.81 μg/m^3 on the first day. Yet, for the next 4 days, the selenium vapor concentration never got higher than 4.76 μg/m^3. Selenium distributions between the solid and vapor phase of the inlet and outlet samples are illustrated in Figure 4.4-48. The high outlet selenium vapor value for the first day is not seen in the inlet vapor concentration of Inlet 1 for

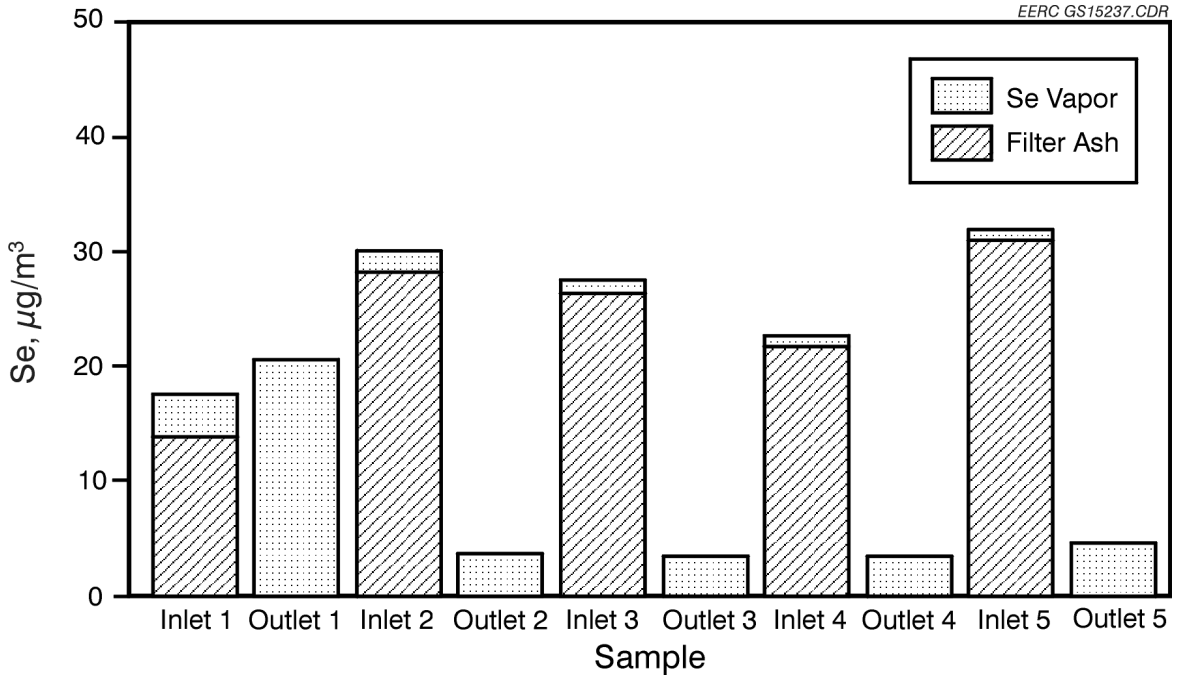

Figure 4.4-48. Selenium distribution between the solid and vapor phase of both inlet and outlet samples.

selenium. The total amount of selenium measured in the first day did not change, yet there is evidence that selenium may have changed form or some other material may be contaminating the clean side of the AHPC. Once the AHPC came to equilibrium with the injection of sorbent, the selenium vapor measurements decreased, indicating that the sorbent was removing some of the selenium.

Total inlet mercury concentrations ranged from 7.61 to 5.28 μg/m^3, averaging 6.84 μg/m^3. The %RSD was 12.07%. The mercury collected on the inlet filter ranged from 0.93 to 0.52 μg/m^3 (see Table 4.4-11).

Figure 4.4-49 shows the distribution of mercury species in the Method 29 inlet sampling. One inlet and one outlet sample was taken each day of PTC-AB-586. In this figure, the concentration of mercury in the solid sample is contrasted to the concentration of mercury sampled in the vapor phase. Speciation measurements of Hg^0 and Hg^{2+} in the gas sample are also shown in Figure 4.4-49. The outlet mercury concentration averaged 2.83 μg/m^3, with a %RSD of

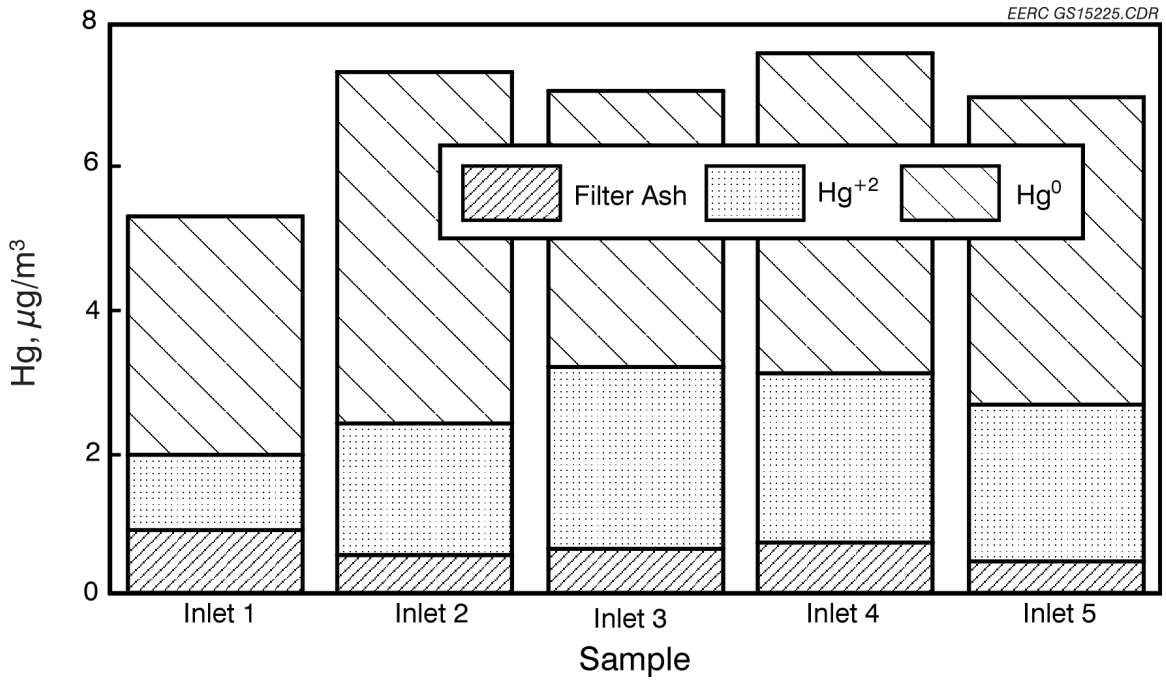

Figure 4.4-49. Distribution of mercury between the solid and vapor phase and speciation of mercury in the inlet gas samples for PTC-AB-586.

14.40%. Outlet 2 and Outlet 6 filters were submitted for trace metal analysis. Mercury concentration in the filter cake was below detection limits. With sorbent injection, the removal efficiency for Test PTC-AB-586 of total mercury averaged 64%. Elemental mercury was the predominant species removed with sorbent injection. The calculated percent removal of Hg^0 is presented in Figure 4.4-50. As in PTC-AB-585, the percent Hg^0 removal increased during the first day of testing and then leveled out.

Distribution of vapor-phase mercury species in the outlet sampling is shown in Figure 4.4-51. Figure 4.4-51 shows the change in the proportion of Hg^0 and Hg^{2+} in the outlet samples from Day 1 to Day 2, which continued through the test duration. It is difficult to draw any conclusions for the proportional shift of Hg^0 to Hg^{2+} in this test because of the addition of sorbent into the gas stream.

Table 4.4-12 presents a summary of trace element data for PTC-AB-585 and PTC-AB-586, with the inlet and outlet averages for the seven trace elements. As in the baseline test,

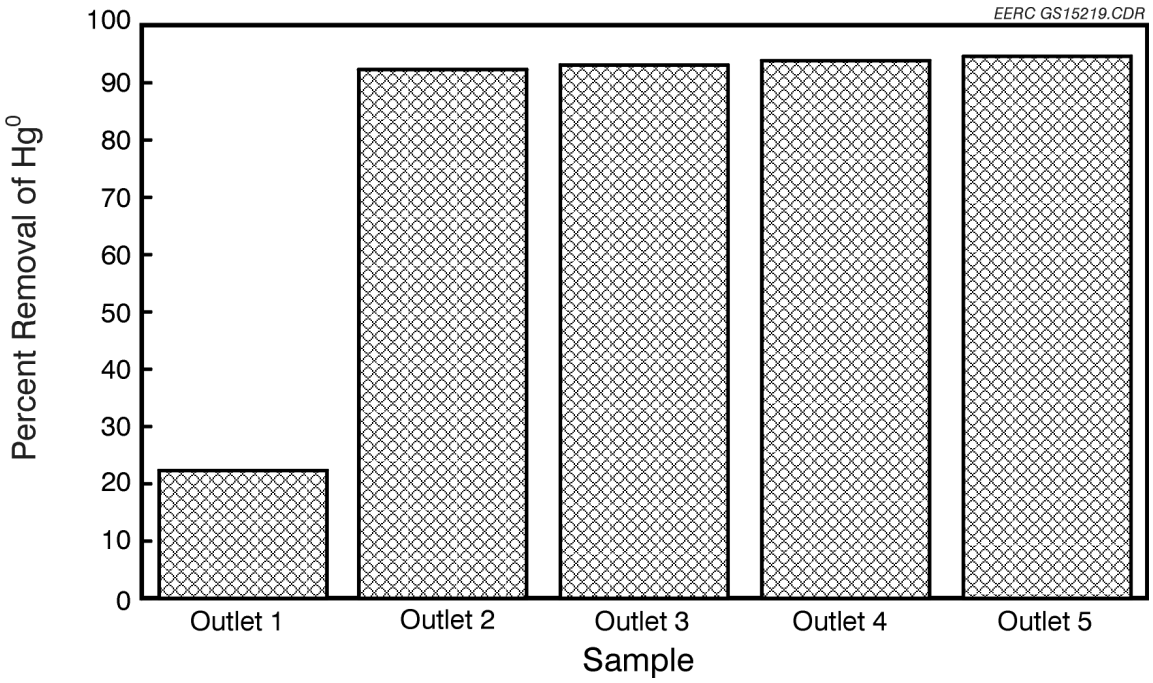

Figure 4.4-50. Percent removal of Hg^0 at the outlet filters for Test PTC-AB-586.

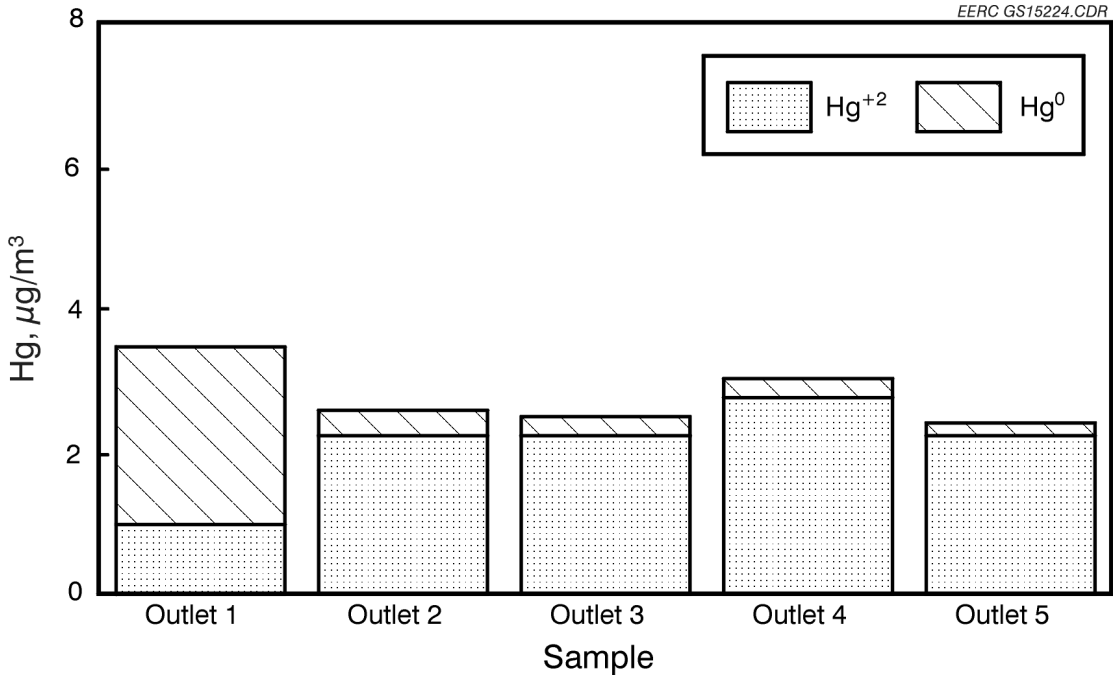

Figure 4.4-51. Distribution of vapor-phase mercury species in the outlet gas samples for Test PTC-AB-586.

TABLE 4.4-12

Summary of Trace Element Data for Tests PTC-AB-585 and PTC-AB-586, μg/m^3

	Hg	As	Cd	Cr	Pb	Ni	Se
PTC-AB-585, Baseline							
Average Inlet	5.5	83.0	1.7	463.0	319.0	223.0	32.0
Average Outlet	3.6	<1.0	<0.08	0.57	<0.50	<2.0	16.0
Percent Removal	34.5	>99.8	>95.3	99.9	>99.8	>99.1	50.0
PTC-AB-586, Sorbent Injection							
Average Inlet	6.8	99.0	1.8	534.0	291.0	229.0	25.0
Average Outlet	2.7	<1.0	<0.08	2.2	<0.50	<2.0	3.8
Percent Removal	60.3	>99.0	>95.6	99.6	>99.8	>99.1	84.8

PTC-AB-585, five trace metals (As, Cd, Cr, Pb and Ni) showed high percent removal. With the addition of the carbon-based sorbents, the percent removal over the baseline increased from 34.5% to 60.3% for mercury and from 50.0% to 84.8% for selenium.

4.4.2.7 Conclusions from Sorbent Injection Test PTC-AB-586 Firing Absaloka Coal

- The AHPC operated successfully on Absaloka subbituminous for 100 hr.
- Pressure drop was controlled, and pulse intervals ranged between 25 to 35 min.
- Particulate removal efficiency of >99.999% was achieved throughout the test period.
- All seven trace elements (As, Cd, Cr, Pb, Ni, Se, and Hg) were found in the filter ash.
- Of the seven elements, only three (Hg, Se, and Cr) appear in detectable quantities in vapor form.

- With sorbent injection, the removal efficiency for Test PTC-AB-586 of total mercury averaged 60%.

- Elemental mercury was the predominant mercury species removed with sorbent injection.

- Selenium was also reduced with sorbent injection.

4.4.3 100-hr Tests Firing Blacksville Bituminous Coal (PTC-BV-587)

The purpose of Test PTC-BV-587 was twofold: first to evaluate the AHPC under baseline conditions firing Blacksville bituminous and second to determine the effects of flue gas conditioning on the AHPC system. The first 48 hr of testing were for establishing baseline conditions. The rest of the test was used to determine the effects of flue gas conditioning agents in the AHPC operation. In addition to the particulate sampling, SO_3 sampling was performed.

The operational parameters are presented in Table 4.4-13. The AHPC was operated at an A/C ratio of 3.7 m/min (12 ft/min) using graphite-impregnated PTFE bags supplied by W.L. Gore. The ESP was set to operate at 50 kV. The temperature of the AHPC was maintained at 149°C (300°F) throughout the test. EPA Method 5 was used to determine particulate loading at the inlet and outlet of the AHPC. Time duration for inlet sampling was 1 hr, while the time duration for the outlet sampling was 4 hr. However, one outlet particulate sample was taken over a 24-hr period. SO_3 concentration in the flue gas stream was determined by selective condensation. A multicyclone sampling system was used to collect a size-fractionated dust sample from the inlet of the AHPC. An APS and a SMPS–CPC were used to get real-time particulate concentration and size distribution data. However, because of the high SO_3 concentration and resulting SO_3 aerosol formation in the SMPS, the SMPS could not be used to obtain a valid submicron particle-size distribution.

TABLE 4.4-13

Test Parameters for PTC-BV-587

Week of March 31–April 4, 1997	
Air/Cloth Ratio, m/min (ft/min)	3.7 (12)
Inlet Temperature, °C (°F)	149 (300)
On-Line and Off-Line Cleaning	On
Baffling	Butterfly
Voltage, kV	50
Type of Bag	Graphite-impregnated PTFE
Bag Identification	Set 13
No. of Bags in Use	4
Pulse Pressure, kPa (psig)	612 (90)
Pulse Duration, s	0.2
Pulsing Initiation Pressure, kPa (in. W.C.)	2.0 (8.0)

The flue gas conditioning agents used in this test were 12 ppm SO_3 and 24 ppm NH_3. The SO_3 was generated by conversion of SO_2 across a vanadium catalyst to SO_3 in the presence of O_2 and heat. The total SO_3 concentration in the flue gas was somewhat uncertain because of the generation of SO_3 from the combustion of Blacksville coal. Therefore, the exact ratio of SO_3/NH_3 was difficult to achieve and maintain constant. The average concentrations of flue gas constituents are listed in Table 4.4-14.

TABLE 4.4-14

Average Flue Gas Concentrations for Test PTC-BV-587[1]

O_2, % by volume	CO_2, % by volume	H_2O, % by volume	SO_2, ppm	SO_3,[2] ppm	NO_x, ppm
4.0	13.5	8	1750	6.3	600

[1] Dry basis except for H_2O.
[2] Without SO^3 injection.

4.4.3.1 Results for Test PTC-BV-587 – Day 1

The AHPC was heated by resistence heating to the specified 149°C (300°F). The AHPC was bypassed during system heatup. After the system equilibrated on coal, the flue gas was directed into the AHPC. Figure 4.4-52 presents the change in dP of the bags versus run time. The initial dP on the clean bags was 0.52 kPa (2.1 in. W.C.). ESP current was 4.00 mA at 50 kV. The change in dP before and after cleaning decreased during the first day of testing, starting with a change in dP of 1.3 kPa at a run time of about 11 hr to a change in dP of 0.9 kPa at 24 hr. The ESP current is also displayed in Figure 4.4-52. The ESP current was at about 4.00 mA at the beginning of the test and rose slightly to 4.25 mA and then decreased to a steady state ranging from 3.30 to 3.50 mA. The pulse interval decreased also from about 110 min on the first pulse interval to about 40 min by the end of the day. The pulse interval information is plotted in Figure 4.4-53.

Dust-loading data for Test PTC-BV-587 is presented in Table 4.4-15. One inlet and one outlet particulate sample were taken on the first day, March 31, 1997. The dust loading calculated

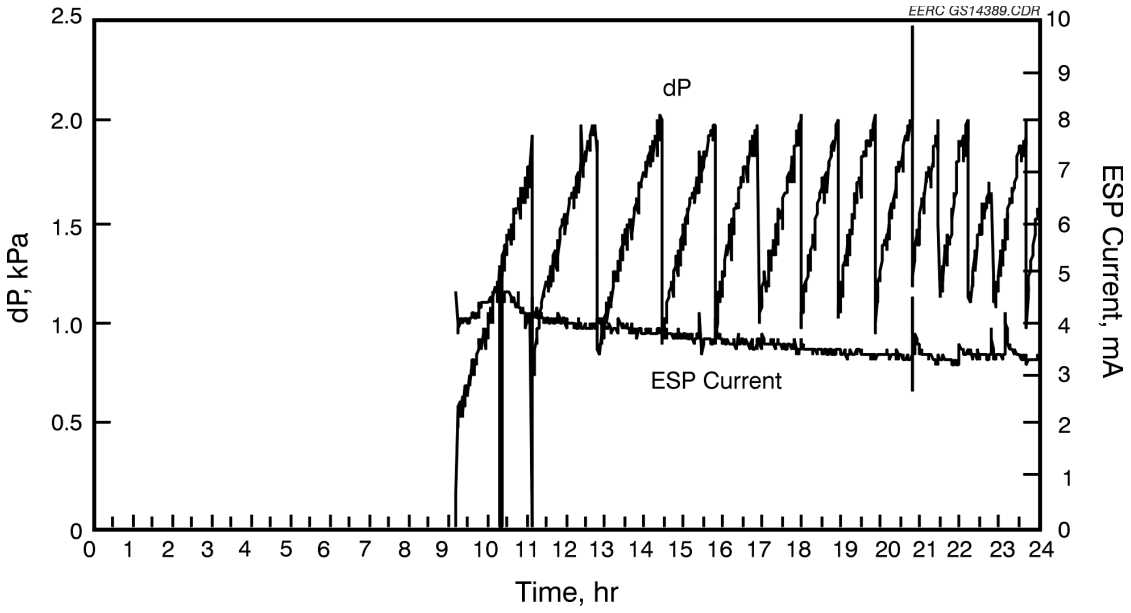

Figure 4.4-52. Pressure drop as a function of time for Day 1, March 31, 1997, Test PTC-BV-587 with on-line cleaning using graphite-impregnated PTFE bags.

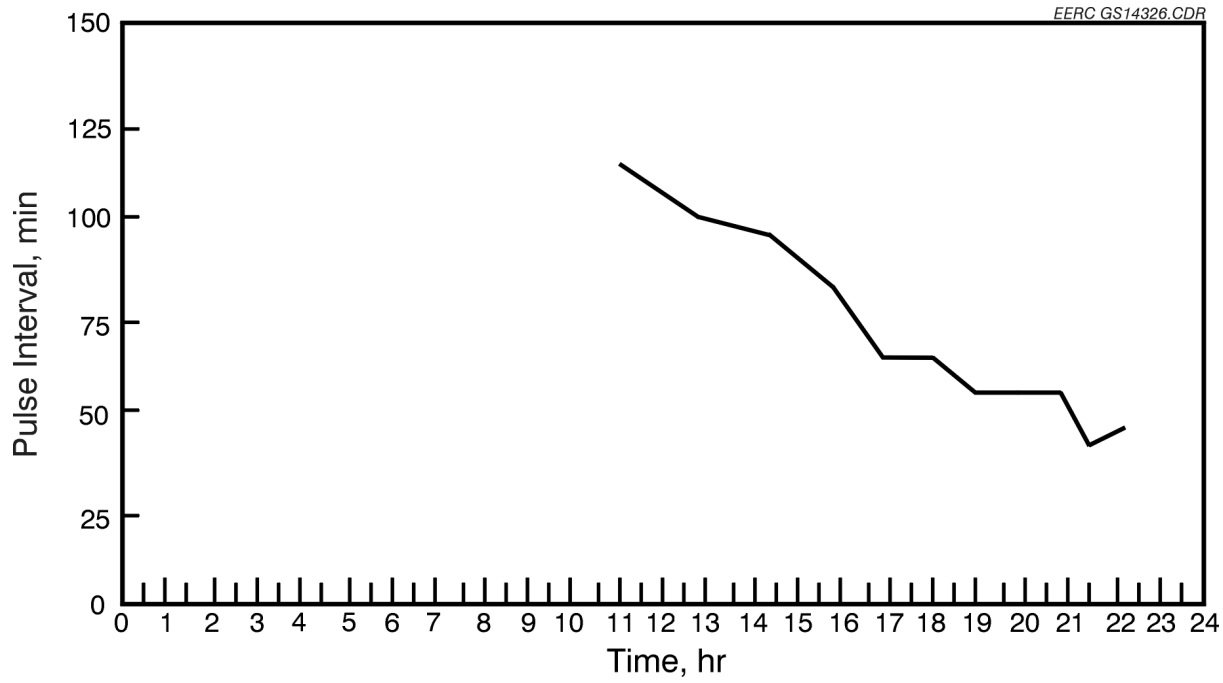

Figure 4.4-53. Pulse interval as a function of time for Day 1, March 31, 1997, Test PTC-BV-587 with on-line cleaning using graphite-impregnated PTFE bags.

TABLE 4.4-15

Dust-Loading Data for Test PTC-BV-587

Date	PTC Test No.	Hopper Ash, g/m^3	Inlet, g/m^3	Outlet, g/m^3	Percent Collection Efficiency[1]
3-31-97	PTC-BV-587	5.83	4.4149	0.0007	99.985
4-1-97	PTC-BV-587	4.53	4.0332	0.0009[2]	99.9773
4-2-97	PTC-BV-587	4.76	5.7722[3]	0.0005[2]	99.9921
4-2-97	PTC-BV-587			<0.00002	
4-3-97	PTC-BV-587	5.26	4.6425	0.0007[2]	99.9852

[1] All outlet dust loadings were contaminated with large particles broken off from the gasket used to seal the outlet plenum.
[2] Sampling time of 24 hr.
[3] Multicyclone.

from the ash collected in the AHPC hopper bottom of 5.83 g/m^3 (2.55 gr/scf) compared favorably with the inlet particulate dust-loading sample of 4.4149 g/m^3 (1.9295 gr/scf). The outlet dust loading for the first day was 0.0007 g/m^3 (0.0003 gr/scf). The higher outlet dust loading was due

to contamination by the silicon rubber gasket used to seal the top of the outlet plenum. SO_3 in the flue gas apparently attacked the silicone rubber and caused particles to break off. The AHPC efficiency was calculated at 99.9845%. APS data, however, showed integrated averages of <0.01 mg/m^3, demonstrating particulate control efficiencies >99.999%. Figure 4.4-54 presents the graph of particulate concentration versus run time. The integrated average of the APS data was 0.0025 mg/m^3.

4.4.3.2. Results for Test PTC-BV-587 – Day 2

The dP versus time graph for Day 2 is found in Figure 4.4-55. The change in dP before and after cleaning remained fairly stable, ranging from 0.95 to 0.75 kPa (3.8 to 3.0 in. W.C.). Pulse intervals decreased from 50 to about 35 min between pulse cycles (Figure 4.4-56). The AHPC came off-line at 32 hr into the run for routine maintenance of the ESP grid and cleaning of AHPC view ports. Additional adjustments were made to the bag cage supports at this time. After the AHPC was returned to on-line status, the pulse interval was 60 min, but quickly reached steady state at about 38 min for the rest of Day 2.

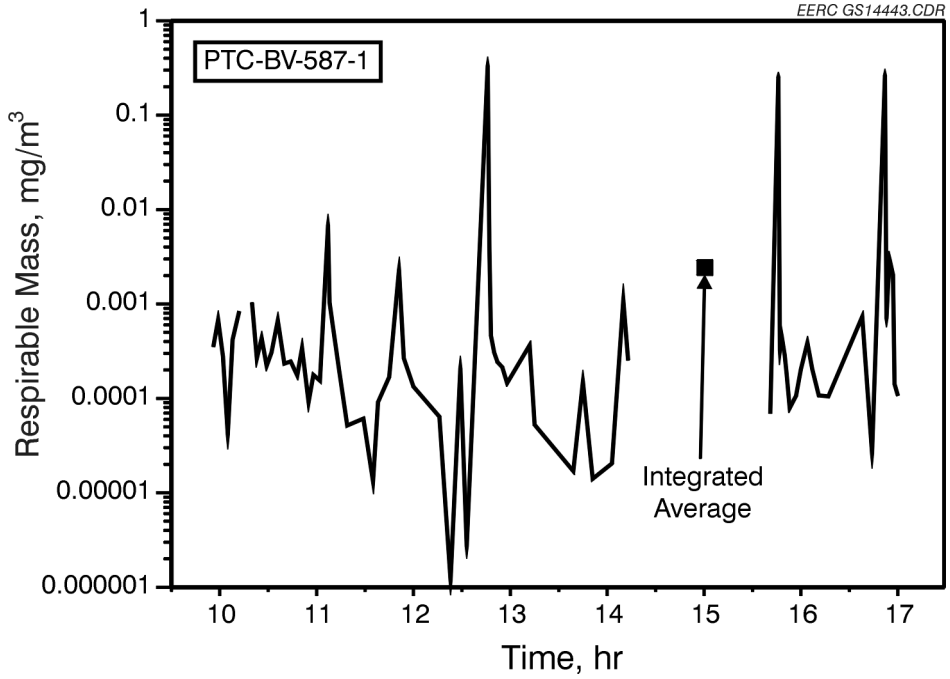

Figure 4.4-54. APS data for Day 1, March 31, 1997, Test PTC-BV-587.

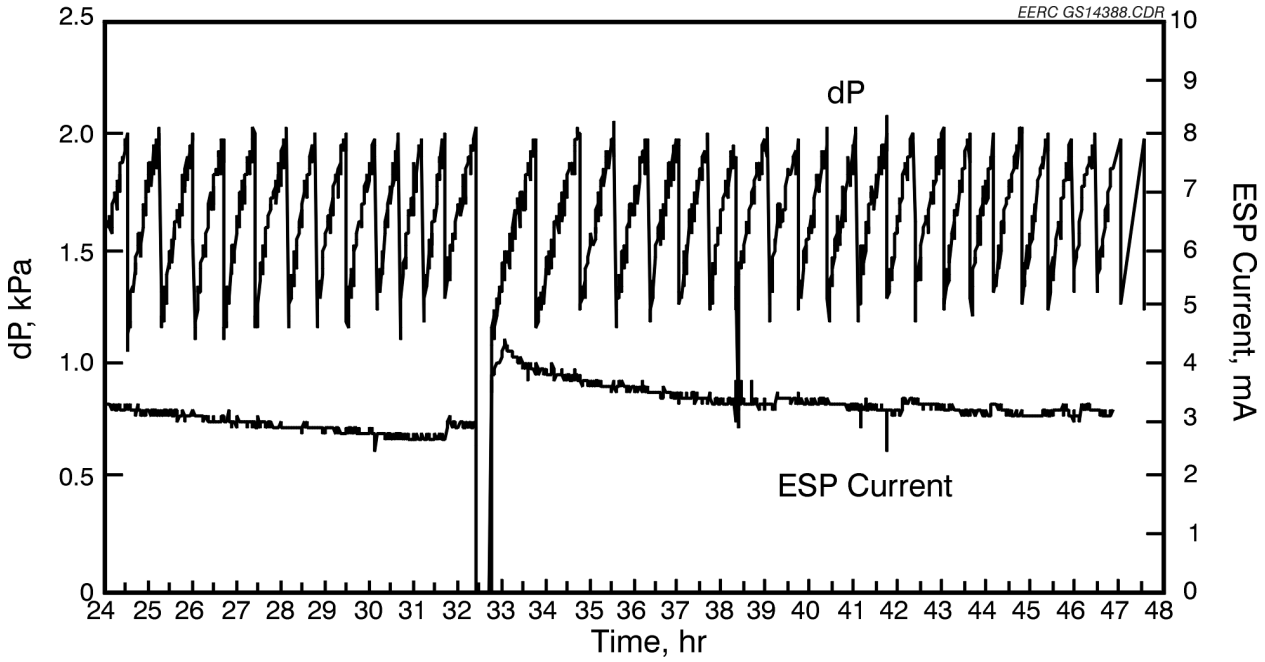

Figure 4.4-55. Pressure drop as a function of time for Day 2, April 1, 1997, Test PTC-BV-587 with on-line cleaning using graphite-impregnated PTFE bags.

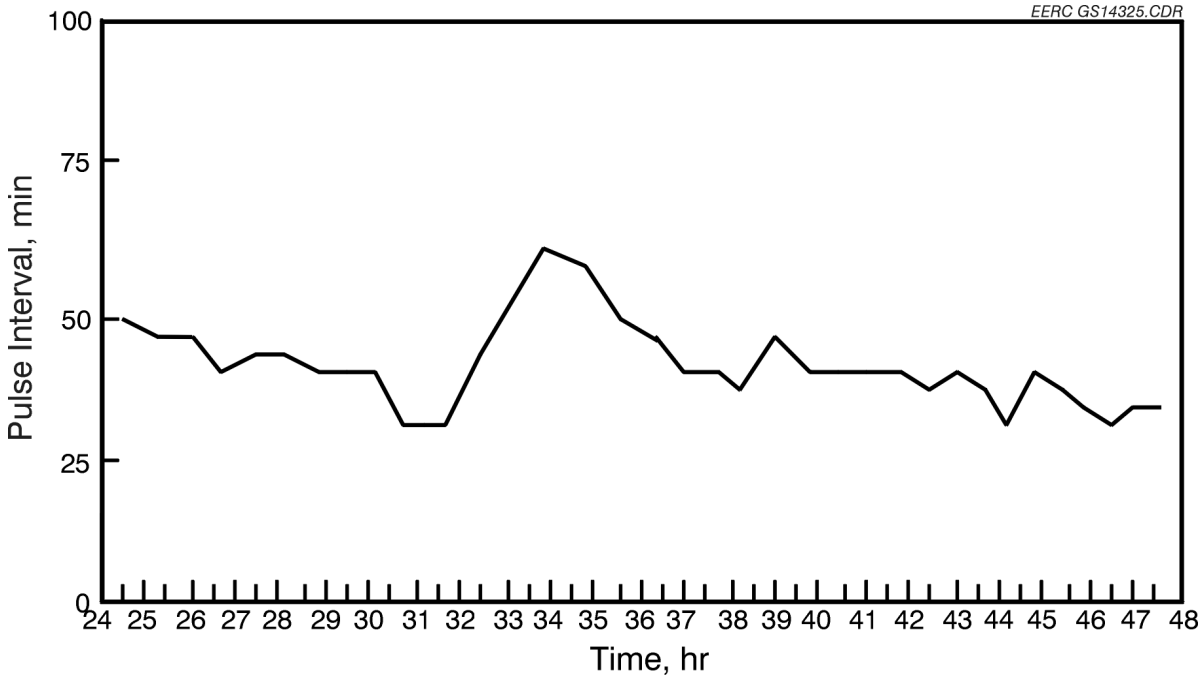

Figure 4.4-56. Pulse interval as a function of time for Day 2, April 1, 1997, Test PTC-BV-587 with on-line cleaning using graphite-impregnated PTFE bags.

Dust-loading data for Day 2 are presented in Table 4.4-15. Inlet dust loading measured at 4.0332 g/m^3 (1.7627 gr/scf). The inlet dust loading, calculated from the mass of ash collected from the AHPC ash hopper, was 4.53 g/m^3 (1.98 gr/scf). Agreement between the two inlet dust-loading values is fair. The outlet dust loading was 0.0009 g/m^3 (0.0039 gr/scf), giving a dust-loading efficiency of 99.9773%, due to gasket contamination. The outlet particulate sample was collected over a period of 4 hr. Respirable mass measurements by the APS are presented in Figure 4.4-57. The APS data confirm the better than 99.999% collection efficiency of the AHPC with an integrated respirable mass value of less than 0.01 mg/m^3. The two integrated averages for Day 2 were 0.0055 and 0.0062 mg/m^3.

4.4.3.3 Results for Test PTC-BV-587 – Day 3 Flue Gas Conditioning

The dP versus time graph for Day 3 is found in Figure 4.4-58. Because of problems logging data, the dP versus time graph for the last 2 days of testing for Test PTC-BV-587 was generated by operator data input. The change in dP before and after the cleaning cycle remained at about

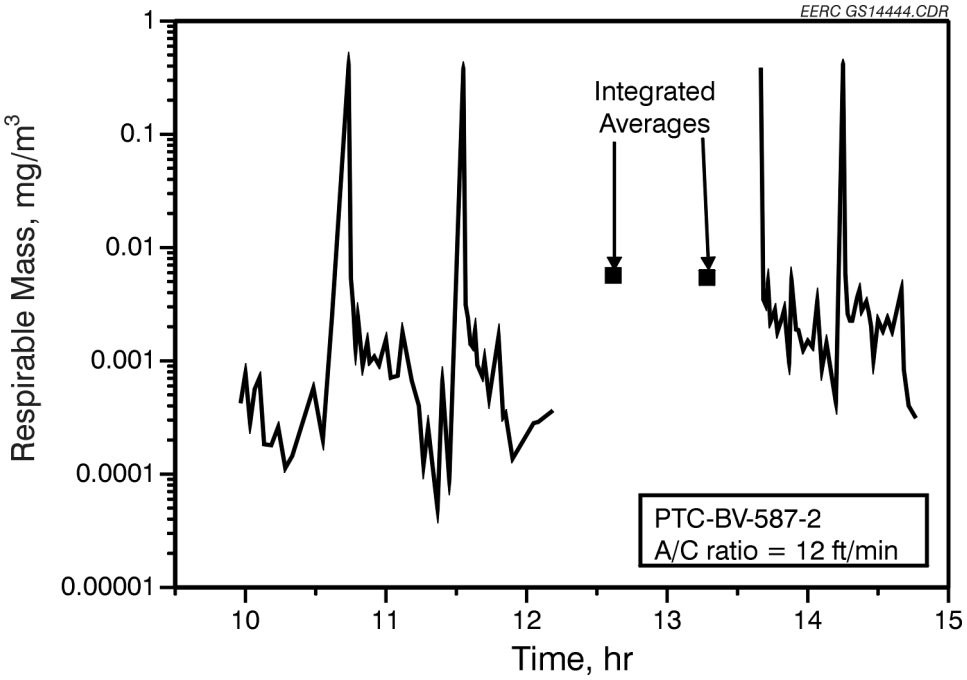

Figure 4.4-57. APS data for Day 2, April 1, 1997, Test PTC-BV-587.

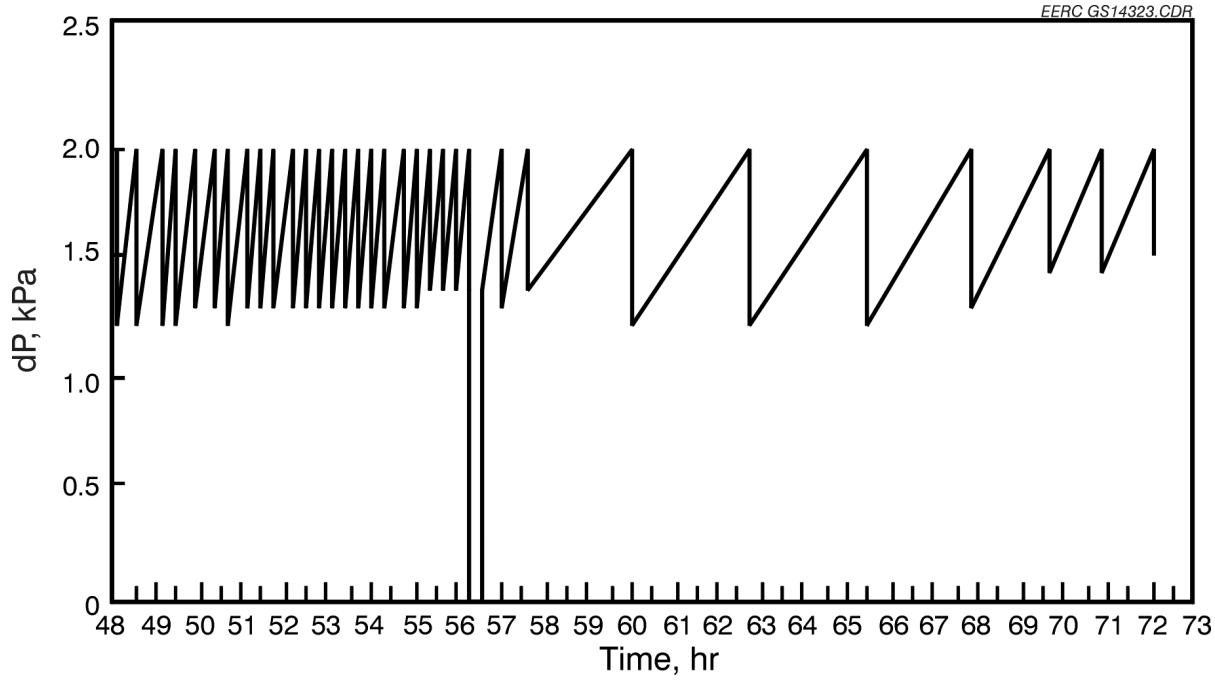

Figure 4.4-58. Pressure drop as a function of time for Day 3, April 2, 1997, Test PTC-BV-587 with on-line cleaning using graphite-impregnated PTFE bags.

0.75 kPa (3.0 in. W.C.) until flue gas conditioning began. The pulse interval ranged between 25 and 35 min before the start of flue gas conditioning. The pulse interval information is plotted in Figure 4.4-59. The AHPC came off-line at 56 hr into the run for routine maintenance of the ESP grid and cleaning of AHPC view ports. An increase in pulse interval from 25 to about 60 min was noted after maintenance, but the pulse interval decreased again to between 35 and 45 min.

Flue gas conditioning began at 57 hr after the AHPC had gone through two cleaning cycles. The dramatic effects of flue gas conditioning can be seen in the graph of dP versus time and pulse interval versus time (Figures 4.4-58 and 4.4-59, respectively). The change in dP before and after cleaning cycle increased from 0.75 kPa (3.0 in. W.C.) to 0.95 kPa (3.8 in. W.C.) and then began to decrease throughout the rest of the day. A possible explanation for the decrease in performance is the variation in SO_3 production from the PTC and possible inconsistent NH_3 addition. Table 4.4-16 presents the SO_3 sampling data for Test PTC-BV-587. The SO_3 concentration decreased from 9.61 ppm SO_3 sampled on Day 1 to 1.99 ppm SO_3 sampled on Day 3 of the test. With NH_3 injection, the ideal would be to neutralize all of the SO_3 and collect it

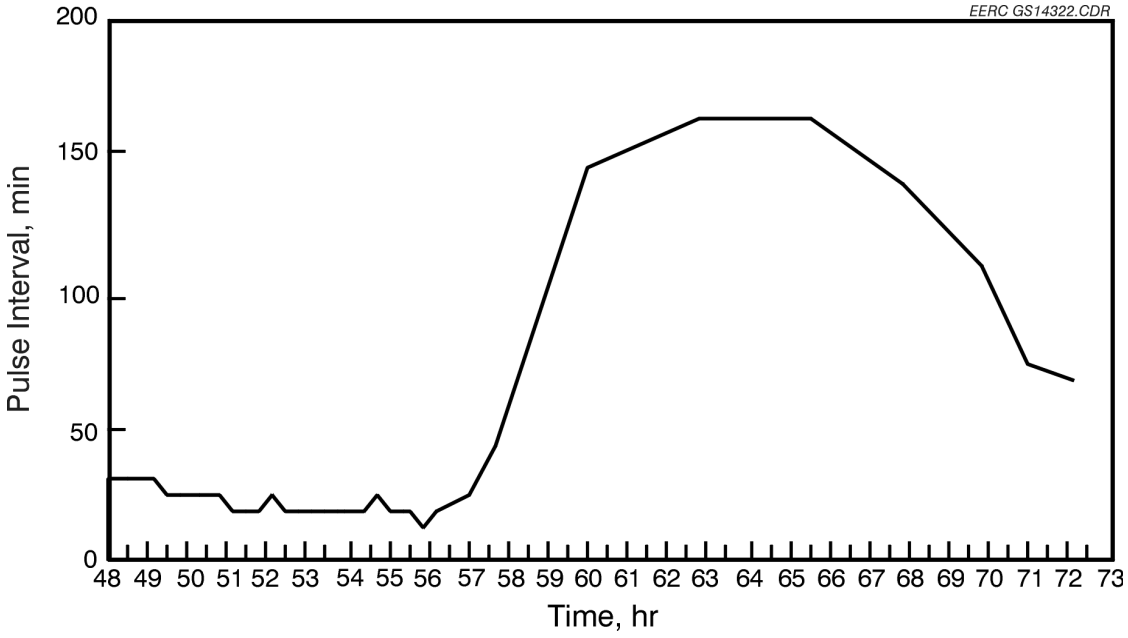

Figure 4.4-59. Pulse interval as a function of time for Day 3, April 2, 1997, Test PTC-BV-587 with on-line cleaning using graphite-impregnated PTFE bags.

TABLE 4.4-16

SO_3 Sampling Data for Blacksville Coal, ppm	
Day 1	9.61
Day 2	6.35
Day 3	1.99
Day 4	7.19
Average	6.29

on the filter. The Day 3 result may have come the closest to achieving that effect, but the increase in SO_3 again on Day 4 indicates that the SO_3/NH_3 ratio was incorrect.

The dust-loading data for Day 3 are presented in Table 4.4-15. A multicyclone sample was taken for the inlet dust loading. The inlet dust loading measured at 5.7722 g/m^3 (2.5227 gr/scf). The inlet dust loading, calculated from the mass of ash collected from the AHPC ash hopper, was 4.76 g/m^3 (2.08 gr/scf). The 24-hr outlet dust loading was 0.000577 g/m^3 (0.000200 gr/scf) and

the 4-hr dust loading was <0.00002 g/m^3 (<0.00001 gr/scf). There was not enough mass collected during the 4-hr outlet sampling to get an acceptable mass measurement. The AHPC collection efficiency was 99.9921% based on the 24-hr sample. Respirable mass measurements by the APS are presented in Figure 4.4-60. No integrated averages were performed on this day. Except for spikes due to cleaning cycles, most of the respirable mass versus time curve was less than 0.01 mg/m^3, confirming a >99.999% collection efficiency.

4.4.3.4 Results for Test PTC-BV-587 – Day 4

The dP versus time graph for Day 4 is found in Figure 4.4-61. The change in dP before and after the cleaning cycle decreased steadily until the AHPC was pulsing almost continuously. At 80 hr, the AHPC was taken off-line for inspection and cleaning. When the AHPC opened up, the ESP grid was severely fouled. The bags were pulsed off-line, with no dust visibly dislodged from any of the bags. An ash sample was taken from one of the bags (Bag D) and submitted for chemical analysis for NH_3 and SO_4. Table 4.4-17 presents the results which, again, indicate not enough NH_3 was used compared to the amount of SO_3 present. All the bags were pulled out and

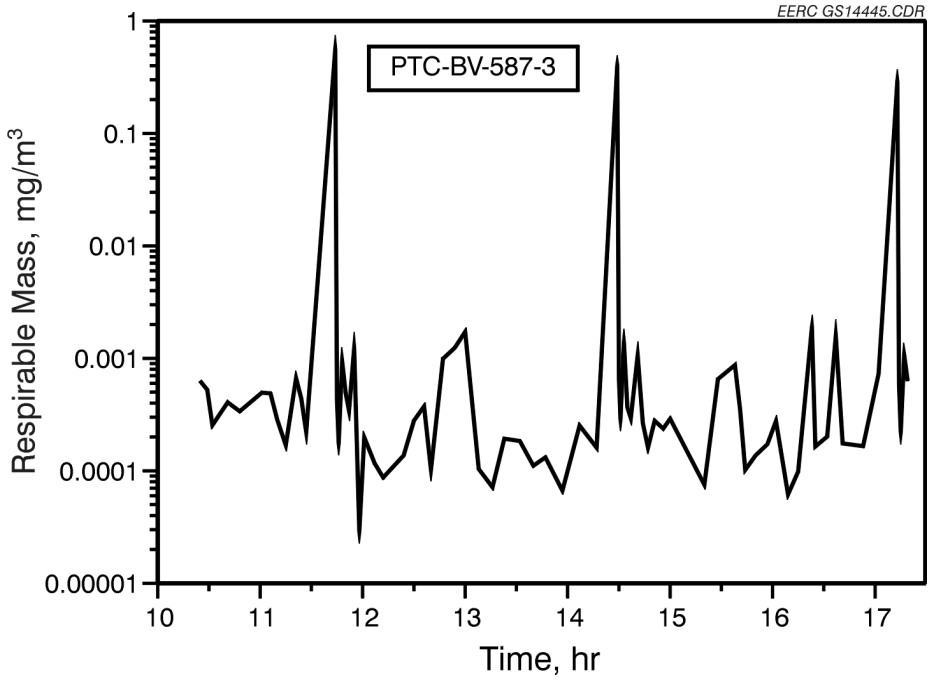

Figure 4.4-60. APS data for Day 3, April 2, 1997, Test PTC-BV-587.

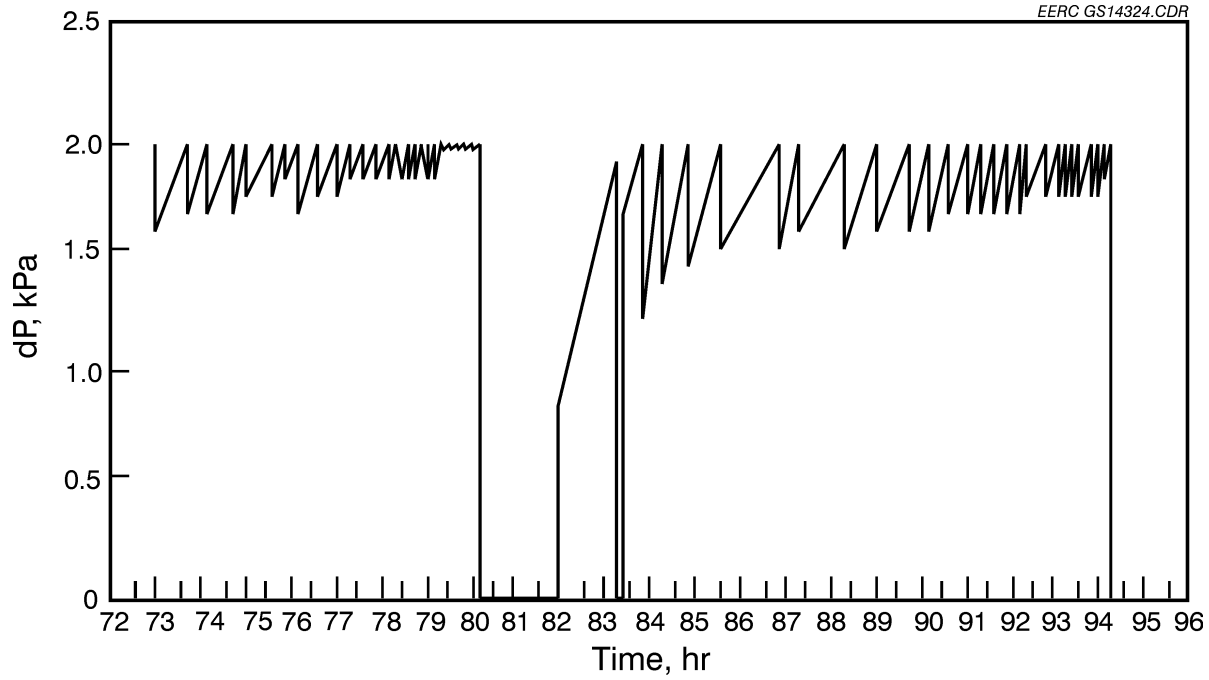

Figure 4.4-61. Pressure drop as a function of time for Day 4, April 3, 1997, Test PTC-BV-587 with on-line cleaning using graphite-impregnated PTFE bags.

TABLE 4.4-17

NH_3/SO_4^{2-} Analysis of Baghouse Ash from Blinded Bag, Test PTC-BV-587

NH_3	13,000 µg/g
SO_4^{2-}	171,000 µg/g

gently brushed clean. The ESP grid was cleaned as well as the site ports. The consistency of the ash was very sticky and hard to clean off. The AHPC was returned to operation at 82 hr. At 83 hr, a slug of unburned carbon filled the AHPC chamber, causing the ESP grid to arc. The AHPC was taken off-line and the ESP grid quickly cleaned and back on-line in 5 min. The AHPC went through two cleaning cycles without flue gas conditioning. Flue gas conditioning resumed at 85 hr. The next two cleaning cycles saw improvement in pulse interval times; however, the bags began to show signs of blinding. It was discovered at this time that the flowmeter on the NH_3 tank was not maintaining a consistent flow rate. The SO_2 flow rate into the SO_3 generator was

also fluctuating. Attempts to correct the flow rate problems were unsuccessful. With the unstable flows of the gas-conditioning agents, the AHPC performance continued to degrade until shutdown at 94 hr. The pulse interval versus time graph is presented in Figure 4.4-62, showing this decrease in AHPC performance at the end of the run.

The dust-loading data for Day 4 are presented in Table 4.4-15. The EPA Method 29 inlet dust loading was 4.6425 g/m^3 (2.10290 gr/scf), and the inlet dust loading, calculated from the mass of ash collected from the AHPC ash hopper, was 5.26 g/m^3 (2.30 gr/scf). The outlet dust loading was 0.0007 g/m^3 (0.00031 gr/scf), giving a dust-loading efficiency of 99.9852%. The outlet particulate sample was collected over a period of 4 hr. Respirable mass measurements by the APS are presented in Figure 4.4-63. The respirable mass integrated average for Day 4 was 0.0099 mg/m^3, indicating >99.999% collection efficiency.

Normally, ashes conditioned with SO_3/NH_3 resemble a fluffy, dry powder and have a reduced bulk density. This ash seemed much more adhesive, especially the ash attached to the ESP grid.

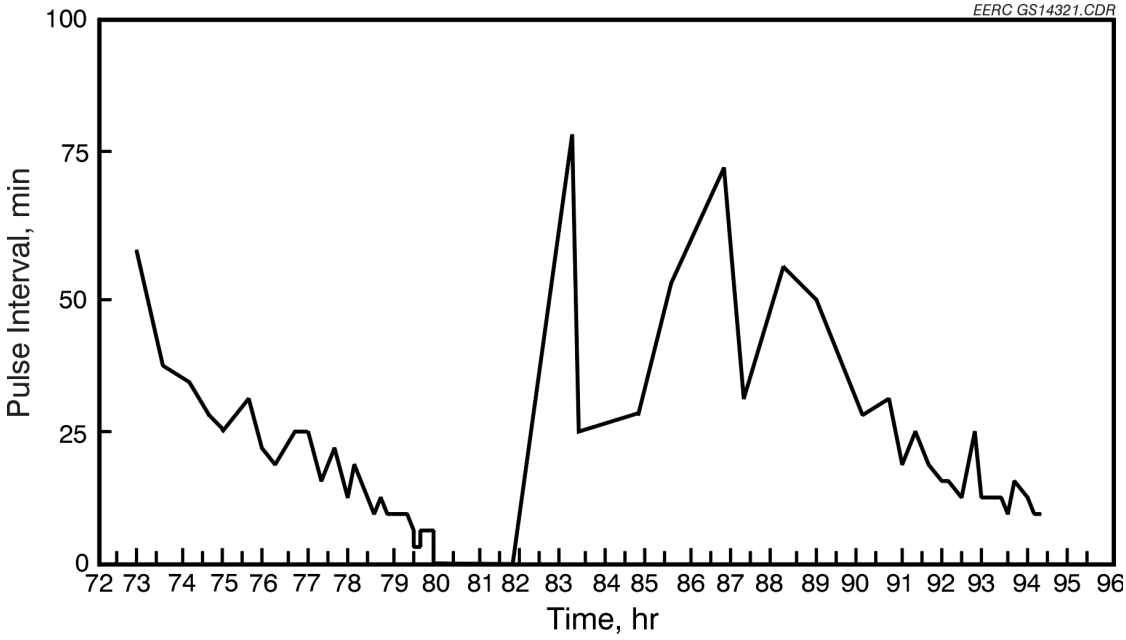

Figure 4.4-62. Pulse interval as a function of time for Day 4, April 3, 1997, Test PTC-BV-587 with on-line cleaning using graphite-impregnated bags.

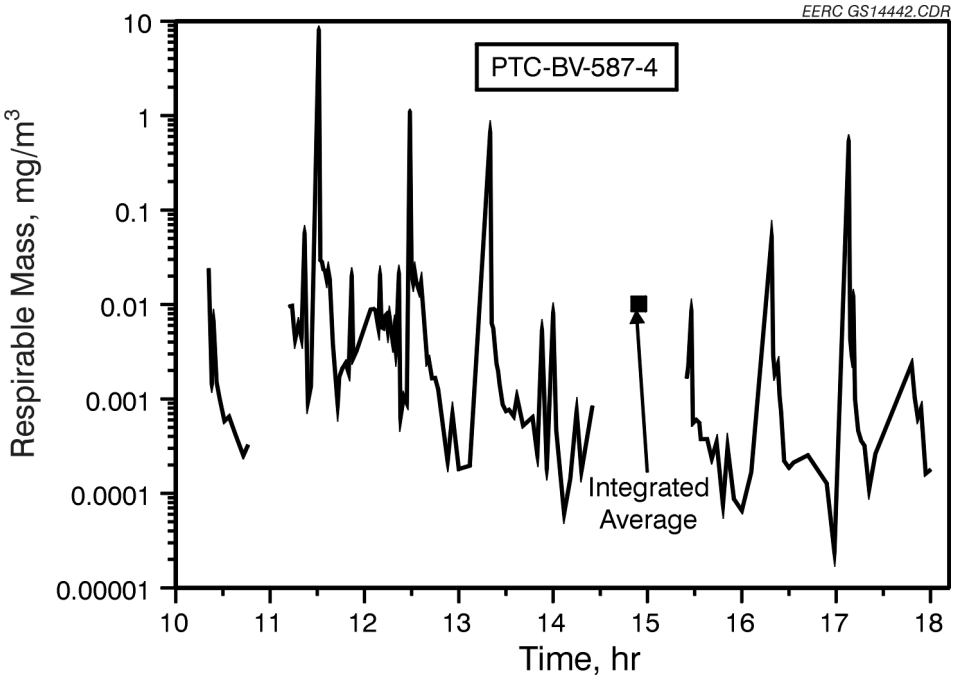

Figure 4.4-63. APS data for Day 4, April 3, 1997, Test PTC-BV-587.

These results indicate that conditioning has the potential to improve performance, but may also cause cleaning problems if the concentrations are incorrect. Performance of the AHPC with Blacksville coal was satisfactory without conditioning, but, if conditioning is to be used, a better understanding of how performance is affected by the conditioning agent concentrations is needed.

4.4.3.5 Conclusions from Test PTC-BV-587 Firing Blacksville Coal

- The AHPC operated successfully on Blacksville bituminous for 50 hr without conditioning.

- Pressure drop was controlled, and pulse intervals ranged between 35 and 40 min.

- Particulate efficiency of >99.99% was achieved throughout the test period.

- Flue gas conditioning had a dramatic effect on the AHPC, initially improving performance but then leading to cleaning problems.

- The NH_3/SO_3 ratio is critical for proper flue gas conditioning.

5.0 STATUS OF DEVELOPMENT AND RECOMMENDATIONS FOR SCALEUP

All of the Phase I objectives were met and the AHPC concept is ready for larger-scale and longer-term evaluation. Two additional developmental questions were identified in Phase I that will affect the scaled-up design. The first question concerns the optimum spacing between the bags and plates. There were no sparking or back corona problems with the directional electrode, grounded bags, and spacing used. This indicates that the spacing can likely be significantly reduced without compromising performance. Closer spacing is attractive because it allows a smaller device footprint, leading to more cost savings. The bag-plate spacing for Phase I was approximately 0.33 m (13–14 in.), but this spacing can likely be reduced up to 50%. Further 5.7-m^3/min (200-acfm) tests are recommended to determine if the bag-to-plate spacing can be reduced without compromising performance.

The second question is whether a bottom inlet configuration would work as well as the side inlet configuration tested in Phase I. Analysis of the flow dynamics within the AHPC indicates that baffling is not important, which suggests that a simpler configuration with an inlet just below the bags and plates would also work well. Again, additional 5.7-m^3/min (200-acfm) tests are recommended to help decide whether a bottom inlet configuration is appropriate for a scaled-up AHPC.

The goal for the scaleup tests is to evaluate the AHPC under the most realistic conditions achievable, including the use of full-scale components where possible. The most important parameters to properly simulate are as follows:

- Bag size: Full size, 0.15-m (6-in.) diameter by 4.6-m (15-ft) length.

- Bag-to-plate spacing: 0.18 m (7 in.) to 0.33 m (13 in.), depending on 5.7-m^3/min (200-acfm) results.

- High-voltage electrode: Directional mast type; the size, geometry, insulators, and rappers will duplicate full scale.

- Plates: Metal gauge, size, geometry, and rappers similar to full scale.

- Pulsing: Nozzles and venturis will be the same as full scale; blow pipes will be sized for 8-bag rows rather than 16-bag full-scale rows.

- Power supply and controller: Power density, voltage range, and controls similar to full scale.

To clearly demonstrate on-line cleaning of a row of bags at a time, a minimum of four rows of bags is required so that during the cleaning the available filtration area is reduced by no more than 25%. The minimum number of bags in a row is eight, which is about half the number that would be used in a full-scale system; however, eight should be sufficient to minimize fringe effects and demonstrate full-scale cleaning of a multibag row. Four rows of eight full-scale bags (0.15-m [6-in.] diameter, 4.6-m [15-ft] length) would total 32 bags, which would filter 257 m^3/min (9081 acfm at) 3.7 m/min (12 ft/min). This represents a large pilot scale (2.4-MW electrical equivalent), which appears to provide the best combination of being large enough to allow meaningful tests with full-scale components, but yet small enough to be transportable and cost-effective. If the plates are each 2.1 m (7 ft) wide by 4.9 m (16 ft) long, the equivalent SCA would be 20 $m^2/m^3/s$ (99 ft^2/1000 acfm). If the 5.7-m^3/min (200-acfm) tests indicate good performance, the field unit will be configured with a bottom inlet, as shown in Figure 5-1. A concern is whether the vertical gas velocity would be too high to expect good precipitation at the bottom entrance of the channels defined by adjacent plates. For the 0.56-m (22-in.) plate-to-plate spacing shown, this velocity would be only 0.88 m/s (2.9 ft/s), which is lower than the gas velocity in typical ESPs. A suggested approach to accommodate possible tests at higher A/C ratios is to oversize the fan and ducting to facilitate operations up to 4.9 m/min (16 ft/min).

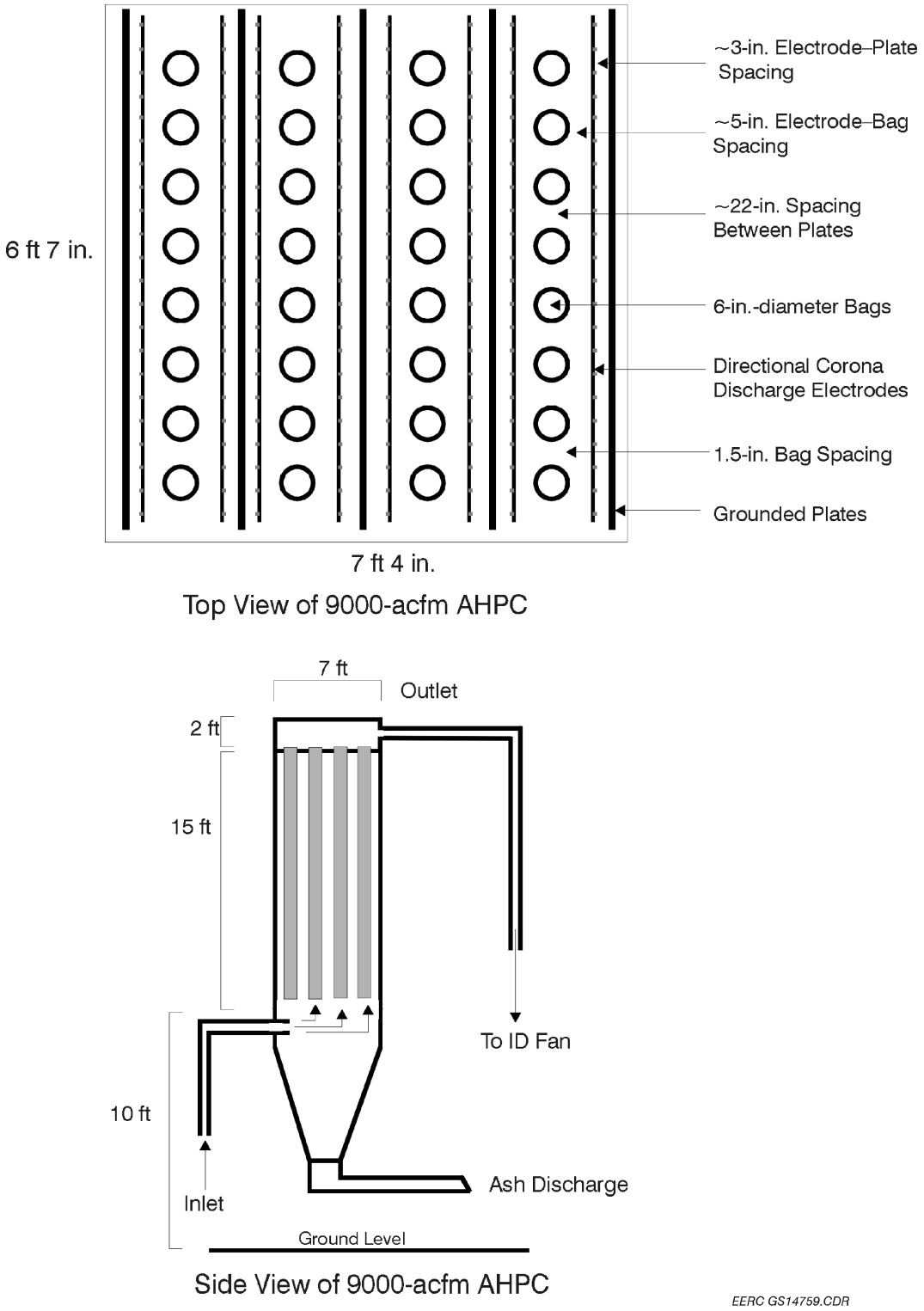

Figure 5-1. Conceptual design of 255 m^3/min (9000-acfm) field AHPC.

6.0 ECONOMIC AND MARKET EVALUATION OF THE AHPC

An economic analysis of the AHPC was not planned as part of Phase I. The intent of this section is not to present a complete economic analysis of the AHPC, but to evaluate the potential for the AHPC based on a review of some economic factors. Particulate control is a broad technology applied to thousands of different processes, so the economic assumptions must be clearly defined before an evaluation can be made. The critical independent parameters that determine the engineering and economic approach to particulate control are as follows:

- Dust type
- Dust loading
- Dust particle-size distribution
- Process conditions: temperature, pressure, and chemical environment
- Level of control required
- Reliability
- Footprint

Discussion of the assumptions for these factors will serve as a basis for comparing the economics and evaluating the market potential for the AHPC.

6.1 Dust Type

The AHPC is expected to function well for a variety of dusts and processes. In cases of extremely high or low electrical resistivity, the performance of the ESP portion of the AHPC could deteriorate to the point where the AHPC would not function well. The AHPC can tolerate a much broader range in resistivity than a conventional ESP because the overall efficiency is determined by the bags. For example, if high resistivity caused the ESP portion to collect only 80% compared to 95%, the AHPC should still function very well. The worst effect would be somewhat more frequent bag cleaning. Therefore, the AHPC should be significantly better at handling low- or high- resistivity dust than conventional ESPs, but may not be able to compete

with conventional baghouses in extreme cases, since conventional baghouses should not be affected at all by the dust resistivity. Extremely high- or low-resistivity dust is likely to occur in very few applications. This refers to dust that is more extreme than the range of resistivity typically found for coal fly ash. An example where this might be a problem is with very conductive dusts such as metallurgical fumes or substances such as pure silica or alumina. The AHPC is expected to function very well for almost all other dust types.

6.2 Dust Loading

The AHPC is applicable to a very wide range in dust loading and is expected to handle high dust loads better than either an ESP or baghouse. An ESP is excellent at handling high dust loads, but efficiency deteriorates. A baghouse may have problems with significantly increased dust load because of the difficulty of controlling pressure drop, and increased bag-cleaning frequency will likely result in increased emissions. The AHPC, however, can achieve the best of both worlds. It can capitalize on the ability of the ESP portion to collect most of the dust, even at high dust loadings, while the filter portion still ensures an ultrahigh collection efficiency. Therefore, the AHPC is superior to either conventional ESPs or baghouses for high dust loadings.

6.3 Dust Particle-Size Distribution

This is an extremely important dust property that is likely to drive the engineering and economic choice for dust control. For dusts that are primarily larger than 20 μm, inertial separation methods, such as cyclones, are reasonably effective and are much more economical than conventional ESPs or baghouses. However, most dusts also have some fines, which pass through cyclones with little or no collection. If emission of even a small amount of fine dust is unacceptable, then cyclones drop out as a viable control method and only ESPs and baghouses are capable of achieving reasonable control. Fabric filters collect fine particles much better than ESPs because fabric filters do not have the same theoretical (and actual) minimum collection efficiency for particles in the range from 0.1 to 0.3 μm. For these particles, the collection

efficiency of a cyclone is close to zero, the efficiency of a modern ESP would be about 99%, and the efficiency of a conventional fabric filter would be about 99.9%. A conservative estimate of the collection efficiency of the AHPC for these fine particles is at least 99.99%, based on extensive test data. Therefore, fine-particle emissions from an AHPC would be at least a factor of 100 times lower than a conventional modern ESP and at least a factor of 10 times lower than a conventional modern baghouse. An economic comparison between the AHPC and a baghouse or ESP must consider the superior performance of the AHPC.

6.4 Process Conditions

The AHPC was developed for applications that include difficult process conditions such as the presence of high levels of acid gases and a range of temperature. ESPs can be designed to operate under hot-side (343°–399°C [650°–750°F]) as well as cold-side conditions (121°–177°C [250°–350°F]), which makes them an attractive choice for high-temperature applications. The choice of filter media in the AHPC will determine the upper temperature limit. The use of GORE-TEX® membrane bags will allow temperatures to about 260°C (500°F), which will cover almost all processes. However, for specialized applications, there is no reason why the AHPC could not operate at higher temperatures by using either high-temperature glass fabric or ceramic filters. In cases of high SO_3 and HCl (which includes most boilers firing eastern bituminous coals), most conventional fabrics cannot withstand the environment and fail in within a few months to a year. All-PTFE fibers, on the other hand, would function very well and are likely to last over 5 years. For process conditions that are less harsh, all-PTFE bags may not be necessary, so the use of GORE-TEX® membrane on either glass or synthetic fabrics might be a more economical choice. ESPs do not have the restriction of having to select a chemically resistant fabric, so they are generally considered more rugged in harsh chemical environments and are generally the logical choice over conventional fabric filtration. What the AHPC offers is a technology that can also operate in a harsh chemical environment and provide superior fine-particle control to an ESP. This means that the AHPC would be able to compete economically with ESPs in cases where conventional fabric filtration could not.

6.5 Level of Control Needed

This factor, along with the particle-size distribution of the dust, is the most critical to the selection of the best economic approach for control. For coal-fired boilers, the NSPS requirement of 0.03 lb/10^6 Btu requires about 99.8% total mass particulate control. It should be recognized that this standard is 20 years old. After the PM_{10} ambient air quality standard was implemented, there was never a subsequent fine-particle emission standard promulgated, even though it would have been a logical step. The new ambient air quality standard for $PM_{2.5}$ is a broad and wide-sweeping regulation designed to ensure that all Americans can enjoy clean air whether they live in remote, pristine regions or in major urban centers. The new standard is based on years of data collection and multiple health studies that indicate the current PM_{10} standard does not adequately protect public health. The standard has major implications for industry, including transportation, power production, oil refining, incineration, chemical production, and agriculture.

The number of counties nationwide that are out of compliance will increase from the present 41 counties that are not in compliance with PM_{10} to 167 that are projected to not meet the new standard. The noncompliance areas represent major urban areas in 37 of the 50 states. States will be required to set up monitoring networks and then develop state implementation plans to bring all areas into compliance. Achieving compliance will require significant reductions in emissions from the primary mobile and stationary sources of $PM_{2.5}$ contamination in the atmosphere. Superior, economically viable technologies will have to be developed that allow efficient operation of processes while at the same time preventing unacceptable pollution of the atmosphere. Protecting public health from the adverse effects of air pollution does not have to present an undue burden on industry if new, economical technologies are available. In many cases, some level of control is already required, so it is simply a matter of replacing an expensive, outdated technology with a modern, less costly, but superior, approach. The AHPC is a technology that can meet this need.

The exact control requirements to meet the new $PM_{2.5}$ standards are difficult to predict, but, it is likely they will be more strict than the 20-year-old NSPS emission limit and will be based on

a fine-particle emission limit. This raises the question of what level of control should be considered for making economic comparisons among competing technologies. The intent of the economic comparison is to evaluate technologies for the future rather than the past. Therefore, the assumed requirement for control should be set at a stricter level than an outdated 20-year-old emission standard. A conservative estimate for a future requirement is 99.9% control of $PM_{2.5}$. This is a level that can be achieved by well-designed baghouses of current design. ESPs may also be able to achieve this level of control by increasing the SCA, so, as a minimum, this appears to be valid control requirement for comparison purposes.

6.6 Reliability

This factor can be considered from both the vendor and client perspective. From a user perspective, the need is for a product that is highly reliable within economic constraints and is backed by the vendor both in terms of a guarantee and the ability of the vendor to correct possible problems. From a vendor perspective, having a superior technology available that can compete economically and is highly reliable is a significant advantage, because the likelihood is high that the customer will be satisfied and the risk in supplying a guarantee is low. For example, an ESP's ability to meet 99.9% $PM_{2.5}$ control and still compete economically would likely require cutting the collection efficiency very close. There would be no margin of safety in meeting the emission limit, while an AHPC would have a wide margin of safety. From a reliability and guarantee perspective, the AHPC would appear to have a significant advantage over either conventional baghouses or ESPs. The reliability issue will be further evaluated in larger-scale testing. However, there are no apparent show stopper issues that would make the AHPC unreliable. The main question concerning reliability of the AHPC is the bag life at high A/C ratios. Since, GORE-TEX® bags have already proven to be highly reliable, bag life with the AHPC is also expected to be excellent.

6.7 Footprint

The land area taken up by the device is typically not a major consideration, except in retrofit applications. The goal would be for a new device to take up the same or less area than conventional technology. Further discussion on the AHPC sizing is given in Section 7.9.1, but initially, the AHPC can be compared with conventional pulse-jet baghouses and conventional ESPs. The plan area required for the device, independent of ducting, can be compared on an acfm of flue gas per ft^2 of plan area. An ESP with a SCA of 100 $m^2/m^3/s$ (500 ft^2/1000 acfm) with a 13-m (42.6-ft) plate height and a 0.31-m (12-in.) plate spacing would be able to treat 52 $m^3/min/m^2$ (170 $acfm/ft^2$) of plan area. A pulse-jet baghouse operating at an A/C ratio of 1.2 m/min (4 ft/min) with 4.6-m (15-ft) by 0.13-m (5-in.) bags and 0.18-m (7-in.) (centerline-to-center) bag spacing could treat 72 $m^3/min/m^2$ (235 $acfm/ft^2$) of plan area, so the pulse-jet baghouse is already smaller than the ESP. Since the AHPC size is based on a conventional pulse jet at 1.2 m/min (4 ft/min), it would also be somewhat smaller than the ESP. Further sizing analysis will show that the AHPC has the potential to be considerably smaller than a conventional pulse-jet baghouse, so from a footprint perspective, the AHPC has the advantage over ESPs or baghouses.

6.8 Economic Questions

Two main questions are, What is the cost of an AHPC? and, What is the cost of competing technologies? At this point only ESPs and baghouses will be considered, since they are the only technologies that can provide fairly good fine-particle collection efficiency. Considerable published information is available on cost estimates for ESPs and baghouses. Scheck and others (9) provide a fairly complete analysis and comparison of ESPs and baghouses along with sensitivity analysis for a number of factors. According to these EPRI estimates, a reverse-gas full-flow (RGFF) baghouse at an A/C of 0.6 m/min (2 ft/min) would require a total capital investment of $53/KW (1982 dollars) for a 500-MW plant. This is equivalent to an ESP with a SCA of 90 $m^2/m^3/s$ 90-m^2/m (450-ft^2/1000 acfm), so the RGFF would be the economic choice for all SCAs larger than this. Another EPRI report (10) lists the capital cost for a pulse-jet baghouse

at $40/KW (1987 dollars) compared to $55/KW for a 90 $m^2/m^3/s$ 90-m^2/m (450-ft^2/1000 acfm) SCA ESP and $57/KW for a 0.6-m/min (2-ft/min) A/C RGFF. All three of these would meet the NSPS for an Appalachian coal. However, for a Powder River Basin coal, a 150-$m^2/m^3/s$ (750-ft^2/1000 acfm) SCA ESP would be required at a cost of $87/KW, while the same reverse-gas and pulse-jet baghouses would meet the emission limit.

Scheck and others (9) also compare ESP and baghouse costs for stricter emission limits down to 0.01 lb/million Btu for several different U.S. coals. In all cases for the stricter emission limit, the ESP is significantly more costly than conventional reverse-gas baghouses. A 99.9% control requirement for $PM_{2.5}$ would be even more difficult for an ESP to achieve than a total mass emission limit of 0.01 lb/million Btu. Therefore, the ESP would not be a viable economic choice for this level of control. That leaves only conventional fabric filters as a competing technology for the AHPC. While low-ratio (A/C 0.6 m/min [2 ft/min] or lower) reverse-gas baghouses have been observed to achieve excellent collection for fine particles, higher-ratio (A/C 1.2 m/min [4 ft/min] or higher) pulse-jet baghouses with conventional fabric typically have much higher emissions and very likely would not achieve 99.9% collection of $PM_{2.5}$. For a valid comparison with the AHPC, the pulse-jet would have to operate at much lower A/C to reduce emissions. The following section compares cost estimates for the AHPC with those for conventional pulse-jet baghouses.

6.9 Costing of the AHPC

The prime factors for costing the AHPC are as follows:

- Size of vessel
- A/C ratio or filtration area
- Fabric cost
- Bag life
- High-voltage power supply
- Plates and high-voltage electrodes

- ESP power
- Fan power
- Pulsing power

6.9.1 Footprint, Size of Vessel, and A/C Ratio

The currently proposed concept is based on a box size that is equivalent to removing approximately three of four rows of bags of a high-ratio baghouse operating at 1.2 m/min (4 ft/min) (assuming 0.13-m [5-in.]-diameter bags and 0.05-m [2-in.] bag spacing). The removed rows of bags are replaced by grounded plates with high-voltage electrodes on both sides of the plate. The resulting distance between rows of AHPC bags for this configuration is 0.58 m (23 in.) Since removal of three out of every four bags is equivalent to increasing the A/C ratio to 4.9 m/min (16 ft/min), an AHPC with a 0.58-m (23-in.) bag spacing operating at 4.9 m/min (16 ft/min) would have the same vessel size as a conventional pulse-jet baghouse at an A/C of 1.2 m/min (4 ft/min). There is potential to make the AHPC more compact by reducing the spacing between the electrodes and still be within typical ESP designs. Going to a 0.41-m (16-in.) spacing alone would reduce the size of the box 25%, and a 0.31-m (12-in.) spacing would result in a box 39% smaller than a pulse-jet baghouse operating at 1.2 m/min (4 ft/min). Another significant enhancement would be to use specialized high-surface-area bags. This could easily result in another 50% reduction in overall size or a unit about 70% smaller than a pulse-jet baghouse operating at 1.2 m/min (4 ft/min). However, there may be a limit to how small the box size could be and still leave enough room for the required ESP collection area. Therefore, in the worst case, the AHPC box is about the same size as a high-ratio baghouse and in the best case, it is 70% smaller than a high-ratio baghouse. A high-ratio pulse-jet baghouse is already much smaller than the reverse-gas baghouses typically used on large boilers and also has a smaller footprint than ESPs.

6.9.2 Cost of Bags and Bag Life

The cost per area of GORE-TEX® fabric is greater than for conventional fabrics such as Ryton, but the higher cost is offset by the much higher A/C ratios and possibility of longer bag

life. To meet a much stricter emission standard with Ryton, the A/C ratio would have to be reduced significantly, making the GORE-TEX® fabrics even more cost-effective. In this case, assuming an A/C ratio of 0.6 m/min (2 ft/min) would be necessary for a conventional fabric, the cost of GORE-TEX® fabrics in an AHPC would be less than for conventional fabrics. It should be noted that GORE-TEX® fabrics have other advantages that make them far superior to Ryton. The upper temperature limit with Ryton is only about 190°C (375°F) compared to about 260°C (500°F) for the either glass or all-PTFE GORE-TEX® fabrics. In addition, the Ryton would not do well in harsh chemical environments, so there are many applications where Ryton simply could not compete from a reliability perspective.

6.9.3 High-Voltage Power Supply, Plates, and High-Voltage Electrodes

These costs would tend to increase the cost of the AHPC over the cost of a conventional pulse-jet baghouse. However, there will also be some offset in costs because of fewer pulse headers and cages for the AHPC. For large ESPs, the cost of an ESP power supply and controller is approximately $30,000 for 2789 m^2 (30,000 ft^2) of plate area. For a full-scale ESP of 100 $m^2/m^3/s$ (500 ft^2/1000 acfm) SCA, this translates to $1.90/kW or $0.50 per acfm. Assuming the AHPC requires 20 $m^2/m^3/s$ (100 ft^2/1000 acfm) SCA, the power supply and controller costs would be $0.38/kW or $0.10/acfm. These costs are considerably lower than the cost for Ryton fabric. While the costs may increase for smaller-size units, it appears that the cost of adding a high-voltage power supply and controller is not significant. The cost of adding plates, insulators, and wires will be partially offset by fewer pulse headers and cages, but a conservative estimate would suggest some increase in cost over a conventional pulse-jet baghouse for the same size vessel. Turner and others (11, 12) provide approximate baghouse vessel costs for several baghouse configurations ranging from about $15 to 30$/kW. Assuming the plates and wires increased the cost of the vessel by 10%, the added cost would be in the range of $1.50 to $3/kW. If the vessel size could be reduced by 10% or more, this additional cost could likely be recovered again. Since there is good potential for a reduced vessel size, it appears that the cost of the power supply and added plates and wires will not add significantly to the overall cost of the AHPC.

6.9.4 ESP, Fan, and Pulsing Power

The power requirements for ESPs can readily be estimated by assuming a power density at the plate and the SCA. Scheck and others (9) list a power density range for ESPs of 0.9 to 2.7 W/ft^2. For the AHPC, assuming a power density on the high end at 3 W/ft^2 and a SCA of 18 m^2/m^3/s (90 ft^2/1000 acfm), the corresponding power requirement is 0.27 W/acfm. This can be compared with the fan requirement for a pressure loss across the AHPC of 2.0 kPa (8 in. W.C.), which is 0.94 W/acfm (assuming 65% fan efficiency). Therefore, the ESP power requirement is approximately equal to the fan power requirement for a 0.5-kPa (2-in.) pressure loss. This indicates that the additional operating cost for ESP power is minor. Analysis of the power requirement for the pulse air shows that this is an insignificant operating cost. Assuming a 0.28-m^3 (1-scf) pulse volume and pulsing once every 15 min for 4.6-m (15-ft) by 0.13-m (5-in.) bags operated at an A/C ratio of 3.7 m/min (12 ft/min), the power requirement is only 0.055 W/acfm. Even if a higher pulse volume were required, the cost of power for bag cleaning appears to be insignificant.

6.10 AHPC Economic Conclusions

- ESPs and baghouses are the only competing technologies that can provide reasonably high levels of control.

- ESPs can compete with the AHPC for some applications to meet current U.S. emission standards; however, ESPs could not compete with the AHPC to meet 99.9% control for $PM_{2.5}$.

- Only baghouses can compete with the AHPC for 99.9% control of $PM_{2.5}$. However, pulse-jet baghouses would either have to use a more sophisticated fabric or reduce A/C ratio to compete with the AHPC for a stricter fine-particle standard.

- The main factors that determine the AHPC cost compared to other technologies are the size of the vessel and the bag costs.

- The size of the AHPC vessel in the worst case is expected to be the same as a pulse-jet baghouse operated at 1.2 m/min (4 ft/min). In the best case, the AHPC could be more than 50% smaller than the pulse-jet baghouse.

- The cost of the high-voltage power supply, plates, and wires is estimated to increase the AHPC vessel cost by about 10% over the same size pulse-jet vessel. However, since the AHPC can likely be smaller than a pulse jet at 1.2 m/min (4 ft/min) and since the pulse jet would likely have to operate at a lower A/C ratio to meet a stricter emission standard, the AHPC has clear economic advantages over a conventional pulse-jet baghouse.

- Fabric cost per unit area for the GORE-TEX® fabric is greater than for conventional fabrics. However, a longer bag life for the GORE-TEX® and the much larger A/C ratio for the AHPC make GORE-TEX® fabric less costly than conventional fabrics.

- The cost of ESP power for the AHPC is equivalent to a 0.5-kPa (2-in. W.C.) pressure loss and is therefore not a significant operating cost. The cost of pulsing air is even less a factor.

- The AHPC is projected to be economically competitive with conventional ESPs and baghouses, even for meeting the old NSPS requirement of 0.03 lb/million Btu. For a new $PM_{2.5}$ emission standard of 99.9% control, the AHPC is projected to be the economic choice over ESPs by a wide margin. The AHPC is projected to also be the economic choice over conventional baghouses for a $PM_{2.5}$ standard.

6.11 Market Potential for the AHPC

The actual market potential of the AHPC depends on how it compares economically to other technologies, the regulations, and the demand. The economics and $PM_{2.5}$ regulation have already been addressed. *EM* magazine (5) projected a world particulate control market of $6.7 billion for the next 12 months. The projection gives the edge to ESPs at $3.9 billion compared to fabric filters at $2.8 billion. This is surprising, considering that ESPs do not provide the level of control that baghouses do. An explanation is that there are still reliability concerns with fabric filters. A new technology such as the AHPC has the potential to break into the ESP market as well as meet the fabric filter market if it can be demonstrated to perform reliably under more harsh chemical conditions where ESPs are frequently the choice. Since the AHPC concept was specifically developed for these applications, the AHPC has much more potential than conventional fabric filters. The combination of wide applicability, competitive cost, and superior performance makes the AHPC highly attractive on a worldwide basis.

7.0 CONCLUSIONS

7.1 Conclusions for Cold-Flow Results

- Visual monitoring showed that when the bags were pulsed, the reentrained dust cloud was propelled back into the ESP zone, according to expectations.

- Voltages up to 70 kV can be applied to the electrodes without generating back corona on the all-PTFE bags. Back corona was not observed with the conductive PTFE bags, even at 70 kV.

- Without the electric field, the bag-cleaning interval was more than 10 times lower, and the bags did not clean to as low a pressure drop. This indicated that the ESP was functioning properly, precollecting most of the dust and improving bag cleaning.

- No significant differences in AHPC performance were noted between the V-baffle and the deflection plate, which indicated that baffling is not highly critical to proper functioning of the AHPC.

- Comparative tests with the conductive and nonconductive bags at 50 kV showed no difference in bag cleanability or AHPC function. This was an encouraging result, because it demonstrated that conductive bags could be used if needed to avoid charge buildup, back corona, or sparking.

7.2 Conclusions of 8-hr Test Results

- The AHPC demonstrated good bag cleanability and operability at an A/C ratio of 3.7 m/min (12 ft/min), firing both Absaloka and Blacksville coals.

- A modified directional electrode increased the corona current flow and improved the distribution of the electric field.

- No significant differences in particulate collection efficiency or operability were observed between the PTFE-only bags and the conductive PTFE bags.

- Particulate collection efficiencies greater than 99.99% were achieved with both coals.

- The collection efficiency of the AHPC shell with no bags and the ESP off was 48%.

- Without bags, the total mass ESP particle collection efficiency in the AHPC was 95% and the respirable mass collection efficiency was 83%.

- Satisfactory bag cleaning was achieved with both off-line and on-line cleaning.

- Successful operation was demonstrated at 4.9 m/min (16 ft/min) with a pulse interval of 10–15 min.

- Injection of NH_3/SO_3 dramatically improved AHPC performance both in pressure drop and pulse interval.

- Under different bag-cleaning modes and different coals, the AHPC demonstrated the ability to recover after an interruption to the ESP power.

7.3 Conclusions for 100-hr Test Results

- Particulate collection efficiencies greater than 99.99% for all particle sizes from 0.01 to 50 μm were achieved.

- Pressure drop was well controlled, steady, and not adversely affected by the injection of carbon. The time interval between bag-cleaning cycles ranged from 25 to 35 min at the end of the 100-hr tests.

- Emissions of arsenic, cadmium, lead, and nickel were below detection limits. Mercury and selenium were detected in measurable quantities in vapor form at the outlet. Chromium was detected at the outlet, but may have been the result of contamination.

- No increased particulate emissions was noted during mercury sorbent injection.

- The AHPC operated successfully on both Absaloka subbituminous and Blacksville bituminous coals for approximately 100 hr.

- The ratio of oxidized mercury to elemental mercury appeared to increase across the AHPC.

- Flue gas conditioning had a dramatic effect on AHPC performance, but the concentrations and NH_3/SO_3 ratio are critical for optimum performance.

8.0 REFERENCES

1. Leutwyler, K. "Pollution, Pollution,...," *Science* **1993**, *269*, 23–28.

2. Lipfert, W.; Wyzga, E. “Air Pollution and Mortality: Issues and Uncertainties,” *Journal of the Air & Waste Management Association* **1995**, *45*, 949–966.

3. U.S. Environmental Protection Agency. *Air Quality Criteria for Particulate Matter*; Vol. III, EPA/600/P-95/001cF, April 1996.

4. Nation Ambient Air Quality Standard for Particulate Matter, Final Rule 40. Code of Federal Regulations, Part 50, *Federal Register* **1997**, *62* (138).

5. “Which Communities Will be Affected by the New Standards?” *EM Air & Waste Management Association’s Magazine for Environmental Managers* **1997**, *Jan*. 19–22.

6. Dennis, R. et al. “Filtration Model for Coal Fly Ash with Glass Fabrics,” EPA-600/7-77-084, Aug. 1977.

7. Leith, D.; Rudnick, S.N.; First, M.W. “High-Velocity, High-Efficiency Aerosol Filtration,” EPA-600/2-76-020, Jan. 1976.

8. Oglesby, S.; Nichols, G.B. *Electrostatic Precipitation*; Marcel Dekker: New York, NY, 1978.

9. Scheck, R.W.; Morra, R.R.; Belba, V.H.; Horney, F.A. *Economics of Fabric Filtration and Electrostatic Precipitators*; EPRI CS-4083, June 1985.

10. Southern Research Institute. “Market Potential and Comparison with Other Technologies” *in* Proceedings of the Workshop on Pulse-Jet Baghouse Technology; EPRI GS-6210, Research Project 1129-8; Jan. 1989; pp 5-1 to 5-15.

11. Turner, J. H.; Viner, A.S.; McKenna, J. D.; Jenkins, R. E.; Vatavuk, W.M. “Sizing and Costing of Fabric Filters, Part I: Sizing Considerations,” *International Journal of Air Pollution Control and Hazardous Waste Management* **1987**, *37* (6), 749–759

12. Turner, J.H.; Viner, A.S.; McKenna, J.D.; Jenkins, R.E.; Vatavuk, W.M. “Sizing and Costing of Fabric Filters, Part II: Sizing Considerations,” *International Journal of Air Pollution Control and Hazardous Waste Management* **1987**, *37* (6), 1105–1112.

MODELING

APPENDIX A

NUMERICAL ANALYSIS OF THE FLOW TROUGH AHPC200

by
Dr. Henry V. Krigmont
&
Dr. Alex V. Potapov

Allied Environmental Technologies, Inc.

The flow through the AHPC200 has been numerically analyzed using the PHOENICS software package. The basis of this analysis is numerical solution of the equations of the fluid motion with appropriate boundary conditions. The computations have been performed using the body-fitted coordinates approach which allows us the exact representation of the geometry of the simulated region. The geometric dimensions has been provided to Allentec by EERC and correspond to the working model of AHPC200. The computational grid consisted of 65x19x54 cells, this grid is presented on Figures 1&2. Due to the symmetry of the problem, only half of the AHPC was actually simulated, the symmetry conditions are assumed on the plane $x=0$ (Figures 1-3). The simulation has been carried out for the normal conditions air (20°C), which corresponds to the cold-flow testing of the AHPC, for the 200 acfm air flow.

The k-e turbulence model has been used for the flow simulation. This model employs the effective viscosity approach on the basis of calculation of the specific kinetic turbulent energy k and rate of the dissipation of this turbulent energy e. Since the conditions at the baghouse inlet are unknown, the uniform distribution of the velocity across the inlet is assumed with uniform turbulence intensity 3%. The model allows us to predict the time-averaged values of the turbulent velocities inside the simulated region (here AHPC).

The details of the simulated region are presented on Figure 3. Here, flow baffle and grounded plate are simulated as plates with zero permeability and appropriate boundary conditions for velocities and turbulent parameters. The surfaces of the pulse jet bags were simulated as porous media with the resistance chosen so that the pressure drop on the bags was about 6 inches of water (about 1,500 Pascals). Due to the small cross-section area and thus negligible influence on the gas flow the high voltage electrodes were actually not simulated. These electrodes are presented on the figures for the reference purposes only.

The results of the simulation are presented in terms of velocity vectors on Figures 4-10. Figure 4 shows the velocity distribution at the vertical plane of symmetry of the AHPC, while Figure 5 shows the velocity distribution at the horizontal plane passing through the center of the baghouse inlet. The rest of the pictures demonstrate the details of velocity distributions at these

planes.

One can see from these figures that the flow does have some recirculation both before and after the flow baffle. However, it appears from the figures that majority of the gas flow does pass between the high voltage electrodes and the grounded plate, which allows charging of the solid particles. The recirculation through the hopper (Figure 6) is minimal and appears to be limited by the top part of the hopper. In general, present geometry of the flow baffle appears to be much better in terms of flow distribution than the curved baffle with 4 inches air path between the baffle and grounded plate which was assumed in the previous simulation. The present geometry can serve as a good first approximation for the problem of the flow baffling.

Figure 1. Computational Grid. View A.

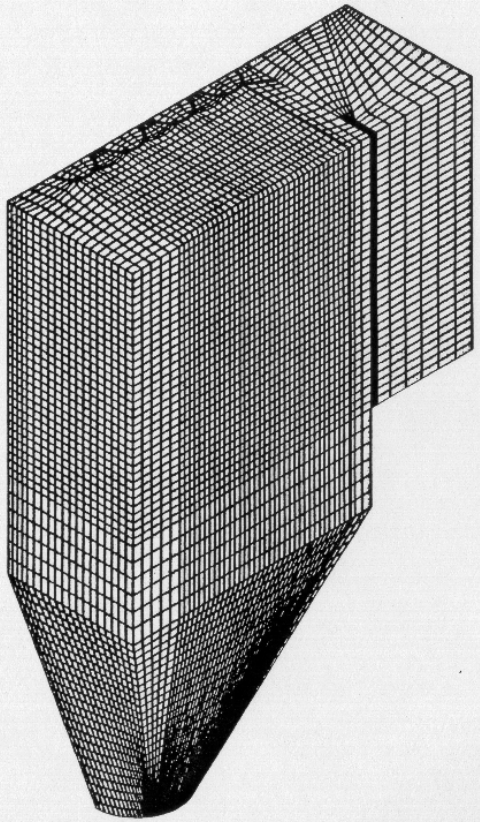

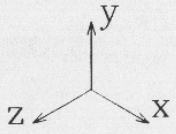

Allied Environmental Technologies, Inc.

EERC

AHPC200, Rev. 2

Computational Grid

Figure 2. Computational Grid. View B.

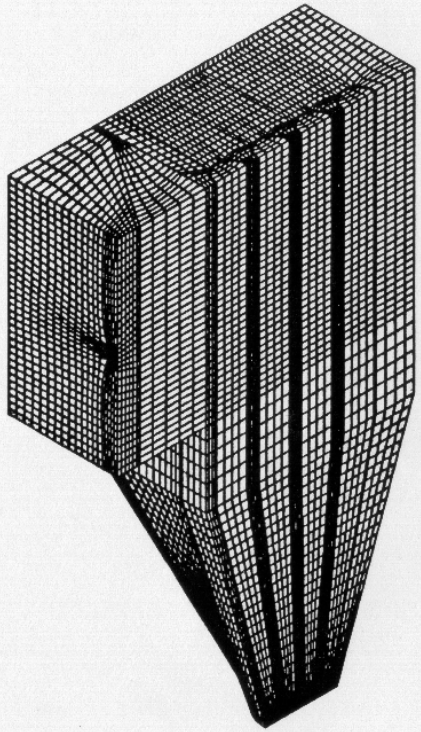

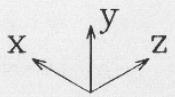

Allied Environmental Technologies, Inc.

EERC

AHPC200, Rev. 2

Computational Grid

Figure 3. Details of the AHPC200.

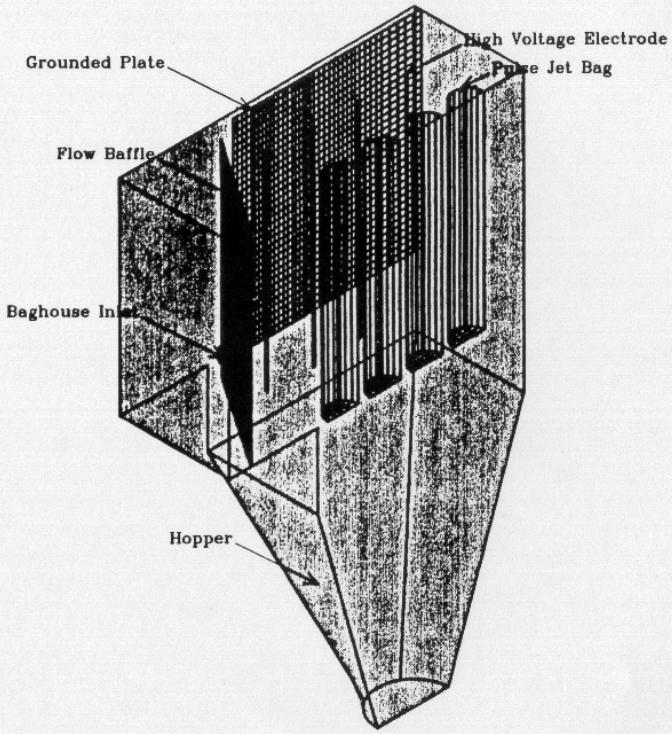

Allied Environmental Technologies, Inc.

EERC

AHPC200, Rev. 2

Simulation Details

Figure 4. Central Section Velocity Vectors.

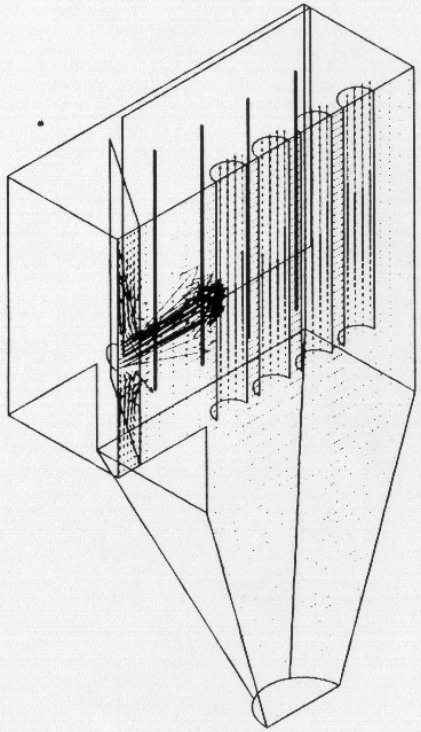

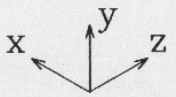

Allied Environmental Technologies, Inc.

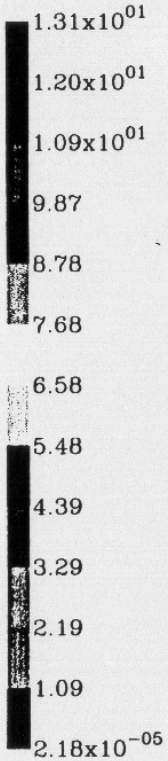

EERC

AHPC200, Rev. 2

Variable: Velocity Vectors

Units : m/sec

Local max: 1.31×10^{01}

Local min: 2.18×10^{-05}

Figure 5. Inlet Centerline Velocity Vectors.

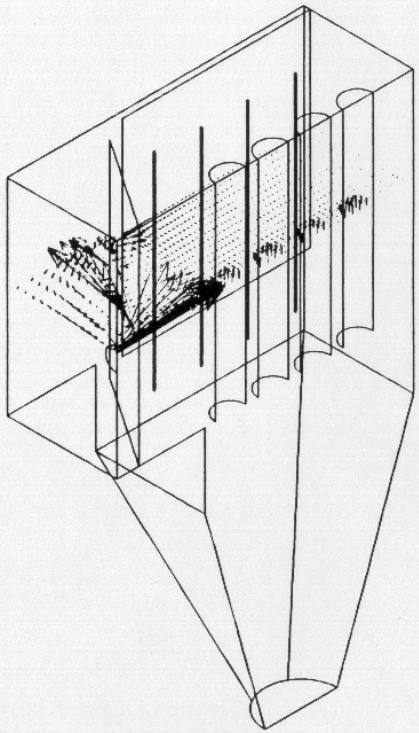

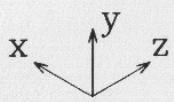

Allied Environmental Technologies, Inc.

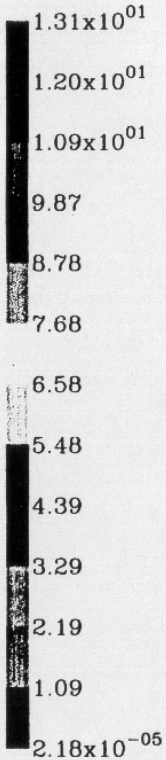

EERC	Variable: Velocity Vectors	Local max: 1.31×10^{01}	Proprietary. Unauthorized Reproduction Prohibited.
AHPC200, Rev. 2	Units : m/sec	Local min: 2.18×10^{-05}	

Figure 6. Central Section Velocity Vectors near the Baghouse Inlet.

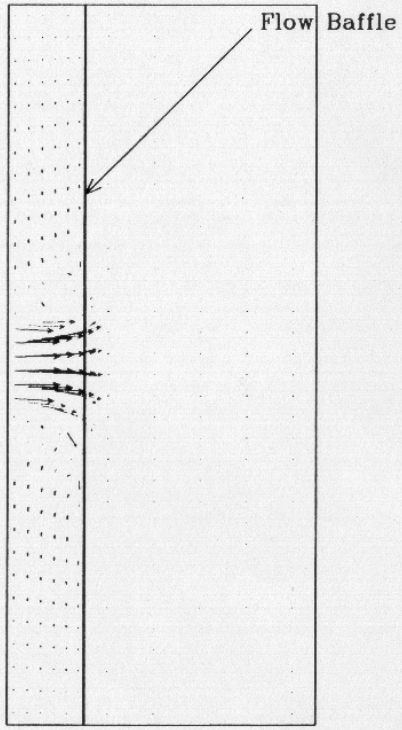

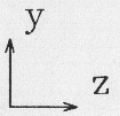

Allied Environmental Technologies, Inc.

1.31×10^{01}
1.20×10^{01}
1.09×10^{01}
9.87
8.78
7.68
6.58
5.48
4.39
3.29
2.19
1.09
2.51×10^{-03}

EERC	Variable: Velocity Vectors	Local max: 1.31×10^{01}
AHPC200, Rev. 2	Units : m/sec	Local min: 2.51×10^{-03}

Figure 7. Central Section Velocity Vectors behind the Flow Baffle.

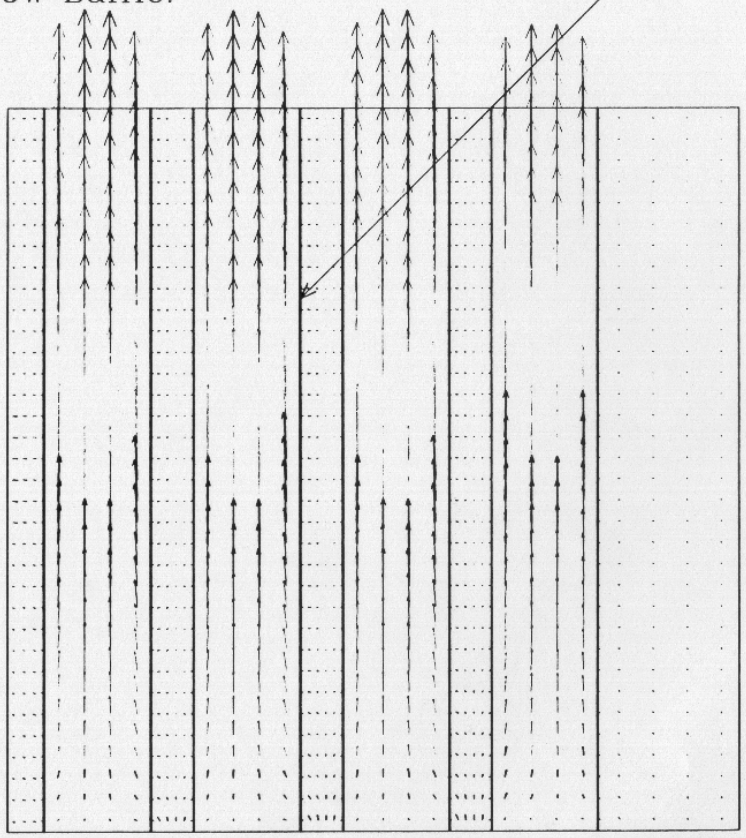

Allied Environmental Technologies, Inc.

2.16
1.99
1.81
1.63
1.45
1.27
1.09
9.14×10^{-01}
7.34×10^{-01}
5.55×10^{-01}
3.76×10^{-01}
1.96×10^{-01}
1.73×10^{-02}

EERC	Variable: Velocity Vectors	Local max: 2.16
AHPC200, Rev. 2	Units : m/sec	Local min: 1.73×10^{-02}

Figure 8. Central Section Velocity Vectors in the Hopper.

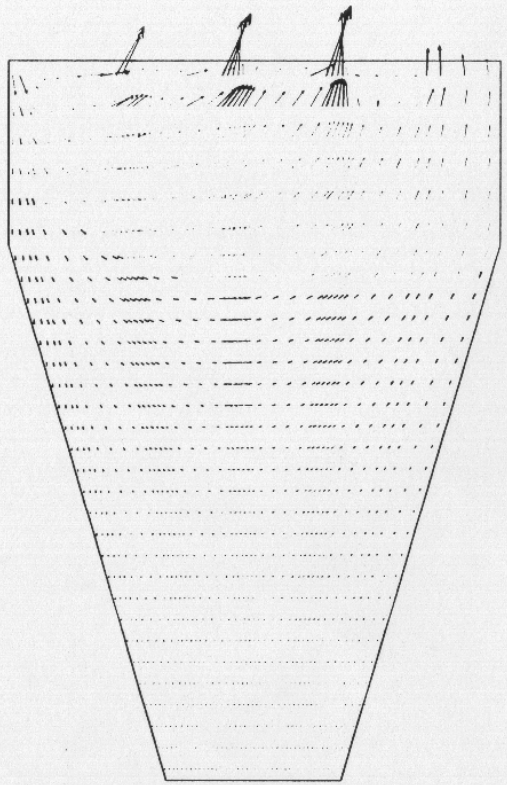

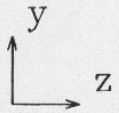

Allied Environmental Technologies, Inc.

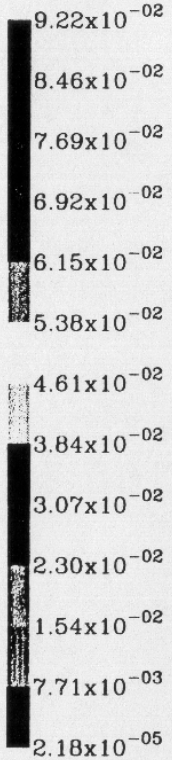

EERC	Variable: Velocity Vectors	Local max: 9.22×10^{-02}	Proprietary. Unauthorized Reproduction Prohibited.
AHPC200, Rev. 2	Units : m/sec	Local min: 2.18×10^{-05}	

Figure 9. Inlet Centerline Velocity Vectors near the Baghouse Inlet.

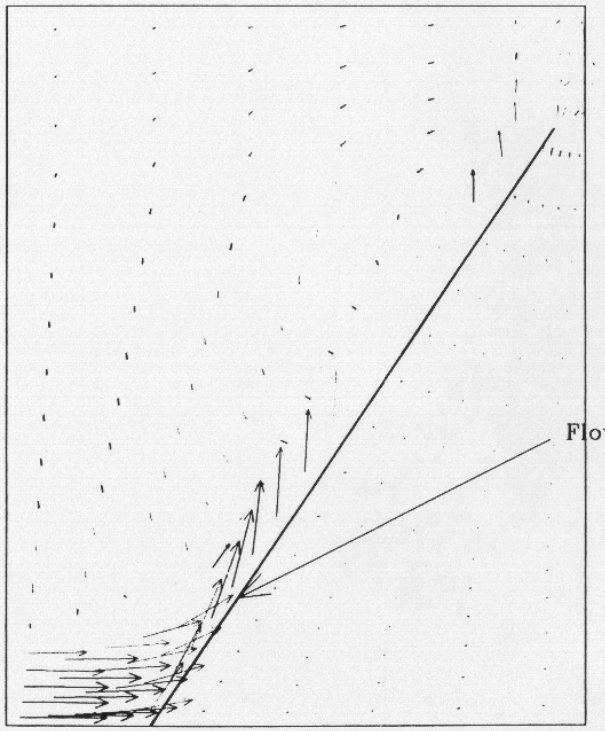

Allied Environmental Technologies, Inc.

1.31×10^{01}
1.20×10^{01}
1.09×10^{01}
9.83
8.74
7.65
6.55
5.46
4.37
3.28
2.19
1.10
9.16×10^{-03}

EERC	Variable: Velocity Vectors	Local max: 1.31×10^{01}	Proprietary. Unauthorized Reproduction Prohibited.
AHPC200, Rev. 2	Units : m/sec	Local min: 9.16×10^{-03}	

Figure 10. Inlet Centerline Velocity Vectors behind the Flow Baffle.

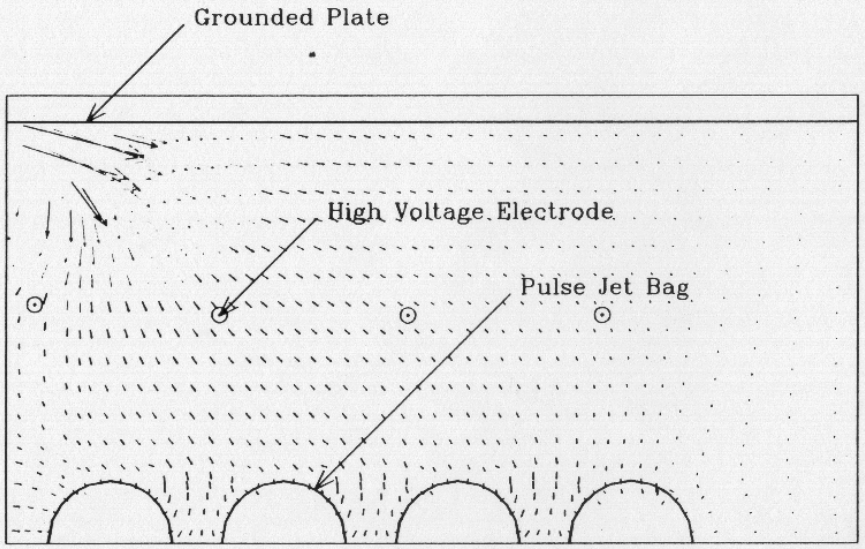

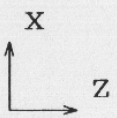

Allied Environmental Technologies, Inc.

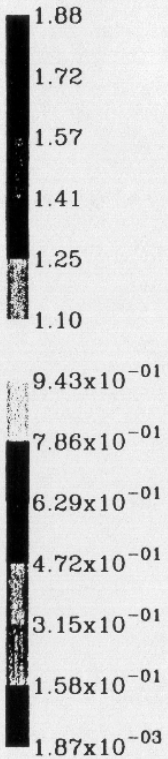

EERC	Variable: Velocity Vectors	Local max: 1.88
AHPC200, Rev. 2	Units : m/sec	Local min: 1.87×10^{-03}

PERFORMANCE ESTIMATION OF ELECTROSTATIC PRECIPITATORS

APPENDIX B

Performance Estimation of Electrostatic Precipitators

Report

Prepared
for
Energy & Environmental Research Center
University of North Dakota
Project:
Advanced Hybrid Particulate Collector
DOE Contract No. DE-AC22-95PC95258

by
Dr. Henry V. Krigmont
and
Dr. Alexander V. Potapov

July 14, 1997

Allied Environmental Technologies, Inc.
ONE PACIFIC PLAZA
7755 Center Ave. Suite 1100
Huntington Beach, CA 92647

EXECUTIVE SUMMARY

The Branch of the Electrostatic Precipitator Computer Model discussed and evaluated below deals, basically, with electric processes, and is a part of the Allied Environmental's precipitator model. The electric part uses geometric and electric parameters of the precipitator together with parameters of the gas and ash to calculate the precipitator performance. Ideally, for the AHPC project, the ESP electrostatic model can predict the amount of the material which is collected by the collecting plate, and, hence, the amount of the material which reaches the bags.

TABLE OF CONTENTS

1.0 Introduction.

The electric part of the computer model of the electrostatic precipitator is the part of the precipitator model. The electric part uses geometric and electric parameters of the precipitator together with parameters of the gas and ash to calculate the precipitator performance. For the AHPC project, the electrostatic model of the ESP can predict the amount of the material which is absorbed by the collecting plate and hence the amount of the material which reaches the bags.

2.0 Description of the ESP Model.

The ESP performance estimation program is based on the algorithms of the ESP model developed by the Southern Research Institute, Birmingham, AL. The original computer code has been modified and rewritten to be suitable for the use on personal computers in FORTRAN 77 computer language (originally, the code has been written on FORTRAN IV computer language), and the performance of the model has been tested using several examples.

The ESP model performs a detailed mathematical simulation of the precipitation process along a single gas passage of a wire-plate precipitator. Each electrical field of the gas passage is subdivided into small computational length increments, with each of which the electrical conditions (including both ionic and particulate space charge density) are approximately uniform. The inlet aerosol particle size distribution is subdivided into small bands, within each of which the particle size is approximately uniform. The ideal collection efficiency for each particle size is calculated using the Deutsch-Anderson equation. This equation is based on the probability of particle transport into a boundary layer of laminar gas flow near the collecting plate (where particle collection is assured) assuming a uniform particle distribution over a cross-sectional plane of the precipitator due to fully-developed small-scale turbulence in the gas flow. That assumption is approximately valid for the fine particles that are of principal importance in the mathematical simulation of the electrostatic precipitation.

The incremental collection fraction, n_{ij}, for the *I-th* particle size in the *j-th* increment of length of the precipitator is mathematically represented in the form of Deutsch-Anderson equation,

$$n_{ij} = 1-\exp(-\varpi_{ij}A_j/V)$$

where, ω_{ij} is the Deutsch migration velocity of the *I-th* particle size in the *j-th* increment of length, V is the volume gas flow, and A_j/V is the specific collection plate area in the *j-th* increment of length. The fractional collection n_i for a given particle size, over the entire length of the precipitator, is determined from

$$n_j = (\sum_j n_{ij}N_{ij})N_{ij}$$

where, N_{ij} is the number of particles of the *I-th* particle size, per cubic meter of gas, entering the *j-th* increment. The quantity N_{ij} can be written in the form

$$N_{ij} = N_{ij-1} \exp(-\varpi_{ij-1} A_{ij}/V)$$

where, N_{i1} is the number of particles of the *I-th* particle size, per cubic meter of gas, in the inlet particle size distribution. The overall ideal collection is given by

$$\eta = \sum_j n_j P_j$$

where, P_i is the percentage by mass of the *I-th* particle size in the inlet particle size distribution.

In the boundary layer of laminar gas flow near the collecting plate of a precipitator, each charged particle has a component of velocity directed toward the collecting plate that is called the migration velocity. The Deutsch migration velocity, ω_{ij}, is a single parameter which incorporates the combined effects of all the electrical mechanisms of particle charging and collecting. The bulk of the time required to execute the ESP model is used in computing the particle charge and the collecting electric field that are needed to compute the Deutsch migration velocity, for each particle size in each computational length increment.

In the computation of the collecting electric field, the ESP model does not assume any explicit spatial distribution of suspended charged particles. Instead, the ESP model performs a self-consistent iterative computation of the inter-electrode space charge distribution in each computational length increment, including approximately both ionic space charge and particulate space charge. The algorithm solves simultaneously Poisson's equation and the current continuity equation in the inter-electrode space. Starting with an estimate of space charge density at the corona electrode, local values of electric potential and space charge density are computed alternately, one from the other, on a rectangular coordinate grid until convergence is obtained. The results are tested against the mathematical boundary conditions of operating voltage and current density specified by the user. If the test fails, the estimate of space charge density at the corona electrode is adjusted, and the whole procedure is repeated until the boundary conditions are satisfied. This procedure requires the simplifying assumption that the average combined motions of ionic and particulate charge carriers can be described by a single effective mobility, reduced from the ionic mobility. The electrostatic potential distribution in wire-plate geometry

is used as a starting point for the iterative computation. Otherwise, the ESP model is not sensitive to the geometrical details of different types of corona electrodes and different collecting plate baffles. The main purpose of this computation is to obtain the value of electric field near the collecting plate.

The charge acquired by particles in each computational length increment is computed using a unipolar ionic charging theory. (The ESP model does not describe bipolar charging under conditions of back corona in a precipitator. The operating current density specified by the user is assumed to be the current density that is useful for unipolar charging.) The algorithm sums the time-rates-of-charging for field charging, until the saturation limit is reached for a given particle size, charging by thermal diffusion of ions, and field-enhanced thermal diffusion charging. The algorithm calculated a fourth-order Runge-Kutta numerical solution to the differential equation for the charging rate. The charge acquired by particles depends on particle size, the density of unipolar ions, the treatment time (the ratio of the computational length increment to the gas velocity) and the average electric field in the inter-electrode space.

The fractional collection η_i for the *I-th* particle size, over the entire length of the precipitator, is translated into an effective migration velocity ω_{ei}. This effective migration velocity is just the numerical factor in the exponent of an equation of the Deutsch-Anderson form that would give the same numerical value of the computed fractional collection. Since the ESP model is structured around an exponential efficiency equation for individual particle size bands, it is convenient to represent non-ideal effects in the precipitation process as correction factors which apply to the exponential arguments. These correction factors are used as divisors for the effective migration velocities.

The degrading effects of gas sneakage and non-rapping re-entrainment in a precipitator are represented by a decimal fraction S (typically 0.05 to 0.10) specified by the user. Non-uniformity in the gas flow distributions is represented by the normalized standard deviation σ_{gas} (typically 0.15 to 0.25) of a matrix of gas velocity measurements over the face of the precipitator. These non-ideal parameters enter into the calculation of correction factors F_i and B_i that are employed as $\acute{\omega}_{ei} = \omega_{ei}/F_i/B_i$. The corrected effective migration velocity $\acute{\omega}_{ei}$ and the corresponding fractional collection efficiency $\acute{\eta}_i$ for the *I-th* particle size are termed "no-rap" parameters. The "no-rap" parameters are of practical interest because they can be measured in a precipitator with the rapper turned off.

The ESP model assumes that all particles re-entrained by rapping upstream of the outlet field are recollected, and that particles re-entrained by rapping in the outlet field are lost. The correction for rapping re-entrainment in the outlet field is based on

data from six field tests of full-scale fly ash precipitators. The total re-entrained mass loading is divided into the particle size bands according to a log-normal particle size distribution with $MMD = 6.0\ \mu m$ and $\sigma = 2.5$, as determined by a fit to the test data. Finally, ESP model writes out the effective migration velocity and collection efficiency for each particle size fraction, for "no-rap" and "no-rap plus rapping" operation of the precipitator. The overall collection efficiency is obtained by summing over the fractional collection efficiencies, with the sum weighted by the inlet particle size distribution.

3.0 Application of the ESP Model.

The ESP model described herein has been utilized to estimate the efficiency of the standard industrial electrostatic precipitators. For this estimate we assumed the ideal conditions of the precipitator operation, i.e. there is no re-entrainment of the collected particles due to rapping into gas flow and there is no non-uniformity of the gas flow in the precipitator ($\sigma_{gas} = 0$). The calculation has bee carried out for three values of the precipitator collecting area (SCA): SCA = 50, 150 and 350 ft^2/1000 acfm of gas flow. For each of these SCA, the precipitator performance has been estimated for four ash particle sizes: 0.1, 1, 2.5 and 10 μm. This estimate has been carried out for wire-to-plate distance equal to 6'' and 8'', the wire-to-wire distance has been assumed to be equal twice wire-to-plate distance. For each case computed, the temperature of the gas in the precipitator was assumed to be 300 °F, and electric field inside the precipitator was assumed to be 5 kV/cm. The gas inside the precipitator was assumed to be conductive (high humidity content in the gas flow).

The results of the calculation are presented in the Table 1 and depicted in the Figures 1 through 5.

Table 1

SCA, ft^2/1000 ACFM	Wire-to-Wire Distance, inches	Particle size, μm	Collection Efficiency, %
50	6	0.1	38.20
50	6	1	42.73
50	6	2.5	64.62
50	6	10	97.52
150	6	0.1	82.56
150	6	1	85.05
150	6	2.5	97.03
150	6	10	99.99
350	6	0.1	98.03

SCA, ft^2/1000 ACFM	Wire-to-Wire Distance, inches	Particle size, μm	Collection Efficiency, %
350	6	1	98.94
350	6	2.5	99.36
350	6	10	99.99
50	8	0.1	43.63
50	8	1	48.37
50	8	2.5	70.77
50	8	10	98.67
150	8	0.1	87.39
150	8	1	89.20
150	8	2.5	98.31
150	8	10	99.99
350	8	0.1	98.57
350	8	1	99.02
350	8	2.5	99.59
350	8	10	99.99

As it could be seen, for small particle sizes, even for ideal conditions considered here the collection efficiency is rather low. In reality, for practical non-ideal conditions this value would decrease even more.

4.0 Conclusions.

The ESP computer model description is presented here together with an example of this model usage.

5.0 Figures

Figure 1.

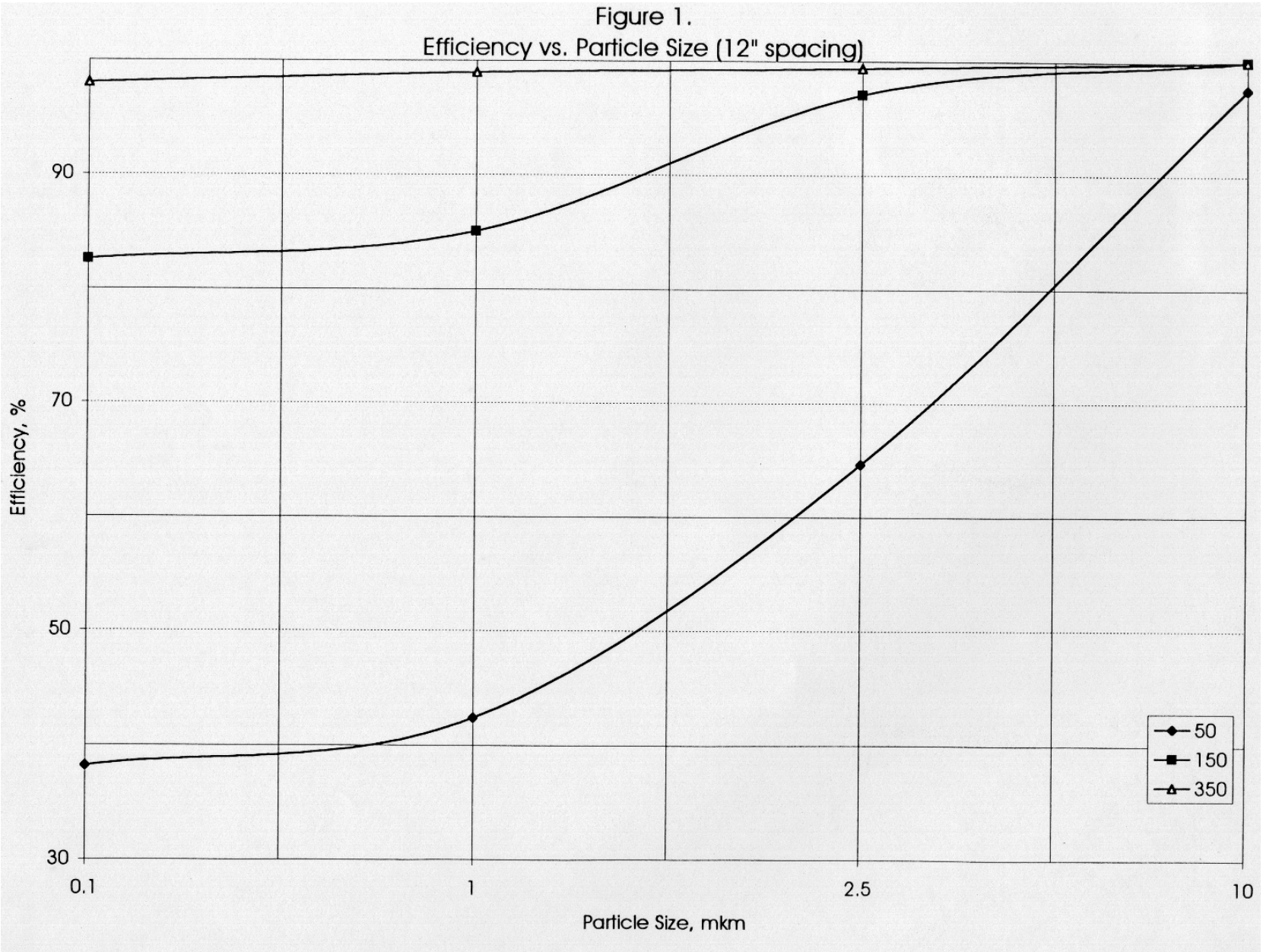
Efficiency vs. Particle Size (12" spacing)
Efficiency, %
90
70
50
30
0.1
1
2.5
10
Particle Size, mkm
50
150
350

Figure 2.

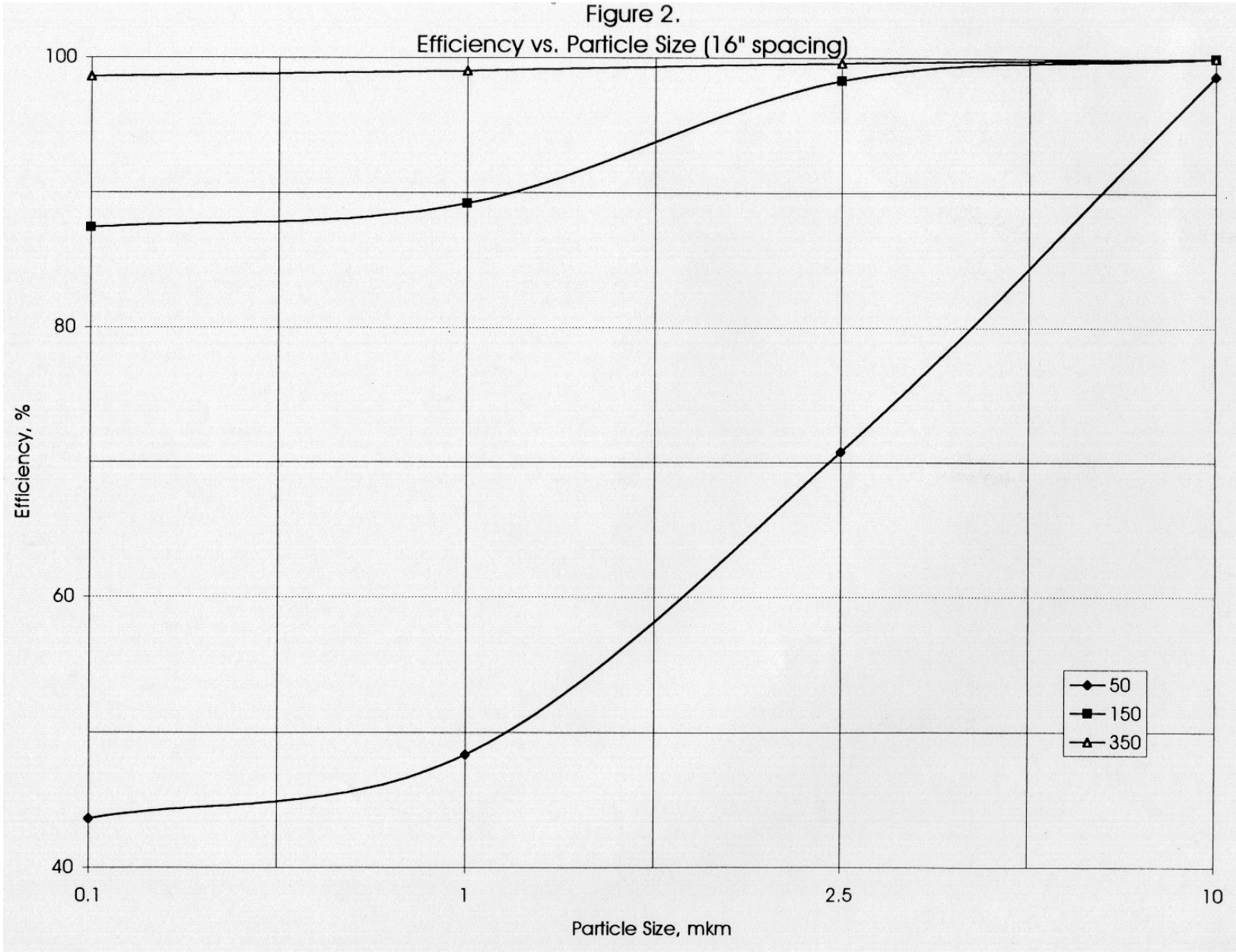
Efficiency vs. Particle Size (16" spacing)
100
80
60
40
Efficiency, %
0.1
1
2.5
10
Particle Size, mkm
50
150
350

Figure 3.
Efficiency vs. Particle Size (SCA=150)

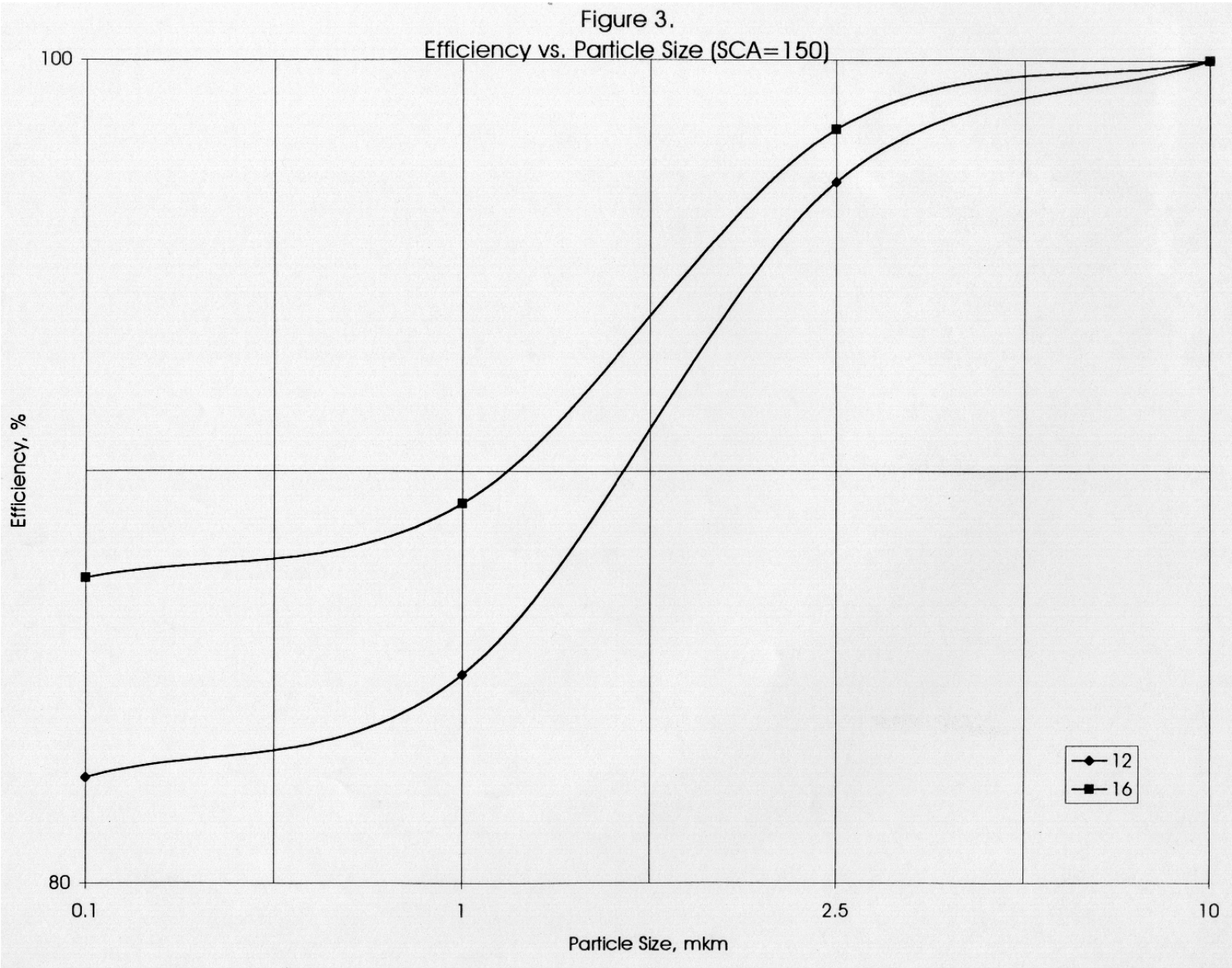

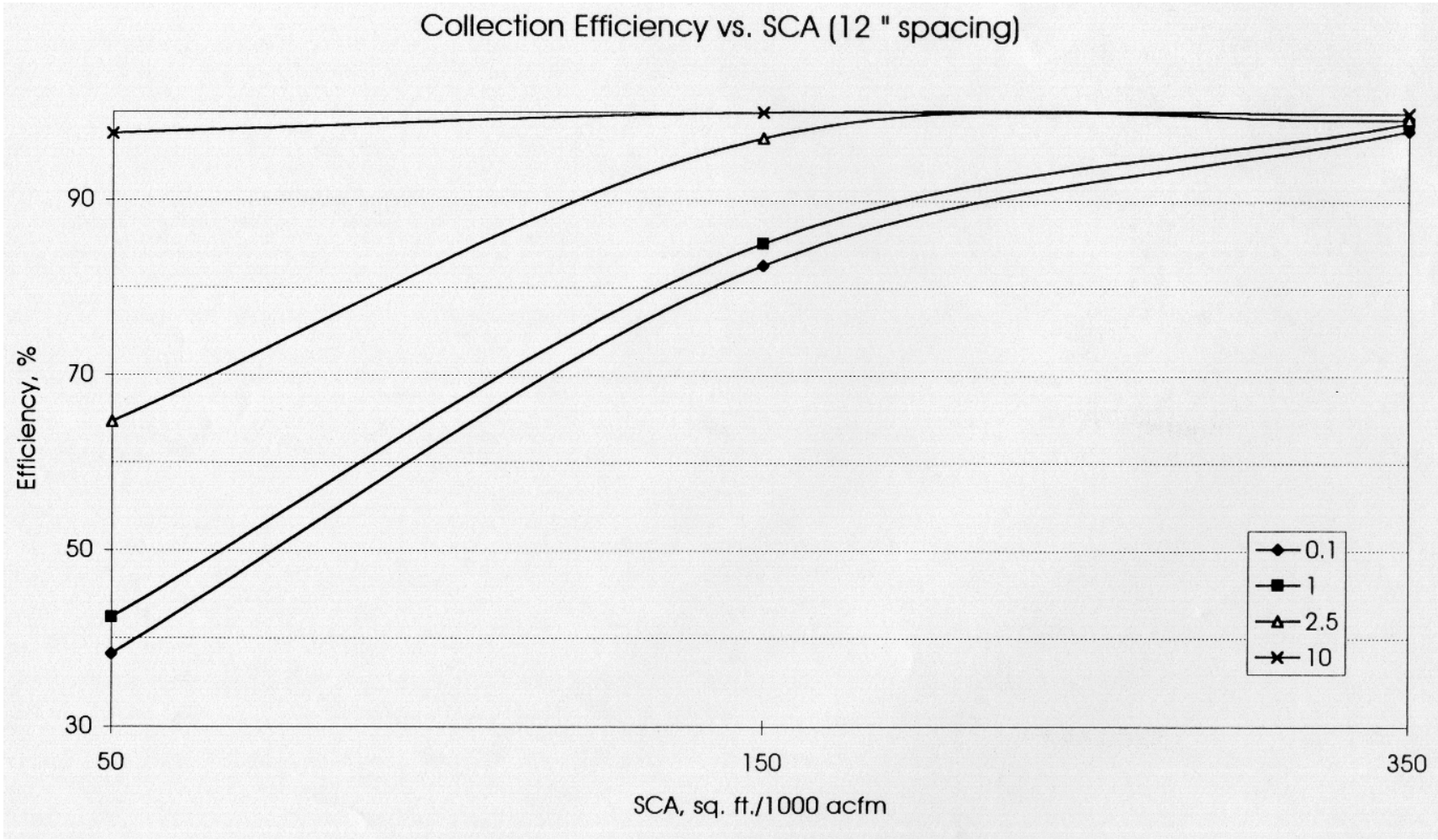
Collection Efficiency vs. SCA (12 " spacing)
Efficiency, %
90
70
50
30
50
150
350
SCA, sq. ft./1000 acfm
0.1
1
2.5
10

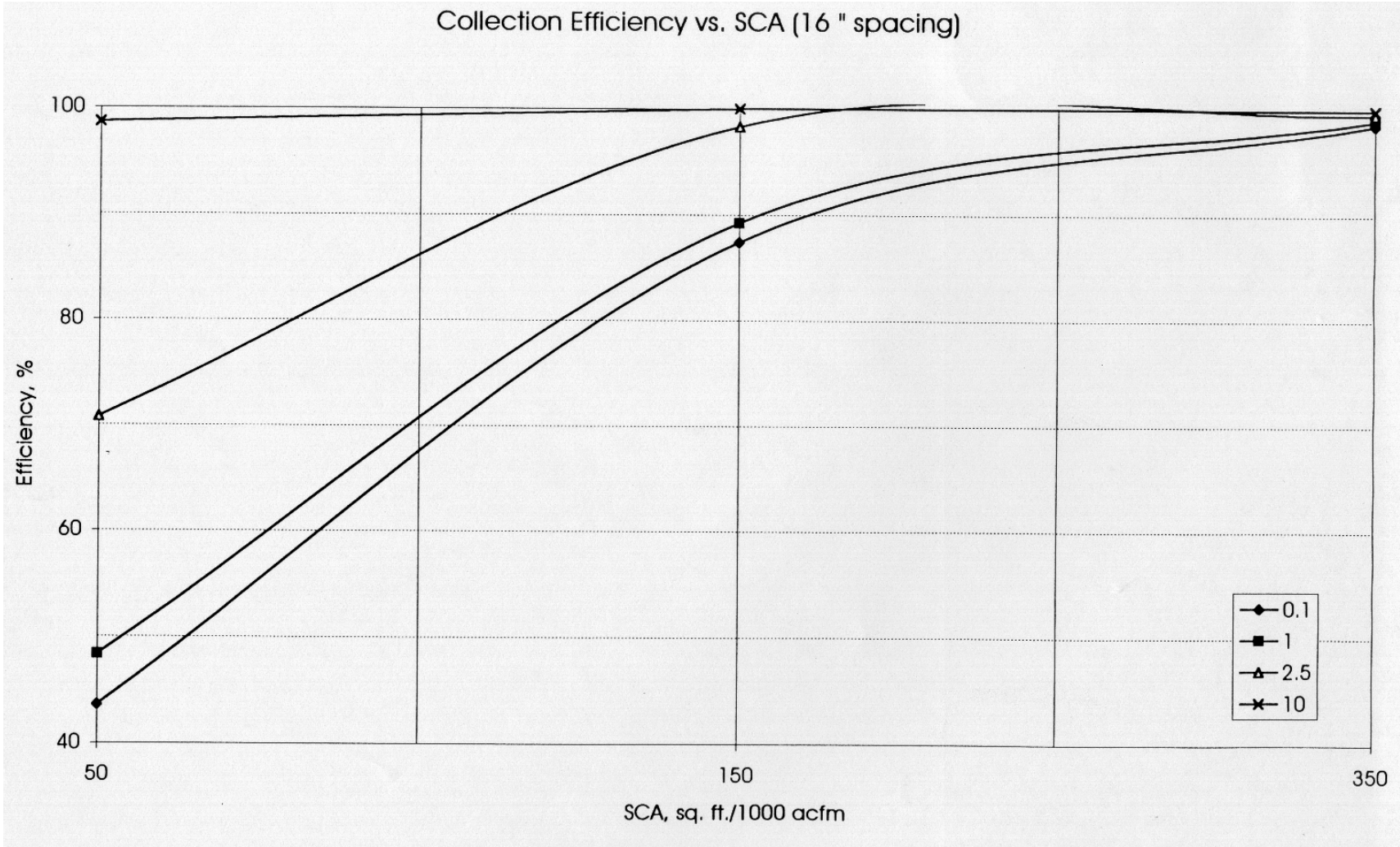
Collection Efficiency vs. SCA (16 " spacing)
100
80
60
40
Efficiency, %
50
150
350
SCA, sq. ft./1000 acfm
0.1
1
2.5
10